DISCOVERY OF AN EFFECTIVE ANTIDOTE FOR *AMANITA PHALLOIDES* POISONING

Juliana Cristina Venera Garcia

TESE APRESENTADA PARA ADMISSÃO A PROVAS DE DOUTORAMENTO À FACULDADE DE FARMÁCIA DA UNIVERSIDADE DO PORTO

The candidate performed the experimental work supported by a PhD grant (SFRH / BD / 74979 / 2010) of Fundação para a Ciência e Tecnologia.

The Faculty of Pharmacy of the University of Porto, the Faculty of Sciences of University of Porto and the Faculty of Sport, University of Porto, Portugal provided the facilities and logistical support for the experimental work.

Juliana Cristina Venera Garcia

DISCOVERY OF AN EFFECTIVE ANTIDOTE FOR *AMANITA PHALLOIDES* POISONING

Tese do 3º Ciclo de Estudos Conducente ao Grau de Doutor em Ciências Farmacêuticas – Especialidade: Toxicologia

Orientador: Professor Doutor Félix Carvalho

(Professor Catedrático da Faculdade de Farmácia da Universidade do Porto)

Co-orientadora: Professora Doutora Maria de Lourdes Pinho de Almeida Souteiro Bastos

(Professora Catedrática da Faculdade de Farmácia da Universidade do Porto)

Co-orientadora: Professora Doutora Vera Marisa Costa

(Professora da Faculdade de Farmácia da Universidade do Porto)

Porto

Abril, 2015

À minha Mãe Carminda e irmã Márcia

Às minhas Tias Mimi e São

Ao Zé

ACKNOWLEDGMENTS / AGRADECIMENTOS

Esta tese não é resultado apenas de um esforço individual. Ela nasce de significativas contribuições que recolhi durante a minha trajetória profissional, acadêmica e como cidadã, ao lidar com pessoas que tanto contribuíram para que este trabalho fosse desenvolvido. Foram 4 anos de intenso trabalho e dedicação, e sem dúvida são 4 anos de puro orgulho por tudo o que consegui conquistar e alcançar. Cresci, aprendi e mergulhei no mundo da ciência com a ânsia de poder ser um pouco melhor todos os dias. Todas as pessoas que aqui mencionarei deram um pouquinho delas e levaram um pouco de mim.

Em primeiro lugar expresso a minha profunda gratidão ao meu Orientador Professor Félix Carvalho. Foi, sem dúvida um honra conhecê-lo como pessoa e profissional. É das pessoas mais entusiastas que conheço transmitindo os seu conhecimentos de forma absolutamente admirável. Obrigada por acreditar em mim e por me ter dado oportunidade de conhecer o mundo da toxicologia de uma forma notável. Foi uma longa caminhada e sei que nada disto era possível sem todo o apoio que prestou nestes 4 anos. Levo comigo todos os ensinamentos transmitidos, toda a força de vencer qualquer obstáculo e todo o ânimo de saber que posso ser capaz. Obrigada professor por me ter tornado uma pessoa melhor.

À minha co-orientadora, Professora Doutora Maria de Lourdes Bastos pelo carinho, pelas palavras entusiastas e pelo apoio que transmitiu nestes 4 anos. Sinto uma profunda admiração por si e pelo trabalho que tem desenvolvido na toxicologia. É notável a forma como abraça todos os alunos e lhe transmite tanto e tão inigualável conhecimento. Não só a nível profissional, como também a nível pessoal contribui para que sejamos pessoas melhores. Obrigada pelo sentido crítico, pela inspiração e pela esperança que deposita em nós que tanto a admiramos.

À minha co-orientadora, Professora Doutora Vera agradeço-lhe todo o carinho e dedicação com que abraçou este projecto. Admiro o seu profissionalismo e a forma como lida dia-a-dia com a toxicologia. Obrigada pelas palavras e pelo apoio que sempre demonstrou. Fez nascer em mim um sentido crítico que até então desconhecia, e sem dúvida tornou-me melhor profissional nesta caminhada que é o doutoramento. Por vezes sentia que o meu mundo estava a desmororar e a professora conseguiu dar-me a mão e caminhou lado-a-lado comigo dando me força e alento para vencer mais uma etapa da minha vida. Muito obrigada professora por pertencer ao mundo da toxicologia e por transmitir todos os conhecimentos (que são muitos) aos alunos que consigo trabalham.

À Senhora Engenheira Maria Elisa agradeço do fundo do coração todo o apoio prestado nestes 4 anos de intenso trabalho. Tenho tanto que lhe agradecer Senhora Engenheira. As suas palavras e carinho fizeram me crescer enquanto pessoa e profissional. Foi o meu porto abrigo, a minha inspiração e o meu ânimo nestes 4 anos. Levo comigo todos os ensinamentos que de forma maternal os transmitiu. Obrigada Senhora Engenheira por existir e por fazer parte do grupo de toxicologia.

À Professora Doutora Paula Baptista agradeço todo o apoio que sempre prestou nestes 4 anos. Agradeço por ter acreditado em mim e por me ter impulsionado para este mundo que é o doutoramento. Tive o privilégio de trabalhar consigo e de conhecer a pessoa admirável que é. Muito obrigada por ter feito parte desta fase da minha vida.

Ao Professor Doutor Fernando Remião agradeço toda a ajuda imprescindível no HPLC. Consigo inicíamos o mundo da toxicologia em aulas que fizeram despertar em mim um gosto que até então desconhecia. As suas aulas são o espelho do profissional que é e por isso é impossível imaginar a toxicologia sem o professor. Obrigada por nos incutir o gosto pela toxicologia.

À Professora Doutora Helena agradeço as aulas que fizeram com que o meu gosto pela toxicologia se intensificasse. É uma professora admirável não só pelo seu profissionalismo, como também pela pessoa que é.

À Doutora Alexandra e ao Doutor Daniel pelos ensinamentos e por por todo o trabalho do *in silico* que tive oportunidade de desenvolver. A amizade com que sempre me abraçaram jamais esquecerei. Xaninha sempre tiveste a palavra certa na hora certa, foi um privilégio trabalhar contigo e conhecer a profissional que és. Daniel sempre acreditaste em mim e fizeste-me sentir quase que uma expert (muito longe disso) no *in silico*. Agradeço aos dois todos os lanches, almoços e jantares que partilhamos, as conversas, as confidências, os sorrisos. Obrigada estais sempre no meu coração.

Ao Professor Doutor José Duarte porque me apresentou o mundo da histologia que tanto admiro e gosto. Consigo tive oportunidade de conhecer e admirar a histologia, e hoje posso dizer que é das análises que mais gosto de fazer. Obrigada por transmitir tantos e tão ingualáveis conhecimentos.

Aos meus co-autores Professor Doutor Ricardo Dinis, Doutor Ricardo Silvestre e Professora Doutora Paula Pinho agradeço toda a ajuda que sempre prestaram para atingir os meus objectivos.

À Cátia Faria e Margarida pela ajuda, pelo suporte técnico e logístico que sempre disponibilizaram. Obrigada por fazerem do laboratório de toxicologia um lugar melhor.

À Dona Celeste agradeço toda a ajuda com os ratinhos e a histologia. Levarei sempre comigo todos os ensinamentos que tão amavelmente tem partilhado. São muitos os alunos que consigo trabalham e que certamente a levarão sempre no coração.

Aos restantes colegas de laboratório, em especial à Mariline, Ana Oliveira, Teresa Baltazar, Vânia, e Maria João, que apesar de pouco tempo de convivência deixaram um carinho muito especial. Obrigada Mariline pelos sorrisos, pelas palavras e pela amizade. Obrigada Ana Oliveira pelas horas infindáveis no HPLC e a ti Teresa por teres teres feito parte do meu trabalho.

Marcelo já sabes o quanto te agradeço toda a ajuda que me deste. Quando me lembrar dos estudos *in vivo* vou certamente lembrar de todos os ensinamentos e de toda a paciência que tiveste comigo. Mas além do trabalho foram tantos os momentos que partilhamos, almoços no bugo, gelados na cremosi e infindáveis conversas das quais tenho tantas saudades.

Emanuele (Manu) és uma pessoa cheia de garra, muito profissional e, sem dúvida uma química de excelência, tens tudo para brilhar na toxicologia e acredito que vais conseguir. Obrigada pelos miminhos (aquele bolinho de côco ainda faz parte da minha memória), e por seres uma pessoa cheia de energia e boa disposição que tanto te caracteriza.

À Doutora Sara agradeço a amizade e carinho. Levo comigo todos os ensinamentos de química que amavelmente se prontificou a partilhar. Tive o privilégio de trabalhar consigo e conhecer a pessoa maravilhosa que é.

Ao Daniel por ser a pessoa que é e por ter tido o privilégio de partilhar uma amizade contigo. És das melhores pessoas que já conheci e que levarei para sempre no meu coração. Dificil de imaginar a toxicologia sem um Daniel. Tanto a nível profissional como pessoal és admirável e cheio de talento. Recordo com saudades as nossas conversas, os nossos almoços e os teus conselhos sempre tão sábios.

À Renata pela amizade e sorrisos que sempre partilhamos. Foste um apoio quando mais precisei e levo para sempre comigo todos os momentos que partilhamos. És uma excelente profissional e amiga, com a qual podemos sempre contar. A toxicologia não seria a mesma sem o teu entusiasmo, a tua dedicação e o teu profissionalismo.

A ti Rita Azevedo porque foste e és uma pessoa muito importante para mim. Admiro o teu profissionalismo e a tua forma de ser. Terás um futuro brilhante e eu estarei na primeira fila para te aplaudir Ritinha. Trago na memória noites de intenso trabalho no laboratório, em que pude partilhar a bancada de trabalho contigo e que numa cumplicidade só nossa partilhávamos conversas mergulhadas de gargalhadas (a história da laranja ainda hoje me faz sorrir). Levo tantos e tão grandes momentos que serão eternos pela intensidade com que os vivemos. Obrigada pelos miminhos, pelas brincadeiras, pelas conversas sérias, por me ouvires e aconselhares, e sobretudo por estares aí.

Ao José Luís porque és simplesmente o Zé. Não me vou esquecer das nossas conversas de surdos mudos, dos momentos que partilhamos na biologia molecular, das confidências, da cumplicidade e sem dúvida da amizade que nos une e unirá sempre. És um grande profissional Zé e o teu gosto pela toxicologia é admirável. Sei que terás um grande futuro e serás reconhecido por isso. É com saudade que recordo os nossos cafés, almoços e jantares e aos quais trouxeste sempre a alegria que tanto te caracteriza. As tuas teorias infindáveis um dia darão um livro Zé (best seller), pois fazem com que os nossos dias sejam um pouco melhores.

A ti Chiara porque és e sempre serás uma das minha melhores amigas. Partilhamos tanto e vivemos tanto. És aquela que sei que posso contar e que estará sempre aí para me ouvir. Obrigada minha flor pelas palavras que tanto me encorajaram e me fizeram sentir que era capaz. Contigo partilhei histórias que são apenas nossas e que tanta saudade me trazem.

A ti João pelo ânimo e entusiasmo que sempre demonstraste. És um grande profissional e é admiravel a forma como lutas pelas teus objectivos. És um exemplo para todos os que lidam contigo e eu tive a sorte de poder cruzar-me contigo e partilhar tantos e tão grandes momentos. Obrigada João por tudo.

Ao Paulo porque os amigos são a segunda família que escolhemos e eu tive o privilégio de te conhecer. Obrigada por todas as palavras de entusiasmo e por todo o apoio nesta fase da minha vida. É tão bom podermos contar com amigos como tu. Sempre tão positivo, tão entusiasta e tão determinado, fazes-me sempre acreditar que tudo é possível.

À Ana Teixeira pela ajuda que sempre prestou, o que seriam das minhas imagens sem a tua opinião e ajuda. Tens a arte dentro de ti e um talento surpreendente que partilhas sem pedir nada em troca. Obrigada Ana não só pela ajuda mas por toda a amizade, foram muitas as noites de trabalho em que tu amavelmente cedeste um pouco do teu tempo para tornar isto possível. É notável o teu altruísmo e és admirável por isso.

À Diana Gesto (minha Deehzinha), por todo o carinho e amizade que ao longo destes 4 anos partilhamos. A minha estadia na faculdade de Ciências não teria sido a mesma senão te tivesse conhecido. Recordo com saudades a nossa viagem a Girona em que te conheci um pouco melhor e pude constatar a pessoa maravilhosa que és. Trago sempre comigo a memória dos nossos lanches, das nossas conversas e dos grandes momentos que temos partilhado.

Aos meus amigos Cristiana Gaspar, Liliana e Richard por toda a amizade que sempre depositaram em mim.

Ao Ricardo Malheiro porque inicíamos juntos esta jornada que é o doutoramento e durante este tempo qualquer dúvida que surgisse sei que podia recorrer a ti. Esse teu espírito de entreajuda ficou bem patente logo no primeiro curso que frequentamos juntos (SPSS lembraste?). Obrigada Ricardo por ter o privilégio de te incluir na minha tese.

À Elsa, amiga desde a primária, já são 20 anos juntas e amizade sempre nos acompanhou. Tu és a irmã que escolhi e que faz parte do meu coração. Não são laços de sangue que nos unem, mas são laços de coração que jamais serão apagados. Já são 20 anos que sei que estás ai e que o que caminhas lado a lado de mãos juntas comigo. Tive o privilégio de te ter na minha vida e é com orgulho que escrevo este agradecimento a ti. Obrigada minha amorinha por existires e por fazeres parte de todos os momentos da minha vida. És a minha jornalista preferida e como tu costumas dizer um dia seremos velhinhas com um monte de histórias para partilhar. E esta é mais uma. Termino com uma célebre frase "Distância não significa nada quando alguém significa tudo".

À minha mãe Carminda porque devo tudo o que sou. É com muito amor que te dedico a minha tese. Foste mãe e pai e por isso orgulho-me muito de ti. Tiveste as palavras certas na hora certa e isso fez me crescer e lutar por tudo o que já consegui. Agradeço todo o esforço que fizeste para conseguirmos alcançar os nossos sonhos. Muito obrigada Mami por existires e por fazeres de nós as pessoas que somos.

À minha irmã Márcia por caminhar sempre lado a lado comigo. Tu és a mais bela expressão de amor que pode existir. O amor de irmão jamais será igualável por ser tão único e tão especial. Contigo partilho alegrias, tristezas, contigo partilho tudo. És o meu porto abrigo, a minha esperança, o meu eu.

A ti Zé porque és simplesmente o meu Zé. Contigo partilho alegrias, tristezas e todos os momentos da minha vida. És o meu sorriso quando mais preciso, a minha alegria quando nada faz sentido. És aquele que escolhi para percorrer uma vida e sem o qual tudo seria mais dificil. Agradeço-te por seres como és e por fazeres de mim a pessoa que sou. Sei que foram duros estes 4 anos mas tu estiveste sempre lá e com muito carinho deste-me força para ultrapassar todos os obstáculos que foram aparecendo no meu caminho.

À minha tia Mimi agradeço todos os conselhos, todo o carinho e todas as partilhas que me fizeram crescer. É, sem dúvida a minha inspiração, a minha força quando me sinto derrotada, e a minha esperança quando tudo parece impossível. Obrigada pelas longas conversas que me fizeram sempre sentir especial. Tenho em si o maior orgulho do mundo, por ser a pessoa admirável que é, e por ser minha tiínha. Obrigada por existir minha tia com sabor a chocolate, e por fazer parte da minha vida.

À minha tia São que sempre se prontificou a ajudar-me. Obrigada tia por todos os ensinamentos, todos os conselhos e todos os momentos que temos partilhados juntas. Tenho o maior orgulho em que faças parte desta fase da minha vida e por poder contar contigo todos os dias.

À restante família, tio Jorge, tio Armando e primos Hugo e Fábio agradeço todo o carinho e amizade.

A minha arianinha por existir e por fazeres dos meus dias, dias melhores.

Finalmente, e não menos importante ao meu Deus porque és a luz que ilumina o meu caminho.

Finalmente agradeço às seguintes instituições:

Fundação para a Ciência e a Tecnologia_FCT pela bolsa de doutoramento (SFRH/BD/74979/2010) e o suporte financeiro para esta dissertação.

FCT Fundação para a Ciência e a Tecnologia
MINISTÉRIO DA EDUCAÇÃO E CIÊNCIA

POPH QUALIFICAR É CRESCER.

QREN QUADRO DE REFERÊNCIA ESTRATÉGICO NACIONAL PORTUGAL 2007.2013

GOVERNO DA REPÚBLICA PORTUGUESA

UNIÃO EUROPEIA
Fundo Social Europeu

Ao "REQUIMTE" pelo suporte financeiro para o trabalho laboratorial decorrido durante esta tese.

Ao Laboratório de Toxicologia da Faculdade de Farmácia da Universidade do Porto, ao Departamento de Bioquimíca da Faculdade de Ciências da Universidade do Porto, e à Faculdade de Desporto da Universidade do Porto pelo apoio logístico prestado para a realização desta dissertação.

PUBLICATIONS

The author states to have afforded a major contribution to the conceptual design, technical execution of the work, interpretation of the results and manuscript preparation of the published or submitted articles included in this dissertation.

Articles in international peer-reviewed journals

Theoretical background

1. Garcia J, Costa VM, Carvalho ATP, Baptista P, Guedes P, Bastos LM, Carvalho F. *Amanita phalloides* poisoning: mechanisms of toxicity and treatment. *Submitted for publication*

Original Research

1. Garcia J, Oliveira A, Guedes P, Freitas V, Carvalho ATP, Baptista P, Pereira E, Bastos ML, Carvalho F. Determination of Amatoxins and Phallotoxins in *Amanita phalloides* mushrooms from Northeast Portugal by HPLC-DAD-MS. *Accepted in Mycologia.*

2. **Garcia J**, Carvalho AT, Dourado DF, Baptista P, de Lourdes Bastos M, Carvalho F. 2014. New in silico insights into the inhibition of RNAP II by α-amanitin and the protective effect mediated by effective antidotes J Mol Graph Model 51:120-7.

3. Garcia J, Costa VM, Baptista P, Bastos LM, Carvalho F. Quantification of alpha-amanitin in biological samples by HPLC using simultaneous UV-diode array and electrochemical detection. *Submitted for publication.*

4. Garcia J, Costa VM, Guedes P, Baptista P, Lourdes Bastos M, Carvalho F. Mushroom poisoning with Amatoxin and isoxazoles-containing mushrooms: A case report. *Submitted for publication.*

5. Garcia J, Costa VM, Carvalho ATP, Dourado D, Silvestre R, Dinis R, Arbo M, Baltazar T, Baptista P, Bastos LM, Carvalho F. Discovery of an effective antidote for *Amanita phalloides* poisoning: a precious extension of polymyxin B pharmacotherapy. *Under preparation.*

ABSTRACT

ABSTRACT

The present dissertation reports a series of studies performed towards a better knowledge on the chemical composition of *Amanita phalloides* and its biological effects, and the successful endeavor of discovering an antidote for intoxications with this poisonous mushroom.

The poisonous *Amanita* mushroom species, particularly *A. phalloides* (Death Cap), are responsible for 90-95% of the fatalities occurring after mushrooms ingestion. Toxins contained in *A. phalloides* include a group of toxic bicyclic octapeptides known as amatoxins. The most relevant amatoxin regarding human intoxications is α-amanitin, for which there is no effective antidote available. Therefore, at present, the greatest clinical interest in this field resumes to the discovery of a new and effective antidote against *A. phalloides* poisoning.

A significant variability in the amount of amatoxins contained in the mushrooms collected at different geographical areas has been described, being the Portuguese data very scarce. In this dissertation, the main composition of amatoxins and phallotoxins in *A. phalloides* collected at two different Portuguese sites were analyzed by liquid chromatography (LC)–diode array (DAD) and mass spectrometry (MS) detection. The results showed that the concentration and distribution of toxins in the fruiting body are variable and influenced by site-specific environmental conditions, in particular the amount of phallotoxins. In sequence, a new high-performance liquid chromatography (HPLC) method was developed to allow simultaneous DAD and electrochemical (EC) quantification of α-amanitin in liver and kidney samples. Most importantly, this developed HPLC method was applied to human samples (urine and gastric juice) in a real case of amatoxins-containing mushrooms poisoning, which assisted in the diagnosis of that mushrooms intoxication.

α-Amanitin is a powerful inhibitor of RNA polymerase II (RNAP II) and this effect is thought to be the main responsible for the hepatic and renal failure that occurs after *A. phalloides* poisoning. As a starting point to achieve our purpose of developing an effective antidote, an *in silico* model using docking and molecular dynamics simulation coupled to molecular mechanics-generalized born surface area method energy decomposition was applied to characterize the *in silico* interactions between the complex formed between RNAP II and α-amanitin. The *in silico* results obtained in this dissertation showed that α-amanitin directly interacts with bridge helix and trigger loop residues, and these interactions possibly contribute to the inhibition of RNAP II. Moreover, the interactions between RNAP II and the classically used *A. phalloides* poisoning antidotes, namely benzylpenicillin, silybin and ceftazidime, were also explored *in silico*. These antidotes show poor efficacy in clinical practice since mortality rate after *A. phalloides* intoxication still remains at 20-30%. *In silico,* benzylpenicillin, ceftazidime and

silybin were able to bind to the same site as α-amanitin, although not replicating the unique α-amanitin binding mode. Our RNAP II α-amanitin binding model provided a reliable platform for the discovery of novel antidotes against α-amanitin poisoning and that model was used in the subsequent study of this dissertation. *In silico* studies were applied to drugs that simultaneously were already in use on the clinical practice, (although with other therapeutic indications not related to mushroom poisonings) and that share structural similarities with α-amanitin. The results obtained *in silico* demonstrate that polymyxin B binds to the same interface as α-amanitin, potentially preventing the toxin from binding to RNAP II. Most importantly, polymyxin B does not interfere with the structures involved in messenger ribonucleic acid (mRNA) synthesis. Subsequent *in vivo* studies in Charles-River CD-1 mice were done as a proof of concept of the *in silico* data. It became demonstrated that a competition between α-amanitin and polymyxin B and/or displacement of α-amanitin from its RNAP II binding site by polymyxin B occurred, since polymyxin B significantly reverted the α-amanitin-induced transcription inhibition of renal specific genes, and decreased the α-amanitin induced liver and renal damage, and also hepatic oxidative stress. The effectiveness of polymyxin B, given 4 hours α-amanitin post-administration was also assessed by a survival rate study. The multiple administration of polymyxin B (at 4, 8 and 12 hours after α-amanitin) guaranteed a 50% of survival of the α-amanitin-treated mice (until 30th day), whereas all animals exposed only to α-amanitin died within 5 days. Moreover, a single dose of polymyxin B administered concomitantly with α-amanitin was able to assure a 100% survival until the 30th day post exposure. Taken together, these results show that polymyxin B potentially acts on RNAP II, preventing α-amanitin from binding, and hence protecting RNAP II from inactivation. These promising results with polymyxin B insured an increase in survival of α-amanitin-treated animals, in clinical realistic human doses (2.5 mg/kg).

In conclusion, the results of this dissertation allowed the full achievement of the established objectives: (i) it is provided an update of the state of the art concerning the toxicity of *A. phalloides,* (ii) new methodologies for measurement of α-amanitin were developed and applied in the analysis of amatoxins and phallotoxins in *A. phalloides* collected at two different Portuguese sites, as well as for clinical purposes and, (iii) polymyxin B is suggested to be the first effective amatoxin's antidote, by acting upon RNAP II. As polymyxin B is already used in the clinical practice for other health issues, it has a great potential to be applied in humans immediately. The addition of polymyxin B to the present standard protocol of *A. phalloides* will improve the overall survival of intoxicated patients and prevent death and/costly treatments.

Keywords: *Amanita phalloides;* α-amanitin; RNA polymerase II; polymyxin B.

RESUMO

RESUMO

A presente dissertação reporta estudos realizados com os objectivos de aumentar o conhecimento sobre a composição química da *Amanita phalloides* e os seus efeitos biológicos, e de desenvolver um antídoto eficaz para as intoxicações resultantes do consumo deste cogumelo tóxico. O género *Amanita*, e particularmente a espécie *A. phalloides* (chapéu da morte), são responsáveis por cerca de 90-95% das fatalidades que resultam da ingestão de cogumelos. As toxinas presentes em *A. phalloides* incluem um grupo de octapéptidos bicíclicos tóxicos denominados genericamente de amatoxinas. Destas, a α-amanitina é considerada a mais relevante no contexto de intoxicações humanas por cogumelos do género *Amanita,* para a qual não existe antídoto eficaz. Deste modo, actualmente, o maior interesse clínico nesta área centra-se na descoberta de um antídoto eficaz para envenenamento por *A. phalloides*.

A variabilidade da concentração de amatoxinas nos cogumelos colhidos em diferentes áreas geográficas tem sido amplamente descrita na literatura, embora dados relativos aos cogumelos colhidos em Portugal sejam praticamente inexistentes. Deste modo, nesta dissertação a composição das principais amatoxinas e falotoxinas presentes nos cogumelos *A. phalloides* colhidos em dois locais diferentes de Portugal foi analisada por cromatografia líquida de alta eficiência com recurso à detecção por um sistema de díodos e espectrometria de massa. Os resultados mostram que a quantidade e distribuição das toxinas no corpo frutífero dos cogumelos, em particular das falotoxinas, são variáveis e influenciadas sobretudo pelas condições ambientais especificas do local de colheita. No seguimentos deste estudo, um novo método de cromatografia líquida de alta eficiência foi desenvolvido com o objectivo de permitir a detecção e quantificação de α-amanitina em amostras de fígado e rim com recurso a dois detectores: um sistema de díodos e um detector electroquímico. O método desenvolvido revestiu-se de grande importância, pois o mesmo permitiu a análise de amostras humanas (urina e suco gástrico) provenientes de um caso clínico de intoxicação por amatoxinas, possibilitando, deste modo, a confirmação do diagnóstico.

A α-amanitina é um inibidor potente da polimerase II do ácido ribonucleico (ARNP II) sendo este efeito apontado como o principal responsável pela falência hepática e renal que ocorre após a intoxicação por *A. phalloides*. Como ponto de partida para alcançar o primordial objectivo desta dissertação, o desenvolvimento de um antídoto eficaz na intoxicação por *A. phalloides*, o complexo formado entre a ARNP II e α-amanitina foi caracterizado *in silico* com recurso a técnicas de *docking* e dinâmicas moleculares acopladas a um método de decomposição de energia (em inglês designado de *molecular mechanics-generalized born surface area method energy decomposition*). Nesta dissertação, os resultados *in silico* demonstram que a α-amanitina interage directamente

com resíduos da hélice-ponte e de uma estrutura designada de *trigger loop* o que, possivelmente, contribui para a inibição da ARNP II. Além disso, as interacções entre a ARNP II e os fármacos actualmente usados na intoxicação por *A. phalloides*, nomeadamente a benzilpenicilina, silibina e ceftazidima, foram também exploradas *in silico*. Estes fármacos têm demonstrado pouca eficácia clínica, uma vez que a mortalidade associada à intoxicação por *A. phalloides* permanece ainda em cerca de 20-30%. *In silico*, a benzilpenicilina, ceftazidima e silibina mostram-se capazes de se ligar no mesmo local que a α-amanitina, sem no entanto reproduzirem o modo de ligação peculiar e único da α-amanitina. O nosso modelo de ligação ARNP II/α-amanitina forneceu uma plataforma ideal para a descoberta de novos antídotos para a intoxicação por α-amanitina, e este mesmo modelo foi usado nos estudos subsequentes desta dissertação. Estudos *in silico* foram aplicados a fármacos que são simultaneamente usados na prática clínica (embora com outras indicações não relacionadas com intoxicação por cogumelos) e que partilham semelhanças estruturais com a α-amanitina. Os resultados obtidos *in silico* demonstram que a polimixina B se liga na mesma interface que a α-amanitina, prevenindo, deste modo, a ligação da toxina à ARNP II. A polimixina B não interfere com as estruturas envolvidas na síntese do ARN mensageiro. Subsequentemente, e com o objectivo de validar os estudos *in silico*, foram conduzidos estudos *in vivo* usando ratinhos. Esses estudos demonstraram que a polimixina B pode competir com a α-amanitina e/ou deslocar a α-amanitina do seu local de ligação à ARNP II, uma vez que a polimixina B reverteu significativamente a inibição da transcrição de genes renais, reduziu os danos hepáticos e renais, assim como o stress oxidativo hepático causado pela α-amanitina. A eficácia da polimixina B, administrada 4 horas após a α-amanitina, foi também avaliada através da realização de um estudo de sobrevivência. A administração múltipla de polimixina B (4, 8 e 12 horas) resultou em 50% de sobrevivência dos ratinhos tratados com α-amanitina (até ao dia 30), enquanto todos os animais expostos apenas ~~com~~ à α-amanitina morreram em 5 dias. Além disso, a administração concomitante de uma dose única de polimixina B com α-amanitina garantiu 100 % de sobrevivência num período de estudo de 30 dias. No seu conjunto, estes resultados mostram que a polimixina B se liga, potencialmente, à ARNP II, prevenindo por isso a ligação da α-amanitina, e deste modo impedindo a inactivação da ARNP II. Estes resultados promissores da polimixina B asseguram uma maior taxa de sobrevivência dos animais tratados com α-amanitina, em doses clinicamente realistas (2.5 mg/kg).

Em conclusão, os resultados desta dissertação permitiram atingir com êxito os objectivos propostos. Foi realizada a actualização do estado de arte no que concerne à toxicidade da *A. phalloides*, e desenvolvidas novas metodologias para a quantificação da α-amanitina,

aplicadas na análise de amatoxinas e falotoxinas de cogumelos *A. phalloides* colhidos em dois locais portugueses diferentes, e também para fins clínicos. Finalmente, descobriu-se o papel antidotal da polimixina B para as intoxicações por amatoxinas, pela sua acção na ARNP II.

Dado que a polimixina B é usada actualmente na prática clínica para outros fins terapêuticos, tem grande potencial de ser aplicada imediatamente em humanos. É nossa convicção que a adição da polimixina B ao actual protocolo hospitalar para a intoxicação por *A. phalloides* vai melhorar a taxa de sobrevivência dos pacientes intoxicados prevenindo mortes, assim como reduzindo os custos dos tratamentos.

Palavras-chave: *Amanita phalloides;* α-amanitin; ARN polimerase II; polimixina B.

OUTLINE OF THE THESIS

OUTLINE OF THE THESIS

The thesis is organized in 5 chapters.

Chapter I is the general introduction to contextualize the actual state of art of the key topics within the thesis. The general introduction section has a focused approach covering aspects of the clinical features of amatoxins poisoning, mechanisms of toxicity, putative treatments and their relevance to the treatment of human poisonings.

Chapter II comprises the aims of the thesis and explains how these articulate with the subsequent experimental results presented.

Chapter III contains the main studies performed, including materials, methods, results and discussion, which are presented in the form of published manuscripts or manuscripts under submission in peer-reviewed journals. For each study, information concerning the journal (upon acceptance or publication) and co-authors is provided.

Chapter IV includes a general discussion and main conclusions of the thesis, highlighting the most relevant achievements and also the future work perspectives in the field.

Chapter V includes the references used in chapter I and IV.

INDEX

TABLE OF CONTENTS

LIST OF FIGURES

LIST OF TABLES

ABBREVIATIONS

LIST OF ABBREVIATIONS

ALT	Alanine aminotransferase
AST	Aspartate aminotransferase
CIAV	Antipoison information center (*Centro de Informação Antivenenos)*
DAD	Diode-array
EC	Electrochemical
GC-MS	Gas chromatography-mass spectrometry
GI	Gastrointestinal
GSH	Reduced glutathione
HPLC	High-performance liquid chromatography
i.p.	Intraperitoneal
LC	Liquid chromatography
LD_{50}	Lethal dose, 50%
LDH	Lactate dehydrogenase
MARS	Molecular adsorbent recirculating system
MD	Molecular dynamics
mm-GBSA	Molecular mechanics/generalized Born surface area
mRNA	Messenger RNA
MTT	3-(4,5-Dimethylthiazol-2-yl)-2,5-Diphenyltetrazolium bromide
NF-κB	Nuclear factor kappa-light-chain-enhancer of activated B cells
OATP	Organic anion-transporting octapeptide
RNA	Ribonucleic acid
RNAP II	RNA polymerase II
ROS	Reactive oxygen species
SOD	Superoxide dismutase
TNF-α	Tumor necrosis factor alpha

CHAPTER I

INTRODUCTION

1. GENERAL ASPECTS

In the past few decades, mushrooms have become popular in the human diet as a result of its exquisite taste and texture, protein content, and an expanding body of scientific research supporting their health benefits (1). The increased public demand for wild edible mushrooms contributes to an increasing interest in their picking and consumption (2), which enhanced the risk of intoxications by toxic mushrooms (3). Despite warnings on the risks, collectors may confuse edible with toxic mushrooms, due to misidentification based on morphological characteristics. Toxic mushrooms can be grouped based on their toxic components: cyclopeptides, gyromitrin, muscarine coprine, isoxazoles, orellanine, psilocybin and gastrointestinal irritants (4). From these, cyclopeptides-containing mushrooms are the most toxic species throughout the world, being responsible for 90-95% of human fatalities (4). The main toxic agents are amatoxins that are present in three genera: Amanita (mainly *A. phalloides*, *A.virosa* and *A.verna*); Lepiota (the most frequently reported is *L. brunneoincarnata*) and Galerina (the most common being *G. marginata*) (Table I) (5). Among these species, *A. phalloides* is responsible for the majority of fatal cases due to mushroom poisoning (6-9). Amatoxin poisoning usually has a bad prognosis due to the risk of death from liver failure. It was estimated that the mortality incidence after *A. phalloides* poisoning ranges at about 10-30% (5, 10, 11). Survival depends on the degree of hepatic destruction, the ability of the remaining liver cells to regenerate, and the management of complications that may develop during the intoxication course (12). Liver transplantation has significantly improved the survival in *A. phalloides* poisoned patients and remains the cornerstone of treatment in selected patients with fulminant hepatic failure (13, 14). However, organ transplant services totally depend on available organ donation, which is not always easy and is a costly and risky procedure.

Accurate estimates of worldwide poison by amatoxins-containing mushrooms are difficult to establish due to lack of case reporting in hospital emergency rooms. In Portugal there is only one retrospective analysis of 93 cases of mushroom poisonings admitted in ten Portuguese hospitals between 1990 and 2008. Of those poisonings 63.4% were attributed to amatoxins-containing mushrooms, 11.8% having a fatal outcome (15). In USA, a total of 6600 mushroom intoxications were reported to the national poison data system of the American association of poison control centers in 2012 (16). Among these cases, 82.7% were attributed to unknown mushroom types while cyclopeptides-containing mushrooms represented 44 cases (4 patients died) (16). A retrospective case study concerning the prevalence and the circumstances of exposure to mushrooms reported to the Swiss toxicological information centre between January 1995 and December 2009

reported a total of 32 confirmed cases of amatoxins poisoning, 5 with a fatal outcome (17). A retrospective study of all amatoxin poisoning cases recorded over 15 years (1988 to 2002) in the Toxicological Unit of Careggi General Hospital (Florence University), reported 111 intoxications by amatoxins-containing mushrooms (2 patients died) (18), while available clinical French data reports 45 patients treated (1984–1989) with an overall mortality of 17.8% (19).

From the above information it is clear that amatoxins poisoning has emerged as a serious public health problem worldwide.

This introduction aims to provide the state of the art concerning the mechanisms of toxicity, patterns of clinical presentation and management of amatoxins poisoning, focusing on the efficacy and limitations of antidotes most commonly used.

Table 1. Amatoxin-containing mushroom species from the genera *Amanita*, *Galerin*a and *Lepiota*

***Amanita* sp.**	***Galerina* sp.**	***Lepiota* sp.**
A. phalloides	*G. badipes*	*L. brunneoincarnata*
A. bisporigera	*G. beinrothii*	*L. brunneolilacea*
A. decipiens	*G. fasciculata*	*L. castanea*
A. hygroscopica	*G. helvoliceps*	*L. clypeolaria*
A. ocreata	*G. marginata*	*L. clypeolarioides*
A. suballiacea	*G. sulciceps*	*L. felina*
A. tenuifolia	*G. unicolor*	*L. fulvella*
A. verna	*G. venenata*	*L. fuscovinacea*
A. virosa		*L. griseovirens*
		L. heimii
		L. helveoloides
		L. kuehneri
		L. langei
		L. lilacea
		L. locanensis

2. *AMANITA PHALLOIDES*

2.1. Biology

Amatoxins are present in several Basidiomycota species belonging to three genera, i.e. *Amanita, Galerina,* and *Lepiota* (20-22). Table I lists the main amatoxin-containing species (5). As case reports of fatalities following consumption of amatoxin-containing mushrooms are mainly associated with *A. phalloides* (20), this species will be the main focus of the present paper.

The smooth moist cap of *A. phalloides* is greenish yellow, darker in the center and faintly streaked radially. The cap is 6-12.5 cm across and easily peeled. The stalk is smooth, white and 6-12.5 cm high. There is an irregular ring near the top of the stalk and a bulbous cup at the base. The fruiting body emanates a sweetish and not unpleasant smell. Its taste is pleasant, according to the survivors after intoxication (7). *A. phalloides* is distinguished from other species like *Volvariella volvacea* by their irregular ring near the top of the stalk, the bulbous cup at the base and white gills under the cap that are not attached to the stem. The morphology of the bulbous cup has been an important feature to distinguish *Amanita* from other resembling genera. However, inexperienced collectors break the specimen off at the stem destroying or neglecting some of these characteristics, which puts the consumers in danger of intoxication (23). Moreover, the above-mentioned characteristics do not exclude the possibility of amatoxins ingestion because other non-*Amanita* containing-amatoxins species exist (23). In fact, mushroom species have variable appearances at different times of year and at different locations, depending on weather, soil, and time of harvest, which makes more challenging the correct mushroom identification.

2.2. Habitat and distribution

Amanita phalloides is the predominant European poisonous mushroom, particularly in Central and Occidental Europe (20). Several cases of A. phalloides poisoning have also been reported in northeastern United States (24), Central and South America, Asia (4), Australia (25) and Africa (26). This species is an ectomycorrhizal fungus that forms symbiotic relationships with a variety of tree species, such as beech, oak, chestnut and pine. The best seasons of the year for *A. phalloides* fructification are spring, late summer, and autumn (7), and therefore the majority of intoxication cases appear in those seasons.

2.3. Main toxins and most poisonous parts of *Amanita phalloides*

Amanita phalloides contains three classes of cyclic peptide toxins, which can be grouped into amatoxins, phallotoxins and virotoxins. All groups of toxins contain a tryptophan residue substituted at position 2 of the indol ring by a sulfur atom (9) (Figure 1,2 and 3). They have distinct toxicological profile: amatoxins are highly toxic [intraperitoneal lethal dose, 50% (LD_{50}) 0.4-0.8 mg/kg, in the white mouse] causing death within 2-8 days, whereas phallotoxins and virotoxins are less toxic (intraperitoneal LD_{50} 1-20 mg/kg, in the white mouse) but act quickly, causing death within 2-5 hours (9).

Several studies investigated the content and distribution of the main toxins in different carpophore tissues and in several development stages of *A. phalloides* (27-29). There is an unequal distribution of the toxins throughout the carpophore. The highest amatoxins content was found in the ring, gills and cap, while the volva was the richest in phallotoxins levels (29). The collection site and the age of the collected species affect the toxin composition of the carpophore elements (27, 29). The collection site (mainly soil characteristics) determines toxins' composition of each mushroom, mostly the predominance of either acidic or neutral phallotoxins (27). Regarding the maturation state, the content of amatoxins is relatively high during the early development stages (button, button with broken outer veil, and pileus revealed from outer veil) and decreases in the mature (completely developed fruit body with convex cap) and old (wilted fruit body with reflexed cap) stages (30).

2.4. Phallotoxins

Phallotoxins are bicyclic heptapeptides, first isolated from *A. phalloides (31)* and formed by at least seven different compounds: phalloidin, phalloin, prophallin, phallisin, phallacin, phallacidin, and phallisacin (Figure 1) (9). The *in vitro* action of phallotoxins has been thoroughly characterized (32-35). Phallotoxins bind to F-actin, which stabilizes the actin filaments and prevents microfilaments depolymerization, disturbing the correct function of the cytoskeleton (35). They are only toxic to mammals if parentally administered since phallotoxins are not absorbed through the gastrointestinal tract (36). The LD_{50} values of phallotoxins for white mouse are listed in Table II. All phallotoxins have similar intraperitoneal LD_{50} (ranging from 1.5 to 4.5 mg/kg), except prophalloin, which appears to be less toxic (>20 mg/kg). The major *in vivo* toxic effect produced by intraperitoneal administration of phallotoxin occurs in the liver (35).

Since phallotoxins are not orally absorbed the overall human intoxication features by *A. phalloides* are not attributed to this class of toxins.

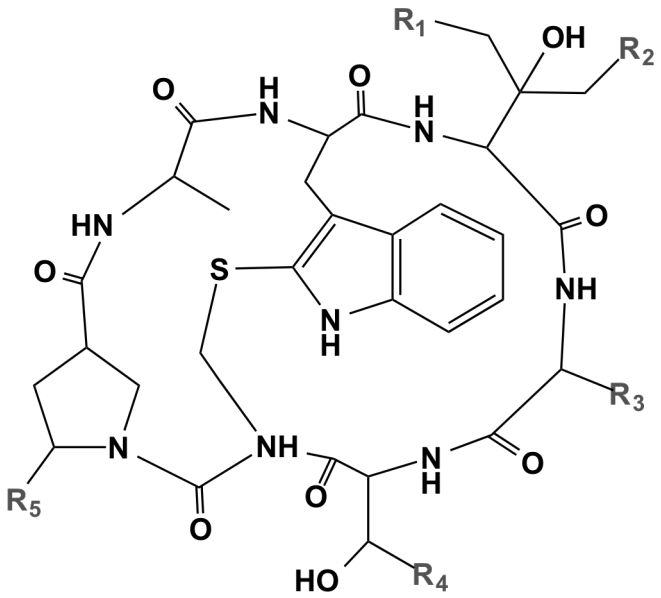

	R1	R2	R3	R4	R5
Phalloidin	OH	H	CH_3	CH_3	OH
Phalloin	H	H	CH_3	CH_3	OH
Prophallin	H	H	CH_3	CH_3	H
Phallisin	OH	OH	CH_3	CH_3	OH
Phallacin	H	H	$CH(CH_3)_2$	COOH	OH
Phallacidin	OH	H	$CH(CH_3)_2$	COOH	OH
Phallisacin	OH	OH	$CH(CH_3)_2$	COOH	OH

Figure 1. Chemical structure of phallotoxins

2.5. Virotoxins

Virotoxins are monocyclic peptides formed by at least five different compounds: alaviroidin, viroisin, deoxoviroisin, viroidin, and deoxoviroidin (Figure 2) (9). The structure and biological activity of virotoxins are similar to that of phallotoxins, thus suggesting that virotoxins are biosynthetically derived from phallotoxins or share common precursor pathways (37, 38). As with phallotoxins, virotoxins are not considered to have significant toxic effects after oral exposure. At molecular level, like phallotoxins, they interact with actin, stabilizing the bonds between actin monomers, which prevent microfilaments depolymerization. However, the ultraviolet-spectra of interaction between actin and virotoxins is different from that of actin-phallotoxins, suggesting a different molecular interaction (39).

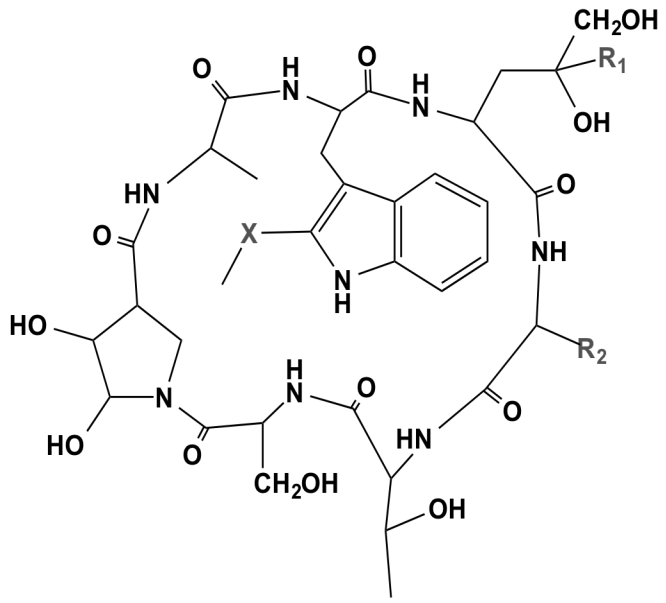

	X	R1	R2
Viroidin	SO_2	CH_3	$CH(CH_3)_2$
Deoxoviroidin	SO	CH_3	$CH(CH_3)_2$
Alaviroidin	SO_2	CH_3	CH_3
Viroisin	SO_2	CH_2OH	$CH(CH_3)_2$
Deoxoviroisin	SO	CH_2OH	$CH(CH_3)_2$

Figure 2. Chemical structure of virotoxins

Virotoxins have a more flexible structure as compared with phallotoxins and the presence of two additional hydroxyl groups may provide different reactivity (Figure 2) (40, 41). The intraperitoneal LD_{50} of virotoxins in mice ranges from 1.0 to 5.1 mg/kg (Table II) and their main toxicological feature is hemorrhagic hepatic necrosis caused by an interaction of the virotoxins with outer surface of the hepatocyte through unknown mechanism (42). At this point, the role of virotoxins in human toxicity remains unclear, although due to its poor oral absorption, little clinical importance is given to this class of toxins.

2.6. Amatoxins

Amatoxins have been identified as bicyclic octapeptides with molecular weight of around 900 g/mol, formed by at least nine different compounds: α-amanitin, β-amanitin, γ-amanitin, ε-amanitin, amanin, amaninamide, amanullin, amanullinic acid and proamanullin (Figure 3) (9). The intraperitoneal LD_{50} of amatoxins in mice ranges from 0.3 to 20 mg/kg (Table II). Amatoxins only differ by the number of hydroxyl groups and by an amide carboxyl exchange (Figure 3) (9). These toxins have great heat stability and this property combined with their solubility in water make them exceptionally toxic as they are not destroyed by cooking or drying (36). In addition, amatoxins are resistant to enzyme and acid degradation, and therefore when ingested they will not be inactivated in the gastrointestinal tract (36). A fatal case was reported after consuming *A. phalloides* frozen during 7-8 months, thus demonstrating that these compounds also resist to freeze/thawing processes (43). Additionally, amatoxins decompose very slowly when stored in open, aqueous solutions or following prolonged exposure to sun or neon light (20).

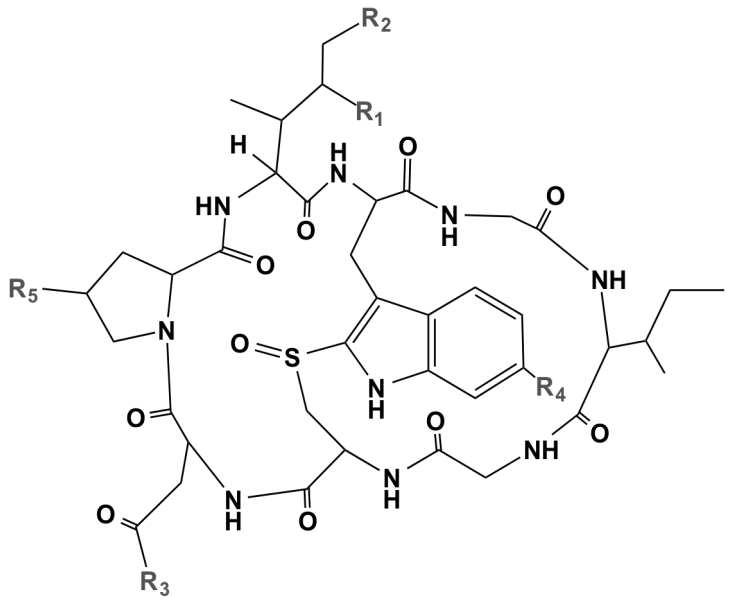

	R1	R2	R3	R4	R5
α-amanitin	CH_2OH	OH	NH_2	OH	OH
β-amanitin	CH_2OH	OH	OH	OH	OH
γ-amanitin	CH_3	OH	NH_2	OH	OH
ε-amanitin	CH_3	OH	OH	OH	OH
Amanin	CH_2OH	OH	OH	H	OH
Amanin amide	CH_2OH	OH	NH_2	H	OH
Amanullin	CH_3	H	NH_2	OH	OH
Amanullic acid	CH_3	H	OH	OH	OH
Proamanullin	CH_3	H	NH_2	OH	H

Figure 3. Chemical structure of amatoxins

Table 2. LD_{50} values for amatoxins, phallotoxins, and virotoxins in different species and administration routes

Toxin	Mice[a]	Rat[a]	Dog[a]	Human[a]	Administration route	Ref.
Amatoxins						
	0.3-0.6	4.0			Intraperitoneal	(36)
α-amanitin	0.002	0.01			Intracerebroventricular	(36)
			0.1		Intravenous	(36)
				0.1	Oral	(9)
β-amanitin	0.5				Intraperitoneal	(44)
γ-amanitin	0.2-0.5				Intraperitoneal	(44)
ε-amanitin	0.3-0.6				Intraperitoneal	(44)
Amanin	0.5				Intraperitoneal	(44)
Amanin amide	0.5				Intraperitoneal	(44)
Amanullin	> 20				Intraperitoneal	(44)
Amanullinic acid	> 20				Intraperitoneal	(44)
Proamanullin	> 20				Intraperitoneal	(44)
Phallotoxins						
Phalloin	1.5				Intraperitoneal	(44)
Phalloidin	2				Intraperitoneal	(44)
Phallisin	2				Intraperitoneal	(44)
Prophalloin	> 20				Intraperitoneal	(44)
Phallacin	1.5				Intraperitoneal	(44)
Phallacidin	1.5				Intraperitoneal	(44)
Phallisacin	4.5				Intraperitoneal	(44)
Virotoxins						
Alaviroidin	3.7				Intraperitoneal	(42)
Viroisin	1.68				Intraperitoneal	(42)
Deoxoviroisin	3.35				Intraperitoneal	(42)
Viroidin	1.0				Intraperitoneal	(42)
Deoxoviroisin	5.1				Intraperitoneal	(42)

2.6.1. Toxicokinetics of amatoxins

The toxicokinetics of α-amanitin has been studied in animals and through data obtained in reports of human poisoning by amatoxins (19, 45). Amatoxins are readily absorbed from the human gastrointestinal tract and can be detected radioimmunologically in the urine as early as 90-120 minutes after ingestion (46). Amatoxins do not bind to albumin (45) being rapidly eliminated from the blood and distributed to liver and kidney within 48 hours (19). After intravenous administration in dogs, the plasma half-life of amatoxins was shown to be short, ranging from 26.7 to 49.6 minutes and were not detectable in plasma after 4-6 hours. The total body clearance was between 2.7 and 6.2 ml/min/kg (45).

The liver is the primary target organ of toxicity of amatoxins, and hepatocellular effects represent the most lethal and the least treatable manifestation of toxicity (4). Amatoxins accumulate in the liver upon uptake via OATP located in the sinusoidal membrane of hepatocytes (Figure 4). Letschert *et al.* (2006) identified OATP1B3 as the main human uptake transporter for amatoxins. Amatoxins were analyzed in the liver following 2 fatal intoxications and in the liver of 2 patients who underwent liver transplantation, showing that high levels of amatoxins levels (α-amanitin ranged from 0 to19 ng/g; β-amanitin ranged from 0 to 3298 ng/g) may be found up to 9 to 22 days post ingestion (19).

Amatoxins do not undergo metabolism and they are excreted in large quantities in the urine during the first days following ingestion, with maximal excretion occurring in the first 72 hours (19). A very small amount can be eliminated in bile and may be reabsorbed via the enteropatic circulation, which prolongs the body burden of these toxins (45). Intestinal elimination also seems to occur. In a human intoxication report (19) 6.3 mg of α-amanitin was eliminated in the faces over a period of 24 hours; this quantity is believed to be lethal in an adult.

Possibly due to the preferential elimination route through the kidney, nephrotoxicity has also been reported (47). The concentration found in the kidney has been shown to be 6 to 90 times higher than in the liver (19). Therefore, although classically amatoxins are considered hepatic toxins, putative renal failure has to be evaluated.

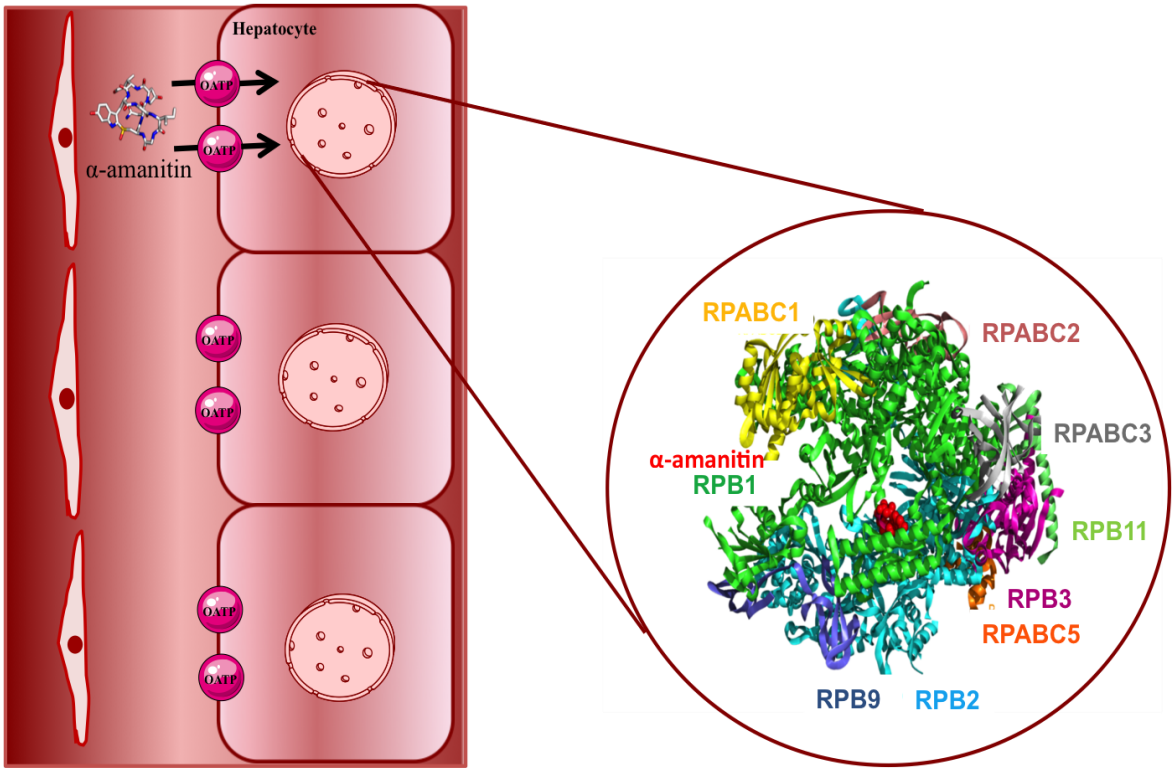

Figure 4. Simplified model of α-amanitin transport and main toxic mechanism in hepatocytes. α-Amanitin accumulation occurs in the liver upon uptake via an organic anion-transporting octapeptide (OATP1B3) located in the sinusoidal membrane of hepatocytes. Once in the hepatocyte, α-amanitin binds to RNA polymerase II causing inhibition of its activity. The α-amanitin binding site is located in the interface of Rpb1and Rpb2 subunits.

2.6.2. Clinical toxicology

The symptomatology of amatoxins poisoning can extend from a simple gastroenterological disorder to death. Signs and symptoms of α-amanitin poisoning are mainly attributable to the accumulation of α-amanitin in the liver and kidney (47).

Three distinct phases of the *A. phalloides* toxic syndrome have been established in the literature: 1) gastrointestinal phase, 2) latent period and 3) the hepatorenal phase (4).

The first stage of *A. phalloides* syndrome occurs abruptly, 6 to 24 hours after ingestion, and is characterized by nausea, vomiting, diarrhea (occasionally bloody), abdominal pain, and hematuria (48). This phase usually lasts about 12-36 hours. Fever, tachycardia, metabolic disorders like hypoglycemia, dehydration, and electrolyte imbalance may occur during this phase (20).

The latent period is characterized by absence of symptoms, whilst progressive deterioration of hepatic and renal function is occurring (48). Hepatic lesions are accompanied by increased serum concentration of aspartate aminotransferase (AST), alanine aminotransferase (ALT) and lactate dehydrogenase (LDH) (49). The blood coagulation is also severely disturbed, which may give rise to internal bleeding (50).

The pathological hallmark of amatoxin poisoning is the development of liver necrosis and this characterizes the hepatorenal phase. The patients progressively lose kidney and liver functions and may develop jaundice, hypoglycemia, oliguria, delirium and confusion (48). This phase culminates in rapid deterioration of central nervous system, severe hemorrhagic manifestations, renal and hepatic failure, which corresponds to a bad prognosis (7). About 20-79% of the intoxicated patients develop chronic liver disease (51).

2.6.3. Mechanism of toxicity induced by amatoxins

There are significant inter and intraspecies variations, concerning the concentration of amatoxins in mushrooms. Therefore, an accurate prediction of toxicity based on the amount of mushrooms consumed is difficult (20). The lethal dose of amatoxins in humans has been estimated (from accidental intoxications) to be about 0.1 mg/kg body weight (Table II), or even lower, and this amount may be present in a single mushroom (4).

Several toxicity mechanisms have been attributed to amatoxins. The main mechanism seems to be their known ability to non-covalently bind and inhibit RNA polymerase II (RNAP II) in the nucleus (52) (Figure 5). Many experimental studies have been conducted to get a better understanding of the interaction with RNAP II (53-55). Cochet-Meilhac and Chambon carried out a kinetic study to evaluate the interaction of amatoxins with RNAP II (53). The authors used purified calf thymus RNAP II and observed that the equilibrium association constant is high, in the order of 10^8-10^{10} (53). Bushnell *et al.* obtained the first X-ray elucidating the RNAP II/ α-amanitin interactions. In this structure, the α-amanitin binding site was located in the interface of subunits Rpb1 and Rpb2 (56). Moreover, the X-ray structure allowed to partially elucidate the key molecular contacts that contribute to RNAP II inhibition. RNAP II residues interacting with α-amanitin are located entirely in the bridge helix (56). In particular, α-amanitin binds directly to the bridge helix residue Glu822, through a hydrogen bond, and indirectly to the bridge helix residue His816 (Figure 5) (56).

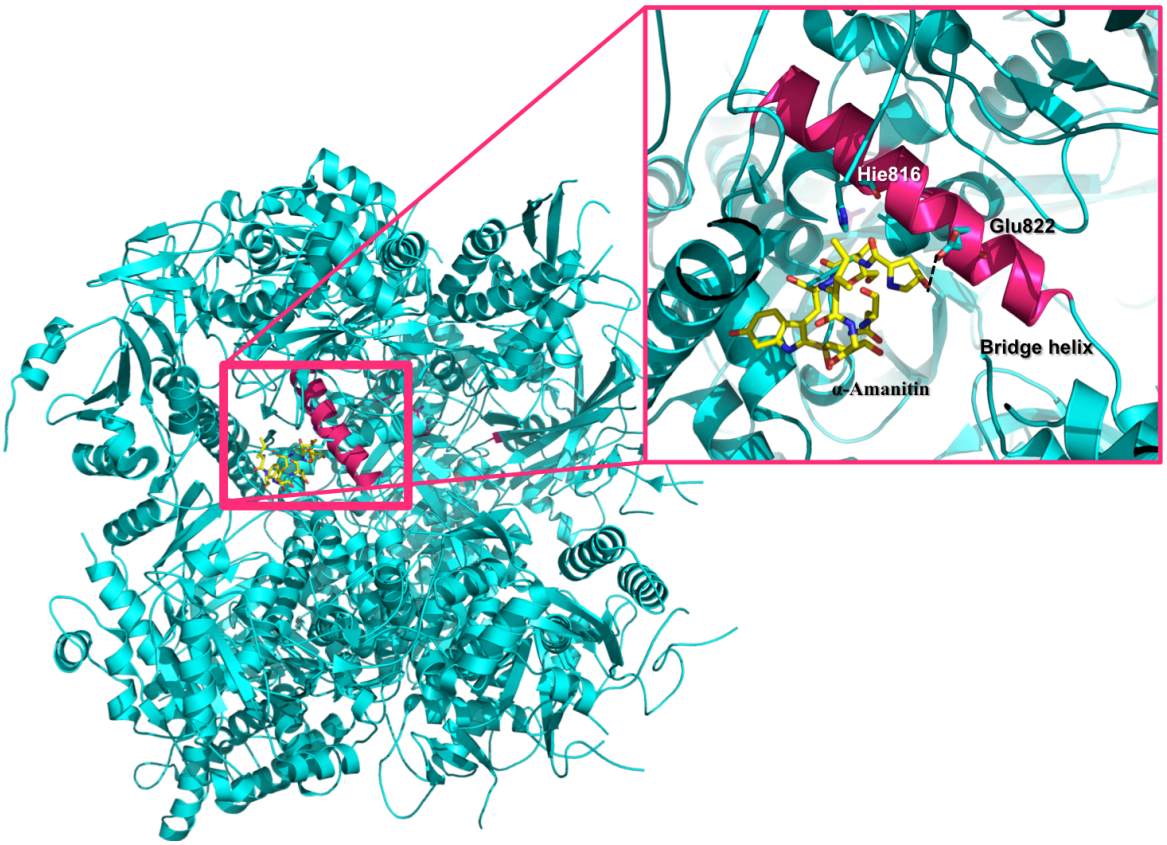

Figure 5. Crystal structure of 10 subunit RNA polymerase II in complex with α-amanitin. Crystal structure elucidates some of the key atomic contacts that contribute to RNA polymerase II inhibition. RNA polymerase II residues interacting with α-amanitin are located entirely in the bridge helix (magenta). α-Amanitin binds directly through a hydrogen bond with bridge helix residue Glu822 and indirectly with bridge helix residue His816. The α-amanitin and residues Glu822 and His816 are in licorice representation.

However, it has been also proposed that α-amanitin inhibits RNAP II by direct interference with the trigger loop (structural element that makes direct substrate contacts and promotes nucleotide addition) (57) therefore preventing the conformational change of RNAP II, inhibiting the deoxyribonucleic acid (DNA) elongation process (58).

The decline of levels mRNA leads to the decrease of protein synthesis and, ultimately, to cell death (52). Moreover, Nguyen *et al.* (1996) suggested that the binding of α-amanitin to RNAP II results in degradation of Rpb1 subunit. The authors have found, in mice fibroblasts, that α-amanitin promotes the degradation of the Rpb1 subunit, resulting in its irreversible inhibition (54). The characterization of this mechanism needs further investigation.

In vitro studies have shown that apoptosis may play an important role in α-amanitin-induced severe liver injury as observed in dog primary hepatocytes (59) and in human hepatocyte cultures (60, 61). The exposure of hepatocytes to α-amanitin (2 μM) resulted in p53- and caspase-3-dependent apoptosis (Figure 6) (Magdalan et al. 2011). In normal neonatal human diploid fibroblasts, α-amanitin (2 μg/mL) treatment for 24 hours resulted in a marked induction of p53. The concentration required for induction of p53 was correlated with the concentration required to inhibit mRNA synthesis, suggesting a link between these two effects (62). To further evaluate the role of p53 in transcription inhibition-mediated cell death, p53 knock-out HTC116 cells and wild-type cells were treated with α-amanitin (10 μg/ml) for 24 hours and the extent of apoptosis was evaluated. The results showed that the knock-out p53 cells were less sensitive to death induced by α-amanitin, corroborating that p53 plays an important role in α-amanitin-induced toxicity. A stress signal is elicited by α-amanitin, which leads to the translocation of cytoplasmic p53 to mitochondria resulting in alteration of mitochondrial membrane permeability through formation of p53 complexes with protective proteins (Bcl-x_L and Bcl-2) (Figure 6). The complexes formation results in the release of cytochrome *c* into the cytosol and the prosecution of the intrinsic apoptotic pathway (Figure 6) (63).These results were further corroborated in *in vivo* assays. Knockout p53/BAK mice showed marked resistance towards α-amanitin (5 μg/g)-induced liver damage, while wild-type mice in the same conditions undergo organ destruction (64). An interaction between p53 and mitochondrial BAK seems to be important for p53's mitochondrial role in the induction of apoptosis (64). Other mechanisms might be involved in α-amanitin-induced toxicity. It has been suggested that TNF-α exacerbates α-amanitin-induced hepatotoxicity *in vivo* (Figure 6) (65). After *in vivo* administration of a high dose of α-amanitin, hepatic TNF-mRNA was increased and hepatocytes underwent apoptosis, whereas in mice treated with anti-TNF antibodies, liver injury caused by α-amanitin was prevented (65). In addition, transgenic mice lacking the 55 kDA TNF-α receptor seem to be relatively resistant to α-amanitin toxicity (65). Therefore hepatocyte apoptosis may result from a synergistic action of α-amanitin with TNF-α (Figure 6) (65). However, the mechanism of such synergistic effects remains unclear at this point and the dependence of α-amanitin toxicity on the presence of TNF-α was not confirmed in another study using rat hepatocyte cultures (66). Thus, TNF-α may not be indispensable for the development of cytotoxicity by α-amanitin but exacerbates it. Actually, TNF-α co-treatment significantly increased lipid peroxidation caused by α-amanitin and this effect was prevented by silybin, indicating the possible involvement of reactive oxygen species (ROS) (66). These results suggest that TNF-toxicity is associated with ROS production (66). In fact, oxidative stress has also been postulated to be important in the development of severe hepatotoxicity in other studies (Figure 6)

(67, 68). *In vivo,* hepatic accumulation of α-amanitin leads to increase of superoxide dismutase (SOD) activity and malondialdehyde products, and also results in the decrease of catalase activity (Figure 6) (68). Lipid peroxidation may contribute to severe hepatotoxicity with massive necrosis (68). Zheleva (2013), using the electron paramagnetic resonance spin trapping technique, studied the *in vitro* and *in vivo* oxidation of α-amanitin. During *in vitro* oxidation, α-amanitin can form unstable phenoxyl radicals by itself. Using the same technique, these authors detected the production of reactive species in mice kidney subjected to an intraperitoneal administration of 1 mg/kg of α-amanitin. Thus, α-amanitin is able to form phenoxyl free radicals that might be involved in generation of ROS (Figure 6) (67). More investigations are needed to completely clarify the pathophysiology of ROS in the α-amanitin-induced toxicity, as it has been a scarcely studied subject.

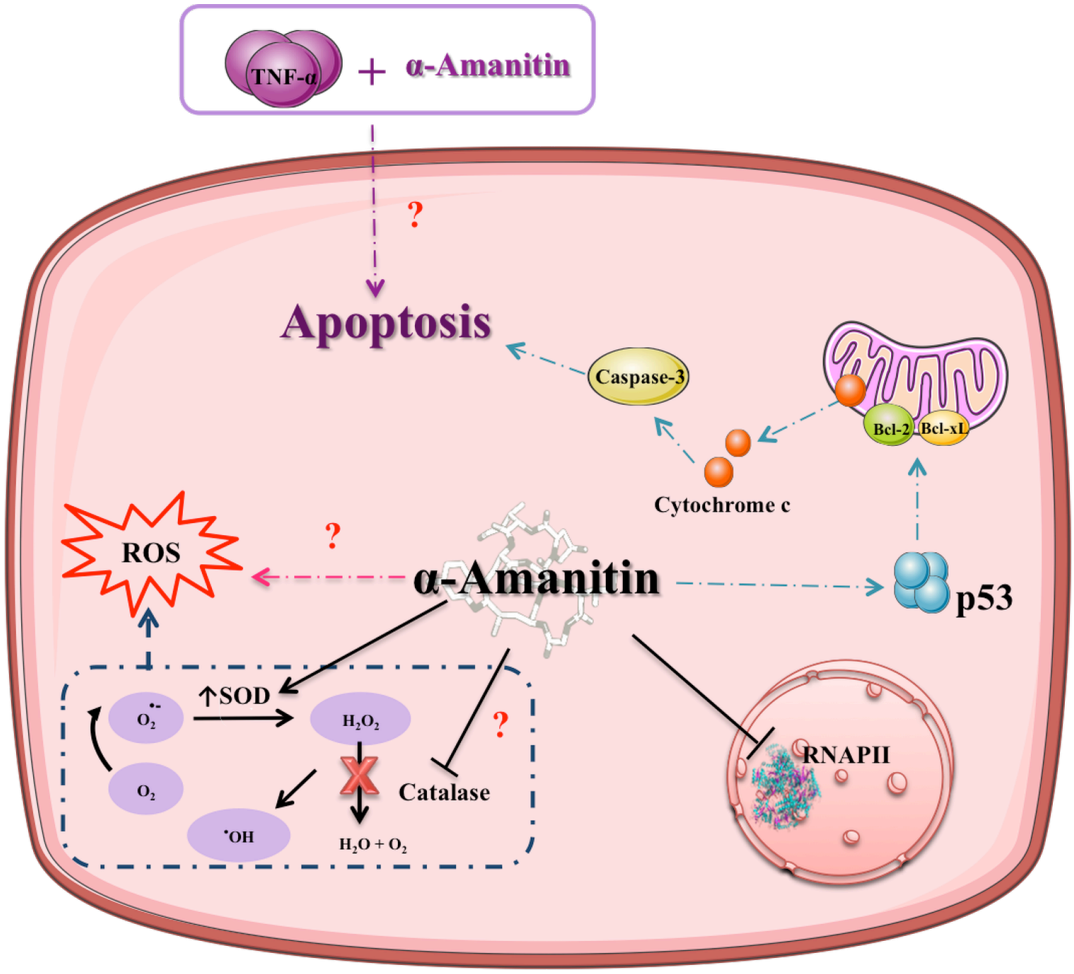

Figure 6. Signaling pathways involved in α-amanitin-induced toxicity. The main toxicity mechanism of α-amanitin is inhibition of RNA polymerase II. Other mechanisms have been suggested and include the formation of reactive oxygen species (ROS) leading to oxidative stress related damage. Generation of ROS may also be induced by increase of

superoxide dismutase (SOD) activity and inhibition of catalase activity. Amatoxins may act synergistically with tumor necrosis factor (TNF), to induce apoptosis, though the underlying mechanisms are not yet known. Amatoxins-induced apoptosis may also be caused by the translocation of p53 to the mitochondria causing alteration of mitochondrial membrane permeability through formation of complexes with protective proteins (Bcl-xL and Bcl-2). These changes result in the release of cytochrome c into the cytosol and activation of the intrisic pathway of apoptosis. Question marks indicate that the mechanism remains unknown.

2.6.4. Pathophysiology of intoxications by amatoxins

2.6.4.1. Liver

As previously referred, the main pathophysiologic feature of intoxication by amatoxins is liver failure. Histopathological findings in liver biopsy specimens have shown massive centrilobular hepatic necrosis (24). Acute toxic hepatitis may develop rapidly, then reaching the state of liver insufficiency and coma (47). Five autopsies were performed on patients fatally poisoned with *A. phalloides* (69). Pathological autopsies revealed intensely yellow liver of creamy consistency and diffuse subcapsular hemorrhaging. The histological examination confirmed stasis in all organs, including liver with diffuse hemorrhagic foci. The liver showed typical features of massive centrilobular necrosis and vacuolar degeneration of hepatocytes (69). Pathological examinations were also performed in two explanted liver after amatoxins poisoning. The cut surface of the explanted livers was hemorrhagic and had a nutmeg appearance. Centrilobular massive hemorrhagic necrosis and fatty degeneration areas were also observed (70).

Liver failure can lead to disseminated intravascular coagulation due to reduced clearance of activated clotting factors, release of pro-coagulants from damaged hepatocytes and reduced synthesis of coagulation inhibitors, contributing to multi-organ failure (71, 72). Consumption and subsequent exhaustion of coagulation proteins and platelets (from ongoing activation of coagulation) may culminate in severe bleeding (71, 72).

2.6.4.2. Kidney

Nephrotoxicity after *A. phalloides* poisoning is also frequent. Patients can develop acute tubular necrosis with kidney failure (47). *Post*-mortem examinations of patients

dying from amatoxin poisoning revealed dark red kidneys with extravasation of blood, especially in the cortical region. Stasis with diffuse hemorrhagic foci, acute tubular necrosis, and massive quantities of hyaline casts in the tubules were also found in patients that died after *A. phalloides* intoxication (69). Fanconi-type renal tubular acidosis associated with *A. phalloides* ingestion has also been reported (20).

2.6.4.3. Central nervous system

Neurologic manifestations, either primarily due to accumulation of ammonia or secondary to multi-organ failure combined with hypotension, may develop in response to abnormal liver and kidney functions (20). Ammonia, a by-product of protein metabolism, is neurotoxic at high concentrations (73). The liver transforms ammonia to urea, which is excreted through the kidneys. Amatoxin-intoxicated patients with continued loss of hepatocellular function are not able to transform ammonia to urea. Blood ammonia levels rise and is delivered to the brain causing encephalopathy, disorientation, confusion, lethargy, somnolence, vertigo, convulsions, and coma (7).

2.6.5. Treatment and management of intoxications by amatoxins

General treatment measures applied to amatoxins' poisoned patients include: stabilization of vital functions, intensive and supportive measures, prevention of the poison absorption, use of putative antidotes, enhanced elimination of the poison and prevention of complications (8). Some of these measures have shown some degree of success, while others show negligible efficacy (Table III). At this point, it can be said that a lot of research work still needs to be done to achieve a satisfactory therapeutic efficacy against amatoxin intoxications.

2.6.5.1. Dealing with intoxication cases

On a putative case of amatoxins intoxication the initial step is to take the clinical history of the patient and perform stabilizing measures, if required. Fluid and electrolyte imbalance may occur in the gastrointestinal phase or result from measures undertaken to eliminate the amatoxins. Intravenous fluids may have to be given for extra-fluid and electrolyte replacement with careful clinical chemistry monitoring (49). The effects of amatoxins on protein synthesis and the damage on liver cells will cause alteration on coagulation factors (49), therefore optimal treatment includes intravenous vitamin K and

fresh-frozen plasma (6). Liver damage should be assessed promptly as it allows determining how far is the damage caused and the best clinical actions to take. Laboratory evaluation should include liver and kidney function, testing aminotransferases, prothrombin time, blood urea nitrogen, creatinine, ammonia, fibrinogen, bilirubin, complete blood count, electrolyte analysis, amylase, lipase, and urinalysis (74).

All basic information, such as the amount, type (a sample of the ingested mushroom is of outmost importance), time of mushrooms ingested, the first evidence of symptoms, and the symptoms present at the moment of hospitalization are of great value in the first contact with the possible amatoxins' poisoned patient. The time between ingestion and onset of symptoms is critical. Sudden onset of intense gastrointestinal symptoms after a delay of 6-24 hours, following a mushrooms meal, should raise the suspicion of amatoxin poisoning.

2.6.5.1.1.Identification of amatoxins and phallotoxins

If *A. phalloides*-type mushrooms is suspected, gastric content, mushroom samples, and stool specimens, if available, should be analyzed to verify the presence of amatoxins and phallotoxins (48). Several methods can be used for identification and quantification of amatoxins and phallotoxins in specimens of *A. phalloides*. Evaluation of these toxins in mushrooms has been performed using reversed-phase high-performance liquid chromatography (RP-HPLC) (27, 29, 30, 66, 75, 76), capillary electrophoresis coupled to mass spectrometry (MS) (77), liquid chromatography (LC) coupled to MS or to tandem MS (78, 79), and LC electrospray ionization time-of-flight-MS (LC/ESI-TOF-MS) (80). RP-HPLC is the most commonly used method, although the LC-MS method appears to provide the most reliable and sensitive results.

The Meixner test can also be used if a specimen of the ingested mushroom is available for analysis (81). The test is based on an acid-catalyzed (using concentrated hydrochloric acid) reaction of amatoxins with the complex biopolymer lignin to form a blue product. As described by Meixner, the test is run by squeezing the juice from a piece of fresh mushroom tissue onto a piece of newsprint, which contains lignin, allowing the spot to dry, and then applying one drop of concentrated hydrochloric acid. Formation of a blue color indicates a positive test (81). Nevertheless, the efficacy of this test is limited by false positive results. Mushrooms containing hydroxyl-substituted tryptamine compounds such as psilocin or serotonin may also produce a positive Meixner reaction (82), and therefore a positive test result requires further confirmation of the mushroom identity.

A rapid and sensitive method that can be performed in the patient bed side, or within minutes in the hospital structures, would be of outmost value for a better clinical

assessment but it is not available presently. Urine analysis is a vital tool for amatoxin poisoning surveillance, contributing to the management of suspected mushroom poisoning (83). If analysis is performed within 36 hours of ingestion, α-amanitin can be detected in urine. After 36 hours the analysis is unreliable in that a negative result cannot rule out poisoning.(4). There are different methods for urine analysis: radioimmunoassay, Enzyme Linked Immunosorbent Assay (ELISA) and HPLC (20).

2.6.5.1.2. Minimizing absorption, and inactivation in the gastrointestinal tract

After careful consideration of the risks to the intoxicated patient, gastrointestinal (GI) decontamination should be considered based upon the time elapsed from ingestion to time of presentation at the hospital. Several methods of GI decontamination that can be used alone or in combination, include gastric lavage, whole bowel irrigation, administration of activated charcoal, and endoscopic or surgical removal of the ingested poison (84). Whole bowel irrigation has a very limited impact in the treatment of human poisoning, and therefore should not be used routinely in the management of the poisoned patient (84-86). Gastric lavage is most useful if attempted within 1 hour after ingestion of a potentially life threatening poison (87), while it is contraindicated in patients with loss of airway protective reflexes, such as in a patient with a depressed state of consciousness, and in patients who are at risk of hemorrhage or gastrointestinal perforation, as well as in patients that underwent recent surgery or have other medical conditions such as coagulopathy (88). Clinical toxicology database of the United Kingdom national poisons information service (TOXBASE) recommends gastric lavage up to 1 hour after *A. phalloides* ingestion (89).

Activated charcoal effectiveness decreases with increased time elapsed after ingestion, while greatest benefit can be observed within 1 hour after ingestion of the poison (84). The efficacy of activated charcoal was not yet proven in controlled clinical settings towards amatoxins ingestion, but activated charcoal (20-40 g every 3-4 hours) has been administered routinely because it may interrupt the enterohepatic circulation of amatoxins and potentially reduce their toxicity (20). The centre of anti-poisoning information (CIAV) in Portugal and TOXBASE recommend a dose of 50 g every 4 hours (89, 90). If vomiting is troublesome the dose can be reduced to 12.5 g charcoal hourly or 25 g every 2 hours (89). As most patients reach the hospital emergency hours after ingesting the mushrooms, these clinical measures have limited efficacy, although they are undertaken to insure the best clinical treatment available in a life risk situation, even before confirmation of amatoxins poisoning.

2.6.5.1.3. Elimination of absorbed amatoxins

As stated, excretion of amatoxins is mainly urinary; therefore diuresis would potentially increase the renal clearance and could be a potential good therapy for this intoxication. Forced diuresis is recommended, with urine output of 100-200 ml/h for 4-5 days (91). This procedure is also recommended by CIAV and national poisons centre of New Zealand, especially in the first 48 hours after ingestion (90, 92).

Amatoxins are only detected in the plasma at the early phase of poisoning and only for a short period of time. For that reason, removing amatoxins by extracorporal elimination, particularly hemodialysis, hemoperfusion or plasmapheresis was previously considered to have no impact on patient survival (19, 93). Some studies present some evidence demonstrating benefits of molecular adsorbent recirculating system (MARS) in management of *A. phalloides* poisonings (94, 95). However, these findings have not been adequately corroborated, since only few case reports have been published and further evidence is needed. In a recent study, the effectiveness and safety of combined extracorporeal techniques using the fractionated plasma separation and adsorption system, FPSA, Prometheus® 4008H, Fresenius Medical Care, Germany, in poisoned patients with *A. phalloides* was investigated (96). This technique consists on the elimination of protein-bound and water-soluble toxin. Prometheus® seemed to be a promising treatment for *A. phalloides* poisoning preventing the need for liver transplantation. However, such treatment was administered associated to other therapies (silybin and N-acetylcysteine). MARS and Prometheus® are based in the same principle, the extracorporeal elimination of toxins. As α-amanitin is rapidly eliminated from plasma, these techniques may be especially useful if patients are presented to the hospital when the first symptoms appear.

2.6.5.2. Drug therapy

Based on pre-clinical findings, several treatments have been applied in intoxications by amatoxin, namely using hormones (insulin, growth hormone, glucagon), steroids, vitamin C, vitamin E, cimetidine, α-lipoic acid, antibiotics (benzylpenicillin, ceftazidime), N-acetylcystein, and silybin (5). From these, only benzylpenicillin, ceftazidime, N-acetylcystein, and silybin were proven to have some degree of therapeutic efficacy, although the death rate remains extremely high (97) (Table III). Some of the most used procedures that showed some clinical effectiveness are addressed below.

2.6.5.2.1. β-Lactam antibiotics

The most widely used drug in the management of amatoxins poisoning, as a monotherapy or in combination with other agents is benzylpenicillin. One study involving 47 patients poisoned with *A. phalloides* demonstrated that benzylpenicillin combined with supportive measures was an effective treatment in 43 cases (Table III) (98). The effectiveness of benzylpenicillin was, also, evaluated in a retrospective study including 111 patients treated from 1988 to 2002 in the Toxicological Unit of Careggi General Hospital for amatoxins poisoning (18). The administration of benzylpenicillin combined with intensive fluid and supportive therapy, restitution of the altered coagulation factors, multiple-dose activated charcoal, mannitol, dexamethasone and glutathione, resulted in complete recovery of all patients treated within 36 hours after mushroom ingestion (Table III) (18). Two patients admitted to the hospital more than 60 hours after mushroom ingestion died (Table III) (18). On the other hand, benzylpenicillin monotherapy administered to 103 intoxicated patients resulted in an overall mortality of 7.8 % (Table III). Higher overall mortality (22.2 %) was observed in Croatia in a study including 18 patients treated in 1988 (Table III) (5). Taken together, these results evidence that benzylpenicillin has some therapeutic effectiveness, although the high mortality rate (Table III) indicates that this antidote is far from ideal.

In vitro studies using human hepatocytes provided some evidence to support the effectiveness of benzylpenicillin in limiting the cytotoxicity of amatoxins (61, 99). *In vivo* studies, dogs (beagles, weighing 8-15 kg) were given an oral dose of lyophilized *A. phalloides*, which contained 0.14 mg/g of acid phallotoxins, 0.04 mg/g of acid amatoxins, 0.04 mg/g of neutral phallotoxins, and 1.1 mg/g of neutral amatoxins. Benzylpenicillin (1000 mg/kg) was intravenously given at 5 hours after poisoning and silymarin (50 mg/kg) was intravenously given at 5 hours followed by a dose of 30 mg/kg at 24 hours after poisoning. The results showed that benzylpenicillin combined with silymarin may help prevent and treat liver damage, since they reverted the increases of aminotransferases (ALT and AST) and also alkaline phosphates induced by *A. phalloides* (100). However, the effectiveness of benzylpenicillin (intraperitoneal dose of 1 million units/kg/day administered at 4 hours after poisoning) may be species dependent, as it was not found to be effective in limiting hepatic injury in mice (weighed an average of 42.4 g) induced by a single intraperitoneal dose of α-amanitin (0.6 mg/kg) (101). Dog seem to be the model that is closest to human concerning intoxications by amatoxins, since the clinical course and symptoms are almost identical to those seen in humans (45). Moreover, dogs and humans share a great oral bioavailability for amatoxins (45). Despite the scarce oral bioavailability in rodents, the toxic effects of amatoxins are similar to those in humans (102). Most in mice studies use intraperitoneal administration that could

intensify the amatoxins-induced organ damage. In fact, that can explain the lack of efficacy of the antidotes in mice injected with high doses of amatoxins.

Several hypothesis have been proposed to explain the mechanism of benzylpenicillin in amatoxins poisoning. It was previously thought that benzylpenicillin could displace α-amanitin from albumin, allowing better renal elimination, but such hypothesis was later refuted by evidences demonstrating that α-amanitin does not bind to serum albumin (103). The influence of benzylpenicillin on the hepatic uptake of amatoxins has also been studied but remains unclear. Kroncke *et al.* studied amatoxins hepatic transport in membrane vesicles from rat liver using radiolabeled α- and γ-amanitins (104). It was observed that amatoxin membrane transport was not inhibited by benzylpenicillin. However, recent *in vitro* findings, using human hepatocytes, suggest that benzylpenicillin blocks α-amanitin uptake, being a potent inhibitor of OATP1B3 transporter (Letschert et al. 2006). Such putative protective effect requires further experimental *in vivo* confirmation.

Despite the reported efficacy of benzylpenicillin, this antidote has safety issues. The administration of benzylpenicillin may result in high sodium salt concentration in the body, which can disrupt electrolyte balance. In addition, it may cause allergic reactions, granulocytopenia and evoke neurotoxic symptoms in patients with nervous system disease and renal insufficiency (5).

Another β-lactam antibiotic used in the management of *A. phalloides* poisoning is ceftazidime. However, the number of amatoxins poisoning cases treated with ceftazidime was limited (97) and this antidote was always administered in combination with silybin (5), which causes bias to its putative protective effect. Further investigations are needed to better understand the underlying protective mechanism of action of ceftazidime.

The Portuguese poisoning information center recommends a dose of benzylpenicillin of 1 million units/kg/day, by continuous intravenous infusion (90) in amatoxins poisoning. This treatment should be maintained until clinical and laboratory improvement is achieved as observed by serum transaminases levels and prothrombin time. TOXBASE recommends a dose of 0.5 million units/kg/day as a continuous infusion for 2-3 days from the day of ingestion, with close monitoring of renal function (89). However the national poisons centre of New Zealand does not recommend the benzylpenicillin administration (92).

2.6.5.2.2. Silymarin

Silybum marianum ('milk thistle') is currently the most well researched plant used in the treatment of liver diseases. The active constituents of milk thistle are flavonolignans

including silybin, silydianin, and silychristine, collectively known as silymarin. Silybin is the component with the highest antioxidant activity, and 'milk thistle' extracts are usually standardized to contain 70-80% silybin (105). Due to its antioxidant activity, silybin has been applied in the management of amatoxin poisoning and evidence on the effectiveness of silybin in poisoned patients has been reported. Forty-six cases of amatoxins poisoning treated with silybin as monotherapy showed that all patients survived (Table III) (Enjalbert et al, 2002). These results indicate that silybin has some effectiveness in the management of amatoxin poisoning exhibiting low mortality rates (Table III). Silybin seems to be more effective as monotherapy than when combined with benzylpenicillin. In fact, in a recent study based on 1500 documented cases, it was concluded that the overall mortality in intoxicated patients with *A. phalloides* treated with silybin, as Legalon® SIL (silibinin-C-2',3-dihydrogen succinate, disodium salt), is less than 10% in comparison to more than 20% when using benzylpenicillin or a combination of silybin and benzylpenicillin (106).

Cytotoxicity evaluation of cultured human hepatocyte using MTT reduction and LDH leakage was performed at 12, 24 and 48 hours of exposure to α-amanitin (2 μM) and/or silybin. The treatment with silybin showed a strong protective effect against cell damage in α-amanitin-induced toxicity (61).

The protective effects of silymarin on amatoxin poisoning have also been studied in different animal models. Again, species differences were found, as a significant hepatoprotective effect was observed for silybin in α-amanitin-induced liver damage in dogs (107), while no protective effect was observed in mice (101). In both species, the α-amanitin LD_{50} was administered, however different routes of administrations were used. α-Amanitin was administered orally to dogs while in mice it was administered intraperitoneally. It is reasonable to consider that α-amanitin-induced toxicity in mice could be enhanced by intraperitoneal administration and the overall protection induced by silybin failed. Moreover inter-species differences may also exist.

As mentioned above, the postulated protective mechanism of action mediated by silybin is associated to its strong antioxidant activity, which could explain its action against hepatotoxic agents that act through oxidative stress. Silybin and silymarin reduce the free radical load, stimulate the activity of SOD and increase reduced glutathione (GSH) levels (108). Moreover, Pradhan and Girish (2006) suggest that silymarin is able to enter the nucleus and specifically stimulate RNA polymerase I. This increased transcription of ribosomal RNA may counterbalance the inhibition of RNAP II induced by amatoxins (109). Nevertheless, this hypothesis needs further confirmation.

Based on animal studies and limited human data, it seems that silybin has been the most promising molecule to prevent pathophysiological events after amatoxin

intoxications, with a good safety profile. Therefore CIAV and the national poisons centre of New Zealand recommend a intravenously dose of 20-50 mg/kg/day in four divided doses. Treatment should be continued for 48 to 96 hours after mushroom ingestion (90, 92). TOXBASE recommendations for *A. phalloides* poisoning treatment do not include silybin administration (89).

2.6.5.2.3. N-acetylcysteine

N-acetylcysteine has been in medical use for more than 50 years as a mucolytic agent. It is also a well-known treatment for acetaminophen overdose, and related liver damage (110). Due to the clinical similarity between acetaminophen overdose and amatoxins poisoning, leading to hepatic and renal necrosis, N-acetylcysteine has been applied in the management of amatoxins poisoning. This compound is a precursor of GSH and due to its antioxidant and liver protecting effects it is postulated to play a protective role in patients poisoned with *A. phalloides*. N-acetylcysteine, administered to 86 amatoxins poisoned patients showed overall survival of 93.0 % (5) (Table III). A retrospective multidimensional multivariate statistical analysis of 2110 clinical cases of amatoxin poisoning was performed in order to optimize therapeutic decision-making (97). The results of this study showed that N-acetylcysteine has a statistically positive impact on amatoxin poisoning (97). A retrospective study including 40 amatoxins-intoxicated patients was performed in order to investigate the benefits of N-acetylcysteine treatment in addition to the standard treatment that included benzylpenicillin in patients with *A. phalloides* intoxication (111). The mortality rate was lower when N-acetylcysteine was co-administered (4.4% vs 18.7 % in the group that received only benzylpenicillin). Thus, the authors concluded that *A. phalloides* intoxication could be successfully treated with N-acetylcysteine in addition with benzylpenicillin (111). N-acetylcysteine can act at two levels: by direct ROS scavenging and/or restoring hepatic GSH (97). In accordance, a recent *in vitro* study showed that treatment of human hepatocyte cultures with N-acetylcysteine, conferred a strong protective effect against subsequent α-amanitin cytotoxicity (61).

On the other hand, research previously conducted by Schneider *et al.* and Tong *et al.* failed to show any relevant clinical efficacy of N-acetylcysteine in the treatment of *A. phalloides* intoxication in mice (101, 112). Both studies used 1.2 g/kg of N-acetylcysteine administered 4 hours after intraperitoneal administration of α-amanitin (0.6 mg/kg). Efficacy data of N-acetylcysteine administration in α-amanitin-intoxicated dogs are lacking. However it is reasonable to consider that there is no reason to not include N-acetylcysteine in the treatment regimen.

CIAV and TOXBASE protocols for *A. phalloides* poisoning do not include administration of N-acetylcysteine (89, 90), whereas the national poisons centre of New Zealand recommends to administer 150 mg/kg in 200 mL vehicle (5 % dextrose in water) intravenously over 15 minutes followed by 50 mg/kg in 500 mL vehicle over 4 hours followed by 100 mg/kg in 1000 mL vehicle over 16 hours (92).

Table 3. Summary of clinical therapy in amatoxins poisoning

Cases	Years	Country	Drug therapy	Prevention of amatoxins absorption	Elimination of absorbed amatoxins	Liver transplantation	Mortality rate (%)	Ref.
47	1971-1975	Italy	BPC				4.0	(98)
205	1971-1980	6 European countries	BPC+SLB				22.4	(113)
2	1980-1981	Austria	SLB				0.0	(114)
16	1980-1981	Austria	BPC + SLB				6.25	(114)
44	1981	Italy	BPC	AC			9.1	(115)
43	1984-1989	France	BPC+ SLB			2	17.8	(19)
4	1994	New York	BPC	AC			25	(116)
21	1984-1993	Germany	BPC + SLB		PL		4.8	(117)
2	2000	Portugal	BPC+SLB	AC			0.0	(6)
2	2000	Portugal	BPC+SLB	AC	PL	2	0.0	(6)
103	1971-1995	Slovak Republic	BPC		HP, HD		7.8	(5)
18	1988	Croatia	BPC		FD, HD, PL		22.2	(5)
86	1987-1993	Italy	NAC				7.0	(5)

Cases	Years	Country	Drug therapy	Prevention of amatoxins absorption	Elimination of absorbed amatoxins	Liver transplantation	Mortality rate (%)	Ref.
25	1980-1986	Europe	SLB		FD, HP, HD		4.0	(5)
20	1991-1999	Slovak Republic	SLB		FD, HP, HD		0.0	(5)
26	1993	Germany	SLB				0.0	(5)
1	2000-2004	Czech Republic	BPC + SLB	AC	HD		0.0	(118)
2	2000-2004	Czech Republic	BPC + SLB	AC, GL	HP		0.0	(118)
1	2000-2004	Czech Republic	BPC + SLB	AC, GL, FD		1	100	(118)
2	2000-2004	Czech Republic	BPC	FD			0.0	(118)
2	2000-2004	Czech Republic	BPC	GL, AC			0.0	(118)
2	2000-2004	Czech Republic	BPC	GL, AC	HP		0.0	(118)
1	200-2004	Czech Republic	BPC	GL			100	(118)
111	1988-2002	Italy	BPC	AC			1.8	(18)
28	1983-1992	NS	SLB				4.0	(106)
126	1983-1992	NS	SLB + BPC				11.0	(106)
118	1957-2005	NS	SLB				5.1	(106)
77	2008	Turkey	BPC + SLB + NAC	AC, GL	HF	1	2.5	(119)
2	2009	Massachusetts	BPC + SLB + NAC	AC			0.0	(120)
2	1999-2012	Australia	BPC + SLB + NAC	AC			0.0	(121)

Cases	Years	Country	Drug therapy	Prevention of amatoxins absorption	Elimination of absorbed amatoxins	Liver transplantation	Mortality rate (%)	Ref.
2	1999-2012	Australia	BPC + SLB				50	(121)
5	1999-2012	Australia	SLB +NAC	AC			40	(121)
24	2001-2006	Turkey	BPC+NAC	AC, GL	HP		4.4	(111)
16	2001-2006	Turkey	BPC	AC, GL	HP		18.7	(111)

PS: plasmapheresis; HD: hemodialysis, HF: hemofiltration; HP: hemoperfusion, FD: forced diuresis; GL: gastric lavage; AC: activated charcoal; BPC: benzylpenicillin; SLB: silybin; NAC: N-acetylcysteine; NS: not specified.

2.6.5.3. Transplantation

In some cases of *A. phalloides* poisoning, acute liver failure can be developed and a consequent liver transplant is needed to guarantee patients' survival. Acute liver failure is a devastating effect characterized by sudden and severe liver cell dysfunction. This catastrophic illness can rapidly progress to coma and death due to cerebral edema and multi-organ system failure (122). Several criteria to decide the timing of liver transplantation have been proposed, although they are not universally accepted. The most widely used criteria for liver transplantation were developed by The Liver Unit at King's College Hospital, (123). Their prognostic model was based on prothrombin time, age, etiology, time passing between appearance of jaundice and onset of encephalopathy, and bilirubin concentration. These criteria differentiate acetaminophen and non-acetaminophen induced acute liver failure. The King's College Hospital prognostic criteria for non-paracetamol-induced fulminant hepatic failure includes: prothrombin time > 100 s; and any three of the following: age <10 or >40 years; jaundice >7 days before onset of encephalopathy, prothrombin time >50 s and bilirubin >300 μmol/l (123). However the application of King's college criteria for non-acetaminophen induced acute hepatic failure on *A. phalloides* poisoning is limited (O'Grady 2012). Not all variables included in these criteria are useful in predicting a fatal outcome. In a distinct rationale, liver transplantation based on the Clichy criteria complies the combination of decrease in factor V below 30% of normal patients over 30 years or below 20% of normal patients below 30 years and grade 3-4 encephalopathy (124). On the other hand, a retrospective study of 198 amatoxin intoxicated patients showed that prothrombin index < 25% in combination with serum creatinine > 106 μmol/L from day 3 to 10 after *A. phalloides* ingestion is a strong predictor of fatal outcome (11). Ganzert's criteria do not include the evaluation of hepatic

encephalopathy due to imprecise data in the patients' records (11). In order to re-assess the transplantation criteria, Escudie *et al.* (2007) studied 27 *A. phalloides* poisoned patients and the above criteria were compared. Encephalopathy, an absolute prerequisite in Clichy criteria for deciding emergency transplantation, was not fully observed in this study (10). Not all patients with a fatal outcome developed encephalopathy and in those who developed, the mean interval between the onset of encephalopathy and death was very short (10). Regarding to Ganzert's criteria, the prothrombin index below or equal to 25% of normal values, between day 3 and day 10 after ingestion, was refuted by Escudie *et al.* (2007). Their findings showed that 52% of patients that had a decrease in prothrombin index recovered without the need of transplantation. The authors concluded that such prothrombin index should be lowered in order to avoid unnecessary transplantation (10). Moreover, it was also shown that the value of serum creatinine has some limitations. Escudie *et al.* (2007) found that not all patients with fatal outcome had a creatinine level over 106 μmol/L 3 days or more after ingestion. The authors suggested that serum creatinine should not be an absolute requirement for emergency transplantation. They also pointed out that liver transplantation should be strongly recommended in patients with an interval between ingestion of mushrooms and the onset diarrhea less than 8 hours (10). In addition to this interval, female sex was also a significant risk factor for a fatal outcome than males. Lastly the decrease in prothrombin index below 10% of normal (international normalized ratio > 6) 4 days or more after ingestion, should lead to consider an emergency transplantation (10).

CHAPTER II

OBJECTIVES

Taking into consideration the above-mentioned regarding the burden of amatoxins poisoning, the potential lethality, and the current inexistence of an effective antidote, the global aim of this thesis was to develop an efficient strategy for the treatment of amatoxins poisoning. The strategy pursued to achieve the proposed main objective comprised the following original studies:

Study I

a) To analyze the contents and distribution of the major amatoxins and phallotoxins in different tissues of *A. phalloides* from two different sites of Portugal by HPLC-DAD-MS.

Study II

a) To develop and validate a HPLC-DAD-EC analytical method for the determination of α-amanitin in biological samples.

Study III

a) Application of the developed HPLC-DAD-EC method in a clinical case of co-ingestion of amatoxins and isoxazoles-containing mushrooms.

Study IV

a) To elucidate, *in silico,* the molecular mechanisms of RNAP II inhibition by α-amanitin.
b) To elucidate the molecular mechanisms underlying the therapeutic effects of current antidotes (benzylpenicillin, silybin, ceftazidime) in amatoxins' poisoning.

Study V

a) To evaluate *in silico* peptides with similar composition and molecular weight to that amatoxins for putative competition and displacement from its binding site in RNAP II.
b) To validate *in vivo* the antidotal effectiveness of polymyxin B through survival rate, biochemical, histological, toxicological and genetic studies.

CHAPTER III

ORIGINAL RESEARCH

Study I

Determination of Amatoxins and Phallotoxins in *Amanita phalloides* mushrooms from Northeast Portugal by HPLC-DAD-MS

(Accepted in Mycologia)

Determination of Amatoxins and Phallotoxins in *Amanita phalloides* mushrooms from Northeast Portugal by HPLC-DAD-MS

Juliana Garcia[1]

Ana Oliveira

Paula Guedes de Pinho

UCIBIO-REQUIMTE/ Laboratory of Toxicology, Department of Biological Sciences, Faculty of Pharmacy, University of Porto, Rua Jorge Viterbo Ferreira nº 228, 4050-313 Porto, Portugal.

Victor Freitas

Centro de Investigação em Química, Departamento de Química, Faculdade de Ciências, Universidade do Porto, Porto, Portugal.

Alexandra Carvalho

Institute of Computational Chemistry and Department of Chemistry, University of Girona, 17071 Girona, Spain.

Paula Baptista

Eric Pereira

CIMO/School of Agriculture, Polytechnic Institute of Bragança, Campus de Santa Apolónia, Apartado 1172, 5301-854 Bragança, Portugal.

Maria de Lourdes Bastos

Félix Carvalho[1]

UCBIO-REQUIMTE/ Laboratory of Toxicology, Department of Biological Sciences, Faculty of Pharmacy, University of Porto, Rua Jorge Viterbo Ferreira nº 228, 4050-313 Porto, Portugal.

Short title: Toxins from *Amanita phalloides*

Abstract: *Amanita phalloides* is a toxic mushroom responsible for the majority of deaths occurring after mushrooms ingestion, mainly due to its high levels of amatoxins. In the

present study the contents and distribution of the major amatoxins and phallotoxins in different tissues of *A. phalloides* from two different sites of Portugal were analyzed by liquid chromatography (LC)–diode array (DAD) and mass spectrometry (MS) detection. The main toxins were separated by LC and its chemical structures confirmed by MS. α-Amanitin contents in caps, stipe and volva tissues were quantified by RP-HPLC. The results show that caps have the highest content of amatoxins, whereas the volva was richest in phallotoxins. Moreover, variability in the toxins composition from different geographic sites was also observed. This study provides, for the first time, the content of toxins in *A. phalloides* from Portugal.

Key words: *Amanita phalloides,* α-amanitin, mass spectrometry, reversed phase high performance liquid chromatography, toxins.

INTRODUCTION

Amanita phalloides (death cap) is one of the most toxic mushrooms worldwide. Fatalities due to *A. phalloides* poisoning account to about 90% of deaths occurring after ingestion of mushrooms (Karlson-Stiber and Persson 2003). This mushroom species grows in symbiosis with arboreal trees, such as beech or oak in Europe and America. *Amanita phalloides* is characterized by greenish yellow cap, darker in the center and faintly streaked radially (FIG. 1). The stipe is smooth and white and it has a distinct ring. The base of the stipe is enclosed in a volva which is a distinctive and morphological diagnostic feature (Bonnet and Basson 2002). Poisoning from the consumption of this mushroom usually occurs as a result of confusion of *A. phalloides* with edible mushroom species, such as *Amanita fulva*, *Agaricus* spp., *Macrolepiota procera* and *Tricholoma portentosum* (Barceloux 2008). Cooking, freezing and drying do not eliminate the toxicity of *A. phalloides* (Vetter 1998).

FIG. 1. Basidiocarp of *Amanita phalloides* (Death Cap) from Vinhais, Portugal.

This species contains two main groups of toxins, amatoxins and phallotoxins. The amatoxins group is composed by α-amanitin (AA), β-amanitin (BA), γ-amanitin (GA), ε-amanitin, amaninamide, amanin, amanullin, amanullic acid and proamanullin (FIG. 2).

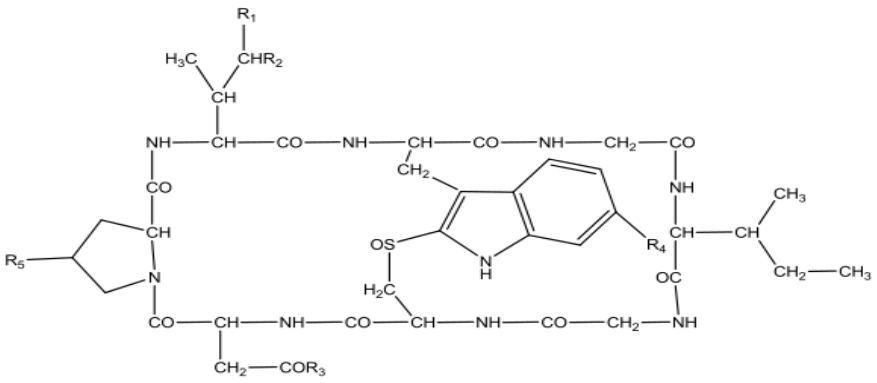

	R1	R2	R3	R4	R5
α-amanitin	CH_2OH	OH	NH_2	OH	OH
β-amanitin	CH_2OH	OH	OH	OH	OH
γ-amanitin	CH_3	OH	NH_2	OH	OH
ε-amanitin	CH_3	OH	OH	OH	OH
Amanin	CH_2OH	OH	OH	H	OH
Amanin amide	CH_2OH	OH	NH_2	H	OH
Amanullin	CH_3	H	NH_2	OH	OH
Amanullic acid	CH_3	H	OH	OH	OH
Proamanullin	CH_3	H	NH_2	OH	H

FIG. 2. Chemical structure of amatoxins The backbone structure is the same in all the amatoxins and five variable groups determine the specific compound.

The phallotoxin group consists of phalloidin (PHD), phalloin, prophallin, phallisin (PHS), phallacin, phallacidin (PCD) and phallisacin (FIG. 3) (Vetter 1998).

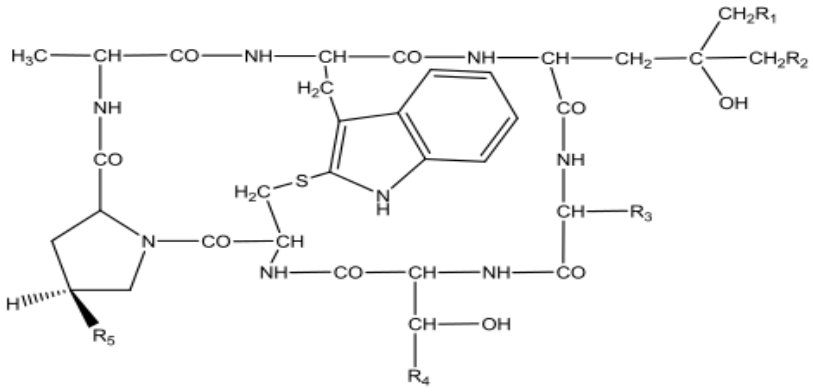

	R1	R2	R3	R4	R5
Phalloidin	OH	H	CH_3	CH_3	OH
Phalloin	H	H	CH_3	CH_3	OH
Prophallin	H	H	CH_3	CH_3	H
Phallisin	OH	OH	CH_3	CH_3	OH
Phallacin	H	H	$CH(CH_3)_2$	COOH	OH
Phallacidin	OH	H	$CH(CH_3)_2$	COOH	OH
Phallisacin	OH	OH	$CH(CH_3)_2$	COOH	OH

FIG. 3. Chemical structure of phallotoxins. The backbone structure is the same in all the phallotoxins and five variable groups determine the specific compound.

Amatoxins are the main toxins responsible for the toxicity and the human fatalities following intoxication with *A. phalloides*. The mechanism of action of amatoxins is not completely understood but it is known that the main target of AA is hepatic RNA

polymerase II enzyme. Following uptake by organic anion-transporting octapeptide (OATP) located in the sinusoidal membrane of hepatocytes, AA inhibits RNA polymerase II, reducing the mRNA synthesis and, consequently, provoking a decrease of protein contents and, ultimately, liver cell death (Mas 2005). The mechanisms of toxicity of AA has been studied by our group and we have focused our efforts on understanding the molecular mechanism of RNA polymerase II inhibition (Garcia et al. 2014).

Several methods for isolation and analysis of amatoxins and phalotoxins have been published, the reversed-phase high performance liquid chromatography (RP-HPLC) being the most common used method (Enjalbert et al. 1996; Enjalbert et al. 1999; Enjalbert et al. 1993; Enjalbert et al. 1992; Enjalbert et al. 2002; Hu et al. 2012). Enjalbert et al. have been analyzed the content of main toxins in *A. phalloides* showing that the amount of toxins depends on climate, topography and soil characteristics (Enjalbert et al. 1996; Enjalbert et al. 1999). In addition, significant differences in amounts of toxins in different tissues of the fruiting body and in different growth phases have also been noted (Enjalbert et al. 1996). The quantification of *A. phalloides* toxins in different part of the globe is important to get the greatest information possible, to ascertain its relative morbidity and lethal potential. To our knowledge, there is no study on the toxin content of *A. phalloides* from Portugal.

In this work *A. phalloides* collected in north of Portugal were investigated for amatoxins and phallotoxins by using liquid chromatography–diode array and mass spectrometry detection (LC-DAD-MS). AA was quantified from caps, stipe and volva by RP-HPLC and DAD.

MATERIAL AND METHODS

Chemicals —α-amanitin (>90% pure) was purchased from Sigma-Aldrich. Acetonitrile (hypergrade) was brought from Fisher Chemicals. Water was purified with a Milli-Q Plus ultra-pure water purification system (Millipore, Bedford, Ma, USA).

Description of the study area ––Considering the geographic differences, the northeast of Portugal province of Trás-os-Montes can be grouped into two areas: the ”Terra Fria” (Cold Land) located in the northern area, with higher altitudes, and the “Terra Quente” (Hot Lands) located in the southern areas, marked by the valleys of the Douro River (Dias et al. 2012). These two areas have significant climatic differences. Cold Land is characterized by cold and prolonged winter, and a brief hot summer with annual mean precipitation of 800 mm and mean temperature of 12.5 C. On the other hand, Hot Land has a warm and dry summer and mild winter with annual mean temperature of 14.0 C and annual precipitation of 1200 mm (Evelpidou et al. 2010). The Vinhais region is located in Cold Land, whereas Mogadouro is in the Hot Land. The varieties of topographic and climatic conditions have a great impact on the type of soil. In fact, according to the Soil Map of

Northeast Portugal, 1: 1 00000 (Agroconcultores and Coba 1991), which follows the FAO system of classification (FAO/UNESCO 1987), leptosols are largely dominant in Mogadouro, whereas cambisols are the most representative soils of Vinhais.

Amanita phalloides *and soil sampling —Amanita phalloides* fruiting body were collected in the Trás-os-Montes region during October and November of 2012 from two different sites named Vinhais and Mogadouro. The set consisted of 25 mature fruiting body. The mushrooms were identified by using morphological features and appropriate keys and monographs including Courtecuisse and Courtecuisse & Duhem (Courtecuisse 1999; Courtecuisse and Duhem 2005). Immediately after harvesting, the mushrooms were dried during three days at 60º C. Each specimen was divided into three parts namely the cap, stipe and volva. Representative voucher specimens (number 447) were deposited at the herbarium of School of Agriculture of the Polytechnic Institute of Bragança (Portugal).

Soils samples from different sites of Vinhais and Mogadorouro regions were collected and represent different soil types (leptosol and cambisol). Bulk soil samples (6 replicates per soil; 0.5 kg per replicate) were collected in plastic bags and thoroughly homogenized before further processing. The soil pH was determined according to ISO 10390:2005 method. The solid samples (weight 10 g) were treated with 50 mL 1M KCl, under stirring for 30 min. After, 1 hour, the pH for the each sample was measured at room temperature.

Extraction of toxins —Several methods have been described in the past few years for the extration of phallotoxins from fungi (Enjalbert et al. 1992; Enjalbert et al. 1996; Kaya et al. 2013). These methods are often laborious and time consuming. This is usually because most of the available protocols include multiple steps of solid/liquid extraction followed by incubation overnight. In addition to being lengthy, these methods also involve large amount of sample (2 g), which is a limitation when the amount of mushrooms available is scarce. Thus, in the present it was used a simpler but fully effective extraction method previously described by Jansson et al. (2012) with minor modifications. Briefly, cap, stipe or volva were ground to a powder in a mortar, after 0.5 g (dry weight) of were extracted during 1 h with 1 ml of milli-Q water and 6 ml acetonitrile. After centrifugation at 3000 rpm for 30 min, the supernatant was used for LC/MS analysis. The same supernatant was used for AA quantification by reversed-phase HPLC.

Identification of A. phalloides *toxins by liquid chromatography–diode array and mass spectrometry detection* —A Finnigan Surveyor series LC, equipped with Lichrocart Purospher® Star reversed-phase column (150 mm x 4.6mm, C18, 5 mm) was used. The mobile phases' flow rate was 0.5 $ml.min^{-1}$, consisted of (A) 0.02 M aqueous ammonium acetate adjusted to pH 5.0 with glacial acetic acid and (B) acetonitrile (Zhao et al. 2006). The gradient profile was: 0→15 min, 0%→2.3% solvent B; 15→35 min, 2.3%→37.9% solvent B; 35→40, 37.9%→37.9% solvent B; 40→45 min, 37.9% →100% solvent B;

45→50 min, 100%→100% solvent B; 50→55 min, 100%→0% solvent B; 55→65, 0%→0% solvent. The sample injection volume was 20 μL. The chromatographic column was stabilized with the initial conditions for 10 min. Double-online detection was done by a DAD and MS detectors. The MS detector was a Finnigan LCQ DECA XP MAX (Finnigan Corp., San Jose, CA) quadrupole ion trap equipped with atmospheric pressure ionization source, using ESI. The vaporizer and the capillary voltages were 5kV and 4V, respectively. The capillary temperature was set at 325 ºC. Nitrogen was used as both sheath and auxiliary gas at flow rates of 90 and 35, respectively (in arbitrary units).

Quantification of amatoxins by high-pressure liquid chromatography with diode array detection —Analyses were performed using a reversed-phase HPLC method (Enjalbert et al. 1992). An HPLC system (Waters model 2690) equipped with a photodiode array detector (Waters model 996) and C-18 column from Waters (150 mm x 4.6mm, C18, 5 μm) was used. The mobile phases' flow rate was 1 $ml.min^{-1}$ and consisted of (A) 0.02 M aqueous ammonium acetate adjusted to pH 5.0 with glacial acetic acid and (B) acetonitrile (Zhao et al. 2006). The gradient was: 0→15 min, 0%→2.3% solvent B; 15→45 min, 2.3%→37.9% solvent B; 45→50, 37.9%→37.9% solvent B; 50→55 min, 37.9% →100% solvent B; 55→60 min, 100%→100% solvent B; 60→65 min, 100%→0% solvent B; 65→70, 0%→0% solvent. The sample injection volume was 20 μL. All analyses were carried out in triplicate and at laboratory temperature. The absorbance was monitored by diode-array detector from wavelength 200 to 400 nm. The amounts of AA in the samples were determined by using a standard curve.

Preparation of calibration curve and quality control samples —A standard sample of AA was dissolved in milliQ distilled water to a concentration of 1 $mg.mL^{-1}$. A six-point curve was obtained with injections of 20 μL of 1, 5, 10, 25, 50, 100 $\mu g.mL^{-1}$ and the linear regression equation and correlation coefficients were calculated. AA in the samples was identified by comparison of retention times and co-injection with standards. Concentrations were calculated using peak areas of reference compound.

Quality control samples (10, 50 and 100 $\mu g.mL^{-1}$) were independently and daily prepared in the extraction medium (acetonitrile/water).

Validation procedure —The limit of detection was defined as the concentration where the signal-to-noise value exceeded 3.0. Intra- and inter-assay precision was also evaluated by considering three concentrations (10, 50 and 100 $\mu g.mL^{-1}$) prepared in triplicate and analysed in the same day (intra-day) and in different days (inter-day). The results are expressed as the coefficient of variation (CV %) of the experimental values at each concentration.

Principal components analysis —Principal components analysis (PCA) was performed using the Matlab software version 7.9.0 (Mathworks, Natick, MA) with PLS Toolbox

version 5.5 (Eigenvector Research Inc., Wenatchee, WA). It was applied as an unsupervised technique for reducing the number of variables (6 variables corresponding to AA, BA, GA, PHD, PHS and PCD) to a smaller number of new derived variables (principal component or factors) that adequately summarize the original information. Moreover it allowed recognizing patterns in the data by plotting them in a multidimensional space, using the new derived variables as dimensions (factor scores). The aim of the PCA is to produce components suitable to be used as predictors or response variables in subsequent analysis (Rencher 1995).

RESULTS

Species identification and pH soil —*A. phalloides* specimens were identified by using morphological features and appropriate keys and monographs including Courtecuisse (1999) and Courtecuisse & Duhem (2005). Morphological features that were important for species level identification of *A. phalloides* include: cap convex or subplanar with a variance of olive-green to brown color; gills free and white to cream; stipe white to pale yellow with fine radial striations; ring in upper part of the stipe, white to pale yellow, with radial striations; and volva globose and white.

The pH of all examined soil samples was strong to moderate acid. The result showed that the means pH for Vinhais and Mogadouro were between 5.170 ± 0.119 (strong acid) and 5.960 ± 0.211 (moderate acid), respectively.

Extraction of toxins ––In order to ensure complete toxins extraction we performed the extraction at different time-points (1, 2 and 3 hours). As the α-amanitin content was the same at different times, we performed a second extraction of the same mushroom sample and an additional rinse under the same conditions. The LC-MS analysis did not recover detectable amounts of residual toxins. The extraction method enabled us to obtain complete toxins extraction, dispensing with the laborious and time-consuming steps. The extraction process involves one solid/liquid extraction step followed by centrifugation. Another advantage of this method is that it only requires a small amount of mushroom sample (0.5 g).

Identification of α-amanitin, β-amanitin, γ-amanitin, phalloidin, phallisin and phallacidin —LC/DAD/MS analyses were performed in order to identify the main amatoxins and phallotoxins present in the mushroom tissues extract. FIG(S). 2 and 3 show the chemical structures of the main amatoxins and phallotoxins. The supposed identification of AA, BA, GA, PHD, PHS and PCD peaks detected under UV were based on their production spectra. Based on TABLE I the base peaks of the mass spectra were *m/z* 919.20 ($C_{39}H_{54}N_{10}O_{14}S$) for AA, *m/z* 920.13 ($C_{39}H_{53}N_9O_{15}S$) for BA, *m/z* 903.20 ($C_{39}H_{54}N_{10}O_{13}S$) for GA, m/z 789.27 ($C_{35}H_{48}N_8O_{11}S$) for PHD, *m/z* 805.27 ($C_{35}H_{48}N_8O_{12}S$) for PHS and *m/z* 847.20 ($C_{37}H_{50}N_8O_{13}S$) for PCD. The chromatographic ion peak $[M+H]^+$

at *m/z* 903.20 ($C_{39}H_{54}N_{10}O_{13}S$) could correspond to either GA or amaninamide. As amaninamide is specific to *Amanita virosa* (Buku et al. 1980), we identified this chromatographic peak as being the GA. The protonated molecular peaks with a $NH4^+$ ion $[M+NH_4]^+$ peaks; m/z 935.67 for AA, m/z 936.67 for BA, m/z 919.67 for GA, m/z 805.60 for PHD, m/z 821.47 for PHS and m/z 863.47 for PCD. A representative chromatogram recorded at 295 nm of *A. phalloides* cap extract is given in FIG. 4.

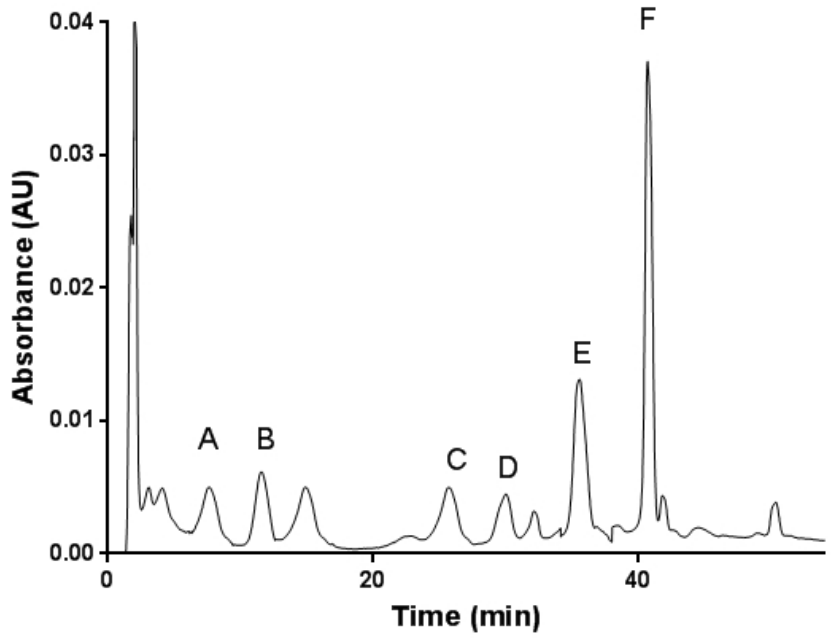

FIG. 4. Representative chromatogram recorded at 295 nm of *A. phalloides* cap from Vinhais. Peaks: A= β-amanitin; B= α-amanitin; C= γ-amanitin; D= phallacidin; E= phallisin; F= phalloidin.

TABLE I. Identified toxins in *A. phalloides* extract

Compound name	Theoretical monoisotopic	Elemental composition	Experimental $[M+H]^+$
α-amanitin	918.35	$C_{39}H_{54}N_{10}O_{14}S$	919.20
β-amanitin	919.34	$C_{39}H_{53}N_9O_{15}S$	920.13
γ-amanitin	902.36	$C_{39}H_{54}N_{10}O_{13}S$	903.20
Phalloidin	788.32	$C_{35}H_{48}N_8O_{11}S$	789.32
Phallisin	804.31	$C_{35}H_{48}N_8O_{12}S$	805.27
Phallacidin	846.32	$C_{37}H_{50}N_8O_{13}S$	847.20

Calibration and validation —The representative regression equation for the calibration curve was y = 10266x + 40831 over range of 1.00-100.00 $\mu g.mL^{-1}$ with a coefficient of 0.991. The lower limits of identification were 0.03$\mu g.mL^{-1}$. The intra- and inter-assay precision and accuracy determined using the blank mushroom extract that had been spiked with AA is indicated in TABLE II. The CV for the intra- and inter-assay was between 0.65 and 2.03% for the three concentrations studied.

TABLE II. Analytical accuracy and precision evaluated using standard spiked blank mushrooms

Concentration known (μg.mL^{-1})	**Concentration found**	**CV (%)**
Intra-assay (n=3)		
1.00	0.90±0.03	3.38
10.00	11.92±0.09	0.76
100.00	101,15±1.27	1.26
Inter-assay (n=3)		
1.00	0.87±0.02	2.02
10.00	11.90±0.24	2.02
100.00	106.58±0.84	0.79

Contents and distribution of α-amanitin in cap, stipe and volva —The retention time for AA was 12.65 min. The concentrations in the samples are shown in TABLE III. The amount of AA in caps of *A. phalloides* from Vinhais and Mogadouro, were 783.94 ± 2.66 μg.g^{-1} and 666.00 ± 1.45 μg.g^{-1} respectively (TABLE III). The stipes from Vinhais and Mogadouro contained 323.48 ±4.03 μg.g^{-1} and 302.53 ± 2.78 μg.g^{-1}respectively (TABLE III). Finally, the lowest concentrations were found in volva from Vinhais and Mogadouro which contained 103.87 ± 1.84 μg.g^{-1} and 73.16 ± 1.66 μg.g^{-1}, respectively (TABLE III).

TABLE III. Content of α-amanitin in different tissues of *A. phalloides*

Tissue	**Vinhais**	**Mogadouro**
caps	783.94 ± 2.66[a]	666.00 ± 1.45[a]
stipes	323.48 ± 4.03[a]	302.53 ± 2.78[a]
volvas	103.87 ± 1.84[a]	73.16 ± 1.66[a]

[a] Content (μg g^{-1} dry weight). Values are mean ± standard deviation (n=3).

Amatoxin and phallotoxin composition in the different tissues —Principal components analysis showed that 96.35% of the total variance of the data is explained using only three principal components. FIG. 5 shows the representation of the two principal components factor scores obtained from the mushrooms harvest in two different geographical sites and the loadings of the variables. The first principal component, accounting for 54.84% of total

variance and was strongly related to the tissue type. On the other hand the third principal component (13.58% of total variance) was related to the collection site. FIG. 5A illustrates the contrast between the two groups: the first group, projected in negative PC3 space composed by CV, SV and VV while the second group (projected in positive PC3 space) is represented by CM, SM and VM. The discrimination between these two groups is associated with the content in PHD and PHS which is correlated with the third PCA axis (FIG. 5B). FIG. 5A shows also a differentiation along PC1 among different tissues, cap, stipe and volva. Volva samples are projected on PC1 negative while caps are projected on PC1 positive and stipe between these two groups.

The separation among these three groups is associated with the content in AA, BA and GA which is very well correlated with the first PCA axis.

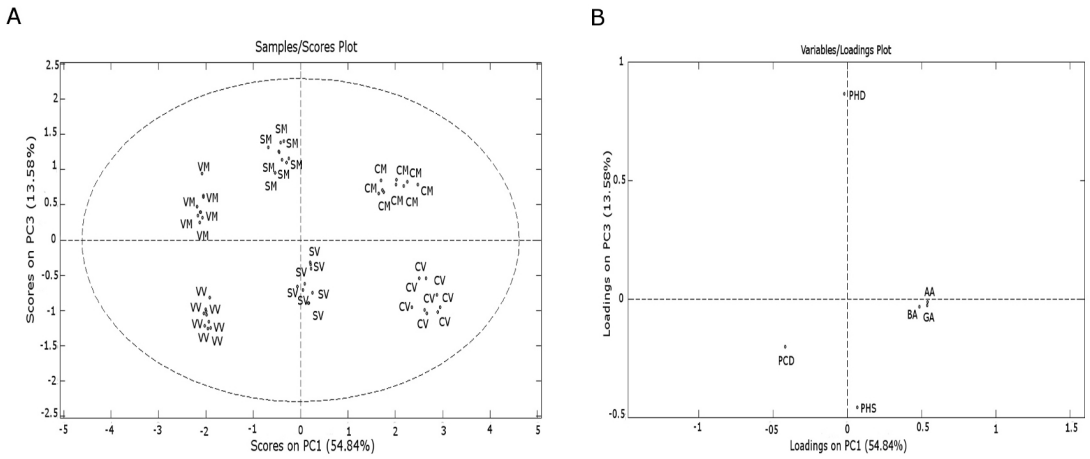

FIG. 5. A. Principal components scores plots of the data from the mushrooms HPLC-DAD spectra. B. Principal components analysis loading plots of the variables α-amanitin (AA), β-amanitin (BA), γ-amanitin (GA), phalloidin (PHD), phallacidin (PCD) and phallisin (PHS). Key: Cap from Vinhais (CV); Stipe from Vinhais (SV); volva from Vinhais (VV); Cap from Mogadouro (CM); Stipe from Mogadouro (SM) and Volva from Mogadouro (VM).

DISCUSSION

As ingestion of *A. phalloides* mushrooms is responsible for several accidental or premeditated fatal intoxications, it is of great importance to have data concerning *A. phalloides* toxin total composition, its distribution in mushroom fruiting body tissues (cap, stipe, and volva) and also its geographic preponderance. Few works are available in literature, and they come from researches performed in Poland, where several cases are reported (Lapinski and Prokopowicz 1998), France (Garrouste et al. 2009) and Czech Republic (Krenova et al. 2007). Portugal is a country where mushrooms take part of eating habits and every year several cases of mushroom intoxications are reported in media. However, no scientific works are available regarding toxins' composition of *A. phalloides* growing in Portugal. Hence, this work aimed at determining the quantitative differences in the toxins amount of the fruiting body tissues from *A. phalloides* mushrooms collected at different sites as at present there is no data for the amount of toxins present in the Portuguese *A. phalloides*. These species exist throughout the Portuguese territory but with higher incidence in the northern part of the country. New cases of *A. phalloides* poisoning have been reported every year, however, it is difficult to estimate the exact number of cases of amatoxin poisoning that occur each year due to under-reporting procedures at hospital emergencies. As described before, this species contains two groups of toxins, amatoxins and phallotoxins. The less-harmful phallotoxins are poorly absorbed through the intestine, although they may contribute to the early gastrointestinal symptoms (Karimi and Razavi 2014). The group of amatoxins is mainly composed of AA. Our results showed that the content of this toxin and its distribution in tissues of *A. phalloides* varied significantly. The highest amounts were found in the cap and stipe and the lowest amount in the volva of the *A. phalloides*. The cap AA content was twice that in the stipe and four times higher than in the volva. The content and distribution of toxins in different tissues of *A. phalloides* were also previously investigated by Enjalbert et al. (1993). Their data revealed significant variations in the amounts of toxins present in the various tissues of *A. phalloides,* which is consistent with our findings, though they found higher amounts. This apparent discrepancy may be explained by environmental factors and genetic differences. The amount of toxin present may also be dependent on the age of the collected species, which may also be reflected in the variation of our values. The collected *A. phalloides* specimens were in mature stage, which explains the lower values that are consistent with results presented by Hu et al. (2012).

Concerning the environmental conditions of the collection area (temperature, microclimate, soil, and pH values) it seems play a determinant role in amatoxin and phallotoxin profile. In accordance, Enjalbert et al. (1996) reported that the geographical local significantly influences toxin composition of the fruiting body tissues, a finding that

is also corroborated in the present study. In fact, the geographic, topographic, climatic, and soil pH differences between the two areas analyzed seems to have an impact on toxin profile. Our findings pointed out that the site-specific environmental conditions have a greater influence on phallotoxin than on amatoxin composition, which is in agreement with Enjalbert et al. (1996). The greatest variations in the toxin concentration were recorded for PHD and PHS in the stipes from Vinhais and Mogadouro. The highest PHD concentration was found in the stipe from Mogadouro. On the other hand the highest PHS concentration was found in the stipe from Vinhais. *A. phalloides* belongs to a category called ectomycorrhizal-symbiotic fungi. These fungi are known to have an intimate relationship (symbiotic) with their host plants. In this context, an ectomycorrhizal fungus gains carbon supply and other essential organic substances from the tree and in return, the plant benefits from receiving water and nutrient resources to grow. Therefore, the close ties between ectomycorrhizal fungi and their plant hosts would lead us to expect greater host influence on chemical composition of ectomycorrhizal mushrooms species. The *A. phalloides* specimens from Vinhais were in a symbiotic association with chestnut tree and specimens from Mogadouro were in a symbiotic association with oak tree. Thus, we strongly believe that host tree and the surrounding flora involved in the symbiotic relationship could influence the chemical composition of mushrooms.

The multivariate techniques of data analysis was used to obtain more information on the variables that mainly influence the sample similarities and/or differences. The same technique has been recently applied by our group to discover molecules that can be used to assist in identifying mushroom species (Carvalho et al. 2014) in which 6 molecules that can be species-or-genus specific were successfully identified. In the present study, we are able to discriminate the different tissues that composed fruiting body mushroom based on toxin composition. Therefore the cap tends to contain more amatoxins (AA, BA and GA) than stipe and volva (FIG. 6). In contrast, volva exhibited the lowest concentration of amatoxins. On the other hand, volva contains more PCD than caps and stipes

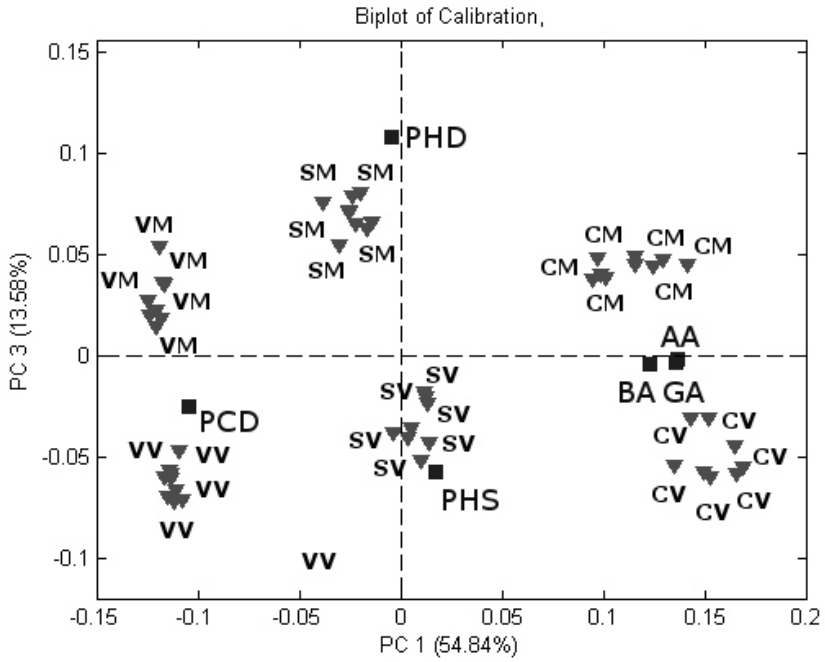

FIG. 6. Principal components scores and loadings plots.

Taken together, these results based on statistical evaluation of HPLC-DAD data revealed that amatoxins and phallotoxins are not equally distributed in the fruiting body tissues and vary from one area to another. Furthermore, findings from this study support the hypothesis that environmental conditions play a significant role in the content of toxins.

ACKNOWLEDGMENTS

Authors are grateful to Dr Zélia dos Santos Azevedo, from Faculty of Sciences, University of Porto, for gently lend us the LC/DAD-ESI/MS and for all precious technical assistance. The authors are also grateful to Foundation for the Science and Technology (FCT, Portugal) for financial support and also thank FCT for PhD grant SFRH/BD/74979/2010.

LITERATURE CITED

Agroconcultores, Coba. 1991. Carta darta dos Solos. Carta do Uso Actual da Terra e Carta de Aptidão da Terra do Nordeste de Portugal. Vila Real: UTAD/PDRITM. p 153-163.

Barceloux DG. 2008. Medical Toxicology of Natural Substances: Foods, Fungi, Medicinal Herbs, Plants, and Venomous Animals. New Jersey: John Wiley & Sons, Inc. 272 p.

Bonnet MS, Basson PW. 2002. The toxicology of Amanita phalloides. Homeopathy 91:249–54.

Buku A, Wieland T, Bodenmuller H, Faulstich H. 1980. Amaninamide, a new toxin of Amanita virosa mushrooms. Experientia 36:33–4.

Carvalho LM, Carvalho F, de Lourdes Bastos M, Baptista P, Moreira N, Monforte AR, da Silva Ferreira AC, de Pinho PG. 2014. Non-targeted and targeted analysis of wild toxic and edible mushrooms using gas chromatography-ion trap mass spectrometry. Talanta 118:292–303.

Courtecuisse R. 1999. Mushrooms of Britain and Europe. London: HarperCollins Publ. 281 p.

Courtecuisse R, Duhem B. 2005. Guia de los hongos de la Península Ibérica, Europa y Norte de África. Barcelona: Ediciones Omega. 301 p.

Dias LG, Pereira AP, Estevinho LM. 2012. Comparative study of different Portuguese samples of propolis: pollinic, sensorial, physicochemical, microbiological characterization and antibacterial activity. Food Chem Toxicol 50:4246–53.

Enjalbert F, Gallion C, Jehl F, Monteil H, Faulstich H. 1992. Simultaneous assay for amatoxins and phallotoxins in Amanita phalloides Fr. by high-performance liquid chromatography. J Chromatogr 598:227–36.

———, Gallion C, Jehl F, Monteil H. 1993. Toxin content, phallotoxin and amatoxin composition of Amanita phalloides tissues. Toxicon 31:803–7.

———, Cassanas G, Guinchard G, Chaumont J. 1996. Toxin composition of Amanita phalloides tissues in relation to the collection site. Mycologia 88:909–921.

———, Cassanas G, Salhi SL, Guinchard C, Chaumont JP. 1999. Distribution of the amatoxins and phallotoxins in Amanita phalloides. Influence of the tissues and the collection site. C R Acad Sci III 322:855–62.

———, Rapior S, Nouguier-Soule J, Guillon S, Amouroux N, Cabot C. 2002. Treatment of amatoxin poisoning: 20-year retrospective analysis. J Toxicol Clin Toxicol 40:715–57.

Evelpidou N, Figueiredo T, Mauro F, Tecim V, vassilopoulos A. 2010. Natural Heritage from East to West: case studies from 6 EU countries. Berlin: Springer Verlag 122 p.

FAO/UNESCO. 1987. Soil Map of the World, Revised Legend, Amended Fourth Draft. Rome: United Nations, Food and Agriculture Organization.

Garcia J, Carvalho AT, Dourado DF, Baptista P, de Lourdes Bastos M, Carvalho F. 2014. New in silico insights into the inhibition of RNAP II by alpha-amanitin and the protective effect mediated by effective antidotes. J Mol Graph Model 51:120–7.

Garrouste C, Hemery M, Boudat AM, Kamar N. 2009. Amanita phalloides poisoning-induced end-stage renal failure. Clin Nephrol 71:571–4.

Hu J, Zhang P, Zeng J, Chen Z. 2012. Determination of amatoxins in different tissues and development stages of Amanita exitialis. J Sci Food Agric 92:2664–7.

Jansson D, Fredriksson SA, Herrmann A, Nilsson C. 2012. A concept study on identification and attribution profiling of chemical threat agents using liquid chromatography-mass spectrometry applied to Amanita toxins in food. Forensic Sci Int 221:44–9.

Karimi G, Razavi B. 2014. Poisonous Mushrooms. In: Gopalakrishnakone P, Faiz SMA, Gnanathasan CA, Habib AG, Fernando R, Yang C-C, eds. Clinical Toxinology. Netherlands: Springer. p. 1-18.

Karlson-Stiber C, Persson H. 2003. Cytotoxic fungi--an overview. Toxicon 42:339–49.

Kaya E, Karahan S, Byram R, Yaykasli KO, Colakoglu S, Saritas A. 2013. Amatoxin and phallotoxin concentration in Amanita phalloides spores and tissues Toxicol Ind Health 1–6.

Krenova M, Pelclova D, Navratil T. 2007. Survey of Amanita phalloides poisoning: clinical findings and follow-up evaluation. Hum Exp Toxicol 26:955–61.

Lapinski TW, Prokopowicz D. 1998. [Epidemiological factors of mushroom poisoning in the north-east of Poland]. Przegl Epidemiol 52:463–67.

Mas A. 2005. Mushrooms, amatoxins and the liver. J Hepatol 42:166–169.

Rencher A. 1995. Methods of Multivariate Analysis. New York, USA: John Wiley & Sons, Inc. 380 p.

Serné EH, Toorians AWFT, Gietema JA, Bronsveld W, Haagsma EB, Mulder POM. 1996. Amanita phalloides, a potentially lethal mushroom: its clinical presentation and therapeutic options. The Netherlands J Med 49:19–23.

van Hoek B, de Boer J, Boudjema K, Williams R, Corsmit O, Terpstra OT. 1999. Auxiliary versus orthotopic liver transplantation for acute liver failure. EURALT Study Group. European Auxiliary Liver Transplant Registry. J Hepatol 30:699–705.

Vetter J. 1998. Toxins of Amanita phalloides. Toxicon 36:13–24.

Zhao J, Cao M, Zhang J, Sun Q, Chen Q, Yang ZR. 2006. Pathological effects of the mushroom toxin alpha-amanitin on BALB/c mice. Peptides 27:3047–52.

FOOTNOTES

[1] Authors to whom correspondence should be addressed (Tel.: + 351 220428597; Fax: + 351 226093390; e-mail: jugarcia_18@hotmail.com and felixdc@ff.up.pt)

Study II

Quantification of alpha-amanitin in biological samples by HPLC using simultaneous UV-diode array and electrochemical detection

(Submitted for publication)

Quantification of alpha-amanitin in biological samples by HPLC using simultaneous UV-diode array and electrochemical detection

Juliana Garcia[a*], Vera M. Costa[a], Paula Baptista[b], Maria de Lourdes Bastos[a], Félix Carvalho[a*]

[a]REQUI*M*TE/ Laboratory of Toxicology, Department of Biological Sciences, Faculty of Pharmacy, University of Porto, Rua José Viterbo Ferreira nº 228, 4050-313 Porto, Portugal.

[b]CIMO/School of Agriculture, Polytechnic Institute of Bragança, Campus de Santa Apolónia, Apartado 1172, 5301-854 Bragança, Portugal.

* Authors to whom correspondence should be addressed (Tel.: + 351 220428597; Fax: + 351 226093390; e-mail: jugarcia_18@hotmail.com and felixdc@ff.up.pt)

Abstract

α-Amanitin is a natural bicyclic octapeptide, from the family of amatoxins, present in the deadly mushroom species *Amanita phalloides*. The toxicological and clinical interests raised around this toxin, require highly sensitive, accurate and reproducible quantification methods for the respective pharmacokinetic and toxicokinetic studies. In the present work, a high-performance liquid chromatographic (HPLC) method with in-line connected diode-array (DAD) and electrochemical detection was developed and validated to quantify α-amanitin in biological samples (namely plasma, liver and kidney) following intoxication. Sample pre-treatment consisted of a simple and unique deproteinization step with 5% perchloric acid followed by centrifugation at 16000*g*, 4ºC, for 20 min. The high recovery found for α-amanitin (≥ 96.8%) makes this procedure suitable for adequately extracting α-amanitin from liver and kidney homogenates. The resulting supernatant was collected and injected into the HPLC, using a commercially pre-packed reverse phase cartridge, Waters Spherisorb RP 18 (5 μm) ODS2 column. Mobile phase was composed by 20% methanol in 50 mM citric acid, and 0.46 mM octanessulfonic acid, adjusted to pH 5.5. The chromatographic runs took less than 22 min and no significant endogenous interferences were observed at the α-amanitin retention time. Calibration curves were linear with regression coefficients higher than 0.994. The overall inter- and intra-assay precision did not exceed 15.3%.

This present method has low interferences and has a simple and fast processing step, being a suitable procedure to support *in vivo* toxicokinetic studies involving α-amanitin. In fact, the validated method was successfully applied to quantify α-amanitin in biological samples following intraperitoneal α-amanitin administration to rats. The results clearly indicate that the proposed method is suitable to investigate the pharmacokinetic and tissue distribution of α-amanitin.

In the present work, human plasma was also used as matrix and the purposed method was adequate for detection of α-amanitin in that matrix. Moreover, the method will be very useful in the development of novel and potent antidotes for amatoxin's poisoning and to improve the knowledge of α-amanitin toxicity.

Keywords: High-performance liquid chromatographic; diode-array; electrochemical; α-amanitin

Abbreviations

HPLC	High-performance liquid chromatography
DAD	Diode-array
EC	Electrochemical
DNA	Deoxyribonucleic acid
LOD	Limit of detection
LOQ	Limit of quantification
LC	Liquid chromatography
MS	Mass spectrometry
RNA	Ribonucleic acid
RNAP II	RNA polymerase II
RSD	Relative standard deviation
SPE	Solid phase extraction
UV	Ultraviolet

1. Introduction

The main toxin of the amatoxins, α-amanitin (Figure 1) is a toxic bicyclic octapeptide present in the deadly mushroom species *Amanita phalloides*. It accounts up to 40% of the amatoxins present in this mushroom and is the main responsible for its toxic effects [1]. α-Amanitin produces hepatic and kidney failure, which result in a potentially fatal outcome in most of the human intoxication cases [2]. The mechanisms underlying the toxicity of α-amanitin are not completely understood, but it is accepted that the inhibition of RNA polymerase II (RNAP II) leads to its the main effects [3]. Other mechanisms also appear to be involved, including oxidative stress [4].

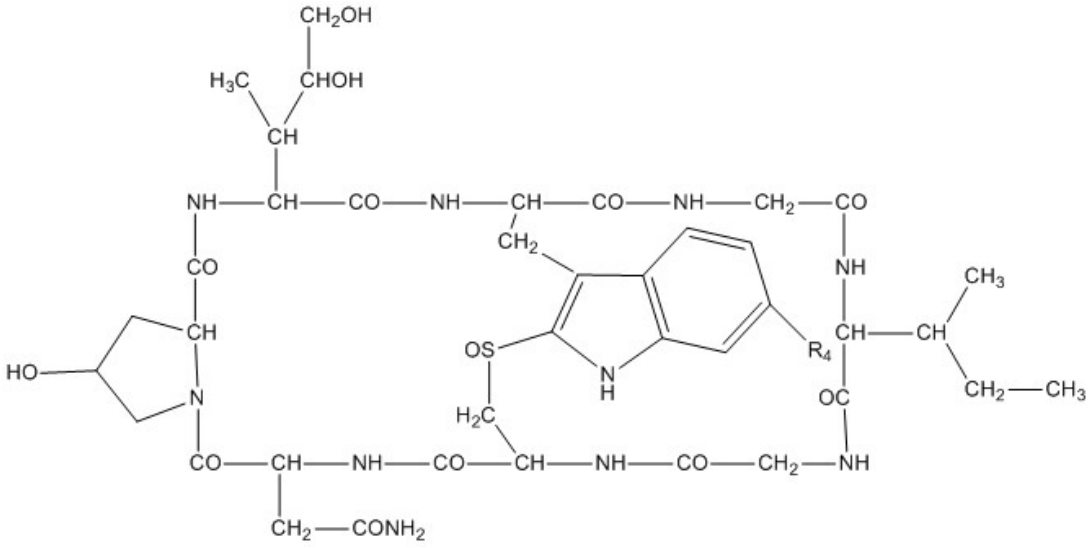

Figure 1. Chemical structure of α-amanitin

So far, there is no specific and totally effective antidote for *Amanita phalloides* poisoning. Benzylpenicillin, ceftazidime, N-acetylcystein, and silybin are the most extensively used antidotes, however mortality remains high [5]. Currently, *in vivo* and *in silico* studies are ongoing in search of effective antidotes, either directed to the toxicokinetics or to the toxicodynamics of amatoxins [6-9]. In both approaches, it is expected that the development of more insightful analytical and physiological methodologies, will provide essential tools for achieving this purpose. From the analytical stand-point, however, sensitive methodologies for α-amanitin to be applied in biological samples are lacking.
Besides the toxicological interest in α-amanitin, recent findings indicate that α-amanitin is emerging as an attractive new class of potent anticancer drug [10]. For this clinical

application, adequate analytical methodologies are also required for the evaluation of α-amanitin pharmacokinetics, both in pre-clinical and clinical studies.

The comprehensive characterization of antidotes in *Amanita phalloides* poisoning and the pharmacokinetics and toxicokinetic studies of α-amanitin require highly sensitive, accurate and reproducible quantification assays. Currently, there are several high-performance liquid chromatography (HPLC)–ultraviolet (UV) [11-17] and HPLC–mass spectrometry (MS) [18-20] methods to determine α-amanitin in mushrooms, liver and fluids. HPLC-MS methods for α-amanitin detection are accurate, sensitive, and specific; nevertheless HPLC-MS is an expensive technique and is not available in many laboratories. To date there are no published HPLC with electrochemical detection methods for the analysis of α-amanitin in biological tissues. Hence, in this paper, we describe a simple acidic extraction and HPLC methodology with in-line connected photodiode array detection (DAD) and EC detection to quantify α-amanitin in rat liver and kidney. Moreover, we applied the validated method to identify α-amanitin in human plasma. The validated method was successfully applied to quantify α-amanitin in plasma, liver and kidney tissues following intraperitoneal administration to rats. The new method provides the required high analytical sensitivity and reproducibility, with a simple and fast pretreatment, as it is required for advanced pharmacokinetic and toxicokinetic research.

2. Material and methods

2.1. Reagents and Chemicals

α-Amanitin (>99%), bovine serum albumin, and 1-octanesulfonic acid sodium salt were purchased from Sigma-Aldrich (St. Louis, Mo, USA). Analytical HPLC grade methanol was obtained from Fisher Scientific (Waltham, Massachusetts, USA). Sodium chloride (NaCl), potassium chloride (KCl), sodium hydrogen phosphate (Na_2HPO_4), potassium dihydrogen phosphate (KH_2PO_4) and perchloric acid were purchased from Merck (Darmstadt, Germany). Water was purified with a Milli-Q Plus ultra-pure water purification system (Millipore, Bedford, Massachusetts, USA).

2.2. Chromatographic conditions

HPLC analysis was performed using a Waters 2690 separation module (Waters, Milford, MA, USA), and a commercially pre-packed reverse phase cartridge of 250mm x 4.6mm, Waters Spherisorb RP-18 (5 μm) ODS2 column. The mobile phase (20% methanol in 50mM citric acid, 0.46mM octanessulfonic acid, adjusted to pH 5.5) was filtered through a 0.45 μm membrane (Millipore, Madrid, Spain) and degassed. An isocratic elution was performed at a flow rate of 1.0mL/min, at room temperature. Sample aliquots of 20 μL

were injected. A Compaq computer fitted with Millenium32 software (Waters) processed the chromatographic and spectral data.

For the spectroscopic and coulochemical analysis, a photodiode array detector (Waters model 996) and/or a Colouchem II (ESA, Chelmsford, USA) equipped with a guard cell (ESA 5020) and analytical cell (ESA 5011A) electrochemical detector were used. In all the studies, both detectors were used, with the analytical cell of the coulochemical detector placed after the photodiode array detector. The electrochemical potential settings of Coulochem II detector were: guard cell, -550 mV, and analytical detector + 500 mV, following a previous reported procedure [21]. A current of 5 μA full-scale was used. Ultraviolet-visible spectra was collected for all samples between from 230 to 400 nm. For quantitative analyses chromatograms were integrated at 305 nm [15].

2.3. Stock solution and calibration standards

A stock solution of α-amanitin was prepared in water Milli-Q and diluted to a final concentration of 1 $mg.mL^{-1}$. All stock solutions were stored of -20 ºC. A set of eleven standards ranging from 0.025 $\mu g.mL^{-1}$ to 10 $\mu g.mL^{-1}$ were prepared at the moment of use by spiking the rat liver and kidney samples with appropriate amounts of α-amanitin. All calibration standards were prepared in triplicate.

2.4. Animals and sample preparation

The liver and kidney tissues were obtained from adult male Wistar rats. These animals were used as healthy controls in other experiments, in which liver and kidney were not used. A minimum number of animals was used in order to obtain valid results. All experiments were approved by local ethical committee. All rats were between 5 and 6 months of age and weighting about 150 to 200 g. Rats were sacrificed by guillotine decapitation by an experienced veterinarian and liver and kidney tissues were immediately collected and kept frozen at -20ºC until homogenization. One gram of each organ was homogenized using an Ultra-Turrax homogenizer in 4 mL of 0.1M phosphate buffer, pH 7.4. The homogenate was placed in perchloric acid (5% final concentration) for protein denaturation, and centrifugated at 16000 *g*, 4ºC for 20 min. The resulting supernatant was collected and injected into the HPLC before or after spiking with α-amanitin, depending on the condition to be tested.

2.5. Method Validation

The HPLC method with simultaneous DAD and EC detection for the determination of α-amanitin in 5% perchloric acid, and in liver and kidney samples was validated by the evaluation of the following parameters: specificity, linearity, recovery, precision, sensitivity, matrix effect and analyte stability.

2.5.1. Specificity

Specificity is the ability to assess unequivocally the analyte in the presence of components that may be expected to be present [22] . Specificity of the method was tested by analysis of three different blanks: 5% perchloric acid, rat liver and kidney extracts and compared to samples spiked with 5 μg.mL $^{-1}$ of α-amanitin to ensure the absence of compounds with similar retention times. The purity of the peak of α-amanitin was investigated by determining the ultraviolet and visible spectrum with maximum absorbance using the DAD and by comparing the retention times between spiked samples and pure controls.

2.5.2. Linearity

The linearity of an analytical procedure is its ability to obtain test results that are directly proportional to the concentration of analyte in the sample within a given range [22]. The linearity response for α-amanitin was initially studied using eleven standards in 5% perchloric acid injected three times, covering the range of 0.025-10μg.mL^{-1}. Subsequently, linearity was studied in biological samples spiked with a series of α-amanitin standards covering the mentioned range. The linearity was evaluated by linear regression analysis.

2.5.3. Recovery

Typically, the accuracy of the analytical methods is determined by recovery studies done by spiking the blank matrix with the analyte prior to sample treatment [23]. Therefore, recovery was used to further evaluate the accuracy of the method in our study. To determine method accuracy, different concentrations of α-amanitin (low, medium and high) were used to spike blank liver and kidney samples (n=3). After homogenization, known concentrations of α-amanitin were added to three different rat liver and kidney preparations placed in 0.1M phosphate buffer. The final hepatic homogenate concentrations used to assess low, medium and high concentrations were: 0.5, 5, and 7.5 μg.mL^{-1}. The final renal homogenate concentrations used to assess low, medium and high concentrations were: 0.82, 5, and 7.5 μg.mL^{-1}. After vortexing for 1 min, the homogenates were placed in perchloric acid (5% final concentration). Centrifugation followed for 10 min at 16000×*g*, the supernatants being collected and injected into the HPLC. The recoveries were assessed by comparing the peak area of the α-amanitin extracted from liver and

kidney homogenates to those of blank deproteinized liver and kidney samples spiked with similar concentrations and injected in the same day and HPLC conditions.

2.5.4. Precision

Precision expresses the degree of scatter between a series of measurements obtained from multiple sampling of the same homogeneous sample. Precision may be considered at three levels: repeatability, intermediate precision, and reproducibility [22]. In this work, method precision (intra-assay repeatability), instrument precision (injection repeatability), and intermediate precision were investigated. To determine method precision (intra-assay), different concentrations of α-amanitin (low, middle and high) were used by spiking blank hepatic and renal samples and performing several replicates (n=6). Known concentrations of α-amanitin were added to biological matrices to obtain final liver matrix concentrations of 0.5 [24], 5 (medium) and 7.5 $\mu g.mL^{-1}$ (high) and kidney matrix concentrations of 0.82 [24], 5 (medium) and 7.5 $\mu g.mL^{-1}$ (high). The samples were analyzed by the same analyst and in the same day. Intermediate precision was also studied in order to determine the agreement of the measurements when the method was used on different days. The inter-assay precision was determined by the analysis of the same concentrations of α-amanitin used in the intra-assay study through the injection of six replicates on three different days over a period of three weeks. The precision was reported as the relative standard deviation (% RSD). The % RSD of the proposed method was calculated using the following equation: %RSD $=S/x$ where S is the standard deviation and x is the mean of response.

2.5.5. Sensitivity

The limit of detection (LOD) of an analytical procedure is the lowest concentration of an analyte in a sample, which can be detected but not necessarily quantitated as an exact value. The limit of quantification (LOQ) is the lowest amount of analyte in a sample that can be quantitatively determined with suitable precision and accuracy [22]. The LOD and LOQ were calculated by using standard solutions prepared in 5% perchloric acid, liver and kidney samples. Two different criteria were applied. Firstly, the LOD and LOQ were measured based on visual evaluation according to International Conference on Harmonization Q2 (ICH Q2) guidelines [25], by successively diluting a stock solution containing 1 $\mu g.mL^{-1}$. The minimum concentrations of α-amanitin that were reliably detected and quantified with acceptable accuracy and precision were considered the LOD and LOQ of our method respectively. Additionally, the LOD and LOQ were determined using the calibration curve method described in the same guidelines [25]. The LOD (k=3.3) and LOQ (k=10) were calculated using the following equation: $A=k\sigma/S$, where A is

LOD or LOQ, σ is the standard deviation of the response, and *S* is the slope of the calibration curve.

2.5.6. Evaluation of the matrix effect

The matrix effect was evaluated by comparing the calibration graphs obtained by spiking liver and kidney samples with known amounts of α-amanitin, and the calibration graph was obtained from standard α-amanitin 5% perchloric acid solutions.

2.5.7. Analyte stability

A stability study was performed in order to assess the stability of the analyte, in different storage and analysis conditions. α-Amanitin stability experiments' were evaluated in 5% perchloric acid, and in deproteinized liver and kidney samples. Perchloric acid (5%) and blank liver and kidney samples were divided into four aliquots, and each aliquot was spiked with α-amanitin at 2.5 $\mu g.mL^{-1}$. Final concentration of each sample was analyzed immediately, while the remaining samples were stored at room temperature, 4°C, -20°C and -80°C and thereafter analyzed after 24h, 7, 14 days without any other freeze-thaw cycles.

Stability was also studied after several freeze–thaw cycles. Perchloric acid (5%), blank liver and kidney samples were divided into two aliquots, each aliquot was spiked with α-amanitin at 2.5 $\mu g.mL^{-1}$ and stored at -20 °C and -80 °C. These samples were analyzed after three freeze–thaw cycles at room temperature. All samples used for stability testing were tested in triplicate. A standard curve was constructed during each analytical evaluation and injected in the same day and conditions.

2.7. Method application

The described analytical method was applied to four different human plasma samples. Aliquots of these plasmas were spiking with α-amanitin to a final concentration of 5 $\mu g.mL^{-1}$ followed by deproteinization using perchloric acid (5% final concentration). The dispersion was vortexed for 1 min and then the samples were centrifugated at 16000 *g* for 10 min at 4°C. The supernatants were then collected and injected into the developed HPLC system.

2.8. Proof of concept

2.8.1. Experimental procedures on animals

Female Wistar rats were used as the animal model for *in vivo* experiments. Animals were obtained from vivarium of Institute of Biomedical Sciences - ICBAS, University of Porto and were between 120-150 g at the time of experiment. The protocol was approved by the local committee for the welfare of experimental animals and was performed in accordance with national legislation. Rats received α-amanitin (dissolved in saline solution) intraperitoneally at a dose of 10 mg/kg and 21.4 mg/kg for different time-points. After two or four hours, the animals were anesthetized with isoflurane and sacrificed by exsanguination, collecting the blood in the inferior vena cava into EDTA-containing tubes. Plasma was isolated from blood by centrifugation at 920 *g* for 10 min at 4 ºC. Livers and kidneys were removed, weighed, and homogenized in ice-cold 0.1M phosphate buffer, pH 7.4. An aliquot of the homogenate was stored (-20°C) for posterior protein quantification. An aliquot of the homogenate was placed in perchloric acid (5% final concentration) for protein denaturation, and centrifugated at 13000 *g*, 4 ºC for 20 min. The supernatant was then collected and injected into the HPLC system. A set of eleven standards ranging from 0.025 μg.mL^{-1} to 10 μg.mL^{-1} were prepared at the moment of use by spiking rat liver and kidney samples with appropriate amounts of α-amanitin. The α-amanitin levels in plasma, liver and kidney that had accumulated at 2 and 4 hours after administration were calculated. As to confirm the identity of the α-amanitin peak, samples were spiked with a standard solution of 5 μg.mL $^{-1}$ of α-amanitin.

2.8.2. Protein determination

Protein content was determined by the method described by Lowry [24]. Bovine serum albumin was used as protein standard. Fifty μL of samples, standards or blank were added in triplicate to a 96-well microtiter plate, followed by addition 100 μL of extemporaneously prepared Reagent A [9.8 mL of 2% sodium carbonate), 100 μL of 2% sodium potassium tartrate and 100 μL of 1% sulfate cupper II]. After 10 min under light protection, 100 μL of extemporaneously prepared Reagent B (Folin–Ciocalteu reagent and H_2O, 1:14) was added. The microtiter plate was kept protected from the light for 20 min, after which the absorbance was measured at 750 nm.

2.9. Statistical analysis

The linearity was evaluated by the linear regression test. Evaluation of the matrix effect was performed by one-way analysis of variance to determine the statistical significance between the slopes of the 5% perchloric acid, liver and kidney standard calibration curves. Statistical significance was set at $p \leq 0.05$. The Tukey multiple comparisons test was used

once a significant *p* was achieved. In the evaluation of stability, different conditions were assessed in different time-points, thus a two-way analysis of variance was performed. If a statistical significant effect was found ($p \leq 0.05$) the Tukey multiple comparisons test was performed. All statistical tests were performed using GraphPad Prism version 6 (San Diego, California, USA).

3. Results

3.1. Optimization of the chromatographic conditions

In order to obtain low background noise in the biological matrices, citric acid/methanol was used as mobile phase, as citrate can be used in a wide range of pH (2.1 <pH <6.4) and provides low background noise [23,26]. It was observed that the ratio of citric acid and methanol (80:20) was key to a good separation and resolution of the peaks. The pH value also studied as it has an important role in the α-amanitin ionization: α-amanitin has an amine ($-NH_2$) group (Figure 1), and therefore the pH of the mobile phase influences both HPLC retention and ionization efficiency. The amine group will be ionized at pH below its pKa (9.72)[27], in which α-amanitin behaves as an extremely polar molecule. For this purpose, a pH of 5.5 was chosen. Taken together, the optimization of the mobile phase and pH led to a optimal chromatographic resolution of the sample components and a low chromatographical run (22 min) (Figure 2).

3.2. Sample preparation

The main goal of the sample preparation was to create a simple method that allowed the elimination of interferences and good stability of the analyte, α-amanitin. Liver and kidney are quite complex matrices, with high level of proteins, thus, a good deproteinizing step was required. For this purpose, we used perchloric acid (5% final concentration). After centrifugation, the resulting supernatant can be directly injected into HPLC, therefore resulting in a simple procedure that can be performed in all laboratory settings.

3.3 Method validation

3.2.1 Specificity

The specificity of the assay was examined using the described chromatographic conditions on section 2. Representative chromatograms recorded at 305 nm of blank 5% perchloric acid and a 5% perchloric acid spiked to contain 5 $\mu g.mL^{-1}$ of α-amanitin (Figures 2A), blank liver sample and a liver sample spiked to contain 5 $\mu g.mL^{-1}$ of α-amanitin (Figures 2C) and a blank kidney sample and a kidney sample spiked to contain 5 $\mu g.mL^{-1}$ of α-

amanitin (Figures 2E) are shown in Figure 2. Representative electrochemical chromatograms of blank 5% perchloric acid and a perchloric acid spiked to contain 5 μg.mL^{-1} of α-amanitin (Figures 2B), blank liver sample and a liver sample spiked to contain 5 μg.mL-1 of α-amanitin (Figures 2D) and a blank kidney sample and a kidney sample spiked to contain 5 μg.mL^{-1} of α-amanitin (Figures 2F) are also shown. There were no endogenous interfering substances in the samples.

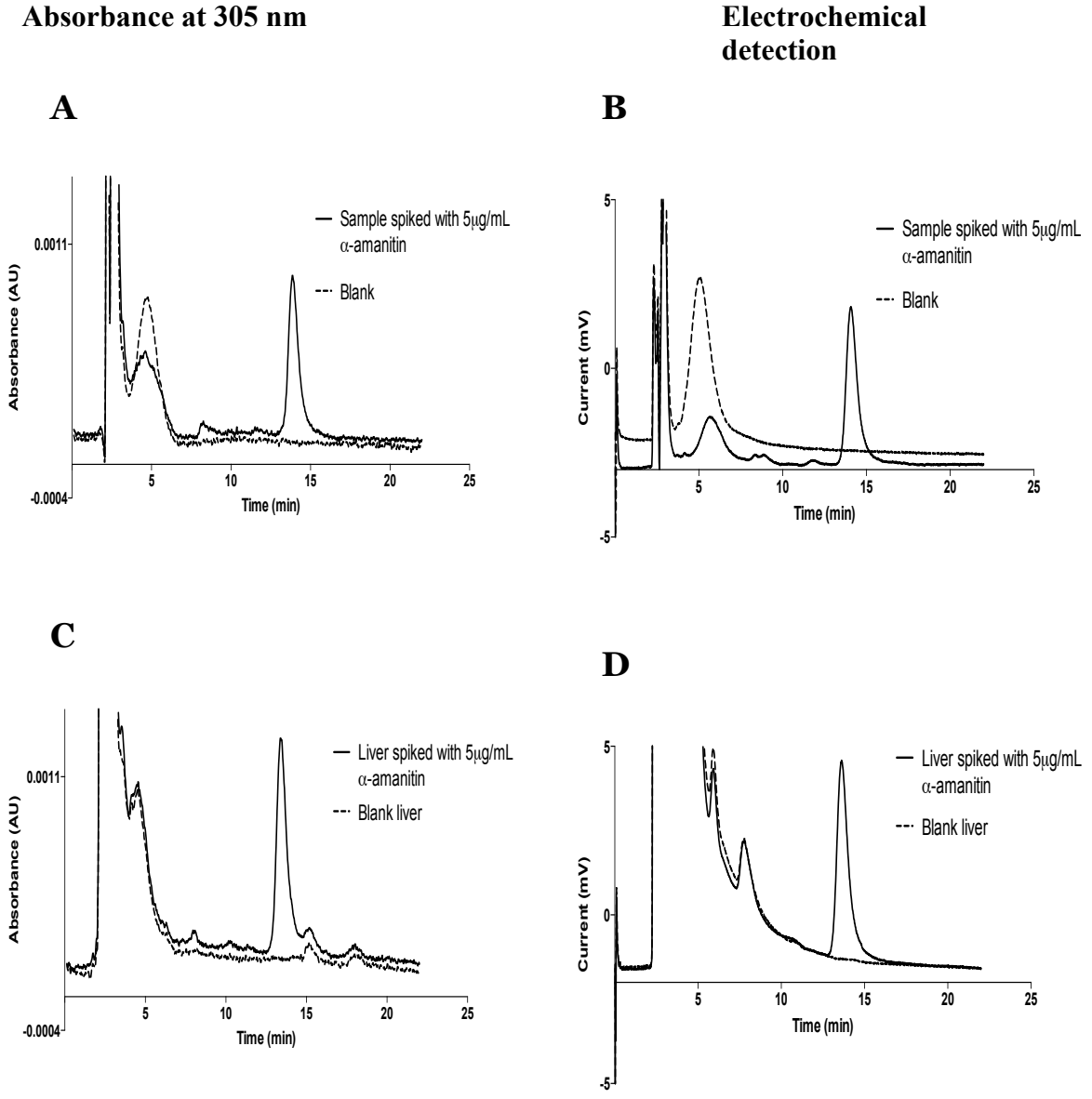

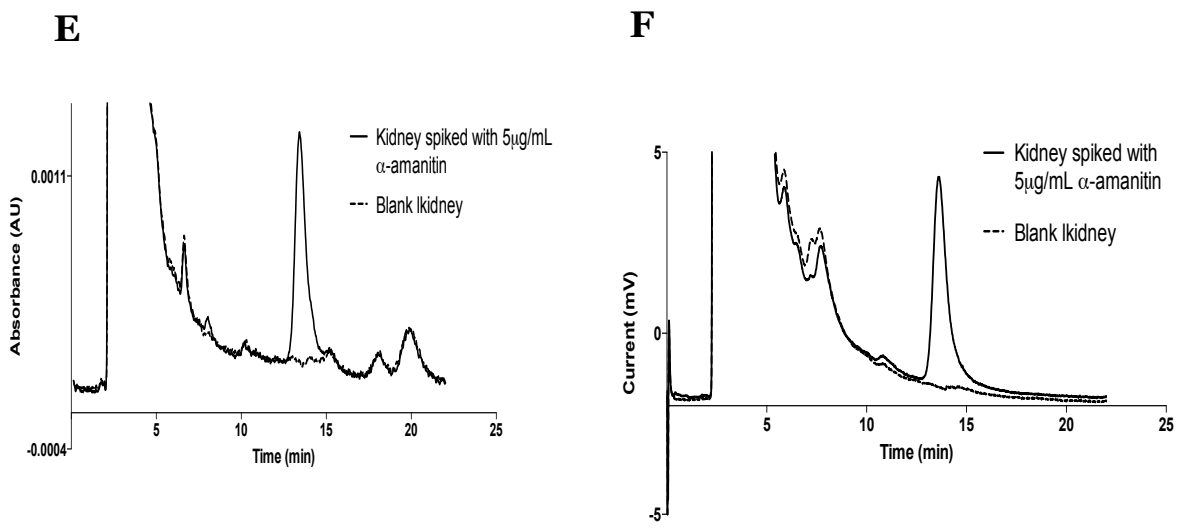

Figure 2. Representative chromatograms recorded at 305nm **(A)** of blank 5% perchloric acid and 5% perchloric acid spiked to contain 5 µg.mL^{-1} of α-amanitin; **(B)** blank liver, and liver sample spiked to contain 5 µg.mL^{-1} of α-amanitin and **(C)** blank kidney, and kidney sample spiked to contain 5 µg.mL^{-1} of α-amanitin. Representative electrochemical chromatograms of **(D)** blank 5% perchloric acid and 5% perchloric acid spiked to contain 5 µg.mL-1 of α-amanitin; **(E)** blank liver, and liver sample spiked to contain 5 µg.mL-1 of α-amanitin and **(F)** blank kidney, and kidney sample spiked to contain 5 µg.mL-1 of α-amanitin**.**

3.2.2. Linearity

The linear least squares regression equation (1/c2) correlation coefficients of the standard curves for α-amanitin in 5% perchloric acid, and for liver and kidney extracts were all above 0.994. The linear equations and corresponding coefficient of determination (r^2) values for solutions of α-amanitin in 5% perchloric acid, liver and kidney matrices are represented in Table 1. All the linearity, range parameters, and their related validation data are shown in Table 1. The regression data for calibration curve shows good linear relationship with $r^2 > 0.990$.

Table 1. Linearity data of α-amanitin analysis in 5% perchloric acid and tissue samples.

	Linear equation	Slope (±SD)	Intercept (±SD)	Determination coeficiente (r^2)	Linear range ($\mu g.mL^{-1}$)
305 nm					
Perchloric acid 5%	y = 9677x– 910.8	9677 ± 121.1	-910.8 ± 556.9	0.9964	0.45-10
Liver	y = 9279x+ 432.2	9279 ± 87.21	432.2 ± 381.8	0.9983	0.33-10
Kidney	y = 6858x + 2404	6858 ± 54.21	2404 ± 256.3	0.9990	0.5-10
Electrochemical detection					
Perchloric acid 5%	y = 54113x - 4772	53759 ± 931.4	-4772 ± 3814	0.9935	0.19-10
Liver	y = 54260x + 77.95	54260 ± 674.8	77.95 ± 2763	0.9966	0.21-10
Kidney	y = 42409x + 951.0	42409 ± 426.4	951 ± 1646	0.9975	0.11-10

3.2.3. Recovery

Recovery from the spiked samples was determined as described in section 2.5.3. Results show an overall mean percent recovery of above 96 % (Table 2).

3.2.4. Precision

The repeatability and the intermediate precision (intra- and inter-assay precision) were calculated as the RSD of replicate samples at three concentration levels of α-amanitin, as described in section 2.5.4.

The intra- and inter-assay precision for detection of α-amanitin in 5% perchloric acid, and rat liver and kidney matrices are presented in Table 2. As shown in Table 2, intra-assay precision for 5% perchloric acid matrix ranged from 1.15% to 2.75% (DAD) and 1.64% to 2.64% [25] whereas the inter-assay precision ranged from 5.57% and 6.10% (DAD) and 3.91% to 10.70% [25]. Intra-assay precision for liver matrix ranged from 0.61% to 8.65% (DAD) and 0.55% to 2.27% [25] whereas the inter-assay precision ranged from 3.54% to 15.30% (DAD) and 6.36% to 9.72% [25]. Finally, intra-assay precision for kidney matrix ranged from 1.73% to 8.16% (DAD) and 2.43% to 3.87% [25] whereas the inter-assay precision ranged from 2.63% to 11.59% (DAD) and 6.64% to 10.94% [25]. Acceptable RSD values (lower than 20%) were obtained for all concentration and for both detectors (DAD and EC), thus the developed method was sufficiently precise.

Table 2. Precision and accuracy results

α-amanitin (µg.mL^{-1})	Intra-assay precision RSD[a] (%) (n=6)	Inter-assay precision RSD[a] (%) (n=18)	Recovery (%)	RSD (%) (n=3)
305 nm				
Perchloric acid 5%				
0.84	2.75	6.10		
5	1.15	5.57		
7.5	1.65	5.66		
Liver				
0.5	8.65	15.30	99.99	2.49
5	3.97	4.27	98.48	2.00
7.5	0.61	3.54	99.89	0.21
Kidney				
0.82	8.16	11.59	101.06	2.13
5	2.18	6.30	99.42	1.05
7.5	1.73	2.63	99.69	0.90
Electrochemical detection				
Perchloric acid 5%				
0.84	2.13	3.91		
5	2.64	5.22		
7.5	1.64	10.70		
Liver				
0.5	2.27	7.49	99.87	3.41
5	1.65	6.36	99.80	1.03
7.5	0.55	9.72	96.87	3.21
Kidney				
0.82	3.87	10.94	99.49	1.99
5	3.60	8.99	98.19	2.16
7.5	2.43	6.64	101.45	2.62

3.2.5. Sensitivity

LOD and LOQ were evaluated and the obtained data are shown in Table 3. Based on visual evaluation, the LOD and LOQ values for 5% perchloric acid were 0.050 and 0.250 μg.mL^{-1} (DAD), and 0.025 and 0.025 μg.mL^{-1} [25], respectively. For liver matrix, the LOD and LOQ values were 0.050 and 0.250 μg.mL^{-1} (DAD) and 0.025 and 0.025 μg.mL^{-1} [25], respectively. For kidney matrix the LOD and LOQ values were 0.125 and 0.250 μg.mL^{-1} (DAD) and 0.05 and 0.100 μg.mL^{-1} [25], respectively. Based on the calibration curve, for 5% perchloric acid matrix, the LOD and LOQ values were 0.150 and 0.450 μg.mL^{-1} (DAD) and 0.060 and 0.190μg.mL^{-1} [25], respectively; for liver matrix the LOD and LOQ values were 0.100 and 0.330 μg.mL^{-1} (DAD) and 0.070 and 0.210 μg.mL^{-1} [25], respectively. Lastly, for kidney matrix, the LOD and LOQ values were 0.160 and 0.500 μg.mL^{-1} (DAD) and 0.040 and 0.110 μg.mL^{-1} [25], respectively.

Table 3. LOD and LOQ values (expressed as μg.mL^{-1}) computed according to different criteria

	Perchloric acid 5%	Liver	Kidney
305nm			
LOD			
Calibration Curve	0.150	0.110	0.160
Based on visual evaluation	0.050	0.050	0.125
LOQ			
Calibration Curve	0.450	0.330	0.500
Based on visual evaluation	0.250	0.250	0.250
Electrochemical			
LOD			
Calibration Curve	0.060	0.070	0.040
Based on visual evaluation	0.025	0.025	0.050
LOQ			
Calibration Curve	0.190	0.210	0.100
Based on visual evaluation	0.025	0.025	0.100

3.2.6. Matrix effect

The matrix effect was evaluated by comparing the slopes of the calibration curves obtained when processing standard 5% perchloric acid solutions and deproteinized liver and kidney samples spiked with standards in the same concentrations. No significant difference was found by comparing 5% perchloric acid and liver. On the other hand, there is a statistically significant difference ($p < 0.0001$) between the 5% perchloric acid standards and the α-amanitin renal spiked samples.

3.2.7. Stability

Stability of α-amanitin was investigated using 5% perchloric acid, liver and kidney matrices. α-Amanitin in all matrices was stable at room temperature and 4ºC over a period of 24h, with no significant degradation observed (Figure 3). On the other hand, in samples kept at room temperature, a degradation of α-amanitin was observed over the period of 14 days. Significant degradation was already observed at 7 days being more pronounced at 14 days. Values of α-amanitin declined to non-detectable concentrations at the 7th day at room temperature. In contrast, a slow degradation was observed in the case of α-amanitin samples stored at 4 ºC. However, a significant degradation was observed at 7 days being more pronounced at 14 days. Excellent stability was obtained either at -20 and -80 ºC as it can be seen in Figure 3. No significant degradation of α-amanitin in 5% perchloric acid, liver and kidney matrices was detected after storing the samples 14 days at -20 and -80 ◦ C. Moreover three freeze-thaw cycles did not cause significant degradation in 5% perchloric acid and in both biological matrices analyzed. Overall the results indicate that α-amanitin in tissue samples is stable during storage, extraction and chromatographic analysis. Moreover, we concluded that the samples can be safely stored at -20 ºC and can be subjected to at least three cycles of freeze-thaw without significant degradation of the analyte.

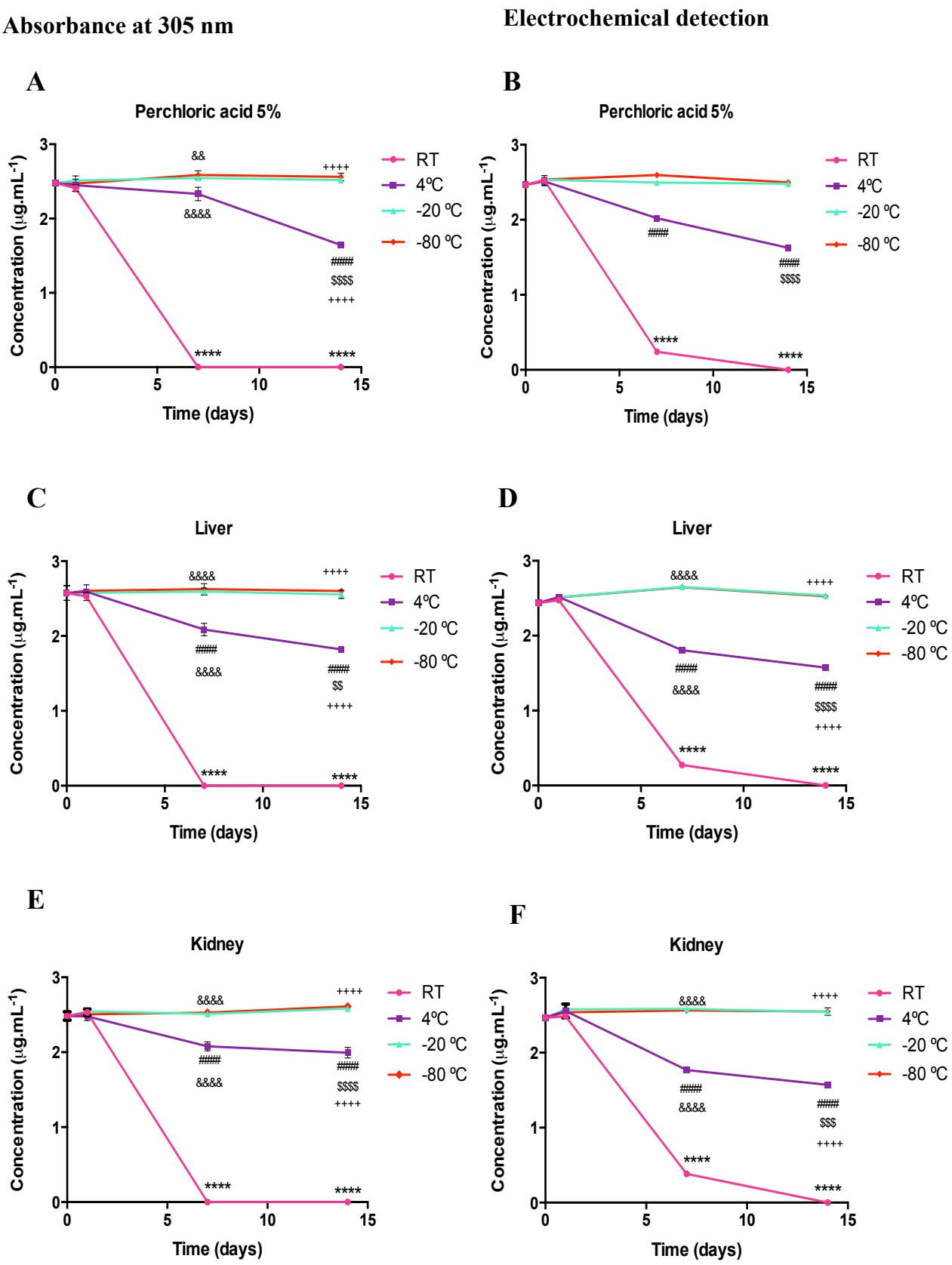

Figure 3. Stability study of α-amanitin on several matrices, temperatures, and time-points. Values of α-amanitin are represented as mean ± standard deviation (SD) of three

independent samples. Each matrix was analyzed by diode array (DAD) and electrochemical [25] after storage at different temperatures [room temperature (RT), 4°C, -20°C and, -80°C] over 1, 7 and 14 days. Stability of α-amanitin was evaluated in **(A,B)** 5% perchloric acid, **(C,D)** liver and **(E,F)** kidney matrices. Statistical analysis was performed using two-way ANOVA. If a statistical significance was achieved ($p < 0.05$), the Tukey's multiple comparisons test was performed. Significant differences (two-way ANOVA, followed by the Turkey's multiple comparisons test post-hoc test): $^{****}p < 0.0001$ vs. RT, time=0min; $^{\#\#\#\#}p < 0.0001$ vs. 4°C, time=0; $^{\$\$\$\$}p < 0.0001$ vs. 4°C, time=7 days; $^{\$\$\$}p < 0.001$ vs. 4°C, time=7 days; $^{\$\$}p < 0.01$ vs. 4°C, time=7 days; $^{\&\&\&\&}p < 0.0001$ 4°C vs -80°C, time= 7 days; $^{\&\&\&\&}p < 0.0001$ 4°C vs -20°C, time=7 days; $^{\&\&}p < 0.01$ 4°C vs -20°C, time=7 days; $^{++++}p < 0.0001$ 4°C vs -80°C, time= 14 days; $^{++++}p < 0.0001$ 4°C vs -20°C, time=14 days.

3.6. Method application

The established HPLC method was applied to human plasma. Figure 4 shows an EC chromatogram **(A)** and a chromatogram recorded at 305 nm **(B)** of blank plasma and plasma spiked to contain 5 μg.mL^{-1} of α-amanitin. There were no endogenous interfering substances in the samples.

A

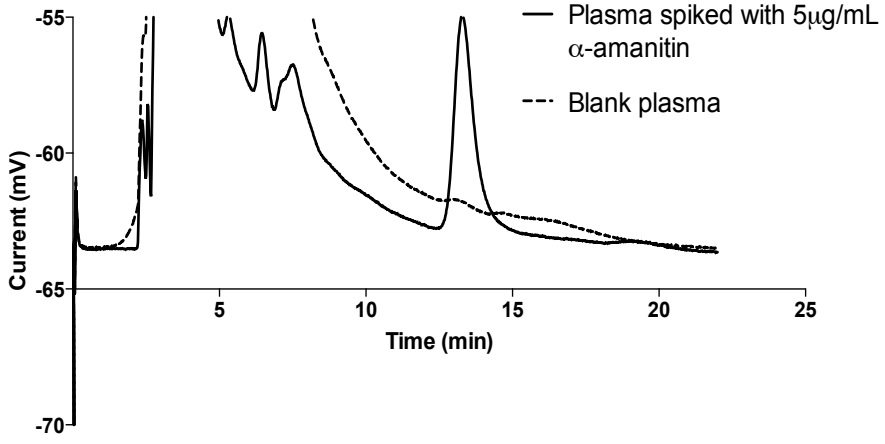

B

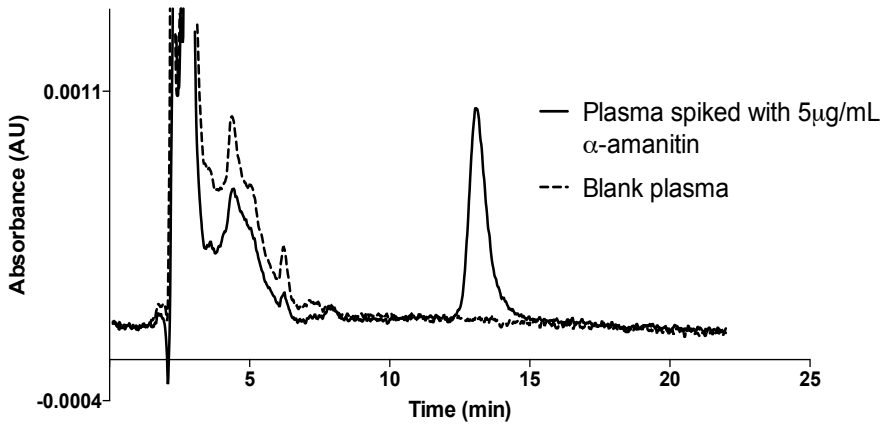

Figure 4. Representative EC chromatograms of **(A)** blank plasma and plasma spiked to contain 5 μg.mL^{-1} of α-amanitin. Representative chromatograms recorded at 305 nm of **(B)** blank plasma and plasma spiked to contain 5 μg.mL^{-1} of α-amanitin.

3.7. α-Amanitin quantification in kidney, liver and plasma after administration of the toxin to rats

The concentrations of α-amanitin in rat plasma and tissues were determined after administration of a single intraperitoneal (10 or 21.4 mg/kg) dose to Wistar rats. Representative EC chromatogram and chromatogram recorded at 305nm of kidney and their respective spiking with α-amanitin are show in Figure 5. Table 4 shows the values obtained by processing the plasma and tissues as indicated in section 2.4 and are expressed as ng of α-amanitin *per* mg of protein. The highest overall concentrations in the tissues examined were in the following order: kidneys> liver. No detectable values were found in plasma. Peak identity was confirmed by spiking samples with α-amanitin.

A

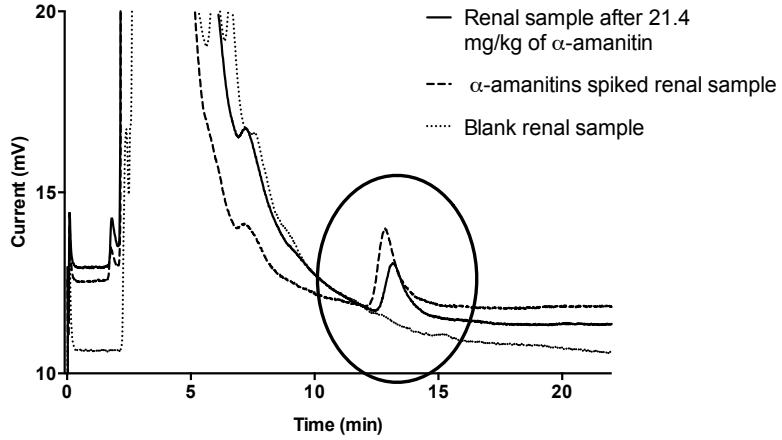

B

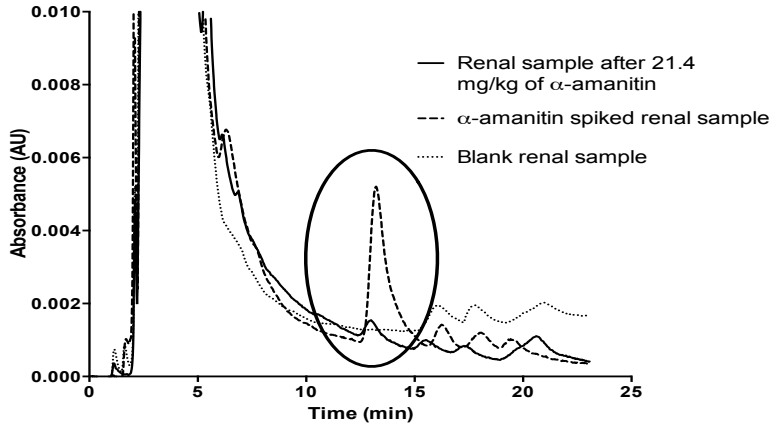

Figure 5. (A) Representative electrochemical chromatogram of rat kidney after an intraperitoneal administration of 21.4 mg. kg^{-1} of α-amanitin that was sacrificed 4 hours later. The same sample was spiked with α-amanitin. **(B)** Representative chromatogram recorded at 305 nm of rat kidney after an intraperitoneal administration of 21.4 mg. kg^{-1} of α-amanitin that was sacrificed 2 hours later. The same sample was spiked with α-amanitin.

Table 4. Quantification of α-amanitin in real samples (plasma, liver, and kidney) from rats injected with α-amanitin

	Plasma (ng.mg^{-1})	Liver (ng.mg^{-1})	Kidney (ng.mg^{-1})
305nm			
Rat (10 mg.kg^{-1} 4h)	N.D.	0.97	1.40
Rat (21.4 mg.kg^{-1} 2h)	N.D.	N.D.	3.16
Rat (21.4 mg.kg^{-1} 4h)	N.D.	0.71	26.58
Electrochemical			
Rat (10mg.kg^{-1} 4h)	N.D.	1.00	1.66
Rat (21.4 mg.kg^{-1} 2h)	N.D.	N.D.	4.00
Rat (21.4 mg.kg^{-1} 4h)	N.D.	0.80	33.74

4. Discussion

Several methods are available in the literature for the analysis and quantification of α-amanitin and in different matrices mainly mushrooms [11-15], plasma [19,28] and urine [21] due to the toxicological importance of this amatoxin. Research studies have been focused on the detection of α-amanitin in body fluids for an early diagnosis of intoxications as to allow the rapid application of therapy [16,19,21]. However, presently the overall toxic mechanisms of α-amanitin remain unclear, hindering the development of new and more effective antidotes, and relevant forensic studies on α-amanitin are scarce. Improved knowledge of the toxicity mechanisms and the kinetics of this toxin will help the development of more efficient antidotes for *A. phalloides* poisoning. Moreover, recent findings suggest that α-amanitin is emerging as an attractive new potent anticancer drug [10]. Therefore the efficacy of α-amanitin as an anticancer agent must be scientifically validated, through animal experiments that include pre-clinical pharmacokinetic and pharmacodynamic studies. However, the lack of analytical methods to quantify α-amanitin in body compartments hinders the quantification of this drug in tissues. To comprehensively characterize the mechanisms of toxicity, pre-clinical pharmacokinetics and efficacy of α-amanitin as anticancer agent, a highly sensitive, accurate, and reproducible quantification assay is required. To date there are no published HPLC

methodologies equiped with EC detector for the analysis of α-amanitin in biological tissues. The presence of a 6-hydroxytryptophan residue in the molecule of α-amanitin suggested the possibility of detecting this compound through an EC detector operating in an oxidative mode [21,28]. Herein, an isocratic HPLC method using DAD and EC detectors was developed and validated for the quantitative measurement of α-amanitin in rat liver and kidney tissues. The extraction of α-amanitin from the tissue homogenates was achieved by a deproteinization step using 5% perchloric acid followed by centrifugation, thus resulting in a simple, convenient and rapid separation of the analyte. Previously described extraction procedures of α-amanitin in liver samples using methylene chloride and acetonitrile are time-consuming use organic solvents and the resulting chromatograms are quite complex showing several interferences [19]. Herein, our procedure was also efficient with plasma samples, which indicates that this simple deproteinization step can be applied to other biological matrices. Deproteinization using 5% perchloric acid can be performed on any biological sample and can be routinely applied in many laboratories all over the world. Moreover, clean chromatograms were obtained, thus improving the analysis. In our method, the buffer of the mobile phase was also optimized. The buffer capacity, the type of detectors used (DAD and EC), the stability of the solution, the solubility and the column were taken into account. Defendenti *et al* (1998) developed and validated a HPLC method with EC detection to measure α-amanitin in urine. For this purpose the authors used a mobile phase composed of phosphate buffer and acetonitrile. One of the major problems with phosphate buffers is the precipitation of phosphates in the HPLC system. As an alternative, we used citrate as a buffer of the mobile phase. Citrate can be used in a wide range of pH (2.1 <pH <6.4) and provides low background noise, which is mainly important electrochemical analysis [23,26]. The ratio of citrate:methanol (80:20) and the pH 5.5 were key to obtain good separation and resolution of the α-amanitin peak. Moreover, the short run time of 22 min enables a large number of samples to be analyzed in a short period of time. Furthermore, the method was highly specific since liver, kidney and plasma samples analyzed did not exhibited chromatographic peaks corresponding to endogenous compounds co-eluting with the target analyte. Calibration curves over the entire ranges of concentrations were adequately described by 1/concentration weighted quadratic regression of the peak–area ratios of α-amanitin, with regression coefficient r^2 always greater than 0.994 in all analytical runs. This shows that our method was linear and a broad range of concentrations can be used. Extraction recovery at a concentrations ranging from 0.5-7.5 $\mu g.mL^{-1}$, results in an overall mean percent recovery of above 96 %. This recovery gives a great deal of confidence as this method can be applied into intoxicated humans, in terms of forensic analysis as well as to post-mortem tissues and confirm the etiology of symptoms.

Considering that intra-assay variations (expressed as RSD), higher variability was found as the analyte levels were lower (Table 2) whereas inter-assay variations (expressed as RSD), higher variability was found in the higher analyte levels (Table 2). Results show an overall RSD of 15.30%, making the developed method precise. The LOD and LOQ values were obtained using two different criteria as to make it comparable to those found in the literature (Table 3) [25]. The values based on visual evaluation are slightly lower than the LOD and LOQ calculated from the linear regression parameters (Table 3). In previous reports, the LOD was about 10 $ng.ml^{-1}$ (corresponding to a signal-to-noise ratio of 25) for urine by HPLC–UV [16], 2 $ng.mL^{-1}$ (corresponding to a signal-to-noise ratio of 2) for plasma by HPLC-EC [28], although most of these methods are specific for a certain matrix. In other matrices our LOD values are comparable with the results by the above methods. To the best of our knowledge, there is only one published study using liver tissue to detect α-amanitin and was made using LC-MS/MS/MS [19]. In that study, liver was prepared by homogenization with aqueous acetonitrile and subsequent removal of acetonitrile using methylene chloride. The aqueous phase was then extracted using solid phase extraction cartridges and α-amanitin was detected with a LOD of about 0.50 $ng.g^{-1}$. The LC-MS/MS/MS method offered the highest specificity and sensitivity, however HPLC–MS instruments are not available in many laboratories. The concentration of α-amanitin in liver and kidney tissues poisoning cases analyzed by HPLC-UV show high variance (0-1719 $ng.g^{-1}$) [29], which indicates that our method is sensitive enough for the quantification of α-amanitin in liver and kidney from suspected human intoxications.

The comparison between the two detectors (DAD and EC) shows that the LOD and LOQ for α-amanitin could be improved through the use of an EC detector. Nevertheless, HPLC-EC instruments are not available in many laboratories. For that reason, validation using UV detector was made since it is a more common instrument all over the world. Moreover does not require a long period of stabilization as it happens with EC detector.

Evaluation of the matrix effect shows that there is a difference between the HPLC response for α-amanitin in 5% perchloric acid and the response for the α-amanitin in kidney matrix. This is probably due to residual components of the kidney matrix, thus demonstrating the importance of the study on equivalent matrices. On the other hand, no statistical difference was found between 5% perchloric acid and liver matrix.

The results of all stability tests indicated that α-amanitin in 5% perchloric acid and tissue samples was stable during sample storage, extraction and chromatographic analysis. Evaluation of more than one freeze–thaw cycle was performed in case that samples require multiple analysis. Three freeze thaw cycles also did not cause any significant degradation in all matrices when stored in acidic matrix. The tissue collection can be done after acidification since our data show that α-amanitin was stable at room temperature

and 4 ºC over a 24 hour period. No liquid nitrogen or urgent freezing seems to be required, making this method very practical and reliable in all laboratories and clinical settings.

As to prove the applicability of our method we performed an *in vivo* study with different α-amanitin doses and sacrifice times. After the intraperitoneal administration of a single dose of α-amanitin (10 or 21.4 mg/kg) to Wistar rats, the validated analytical method was successfully applied. In rats, there are no α-amanitin pharmacokinetic data available at this point. Therefore based on *in vivo* studies [8,30], in murine models we selected the 2 and 4 hours post-administration periods to perform sample collection. The toxicokinetic of α-amanitin has been studied in intoxicated humans and dogs and shows a short half-life (is totally eliminated from the blood after 41.02 minutes), being widely distributed to target tissues (liver and kidney). Our method was able to detect α-amanitin in several samples. The short half-time of α-amanitin was confirmed, as no analyte was found in plasma. Our results show higher levels of total α-amanitin in kidney than in liver. These differences may be explained by the fact that the kidney serves as an elimination organ of α-amanitin.

Of interest, this method was also successfully applied to quantify α-amanitin in human plasma since there were no endogenous substances in the samples co-eluting with the peak of interest. Considering this, we suggest that this method can be used for early diagnosis of *A. phalloides* poisoning, tissues analysis and other pharmacokinetic studies. In fact, this method is a suitable tool to support *in vivo* toxicokinetic studies designed to elucidate the mechanisms of toxicity of α-amanitin, being able to assist in the development of novel and potent antidotes for amatoxin's poisoning.

5. Conclusion

A selective and sensitive HPLC method using DAD and EC detectors has been developed and validated for the quantitative measurement of α-amanitin in 5% perchloric acid, rat liver and kidney. The extraction of α-amanitin from tissue homogenates was achieved by a simple deproteinization step with a high recovery of the analyte. Validation was carried out by the evaluation of the most relevant parameters for checking the quality of the method. The method proved to be linear in the concentration range studied as well as selective, accurate, precise and sensitive. All stability tests indicated that α-amanitin was stable during sample storage, extraction, and chromatographic analysis. Moreover this method was successfully applied to real samples, after α-amanitin administration to Wistar rats. Taken together, these characteristics combined with a short chromatographic run time of 22 min, allows this assay to be easily applied for the determination of α-

amanitin in liver and kidney and other biological samples. This method provides a convenient tool for the future toxicological and clinical studies involving α-amanitin.

Acknowledgments

This work received financial support from the European Union (FEDER funds through COMPETE) and National Funds (FCT, Fundação para a Ciência e Tecnologia) through project Pest-C/EQB/LA0006/2013.

Juliana Garcia and Vera Marisa Costa thank FCT - Foundation for Science and Technology -for their PhD grant (SFRH/BD/74979/2010) and Post-doc grant (SFRH/BPD/63746/2009), respectively.

Table legends

Table 1. Calibration data resulting from linear least squares regression analysis for the determination of α-amanitin in perchloric acid 5% and tissue samples. Slope of calibration curves, intercept, and the determination coefficients were calculated.

Table 2. Method precision was evaluated by the intra-assay repeatability and intermediate precision (inter-assay). To determine intra-assay and inter-assay precision, different concentrations of α-amanitin (low, middle and high) were used by spiking blank liver and kidney samples and performing several replicates (n=6). The precision was reported as the relative standard deviation (% RSD). Recovery was used to further evaluate the accuracy of the method.

Table 3. Limits of detection (LOD) and quantification (LOQ) of α-amanitin in perchloric acid 5%, liver and kidney samples based on two criteria. The two criteria adopted were based on visual evaluation and on the standard deviation of the response and slope of the calibration curve.

Table 4. Quantification of α-amanitin in real samples (plasma, liver, and kidney) obtained from Wistar rats exposed to α-amanitin. Two different concentrations of α-amanitin (10 mg/kg and 21.4 mg/kg) and two different time points (2 and 4 hours) were used.

References

[1] J. Vetter, Toxicon 36 (1998) 13.
[2] A.W. Hayes, Principles and Methods of Toxicology, Fifth Edition, Taylor & Francis, 2008.
[3] T.J. Lindell, F. Weinberg, P.W. Morris, R.G. Roeder, W.J. Rutter, Science 170 (1970) 447.
[4] A. Zheleva, A. Tolekova, M. Zhelev, V. Uzunova, M. Platikanova, V. Gadzheva, Med Hypotheses 69 (2007) 361.
[5] F. Enjalbert, S. Rapior, J. Nouguier-Soule, S. Guillon, N. Amouroux, C. Cabot, J Toxicol Clin Toxicol 40 (2002) 715.
[6] J. Magdalan, A. Ostrowska, A. Piotrowska, A. Gomułkiewicz, A. Szeląg, P. Dzięgiel, Arch Toxicol 83 (2009) 1091.
[7] P. Poucheret, F. Fons, J.C. Dore, D. Michelot, S. Rapior, Toxicon 55 (2010) 1338.
[8] T.C. Tong, M. Hernandez, W.H. Richardson, 3rd, D.P. Betten, M. Favata, R.H. Riffenburgh, R.F. Clark, D.A. Tanen, Ann Emerg Med 50 (2007) 282.
[9] J. Garcia, A.T.P. Carvalho, D.F.A.R. Dourado, P. Baptista, M. de Lourdes Bastos, F. Carvalho, J Mol Graphics Modell 51 (2014) 120.
[10] G. Moldenhauer, A.V. Salnikov, S. Luttgau, I. Herr, J. Anderl, H. Faulstich, J Natl Cancer Inst 104 (2012) 622.
[11] F. Enjalbert, G. Cassanas, G. Guinchard, J.P. Chaumont, Mycologia 88 (1996) 909.
[12] F. Enjalbert, G. Cassanas, S. Rapior, C. Renault, J.P. Chaumont, Mycologia 96 (2004) 720.
[13] F. Enjalbert, G. Cassanas, S.L. Salhi, C. Guinchard, J.-P. Chaumont, Comptes Rendus de l'Académie des Sciences - Series III - Sciences de la Vie 322 (1999) 855.
[14] F. Enjalbert, C. Gallion, F. Jehl, H. Monteil, Toxicon 31 (1993) 803.
[15] F. Enjalbert, C. Gallion, F. Jehl, H. Monteil, H. Faulstich, J Chromatogr A 598 (1992) 227.
[16] F. Jehl, C. Gallion, P. Birckel, A. Jaeger, F. Flesch, R. Minck, Anal Biochem 149 (1985) 35.
[17] E. Kaya, M.G. Surmen, K.O. Yaykasli, S. Karahan, M. Oktay, H. Turan, S. Colakoglu, H. Erdem, Cutan Ocul Toxicol 14 (2013) 14.
[18] W.C. Chung, S.C. Tso, S.T. Sze, J Chromatogr Sci 45 (2007) 104.
[19] M.S. Filigenzi, R.H. Poppenga, A.K. Tiwary, B. Puschner, J Agric Food Chem 55 (2007) 2784.
[20] D. Jansson, S.A. Fredriksson, A. Herrmann, C. Nilsson, Forensic Sci Int 221 (2012) 44.
[21] C. Defendenti, E. Bonacina, M. Mauroni, L. Gelosa, Forensic Sci Int 92 (1998) 59.
[22] R. Singh, J Adv Pharm Educ Res 4 (2013) 26.
[23] L.R. Snyder, J.J. Kirkland, J.L. Glajch, Practical HPLC Method Development, Wiley, 2012.
[24] O.H. Lowry, N.J. Rosebrough, A.L. Farr, R.J. Randall, J Biol Chem 193 (1951) 265.
[25] ICH, 1996.
[26] V.M. Costa, R. Silva, L.M. Ferreira, P.S. Branco, F. Carvalho, M.L. Bastos, R.A. Carvalho, M. Carvalho, F. Remião, Chem Res Toxicol 20 (2007) 1183.
[27] P.W. Morris, D.L. Venton, K.M. Kelley, Biochemistry 17 (1978) 690.
[28] F. Tagliaro, G. Schiavon, G. Bontempelli, G. Carli, M. Marigo, J Chromatogr B Biomed Sci Appl 563 (1991) 299.
[29] A. Jaeger, F. Jehl, F. Flesch, P. Sauder, J. Kopferschmitt, J Toxicol Clin Toxicol 31 (1993) 63.
[30] S.M. Schneider, E.A. Michelson, G. Vanscoy, J Appl Toxicol 12 (1992) 141.

Study III

Co-ingestion of amatoxins and isoxazoles-containing mushrooms and successful treatment: A case report

(Submitted for publication)

Co-ingestion of amatoxins and isoxazoles-containing mushrooms and successful treatment: A case report

Juliana Garcia[a*], Vera M. Costa[a], Ana Elisa Costa[b], Sérgio Andrade[c], Ana Cristina Carneiro[c], Filipe Conceição[c], José Artur Paiva[b], Paula Guedes de Pinho[a], Paula Baptista[d], Maria de Lourdes Bastos[a], Félix Carvalho[a*]

[a]UCIBIO-REQUIMTE/ Laboratory of Toxicology, Department of Biological Sciences, Faculty of Pharmacy, University of Porto, Rua José Viterbo Ferreira nº 228, 4050-313 Porto, Portugal.

[b] Internal Medicine Service São João Hospital Center, 4200-319 Porto. Portugal.

[c] Intermediate Care Unit of Emergency Service, São João Hospital Center, 4200-319 Porto, Portugal.

[d]CIMO/School of Agriculture, Polytechnic Institute of Bragança, Campus de Santa Apolónia, Apartado 1172, 5301-854 Bragança, Portugal.

* Authors to whom correspondence should be addressed (Tel.: + 351 220428597; Fax: + 351 226093390; e-mail: jugarcia_18@hotmail.com and felixdc@ff.up.pt

Abstract

Mushrooms poisoning occurs when ingestion of wild mushrooms containing toxins takes place putting the consumers at life-threatening risk. In the present case report, an unusual multiple poisoning with isoxazoles- and amatoxins-containing mushrooms in a context of altered mental state and poorly controlled hypertension is presented. A 68-year-old female presented to São João hospital (Portugal) with complaints of extreme dizziness, hallucinations, vertigo and imbalance, 3 hour after consuming a stew of wild mushrooms. The first observations revealed altered mental state and elevated blood pressure. The examination of cooked mushroom fragments allowed a preliminary identification of *A. pantherina*. Gas chromatography–mass spectrometry (GC-MS) showed the presence of muscimol in urine. Moreover, through high-performance liquid chromatography-ultraviolet detection (HPLC-UV) analysis of the gastric juice it was revealed the presence of α-amanitin, indicating that amatoxins-containing mushrooms were also included in the stew. After 4 days of supportive treatment, activated charcoal, silybin and N-acetylcysteine, the patient recovered being discharged 10 days post-ingestion with no organ complications. The prompt and appropriate therapy protocol for life-threatening amatoxins toxicity probably saved the patient's life as oral absorption was decreased and also supportive care was immediately started.

Keywords: Wild mushrooms; *Amanita pantherina; Amanita phalloides;* isoxazoles, amatoxins, intoxication

Abbreviations

CNS	Central Nervous System
DAD	Diode-array
EC	Electrochemical coulometric detection
DNA	Deoxyribonucleic acid
GC-MS	Gas chromatography-mass spectrometry
HPLC	High Performance Liquid Chromatography
RNA	Ribonucleic acid
RNAP II	RNA polymerase II
TIC	Total ion chromatogram
UV	Ultraviolet

1. Introduction

An altered mental state is a very common occurence in the emergency room and the diagnosis/treatment is highly challenging (Xiao et al., 2012). In fact, two or more etiologies may coexist, including pathological disorders, (e.g. hypoglycemia; cranial trauma; alcohol; infection; psychoses; stroke; hypertensive, metabolic, hepatic, or uremic encephalopathies), consumption of psycho-active substances; and others (Schwartz et al., 1992). Among these, possible accidental or intentional exposure to psycho-active substances present in some wild mushrooms species should not be neglected (Tsujikawa et al.). In fact, consumption of wild mushrooms has increased substantially in the last decades (Thimmel and Kluthe, 1998). Mushrooms are appreciated worldwide as a delicacy, due to their exquisite palatability and texture. Moreover, their chemical, nutritional, and functional properties make them exceptional in the human diet (Cheung, 2010). Despite these benefits, the ingestion of wild mushrooms containing toxins frequently occurs, which can put the consumers at life-threatening risk. Mushroom poisoning is usually accidental, rarely suicidal, and frequently occurs as a result of misidentification of a toxic mushroom as an edible species (Barbato, 1993; Cochran, 1987). The severity of mushroom poisoning depends on the species of mushroom, the amount of mushroom consumed, the prompt therapy and the health status of the individual (Broussard et al., 2001; Durukan et al., 2007). The main toxins associated to mushroom poisoning are: cyclopeptides, orellanine, gyromitrin, isoxazoles, muscarine, psilocybin and gastrointestinal specific irritants (Koppel, 1993). Of the mentioned toxins, the most dangerous and potentially fatal poisonings are caused by cyclopeptides (mainly amatoxins) (Karlson-Stiber and Persson, 2003), while orellanine, isoxazoles, muscarine, psilocybin, and gyromitrin can cause a serious illness but are rarely fatal (Koppel, 1993). Amatoxins are natural toxic bicyclic octapeptides present in mushroom species from three different genera: *Amanita*, *Galerina*, and *Lepiota* (Vetter, 1998). The species *A. phalloides* is involved in the majority of human fatal cases of mushroom poisoning (Karlson-Stiber and Persson, 2003). Its main toxin is α-amanitin, which causes hepatic and kidney damage, often fatal (Faulstich, 1979; Klein et al., 1989; Santi et al., 2012). The mechanisms of toxicity of α-amanitin are complex, but its most known mechanism is the inhibition of RNA polymerase II (RNAP II) (Vetter, 1998).

Muscimol and ibotenic acid belong to the family of toxins known as isoxazoles. *Amanita pantherina* and *A. muscaria* are the most commonly known isoxazoles-containing mushrooms (Diaz, 2005). Data on the incidence of intoxication by isoxazoles-containing mushrooms are scarce. The severity of the symptoms is mild, thus intoxicated people often do not seek medical attention. In Portugal, only a few cases of isoxazoles-containing mushrooms intoxications have been reported (Morgado et al., 2006). The American

Association of Poison Control Centers annual report of 2012 presents 36 cases of isoxazoles-containing mushroom intoxications in the United States of America, with no death cases associated (Mowry et al., 2013). Ibotenic acid is an agonist of glutamic acid receptors; its decarboxylated derivative, muscimol, is an agonist at gamma-aminobutyric acid (GABA) receptors. The central effects of these toxins are generally attributed to these pharmacological properties (Krogsgaard-Larsen et al., 1980; Michelot and Melendez-Howell, 2003; Snodgrass, 1978) and include hallucinations, confusion, dizziness, visual and auditory aesthesia (hypersensitivity), space distortion, and unawareness of time (Michelot and Melendez-Howell, 2003).

In this work, we describe a case of a 68-years-old patient with poorly controlled hypertension and altered mental state after eating wild mushrooms, and the respective clinical management of the case. The suspicion of a hypertensive crisis and isoxazoles- and amatoxins-containing mushrooms poisoning were taken into consideration in the medical decisions.

2. Case report

A 68-years-old female with hypertension was admitted to the emergency room of São João Hospital (Porto, Portugal) after ingestion of mushrooms. After specific query, her son reported that the patient had ingested several wild mushrooms that where collected in a public yard by the patient. She stewed the mushrooms, and, immediately after ingestion, she started experiencing dizziness, vertigo and imbalance. She self-induced vomiting and had no symptoms of nausea, spontaneous vomiting or diarrhea. On admission, 3 hours post-ingestion, the examination revealed an altered mental status including confusion and repetitive speech, only responsive to severe painful stimuli, and mydriatic pupils. These symptoms resolved in a few hours after admission. Initial emergency room vital signs were: blood pressure 230/108 mmHg, normal pulse and respiratory rate, temperature 96.8 degrees Fahrenheit, and oxygen saturation of 97.5 percent using an oxygen mask at 10L/min. Physical exam demonstrated dry skin and dry mucous membranes. Additionally, she had clear breath and heart sounds, no abdominal tenderness, and no gross focal neurologic deficits. A brain computed tomography was immediately performed revealing no abnormalities. Additionally, electrocardiogram, funduscopy and urinary sediment were analyzed demonstrating no evidence of lesions. Her serial hematological parameters, coagulation profile, liver and renal function tests were normal and are in Table 1.

Table 1. Clinical parameters over three days post-ingestion

Parameters	1st day[a]	3rd day	Reference values[b]
Hematological parameters			
White blood cell count (x 10^9/L)	6.69	6.98	4-11
Mean Corpuscular Volume (fL)	88.4	89.0	87-103
Mean Corpuscular Hemoglobin (pg)	30.8	31.2	27-35
Mean Corpuscular Hemoglobin Concentration (g/dL)	34.8	35.1	28-36
Platelet Count (x 10^9/L)	212	187	150-400
Red Cell Distribution (%)	12.5	13.0	11-16 (Width-coefficient of variation %)
Red Cell Distribution (fL)	40.0	42.1	37-54 (Width-standard deviation)
Red Blood Cell Count (x10^{12}/L)	4.84	4.29	12.0-16.0
Hemoglobin (g/dL)	14.9	13.4	12.0-16.0
Blood Chemistry Tests			
Lactate dehydrogenase (U/L)	273	182	135-225
Albumin (g/L)		34.2	38-51
Alanine aminotransferase (U/L)	38.0	24.0	10-31
Aspartate aminotransferase (U/L)	31.0	34.2	10-31
Alkaline phosphatase (U/L)	102	75.0	30-120
Total bilirubin (mg/dL)	1.06	2.00	< 1.2
Conjugated bilirubin (mg/dL)	0.50	0.52	<0.4
Gamma-glutamyl transpeptidase (U/L)	74.0	53.0	7-32
Creatine phosphokinase (U/L)	193	88.0	10-149
Urea (mg/dL)	36.0	21.0	10-50
Creatinine (mg/dL)	0.74	0.55	0.51-0.95
Ammonia (μmol/L)	30.0	45.0	
Amylase (U/L)	38.0		22-80
Lipase (U/L)	22.0	36.0	7-60
Activated Partial Thromboplastin Time (s)	30.1	30.4	24.5-36.5
Prothrombin Time (s)	12.5	11.5	9.5-13.8
Fibrinogen (mg/dL)	506	557	190-400
C-reactive protein (mg/L)	8.80	20.5	<3.0

[a] Clinical parameters three hours post-ingestion
b Reference values adopted by São João Hospital

As a standard procedure for intoxications with wild mushrooms, until species identification by laboratory, the general detoxification treatment with oral-activated charcoal was immediately instituted on admission, and it was followed by the specific treatment for *A. phalloides* poisoning, through the administration of silybin and N-acetylcysteine. N-acetylcysteine and silybin were administered in a loading dose of 10.5 g (150 mg/kg) and 350 mg (5 mg/kg), respectively, followed by perfusion. The perfusion of silybin was maintained at a dosage of 58 mg/h (20 mg/kg/d) and N-acetylcysteine at 875 mg/h (12.5 mg/kg/h) for the following 4 hours. Labetalol perfusion was also administered for blood pressure control. The patient was then transferred to intermediate care unit to continue with the treatment with continuous surveillance. A total of 300 mg/kg of N-acetylcysteine was administered in the first 21 hours after admission. The perfusion of activated charcoal and silybin were kept until the fourth day in which day a normal coagulation profile and liver function were observed). Serum aminotransferases and coagulation profile were normal during all the time that surveillance was maintained, although an elevation of total bilirubin (twofold the normal value) was observed at day 2 (conjugated bilirubin was normal at that time). Two days after, total bilirubin level started to decline, and it normalized within one week. After labetalol perfusion, the blood pressure control was achieved by administration of sublingual captopril until the fourth day.

The patient kept some of the stew after ingestion, which was then provided for analysis. The identification of the mushrooms was firstly performey 2 experts based on the macroscopic features of the fruiting body (Courtecuisse, 1999; Courtecuisse and Duhem, 2005). In the stewed mushrooms, the color of some of the cap fragments resembled *A. pantherina,* namely brown with whitish-brown warts (Figure 1). The gills were free and whitish-brown color and the stipe was cylindrical and seemed to be white.

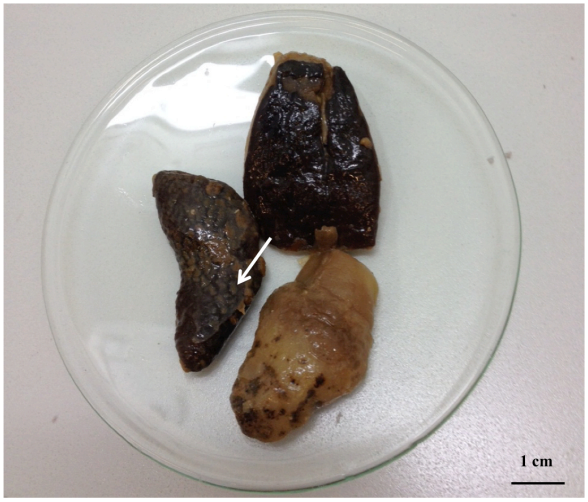

Figure 1. Macroscopic identification of *Amanita pantherina* found in the stew, showing a mushroom fragment (left), with its characteristic features. The cap fragments are brown with whitish-brown warts (white arrow). The stipe is cylindrical.

Therefore, to confirm the intoxication by *A. pantherina*, we looked for the presence of muscimol in the urine. Gas chromatography–mass spectrometry (GC-MS) analysis confirmed the presence of muscimol (Figure 2) in the patient's urine. These data allowed to identify the putative responsible for the patient's hallucinogenic effects, since she possibly ingested ibotenic acid and muscimol-containing mushrooms.

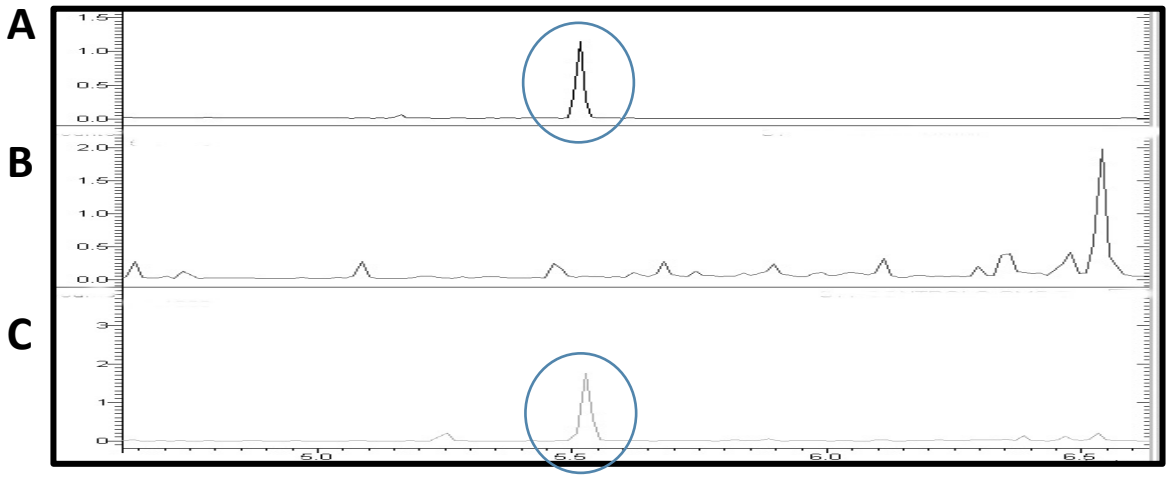

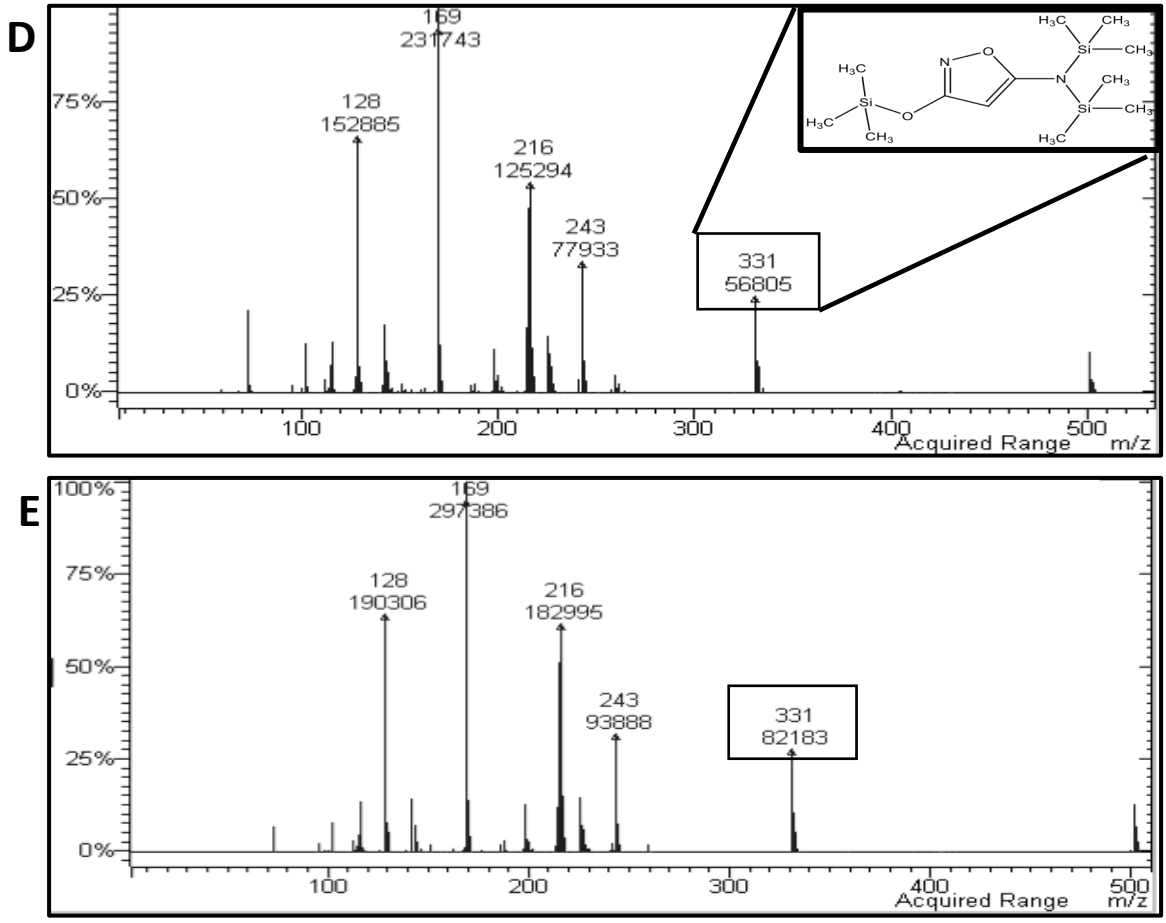

Figure 2. Zoomed views for the part of GC-MS total ion chromatograms corresponding to peak of muscimol after the derivatization. A) muscimol standard, B) blank urine, and C) patient's urine. Mass spectrum of D) derivatized muscimol standard and E) patient's urine. The molecular ion m/z 331 and chemical formula of derivatized muscimol are represented.

As a result of the severity of possible *A. phalloides* intoxication, the presence of the main toxin of this mushroom was investigated in the biological fluids (urine and gastric juice) and in the mushrooms collected. α-Amanitin was identified in the gastric fluid by high-performance liquid chromatography with ultraviolet detection (Figure 3), as previously described (Garcia et al., 2014). The α-amanitin levels in the gastric fluid were 1.12 μg/mL, whereas no detectable levels of α-amanitin were found in the urine [the methods limit of detection is 0.05 μg/mL (Garcia et al., 2014)].

In the fifth day after mushroom ingestion, the patient was discharged from the intermediate care and transferred to the ward without evidence of liver abnormalities and with better blood pressure control. Ten days post-ingestion the patient was discharged home with no organ complications.

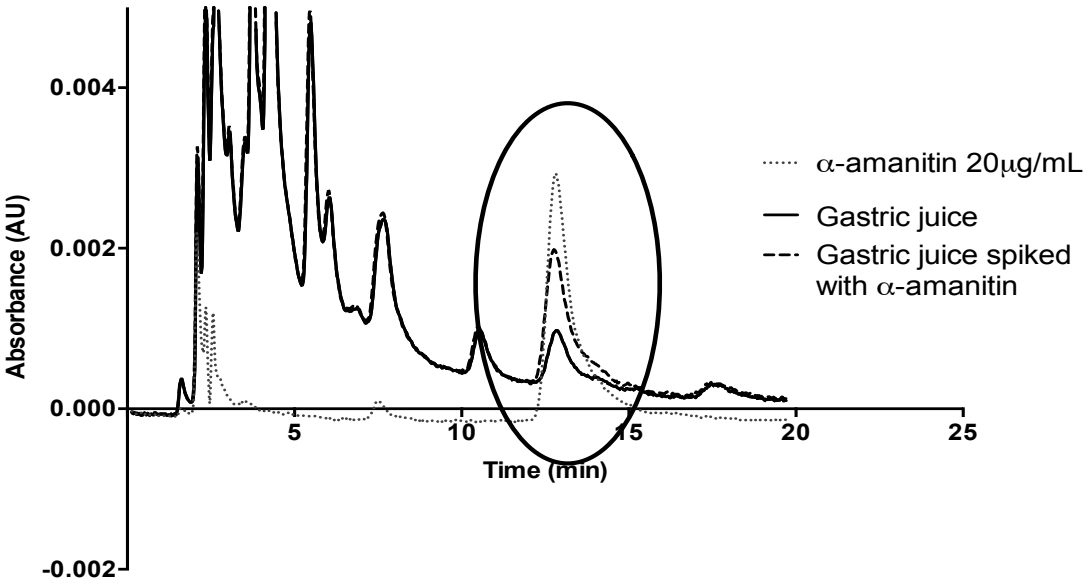

Figure 3. Chromatogram of the patient's gastric juice recorded at 305 nm superposed to the chromatograms of the same sample spiked with α-amanitin and standard solution of 20 μg/mL of α-amanitin.

3. Discussion

Altered mental status comprises clinical symptoms including cognitive disorders, attention disorders, arousal disorders, and decreased level of consciousness (Xiao et al., 2012). It is a very common situation in the emergency room, and has many possible causes including pathological disorders and consumption of psycho-actives substances (Xiao et al., 2012). In the case presented herein, the high blood pressure in association with altered mental status lead to suspicion of a hypertensive crisis case. However, the clinical evaluation showed no lesion of target organs (normal brain computed tomography, electrocardiogram, funduscopy and urinary sediment), thus that hypothesis was discarded. At the same time, the history of wild mushroom consumption implied measures to counteract its putative life-threatening toxicity. Worldwide most cases of intoxications by wild mushrooms have been attributed to amatoxin-containing mushrooms (Brandão et al., 2011; Mowry et al., 2013), with only a very small percentage of cases attributed to ibotenic acid and muscimol-containing mushrooms (Morgado et al., 2006; Mowry et al., 2013).

In the case presented herein, the features of the clinical presentation are consistent with the diagnosis of intoxication by isoxazoles-containing mushrooms. Positive identification of *A. pantherina* mushroom, found in the patient's home, was accomplished by 2 experts. This species contains the toxins ibotenic acid and muscimol (Michelot and Melendez-Howell, 2003). Ibotenic acid is metabolized to muscimol (Michelot and Melendez-Howell, 2003) and the presence of muscimol was confirmed in the patient´s urine sample. Muscimol and ibotenic acid cross the blood-brain barrier exerting their effects primarily on the Central Nervous System (CNS), where they act as neurotransmitter agonists (Michelot and Melendez-Howell, 2003). Ibotenic acid mimics the excitatory amino acid glutamic acid and acts on N-methyl-D-aspartic acid (NMDA) receptors. Muscimol is a potent agonist of $GABA_A$ receptors and also exerts CNS effects (Michelot and Melendez-Howell, 2003). Nausea, hallucinations, delirium, and sleepiness are often described after isoxazoles-containing mushrooms ingestion (Diaz, 2005; Satora et al., 2006). The toxic threshold estimated for ibotenic acid and muscimol is 30-60 mg and 6 mg, respectively (Halpern, 2004) and these amounts can be found in a single mushroom (Rumack and Spoerke, 1994). At this point, the toxicokinetics of muscimol and ibotenic acid remains largely unknown, but based on the rapid onset of symptoms after mushrooms ingestion, a fast absorption of toxins is presumed. Moreover, the toxins are readily excreted in urine, where they can be detected within 1 hour after ingestion (Stribrny et al., 2012). Clinical symptoms have been reported 30 min to 2 hours after ingestion and include nausea, hallucinations, delirium, muscular spasm, and sleepiness (Diaz, 2005; Satora et al., 2006). The CNS effects are usually short-lived, and fatalities rarely occur (Benjamin, 1992; Diaz,

2005), thus the recommended treatment after isoxazoles-containing mushrooms consists of eliminating the toxins from gastrointestinal tract, administration of activated charcoal, and supportive measures to alleviate CNS symptoms (Michelot and Melendez-Howell, 2003). Even when the intoxication symptoms largely indicate a self-limited mushroom intoxication, if the patient's meal contained wild mushrooms, the possible presence of amatoxins should be taken into consideration in the medical protocol to be followed. Amatoxins are a group of toxic bicyclic octapeptides present in the genus *Amanita*. α-Amanitin is considered the main responsible for the human toxic effects. Upon ingestion, α-amanitin binds to the RNAP II enzyme, inhibits the transcription process and, ultimately, causes cell death. The main target organ seems to be the liver, as α-amanitin undergoes enterohepatic circulation (Letschert et al., 2006) but the kidneys can also be compromised (Amini et al., 2011). In the liver, α-amanitin causes broad necrosis that results in acute hepatic failure and further complications, such as hepatic coma, coagulation disorders, and renal failure (Enjalbert et al., 2002). The estimated lethal dose of amatoxins in humans is about 0.1 mg/kg body weight, or even lower, and this lethal amount may be present in a single mushroom (Faulstich, 1980). Upon ingestion, amatoxins seem to be gradually absorbed from the gastrointestinal tract. In the present case, the patient was taken to the hospital emergency room 3 hour after mushrooms ingestion and the presence of α-amanitin was confirmed in gastric juice but not in urine. We can presume that the fast CNS symptoms elicited the hospital attendance even before the amatoxins were fully absorbed. The gastric lavage undertaken in the hospital settings, as it was immediately performed, decreased or even abrogated the absorption of the toxins. The clinical course after amatoxins intoxication is initially characterized by a latent period followed by gastrointestinal symptoms, which include nausea, diarrhea and vomiting. However, no amatoxins toxicity signs or symptoms are usually found until 6-24 hours after ingestion (Enjalbert et al., 2002). Presently, there is currently no specific and effective antidote for *A. phalloides* poisoning but several therapeutic drugs are used to protect the target organs of amatoxins poisoning. Intravenous silybin is the pharmacologic treatment of choice in Europe (Mengs et al., 2012) and USA (French et al., 2011). Other therapies have been suggested and includ benzylpenicillin, ceftazidime, or N-acetylcysteine (Enjalbert et al., 2002). The administration of silybin used in amatoxin poisoning cases is based on its strong antioxidant activity and the ability of stimulate RNA polymerase I, counterbalancing the activity inhibition of RNAP II (Fraschini et al., 2002), whereas N-acetylcysteine's potential therapeutic effect is due to its known antioxidant activity (Montanini et al., 1999).

Since α-amanitin undergoes extensive enterohepatic recycling, repeated doses of activated charcoal were, also, administered, to enhance the elimination. The administration of

activated charcoal had implications in the choice of the route of administration of the antihypertensive drug to be used. Activated charcoal may prevent the absorption of orally administered therapeutic agents; therefore sublingual captopril was administered..

In summary, in the present case, the treatment of a patient that suffered mushroom intoxication was immediately started after patient's admission and consisted of gastric lavage, oral-activated charcoal, silybin and N-acetylcysteine, and anti-hypertensive therapy. It can be inferred that the early hospitalization, rapid diagnosis and aggressive management concurred for the successful of the therapy after *A. phalloides* lethal mushroom poisoning. Every effort should be made to identify the toxins present in the mushrooms ingested as to continue with supportive therapy or not, but clinical measures should not wait for the analytical results, as time is of the essence in these cases. In the present case, the simultaneous ingestion of isoxazoles toxins and amatoxins lead to the early application of the *A. phalloides* therapy protocol in hospital settings, since the former caused rapid hallucinogenic symptoms. The facilities for toxicological analysis are not commonly available in most Hospitals. The collaboration between hospitals and toxicological laboratories and the communication between physicians and toxicologists could be helpful in reducing the time of therapy implemented as well as the morbidity and mortality in cases of poisoning. The rapid hospitalization and the history of mushrooms ingestion lead to an early therapeutic intervention for amatoxins poisoning, which was key to prevent complications resulting from amatoxins intoxication.

Acknowledgments

This work received financial support from the European Union (FEDER funds through COMPETE) and National Funds (FCT, Fundação para a Ciência e Tecnologia) through project Pest-C/EQB/LA0006/2013.

Juliana Garcia and Vera Marisa Costa thank FCT - Foundation for Science and Technology - for their PhD grant (SFRH/BD/74979/2010) and Post-doc grant (SFRH/BPD/63746/2009), respectively.

References

Amini, M., Ahmadabadi, A., Kazemifar, A.M., Solhi, H., Jand, Y., 2011. Amanita Phalloides Intoxication Misdiagnosed as Acute Appendicitis: A Case Report. Iran J Toxicol 5, 527-530.

Barbato, M.P., 1993. Poisoning from accidental ingestion of mushrooms. Med J Aust 158, 842-847.

Benjamin, D.R., 1992. Mushroom Poisoning in Infants and Children: The Amanita Pantherina/Muscaria Group. Clin Toxicol 30, 13-22.

Brandão, J.L., Pinheiro, J., Pinho, D., Correia da Silva, D., Fernandes, E., Fragoso, G., Costa, M.I., Silva, A., 2011. Intoxicação por cogumelos em portugal. Acta Med Port 24, 269-278.

Broussard, C.N., Aggarwal, A., Lacey, S.R., Post, A.B., Gramlich, T., Henderson, J.M., Younossi, Z.M., 2001. Mushroom poisoning - from diarrhea to liver transplantation. Am J Gastroenterol 96, 3195-3198.

Cheung, P.C.K., 2010. The nutritional and health benefits of mushrooms. Nutrition Bulletin 35, 292-299.

Cochran, K., 1987. Poisonings due to misidentified mushrooms. McIlvainea 8, 27-29.

Courtecuisse, R., 1999. Mushrooms of Britain and Europe. HarperCollins Publ., London.

Courtecuisse, R., Duhem, B., 2005. Guía de los hongos de la Peninsula Ibérica, Europa y Norte de África., in: Omeda, E. (Ed.), Barcelona.

Diaz, J.H., 2005. Syndromic diagnosis and management of confirmed mushroom poisonings. Crit Care Med 33, 427-436

Durukan, P., Yildiz, M., Cevik, Y., Ikizceli, I., Kavalci, C., Celebi, S., 2007. Poisoning from wild mushrooms in Eastern Anatolia region: analyses of 5 years. Hum Exp Toxicol 26, 579-582.

Enjalbert, F., Rapior, S., Nouguier-Soule, J., Guillon, S., Amouroux, N., Cabot, C., 2002. Treatment of amatoxin poisoning: 20-year retrospective analysis. J Toxicol Clin Toxicol 40, 715-757.

Faulstich, H., 1979. New aspects of Amanita poisoning. Klinische Wochenschrift 57, 1143-1152.

Faulstich, H., 1980. Mushroom poisoning. The Lancet 316, 794-795.

Fraschini, F., Demartini, G., Esposti, D., 2002. Pharmacology of Silymarin. Clin Drug Investig 22, 51-65.

French, L.K., Hendrickson, R.G., Horowitz, B.Z., 2011. Amanita phalloides poisoning. Clin Toxicol 49, 128-129.

Garcia, J., Costa, V.M., Baptista, P., Bastos, M.L., Carvalho, F., 2014. Quantification of alpha-amanitin in biological samples by HPLC using simultaneous UV-diode array and electrochemical detection. Submitted.

Halpern, J.H., 2004. Hallucinogens and dissociative agents naturally growing in the United States. Pharmacol Ther 102, 131-138.

Karlson-Stiber, C., Persson, H., 2003. Cytotoxic fungi—an overview. Toxicon 42, 339-349.

Klein, A.S., Hart, J., Brems, J.J., Goldstein, L., Lewin, K., Busuttil, R.W., 1989. Amanita poisoning: Treatment and the role of liver transplantation. Am J Med 86, 187-193.

Koppel, C., 1993. Clinical symptomatology and management of mushroom poisoning. Toxicon 31, 1513-1540.

Krogsgaard-Larsen, P., Honore, T., Hansen, J.J., Curtis, D.R., Lodge, D., 1980. New class of glutamate agonist structurally related to ibotenic acid. Nature 284, 64-66.

Letschert, K., Faulstich, H., Keller, D., Keppler, D., 2006. Molecular characterization and inhibition of amanitin uptake into human hepatocytes. Toxicol Sci 91, 140-149.

Mengs, U., Pohl, R.T., Mitchell, T., 2012. Legalon(R) SIL: the antidote of choice in patients with acute hepatotoxicity from amatoxin poisoning. Curr Pharm Biotechnol 13, 1964-1970.

Michelot, D., Melendez-Howell, L.M., 2003. Amanita muscaria: chemistry, biology, toxicology, and ethnomycology. Mycol Res 107, 131-146.

Montanini, S., Sinardi, D., Pratico, C., Sinardi, A.U., Trimarchi, G., 1999. Use of acetylcysteine as the life-saving antidote in Amanita phalloides (death cap) poisoning. Case report on 11 patients. Arzneimittelforschung 49, 1044-1047.

Morgado, L., Martins, L., Gonçalves, H., Oliveira, P., 2006. Estudo de intoxicações causadas por ingestão de macrofungos na região do Alto Alentejo. Anais da Associação Micológica A Pantorra 6, 65-74.

Mowry, J.B., Spyker, D.A., Cantilena, L.R., Jr., Bailey, J.E., Ford, M., 2013. 2012 Annual Report of the American Association of Poison Control Centers' National Poison Data System (NPDS): 30th Annual Report. Clin Toxicol 51, 949-1229.

Rumack, B.H., Spoerke, D.G., 1994. Handbook of Mushroom Poisoning: Diagnosis and Treatment. Taylor & Francis.

Santi, L., Maggioli, C., Mastroroberto, M., Tufoni, M., Napoli, L., Caraceni, P., 2012. Acute Liver Failure Caused by Amanita phalloides Poisoning. In J Hepatol 2012, 6.

Satora, L., Pach, D., Ciszowski, K., Winnik, L., 2006. Panther cap Amanita pantherina poisoning case report and review. Toxicon 47, 605-607.

Schwartz, R.B., Jones, K.M., Kalina, P., Bajakian, R.L., Mantello, M.T., Garada, B., Holman, B.L., 1992. Hypertensive encephalopathy: findings on CT, MR imaging, and SPECT imaging in 14 cases. Am J Roentgenol 159, 379-383.

Snodgrass, S.R., 1978. Use of 3H-muscimol for GABA receptor studies. Nature 273, 392-394.

Stribrny, J., Sokol, M., Merova, B., Ondra, P., 2012. GC/MS determination of ibotenic acid and muscimol in the urine of patients intoxicated with Amanita pantherina. Int J Legal Med 126, 519-524.

Thimmel, R., Kluthe, R., 1998. The nutritional database for edible mushrooms. Ernahrung 22, 63-65.

Tsujikawa, K., Mohri, H., Kuwayama, K., Miyaguchi, H., Iwata, Y., Gohda, A., Fukushima, S., Inoue, H., Kishi, T., 2006. Analysis of hallucinogenic constituents in Amanita mushrooms circulated in Japan. Forensic Sci Int 164, 172-178.

Vetter, J., 1998. Toxins of Amanita phalloides. Toxicon 36, 13-24.

Xiao, H., Wang, Y., Xu, T., Zhu, H., Guo, S., Wang, Z., Yu, X., 2012. Evaluation and treatment of altered mental status patients in the emergency department: Life in the fast lane. World J Emerg Med 3, 270-277.

Study IV

New *in silico* insights into the inhibition of RNAP II by α-amanitin and the protective effect mediated by effective antidotes

(Published in Journal of Molecular Graphics and Modelling)

Journal of Molecular Graphics and Modelling 51 (2014) 120–127

Contents lists available at ScienceDirect

Journal of Molecular Graphics and Modelling

journal homepage: www.elsevier.com/locate/JMGM

New *in silico* insights into the inhibition of RNAP II by α-amanitin and the protective effect mediated by effective antidotes

Juliana Garcia [a,*], Alexandra T.P. Carvalho [b], Daniel F.A.R. Dourado [b], Paula Baptista [c], Maria de Lourdes Bastos [a], Félix Carvalho [a,*]

[a] REQUIMTE Laboratory of Toxicology, Department of Biological Sciences, Faculty of Pharmacy, University of Porto, Rua José Viterbo Ferreira n° 228, 4050-313 Porto, Portugal
[b] Department of Cell and Molecular Biology, Computational and Systems Biology, Uppsala University, Biomedical Center Box 596, 751 24 Uppsala, Sweden
[c] CIMO/School of Agriculture, Polytechnic Institute of Bragança, Campus de Santa Apolónia, Apartado 1172, 5301-854 Bragança, Portugal

ARTICLE INFO

Article history:
Accepted 3 May 2014
Available online 14 May 2014

Keywords:
α-Amanitin
Benzylpenicillin
Ceftazidime
Silybin
RNA polymerase II
Trigger loop
Bridge helix

ABSTRACT

Poisonous α-amanitin-containing mushrooms are responsible for the major cases of fatalities after mushroom ingestion. α-Amanitin is known to inhibit the RNA polymerase II (RNAP II), although the underlying mechanisms are not fully understood. Benzylpenicillin, ceftazidime and silybin have been the most frequently used drugs in the management of α-amanitin poisoning, mostly based on empirical rationale. The present study provides an *in silico* insight into the inhibition of RNAP II by α-amanitin and also on the interaction of the antidotes on the active site of this enzyme.

Docking and molecular dynamics (MD) simulations combined with molecular mechanics-generalized Born surface area method (MM-GBSA) were carried out to investigate the binding of α-amanitin and three antidotes benzylpenicillin, ceftazidime and silybin to RNAP II.

Our results reveal that α-amanitin should affects RNAP II transcription by compromising trigger loop (TL) function. The observed direct interactions between α-amanitin and TL residues Leu1081, Asn1082, Thr1083, His1085 and Gly1088 alters the elongation process and thus contribute to the inhibition of RNAP II. We also present evidences that α-amanitin can interact directly with the bridge helix residues Gly819, Gly820 and Glu822, and indirectly with His816 and Phe815. This destabilizes the bridge helix, possibly causing RNAP II activity loss.

We demonstrate that benzylpenicillin, ceftazidime and silybin are able to bind to the same site as α-amanitin, although not replicating the unique α-amanitin binding mode. They establish considerably less intermolecular interactions and the ones existing are essential confine to the bridge helix and adjacent residues. Therefore, the therapeutic effect of these antidotes does not seem to be directly related with binding to RNAP II.

RNAP II α-amanitin binding site can be divided into specific zones with different properties providing a reliable platform for the structure-based drug design of novel antidotes for α-amatoxin poisoning. An ideal drug candidate should be a competitive RNAP II binder that interacts with Arg726, Ile756, Ala759, Gln760 and Gln767, but not with TL and bridge helix residues.

1. Introduction

The poisonous Amanita mushroom species *Amanita phalloides* (Death Cap), *Amanita verna* (White Deadly Amanita) and *Amanita virosa* (Destroying Angel) are responsible for 90–95% of the fatalities occurring after mushroom ingestion [1]. Toxins contained in these species include bicyclic octapeptides and consist of nine defined members: α-amanitin, β-amanitin, γ-amanitin, ε-amanitin, amanin, amanin amide, amanullin, amanullinic acid, and proamanullin [2]. From these, α-amanitin accounts for about 40% of the amatoxins [2].

Specific properties characterize these toxins. They are thermostable and are not removed by boiling and discarding water or by any form of cooking or drying, and belong to the most violent

* Corresponding authors. Tel.: +351 220428597; fax: +351 226093390.
E-mail addresses: jugarcia_18@hotmail.com, garciaju1987@gmail.com (J. Garcia), felixdc@ff.up.pt (F. Carvalho).

http://dx.doi.org/10.1016/j.jmgm.2014.05.002
1093-3263/

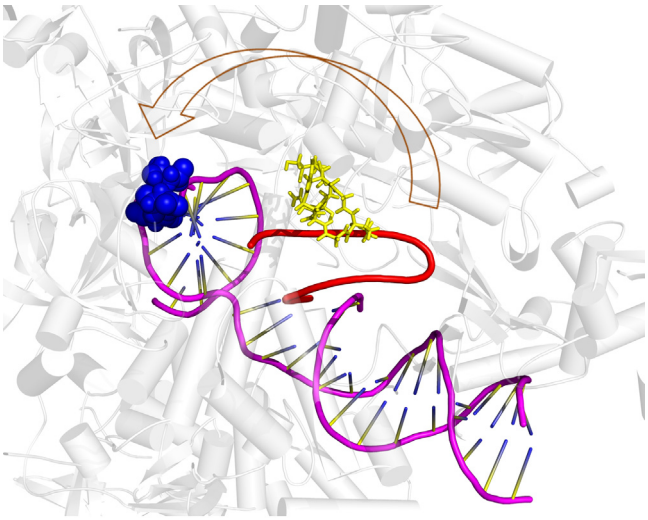

Fig. 1. Structure of RNAP II/α-amanitin complex. Trigger loop, active site, DNA and α-amanitin are colored red, blue, magenta and yellow, respectively. Active site is represented by the Asp 481, Asp 483 and Asp 485 catalytic residues. (For interpretation of the references to color in this figure legend, the reader is referred to the web version of the article.)

poisons from higher fungi: only one medium-size amatoxin-containing specimen contains from 10 to 12 mg amatoxins, a potential lethal dose for human adults (lethal dose: LD_{50} of 0.1–0.5 mg/kg body weight) [3].

After ingestion poisonous Amanita mushrooms, amatoxins are readily absorbed and accumulate in the liver upon uptake *via* an organic anion-transporting octapeptide (OATP) located in the sinusoidal membrane of hepatocytes [4], which is the same transport system for biliary acids. The main molecular mechanism of toxicity is their strong inhibition of RNAP II [5] which is responsible for the transcription of the precursor of messenger RNA. This in turn causes inhibition of DNA and protein synthesis processes and leads to cell death [6].

RNAP II consists of a 10-subunit core enzyme and a peripheral heterodimer of subunits Rpb4 and Rpb7 (Rpb4/7 subcomplex). The core enzyme comprises subunits Rpb1, Rpb2, Rpb3, Rpb5, Rpb6, Rpb8, Rpb9, Rpb10, Rpb11 and Rpb12 [7]. The active site is located in the interface between the core subunits Rpb1 and Rpb2. The catalytic process involves the nucleotide addition cycle (NAC) and begins with binding of a nucleoside triphosphate (NTP) substrate to the elongation complex (EC). Catalytic addition of the nucleotide to the growing 3′-end of the RNA leads to formation of a pyrophosphate ion. Pyrophosphate release leads to the pre-translocation state, in which the newly added, 3′-terminal RNA nucleotide remains in the substrate site. Finally, translocation of DNA and RNA results in the post-translocation state, in which the substrate site is free for binding the next NTP, and the NAC can be repeated [8]. This process involve a structural element named trigger loop (TL), which makes both direct and indirect contact with all features of the nucleotide in the polymerase active center and the bridge helix which guides the template DNA strand in the active site and positions the DNA-RNA hybrid relative to the active site [9]. TL has been hypothesized to have several conformations, but two of them, the "open" (Fig. 1) and "closed" conformations were observed in X-ray structures [9,10]. In the open TL structure the substrate enters on the enzyme, and then the TL rotates (see arrow in Fig. 1) to the active site (closed conformation) [9]. The flexibility of the trigger loop on the catalysis is directly influenced by the conformation of the bridge helix [11]. Recently a crystal structure of α-amanitin with yeast RNAP II was published revealing several key molecular interactions that may contribute to inhibition of RNAP II [10]. Multiple relevant interactions between α-amanitin with RNAP II are located in the bridge helix (previously defined "cleft" region) and in adjacent part of Rpb1 (previously defined funnel region). Based on this α-amanitin may block translocation by interacting with bridge helix and preventing the conformational change of the TL and consequently transcriptional elongation (Fig. 1) [12].

No specific antidote for intoxications with amatoxins is available. Based on pre-clinical findings several antidotes have been used in amatoxin poisonings, including hormones (insulin, growth hormone, glucagon), steroids, vitamin C, vitamin E, cimetidine, thioctic acid, antibiotics (benzylpenicillin, ceftazidime), N-acetylcysteine, and silybin. From these, only benzylpenicillin, ceftazidime, N-acetylcysteine and silybin been reported some success in the pharmacologic management of amatoxin poisonings, though with varying extent [1]. Furthermore, the precise pharmacological mechanism of action for these drugs remains to be elucidated.

In the current study we report the mode of interaction of α-amanitin and three antidotes (benzylpenicillin, ceftazidime and silybin) with RNAP II, using docking methods and molecular dynamics simulations. To secure significant sampling, we performed 3 molecular dynamic simulations (in a total of 34 ns) in explicit water of each one of the RNAP II/α-amanitin/antidotes complexes. In order to provide a new insight into the inhibition mechanism of RNAP II by α-amanitin, and the possible therapeutic mechanism of action of benzylpenicillin, ceftazidime and silybin in amatoxin poisoning, we used binding energy decomposition based on the molecular mechanics generalized Born surface area (MM-GBSA) approach.

2. Materials and methods

2.1. Molecular docking

Molecular Docking of several compounds is helpful in elucidating key features of ligand–receptor interactions. This method allows us to explore the interaction of the antidotes with RNAP II and predict their preferred orientation, which would form a complex with overall minimum energy. The crystal structure of RNAP II complexed with α-amanitin (Protein Data Bank entry 3CQZ and 2VUM) was used to obtain the starting structures for the molecular docking [8,11] and only subunits Rpb1 and Rpb2 were used.

The optimized Rpb1 and Rpb2 subunits were docked with α-amanitin, benzylpenicillin, silybin and ceftazidime. The docking procedure was made with the AutoDock 4 program [13,14]. This automated docking program uses a grid based method for energy calculation of the flexible ligand in complex with a rigid protein. The program performs several runs in each docking experiment. Each run provides one predicted binding mode. The Lamarckian genetic algorithm (LGA) was used in all docking calculations. The $48 \times 44 \times 44$ grid points along the *x*, *y* and *z* axes was centered on the α-amanitin which was large enough to cover all possible rotations of the toxin and antidotes. The distance between two connecting grid points was 0.375 Å. The docking process was performed in 250 LGA runs. The population was 150, the maximum number of generations was 27,000 and the maximum number of energy evaluations was 2.5×106. After complete execution of AutoDock ten conformations of ligand in complex with the receptor were obtained, which were finally ranked on the basis of binding energy [15]. The resulting conformations were visualized in the Visual Molecular Dynamics [16].

After analysis of all the solutions obtained, the best docking solutions were chosen as starting structures for the subsequent minimization and molecular dynamic studies.

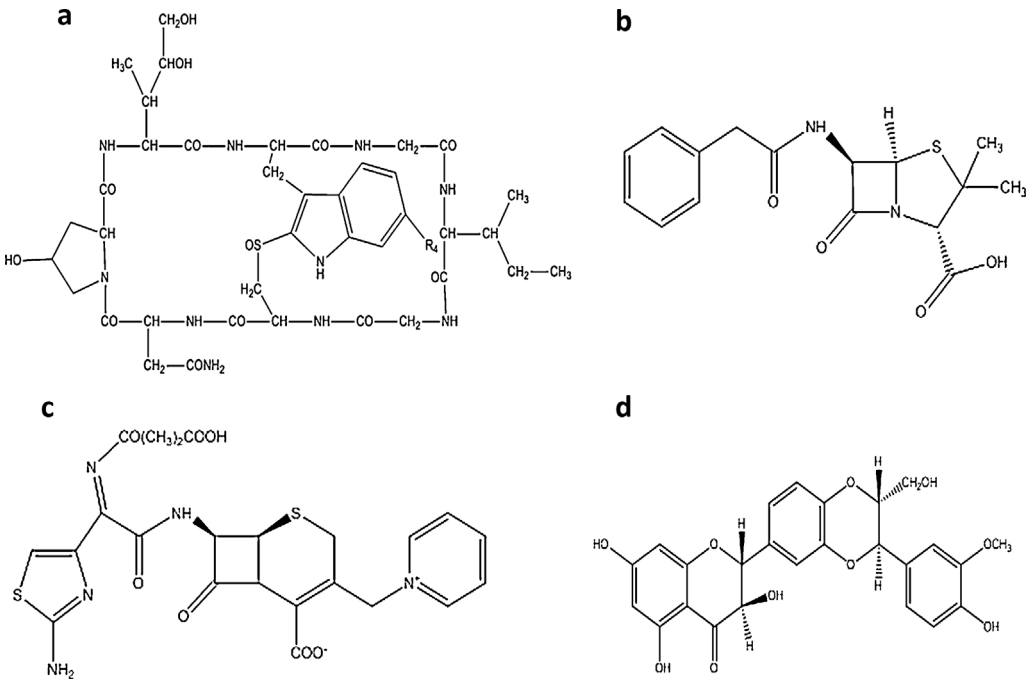

Fig. 2. Chemical structures: (a) α-amanitin; (b) benzylpenicillin; (c) ceftazidime; and (d) silybin.

2.2. Optimization of antidotes and α-amanitin

The structures of α-amanitin, benzylpenicillin, ceftazidime and silybin (Fig. 2) were constructed and optimized in Gaussian at the HF/6-31G* level of theory. For each antidote, we performed two optimizations: one in vacuum and another in the condensed phase. The partial charges were calculated resorting to the RESP method.

2.3. Molecular dynamic simulations

The enzyme was first neutralized by adding Na^+ ions and solvated in a cubic box of TIP3 water molecules, such that there were at least 10.0 Å of water between the surface of the protein and the edge of the simulation box. The initial geometry optimization of the enzyme was minimized in two stages. In the first stage only the hydrogen and water atoms were minimized; in the second stage the entire system was minimized.

The parameters of the chosen models were validated with MD simulations in explicit solvent. The MDs were performed with ff99SB force field and the generalized amber force field (Gaff) [17]. An initial minimization was performed followed by an equilibration of 500 ps. The equilibration was performed in a NVT ensemble using Langevin dynamics with small restraints on the protein (100 kcal mo1^{-1}). For each of the four systems an initial production simulation of 10 ns was performed followed by two random initial velocities replica runs, totaling 34 ns per substrate. This represented a substantial computational effort, since each system is composed by ≈44,000 atoms containing protein, DNA and RNA. Temperature was maintained at 300 K in the NPT ensemble using Langevin dynamics with a collision frequency of 1.0 ps^{-1}. The time step was set to 2 fs. The trajectories were saved every 500 steps for analysis. Constant pressure periodic boundary was used with an average pressure of 1 atm. Isotropic position scaling was used to maintain the pressure with a relaxation time of 2 ps. SHAKE constraints were applied to all bonds involving hydrogen. The particle mesh Ewald (PME) method was used to calculate electrostatic interactions with a cutoff distance of 8.0 Å.

2.4. Calculation of the binding energy

MM-GBSA was applied to compute the binding energy between the protein and each ligand and to decompose the interaction energies on a per residue basis by considering molecular mechanics energies and solvation energies [18].

The energy decomposition was performed for gas-phase energies, desolvation free energies calculated by GB model [19] and nonpolar contributions to desolvation using the linear combinations of pairwise overlaps (LCPO) method [20].

Conformational entropy was not considered because our aim was to identify important interactions between the α-amanitin and the antidotes with RNAP II residues, rather than to obtain very accurate absolute values for the binding free energy.

3. Results and discussion

The determination of the crystal structures with bound α-amanitin it showed that this toxin binding site was quite far from the RNAP II active site. Inhibition could only be explained if α-amanitin binding could lead to some conformational change that would affect the active site. The mystery was partially solved with the determination of the complex RNAP II/DNA.RNA/substrate [9]. In this complex the TL is in the opposite direction and interacting with the substrate. The TL is thus a highly flexible structural motif within the enzyme capable of large conformational changes at each catalytic cycle. Superposition of the pre-catalytic complex with the complex with α-amanitin shows that the large size of the toxin could prevent the movement of the TL (Fig. 3).

Consequently, a description of the full TL movement is still missing. Many TL conformations are still not described and the crystal structures only give initial and final snapshots for this movement. To gain detailed insight about the most important residues for the α-amanitin/antidotes dynamical interaction with RNAP II we performed and analyzed MD simulations on docked complexes of RNAP II/α-amanitin and with the antidotes. Moreover, we performed detailed hydrogen bonds analyses (Table 1), measured the most relevant distances between the protein residues and the

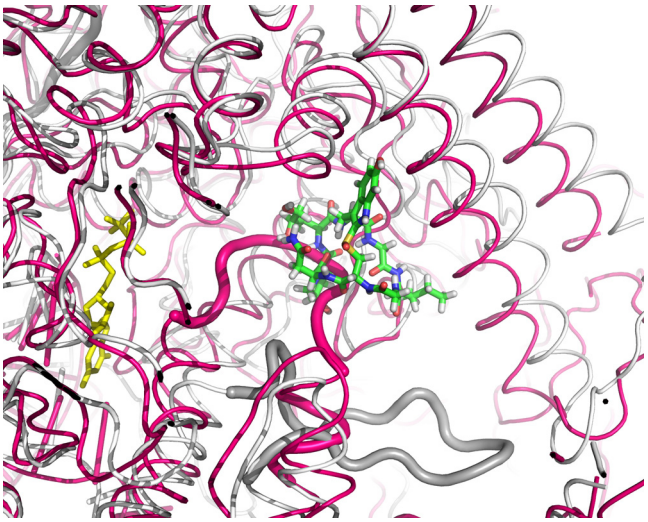

Fig. 3. Interaction of α-amanitin with RNAP II, demonstrated *in silico*. Superposition of the lowest RMSD for the average structure of the simulation (gray), pre-catalytic complex (magenta, pdb code 2E2H), complex with α-amanitin. The α-amanitin is in licorice representation and the substrate is in yellow licorice representation). (For interpretation of the references to color in this figure legend, the reader is referred to the web version of the article.)

toxin/antidotes. Finally, we performed energy decomposition. The protein per residue energy values gives us a fast and relatively reliable estimation of the contribution of each residue to the binding [21]. Our goal was provide a new insight into the inhibition mechanism of RNAP II by α-amanitin by identifying the critical residues for RNAP II binding and subsequently understanding how antidotes interact with RNAP II and if they can bind to the same position without inhibiting the enzyme.

3.1. Identification of critical residues for α-amanitin binding

Superposition of the average simulation structure and the crystal structure is shown in Fig. 4. The most noticeable differences between the crystal structure and our simulation structure rely in the displacement of TL (Fig. 4), which may be attributed to the high flexibility and intrinsic mobility of the TL. In the our simulation structure, Gly1088 residue interacts with α-amanitin oxygen (O33), while in the crystal structure this residue is far away from the α-amanitin. The demonstrated accuracy of the docked complex validates our protocol and supports the results obtained for the antidotes, for which there is no crystal structure (described in Section 3.2).

In order to more easily and accurately grasp the interactions between the protein and α-amanitin we performed an energy decomposition analysis of the simulations. We resorted to the MM-GBSA method. The calculated binding energies of each complex can be seen in Table 2. Even not considering the entropy, computational studies using MM-GBSA calculations on different complexes of protein-inhibitors showed good correlations with respect to experimental data [21]. Individual energy decomposition of all residues in the complex was also calculated in order to qualitatively find the key residues that play a more important role in the α-amanitin binding (Figs. 5a and 6a). Values are expressed as mean ± SD of the 3 replicates. Fig. 5a depicts the relative position of the inhibitor and important residues in the binding complex by using the lowest root-mean-square deviation RMSD structure in respect to the average of the simulation. The toxin α-amanitin interacts with residues Arg726, Ile756, Ala759, Gln760, Gln767, Gln768, Ser769, Gly819, Gly820, Glu822, Leu1081, Asn1082, Thr1083, His1085 and Gly1088 (Figs. 5a and 6a). The guanidinium group of Arg726 forms cation–π interactions with α-amanitin phenyl group, which corresponds to energy of -1.71 ± 1.51 kcal mo1^{-1}. The binding energy of residue Ile756 is -2.53 ± 0.83 kcal mol^{-1}, agreeing with the CH–π interaction of Ile756 alkyl group with α-amanitin phenyl ring. At the same time, Ala759 alkyl group also forms CH–π interactions with α-amanitin phenyl group (-0.67 ± 0.04 kcal mol^{-1}). The side-chain nitrogen atom of Gln760 forms a hydrogen bond with α-amanitin O4 (Table 1), leading to a favorable binding energy of -1.40 ± 0.89 kcal mol^{-1}. Thus the indole portion of α-amanitin inserts in the hydrophobic pocket created by Arg726, Ile756, Ala759 and Gln760 (Fig. 5a). The side-chain oxygen of Gln767 forms a hydrogen bond with α-amanitin N30, which

Table 1
Hydrogen bonds formed between the toxin/antidotes and RNA polymerase II[a].

Toxin/Antidote	Donor	AcceptorH	Acceptor	Distance[b](Å)	Angle[b] (°)	% per time frame
	Gln767:OE1	α-amanitin:H77	α-amanitin:N30	1.81	166.53	60
	α-amanitin:O4	Gln768:HE2	Gln768:NE2	2.87	157.06	80
α-amanitin	α-amanitin:O4	Gln760:HE2	Gln760:NE2	2.11	148.55	26
	α-amanitin:O59	Ser769:H	Ser769:N	2.04	157.88	88
	Glu822:OE1	α-amanitin:1H11	α-amanitin:O63	2.55	172.43	60
Benzylpenicillin	Benzilpenicillin:O3	Hie816:HE2	Hie816:NE2	2.51	134.78	48
	Benzilpenicillin:O1	Gln760:1HE2	Gln760:NE2	1.96	167.45	56
Silybin	Silybin:O56	Gln760:1HE2	Gln760:NE2	2.17	142.68	75
	Silybin:O4	Gly823:H	Gly823:N	2.08	150.30	47

[a] Hydrogen bonds were analyzed in the average structures from MD simulation.

[b] The geometric criterion for the formation of H-bonds is common with an acceptor-donor distance less than 3.5 Å and the donor-H-acceptor angle larger than 120.

Table 2
Binding energy calculation between the three antidotes and α-amanitin with Rpb1 and Rpb2 subunits (all energies are in kcal mol^{-1}).

Complex	ΔG_{ele}	ΔG_{vdw}	ΔG_{Int}	ΔG_{Gas}	ΔG_{GBSUR}	ΔG_{GB}	ΔG_{GBsol}	ΔG_{GBele}	ΔG_{tot}
Rpb1Rpb2/α-amanitin	−60.97	−60.91	0.00	−121.88	−8.16	108.70	100.53	47.73	−21.34
Rpb1Rpb2/benzylpenicillin	−19.78	−31.34	0.00	−51.12	−4.27	41.53	37.26	21.75	−13.87
Rpb1Rpb2/silybin	−21.00	−42.58	0.00	−63.62	−5.87	47.96	42.09	26.95	−21.53
Rpb1Rpb2/ceftazidime	−59.96	−38.20	0.00	−98.16	−5.31	89.94	84.63	29.98	−13.53

ΔG_{ele}: electrostatic energy. ΔG_{vdw}: van der waals energy; ΔG_{int}: internal energy; ΔG_{Gas}: total gas phase energy (sum ΔG_{ele}, ΔG_{vdw}, ΔG_{int}); ΔG_{GBSUR}: nonpolar contribution to solvation; ΔG_{GB}: the electrostatic contribution to the solvation free energy; ΔG_{GBSOL}: sum of nonpolar and polar contributions to solvation; ΔG_{GBELE}: sum of the electrostatic solvation free energy and electrostatic energy; ΔG_{TOT}: estimated total binding energy.

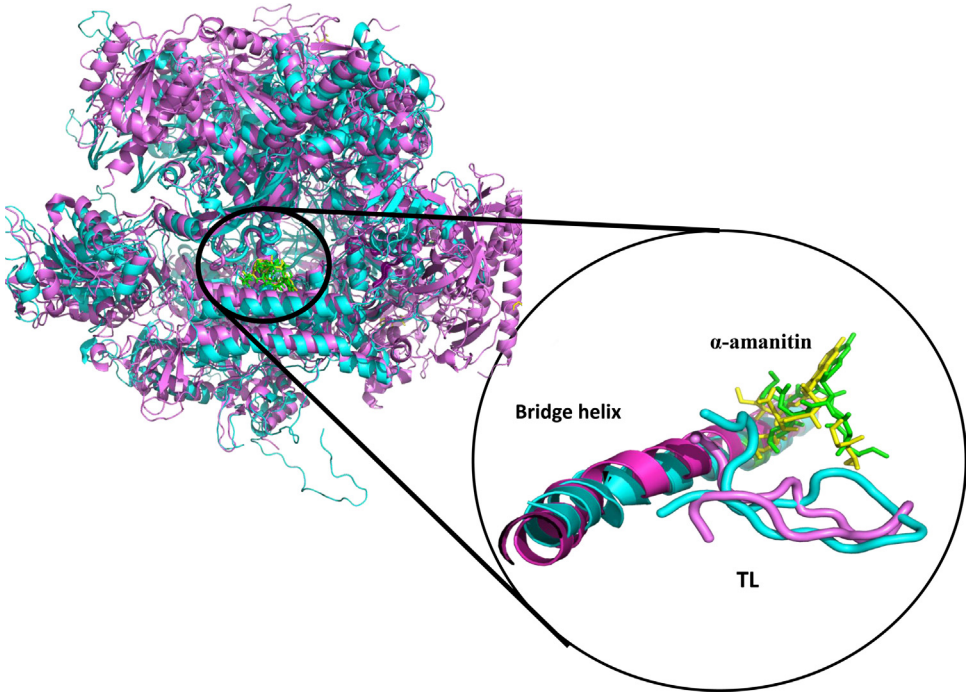

Fig. 4. Superposition of the lowest RMSD for the average structure of RNAP II (cyan) with α-amanitin (green), crystal structure of RNAP II (magenta, pdb code 3CQZ) in complex with α-amanitin (yellow).

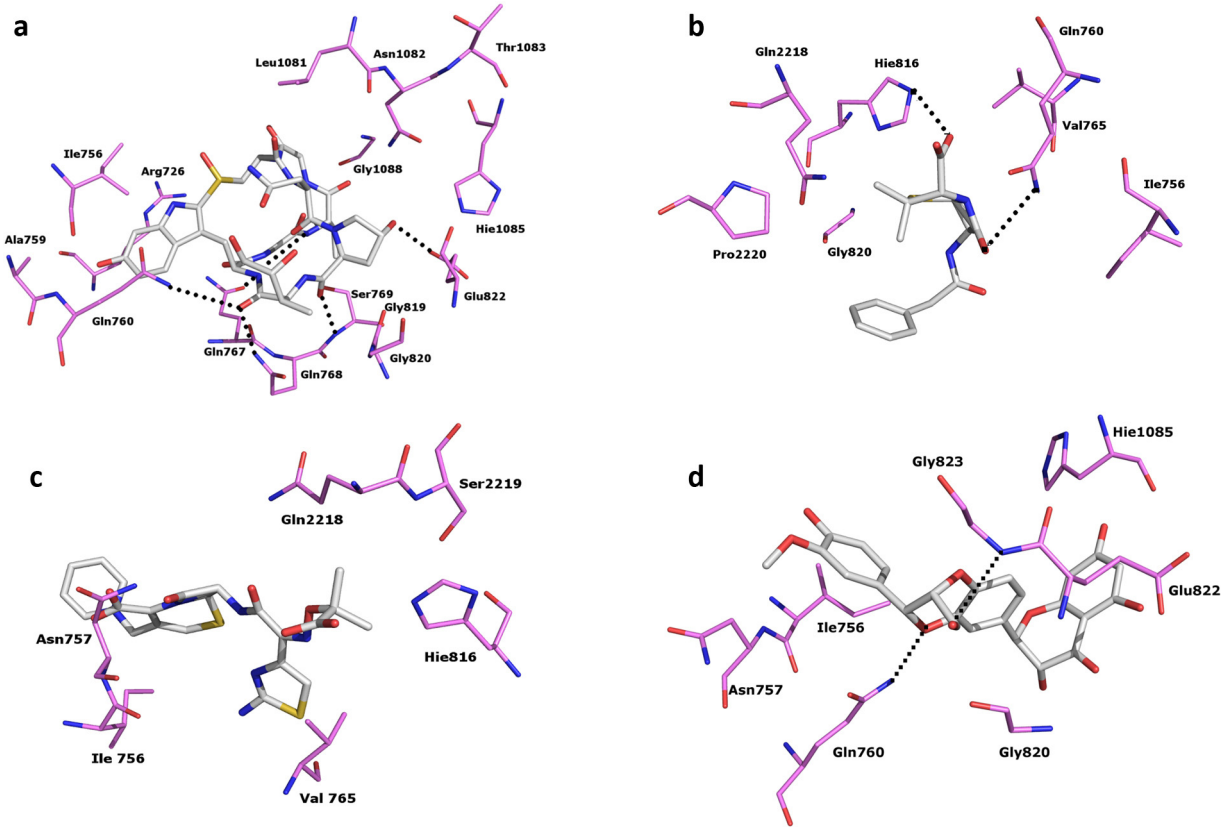

Fig. 5. Geometries of key residues, which produce some favorable interactions with RNAP II, are plotted in the complexes according to the average structure from the MD trajectory. (a) RNAP II/α-amanitin complex; (b) RNAP II/benzylpenicillin complex; (c) RNAP II/ceftazidime complex; and (d) RNAP II/silybin complex. The dashed lines represent hydrogen bonds between the α-amanitin/antidotes and RNAP II.

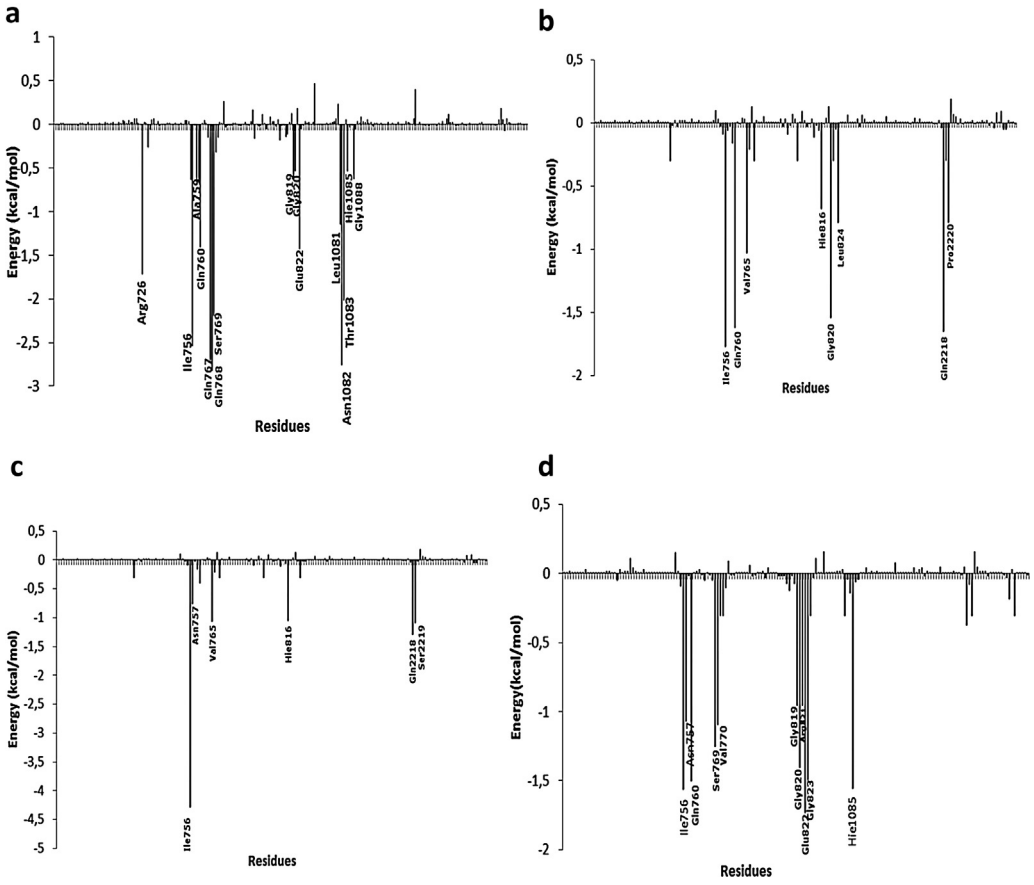

Fig. 6. α-Amanitin/antidotes-residues interaction spectrum of (a) RNAP II/α-amanitin complex; (b) RNAP II/benzylpenicillin complex; (c) RNAP II/ceftazidime complex and (d) RNAP II/silybin complex. The residues with interaction energy than −0.5 kcal mol^{-1} are labeled. Values are expressed as mean ± s.d. of the 3 replicates.

corresponds to interaction energy of −2.70 ± 1.60 kcal mol^{-1}. The nitrogen atom of Gln768 also forms a hydrogen bond with α-amanitin O4 (Table 1), which is the strongest interaction among all residues (−2.82 ± 0.88 kcal mol^{-1}). The α-amanitin/Ser769 interaction energy is −2.18 ± 0.80 kcal mol^{-1}, which is due to a hydrogen bond between Ser769 nitrogen atom and α-amanitin O59 (Table 1). Hydrophobic interactions may be the main force between bridge helix residues Gly819, Gly820 and α-amanitin, which correspond to energies of −0.61 ± 0.08 and −0.53 ± 0.00 kcal mol^{-1}, respectively. The interaction energy of the bridge helix residue Glu822 with α-amanitin is −1.90 ± 0.97 kcal mol^{-1}, corresponding to a hydrogen bond between the Glu822 side chain oxygen and α-amanitin hydroxyproline OH (Table 1). The alkyls group of Leu1081 and Asn1082 interact with α-amanitin alkyls by hydrophobic interactions, which correspond to energies of −1.14 and −2.75 kcal mol^{-1}, respectively. The interaction energy of Thr1083 with α-amanitin is −2.01 kcal mol^{-1}, mostly attributed to dipole–dipole interactions. TL residues His1085 and Gly1088 form dipole–dipole interactions with α-amanitin hydroxyproline and produce interaction energies of −0.53 ± 0.12 and −0.62 kcal mol^{-1}, respectively, which is supporting by experimental data [22].

According to Figs. 5a and 6a and the above analysis, three valuable findings can be observed: (1) Hydrogen bonds, CH–π and hydrophobic interactions drive the bindings of α-amanitin to RNAP II. (2) Our results indicate interactions with bridge helix residues Gly819, Gly820 and Glu822. Moreover, indirect contacts to the bridge helix were also observed. α-Amanitin binds to residue Gln768, which in turn binds to His816 and Phe815 and forms a hydrogen bond with Ser769. Ser769 interacts with the bridge helix residue Gly819. (3) α-Amanitin interacts with TL residues Leu1081, Asn1082, Thr1083, His1085 and Gly1088. These interactions can prevent TL movement and hence contributing to inhibit transcription.

3.2. Binding mode predictions of antidotes to RNAP II

In order to provide a new insight into the mechanism of action of benzylpenicillin, ceftazidime and silybin in amatoxin poisoning we analyzed the antidotes binding to RNAP II.

According to Figs. 5b and 6b, several residues are involved in the RNAP II/benzylpenicillin binding. The binding energy of benzylpenicillin to Ile756 is −1.77 ± 0.49 kcal mol^{-1}, agreeing with CH–π interactions between Ile alkyls and benzylpenicillin phenyl ring (Fig. 5b). Gln760 nitrogen atom binds to benzylpenicillin O1 by a hydrogen bond, corresponding to energy of −1.63 ± 0.45 kcal mol^{-1} (Table 1). At same time, other hydrogen bond between His816 nitrogen and benzylpenicillin O3 contributes with −0.69 ± 0.14 kcal mol^{-1} (Table 1). Val765 alkyl group and benzylpenicillin alkyl group generate dispersive interactions (−1.03 ± 0.14 kcal mol^{-1}). Dipole–dipole interactions are observed between Gly820 and benzylpenicillin (−1.54 ± 0.00 kcal mol^{-1}). Leu824 alkyls groups interact with benzylpenicillin alkyls groups by hydrophobic interactions (−0.79 ± 0.23 kcal mol^{-1}). Finally, Gln2218 and Pro2220 form dipole–dipole interactions with benzylpenicillin carboxyl group, corresponding to energies of −1.65 ± 0.45 and −0.79 ± 0.20 kcal mol^{-1}, respectively. Based on the above analysis, two valuable findings can be described: (1) Residues Ile756, Gln760 and Gly820 are common sites for α-amanitin and benzylpenicillin. (2) Our results indicate that

benzylpenicillin interacts with bridge helix residues His816, Gly820 and Leu824.

In the case of the RNAP II/ceftazidime complex the following residues contribute for binding energy (Figs. 5c and 6c). Ile756 alkyl group and ceftazidime dihydrothiazine ring generate CH–π interactions (Fig. 5c), corresponding to an interaction energy of -4.28 ± 1.70 kcal mol^{-1}. The interaction energy of Asn757 is -0.80 ± 0.10 kcal mol^{-1}, which can be attributed to dipole–dipole interactions with ceftazidime carboxylic acid group. Dipole–dipole interactions between Val765 and ceftazidime propylcarboxy moiety are responsible for energy of -1.06 ± 0.51 kcal mol^{-1}. At same time, identical interactions can be seen between His816 imidazole ring and ceftazidime propylcarboxy moiety (-1.04 ± 0.18 kcal mol^{-1}). Hydrophobic and dipole–dipole interactions are the main forces between Gln2218 and ceftazidime propylcarboxy moiety (-1.30 ± 1.11 kcal mol^{-1}). At same time Ser2219 forms dipole–dipole interactions with the same moiety, which correspond to interaction energy of -1.09 ± 0.38 kcal mol^{-1}. Based on the above analysis, two important conclusions can be obtained: (1) Residue Ile756 and is common site for α-amanitin and ceftazidime. (2) Our results indicate that ceftazidime interact with bridge helix residue His816.

Finally, for RNAP II/silybin binding the key residues are seven (Figs. 5d and 6d). The binding energy of silybin to Ile756 is -1.58 ± 0.27 kcal mol^{-1}, corresponding to a CH–π interaction between Ile756 alkyl and silybin phenyl group. The interaction energy of Asn757 with silybin phenyl ring has energy of -1.06 ± 0.81 kcal mol^{-1}, which mostly results of NH–π interactions. Gln760 side-chain nitrogen forms a hydrogen bond with silybin O56 (-1.50 ± 0.79 kcal mol^{-1}) (Table 1). Dipole–dipole interactions between residues Ser769, Val770, Gly819, Gly820 and Arg821 with silybin result in the energies contributions of -1.25 ± 0.14, -1.01 ± 0.10, 0.95 ± 0.29, -1.40 ± 1.17 and -0.95 ± 0.50 kcal mol^{-1}, respectively. Silybin phenyl ring contacts with Glu822 alkyl group to generate a hydrophobic CH–π interaction (-1.38 ± 0.60 kcal mol^{-1}). The Gly823 forms a hydrogen bond with silybin O4 (-1.49 ± 0.89 kcal mol^{-1}) (Table 1). The π–π contacts and dipole–dipole interactions between residue His1085 and silybin diphenol ring result in an energy contribution of -1.50 ± 0.07 kcal mol^{-1}. From these results, we can conclude: (1) Residues Ile756, Gln760, Gly819, Gly820, Glu822 and His1085 are common sites for α-amanitin and silybin. (2) Our results indicate that silybin interact with bridge helix residues Gly819, Gly820 and Glu822 and TL residue His1085.

4. Conclusions

In this study, docking and MD simulation coupled with MM-GBSA energy decomposition have been carried out to clarify the inhibition mechanism of RNAP II by α-amanitin and to provide a new insight into the plausible mechanism of action of three antidotes used in amatoxin poisoning.

We hypothesize that TL residues Leu1081, Asn1082, Thr1083, His1085 and Gly1088, and bridge helix residues Gly819, Gly820 and Glu822 contribute for the high binding affinity of α-amanitin with RNAP II. Our data clearly reinforces the hypothesis of an important role of the bridge helix [23] and TL in the elongation process and are consistent with the existence of a network of functional interactions between the bridge helix and TL that control fundamental parameters of RNA synthesis. Our data suggest that α-amanitin interferes with bridge helix movement during the translocation and with the movement of the TL, which closes over the active site during the nucleotide incorporation (Fig. 1). Moreover, according to Kaplan et al. (2008), we show that the interaction of α-amanitin with His1085 contributes for the inhibition of the enzyme. This is supported by the findings that a substitution of alanine or phenylalanine at position 1085 specifically renders RNAP II highly resistant to α-amanitin [22]. Also, there are evidences that residue 1085 may play a critical role in the catalytic mechanism [24]. Taken together our results are in good agreement with all literature data.

In the analysis of the antidotes we focused on the TL, bridge helix and other additional residues that are involved in α-amanitin binding. It seems that benzylpenicillin, ceftazidime and silybin, although binding to the same RNAP II binding site, cannot replicate α-amanitin binding mode. The antidotes establish considerably less intermolecular interactions and the ones existing are essential confine to the bridge helix and adjacent residues. The therapeutic effect of the studied antidotes on α-amatoxin poisoning seems not to be directly related with binding to RNAP II.

These structural insights about the molecular aspects of RNAP II inhibition can provide a reliable platform for the structure-based drug design against α-amatoxin poisoning. We suggest that an ideal drug should be a competitive RNAP II binder able to strongly interact with Arg726, Ile756, Ala759, Gln760 and Gln767, but not with bridge helix and TL residues.

Acknowledgements

The authors gratefully acknowledge the Foundation for the Science and Technology (FCT, Portugal) for financial support and also thank FCT for PhD grant SFRH/BD/74979/2010. We acknowledge Qtrex cluster and SNIC-UPPMAX for CPU time allocation.

References

[1] F. Enjalbert, S. Rapior, J. Nouguier-Soule, S. Guillon, N. Amouroux, C. Cabot, Treatment of amatoxin poisoning: 20-year retrospective analysis, J. Toxicol. Clin. Toxicol. 40 (2002) 715–757.
[2] J. Vetter, Toxins of amanita phalloides, Toxicon 36 (1998) 13–24.
[3] T. Wieland, Progress in Tryptophan and Serotonin Research, Walter de Gruyter & Co, Berlin, New York, 1984.
[4] K. Letschert, H. Faulstich, D. Keller, D. Keppler, Molecular characterization and inhibition of amanitin uptake into human hepatocytes, Toxicol. Sci. 91 (2006) 140–149.
[5] T.J. Lindell, F. Weinberg, P.W. Morris, R.G. Roeder, W.J. Rutter, Specific inhibition of nuclear RNAP II by alpha-amanitin, Science 170 (1970) 447–449.
[6] T. Wieland, The toxic peptides from amanita mushrooms, Int. J. Pept. Protein Res. 22 (1983) 257–276.
[7] P. Cramer, K.J. Armache, S. Baumli, S. Benkert, F. Brueckner, C. Buchen, et al., Structure of eukaryotic RNA polymerases, Annu. Rev. Biophys. 37 (2008) 337–352.
[8] F. Brueckner, J. Ortiz, P. Cramer, A movie of the RNA polymerase nucleotide addition cycle, Curr. Opin. Struct. Biol. 19 (2009) 294–299.
[9] D. Wang, D.A. Bushnell, K.D. Westover, C.D. Kaplan, R.D. Kornberg, Structural basis of transcription: role of the trigger loop in substrate specificity and catalysis, Cell 127 (2006) 941–954.
[10] D.A. Bushnell, P. Cramer, R.D. Kornberg, Structural basis of transcription: alpha-amanitin-RNAP II cocrystal at 2.8 A resolution, Proc. Natl. Acad. Sci. U. S. A. 99 (2002) 1218–1222.
[11] L. Tan, S. Wiesler, D. Trzaska, H. Carney, R. Weinzierl, Bridge helix and trigger loop perturbations generate superactive RNA polymerases, J. Biol. 7 (2008) 1–15.
[12] X.Q. Gong, Y.A. Nedialkov, Z.F. Burton, Alpha-amanitin blocks translocation by human RNAP II, J. Biol. Chem. 279 (2004) 27422–27427.
[13] G.M. Morris, D.S. Goodsell, R.S. Halliday, R. Huey, W.E. Hart, R.K. Belew, et al., Automated docking using a Lamarckian genetic algorithm and an empirical binding free energy function, J. Comput. Chem. 19 (1998) 1639–1662.
[14] G.M. Morris, R. Huey, W. Lindstrom, M.F. Sanner, R.K. Belew, D.S. Goodsell, et al., AutoDock4 and AutoDockTools4: automated docking with selective receptor flexibility, J. Comput. Chem. 30 (2009) 2785–2791.
[15] R. Huey, G.M. Morris, A.J. Olson, D.S. Goodsell, A semiempirical free energy force field with charge-based desolvation, J. Comput. Chem. 28 (2007) 1145–1152.
[16] W. Humphrey, A. Dalke, K. Schulten, VMD: visual molecular dynamics, J. Mol. Graph. 14 (1996) 33–38.
[17] D.A. Case, T.E. Cheatham, T. Darden, H. Gohlke, R. Luo, K.M. Merz, et al., The Amber biomolecular simulation programs, J. Comput. Chem. 26 (2005) 1668–1688.
[18] P.A. Kollman, I. Massova, C. Reyes, B. Kuhn, S. Huo, L. Chong, et al., Calculating structures and free energies of complex molecules: combining molecular mechanics and continuum models, Acc. Chem. Res. 33 (2000) 889–897.

[19] A. Onufriev, D. Bashford, D.A. Case, Modification of the generalized born model suitable for macromolecules, J. Phys. Chem. B 104 (2000) 3712–3720.
[20] J. Weiser, P.S. Shenkin, W.C. Still, Approximate atomic surfaces from linear combinations of pairwise overlaps (LCPO), J. Mol. Biol. 20 (1999) 217–230.
[21] P.D. Lyne, M.L. Lamb, J.C. Saeh, Accurate prediction of the relative potencies of members of a series of kinase inhibitors using molecular docking and MM-GBSA scoring, J. Med. Chem. 49 (2006) 4805–4808.
[22] C.D. Kaplan, K.M. Larsson, R.D. Kornberg, The RNAP II trigger loop functions in substrate selection and is directly targeted by alpha-amanitin, Mol. Cell 30 (2008) 547–556.
[23] Y.A. Nedialkov, K. Opron, F. Assaf, I. Artsimovitch, M.L. Kireeva, M. Kashlev, et al., The RNA polymerase bridge helix YFI motif in catalysis, fidelity and translocation, BBA – Gene Regul. Mech. 1829 (2013) 187–198.
[24] A.T.P. Carvalho, P.A. Fernandes, M.J. Ramos, The catalytic mechanism of RNAP II, J. Chem. Theory Comput. 7 (2011) 1177–1188.

Study V

Discovery of an effective antidote for *Amanita phalloides* poisoning: a precious extension of polymyxin B pharmacotherapy

(Under preparation)

Discovery of an effective antidote for *Amanita phalloides* poisoning: a precious extension of polymyxin B pharmacotherapy

Juliana Garcia[a]*, Vera Marisa Costa[a], Alexandra T.P. Carvalho[b], Ricardo Silvestre[c,d], José Alberto Duarte[e], Daniel F.A.R. Dourado[b], Marcelo D. Arbo[a], Tereza Baltazar[a], Ricardo Jorge Dinis-Oliveira[a,e,f], Paula Baptista[h], Maria de Lourdes Bastos[a], Félix Carvalho[a]*

[a]UCIBIO/REQUI*M*TE-Laboratory of Toxicology, Department of Biological Sciences, Faculty of Pharmacy, University of Porto, Rua José Viterbo Ferreira nº 228, 4050-313 Porto, Portugal.

[b]Department of Cell and Molecular Biology, Computational and Systems Biology, Uppsala University, Biomedical Center Box 596, 751 24, Uppsala, Sweden.

[c]Life and Health Sciences Research Institute (ICVS), School of Health Sciences, University of Minho, Braga, Portugal

[d] ICVS/3B's - PT Government Associate Laboratory, Braga/Guimarães, Portugal

[e]CIAFEL, Faculty of Sport, University of Porto, Porto, Portugal.

[f]Department of Legal Medicine and Forensic Sciences, Faculty of Medicine, University of Porto, Porto, Portugal.

[g]IINFACTS - Institute of Research and Advanced Training in Health Sciences and Technologies, Department of Sciences, Advanced Institute of Health Sciences – North (ISCS-N), CESPU, CRL, Gandra, Portugal

[g]CIMO/School of Agriculture, Polytechnic Institute of Bragança, Campus de Santa Apolónia, Apartado 1172, 5301-854 Bragança, Portugal.

* Authors to whom correspondence should be addressed (Tel.: + 351 220428597; Fax: + 351 226093390; e-mail: up200502554@ff.up.pt and felixdc@ff.up.pt)

Abstract

Amanita phalloides is responsible for more than 90% of mushroom-related fatalities and no effective antidote is clinically available. α-Amanitin, the most powerful toxin of *A. phalloides,* causes hepatic and kidney failure and its main toxicity mechanism relies on the inhibition of RNA polymerase II (RNAP II). In the present study, *in silico* and *in vivo* studies involving RNAP II were performed to find a potential α-amanitin antidote among clinically available drugs. *In silico* studies included docking and molecular dynamics (MD) simulation coupled to molecular mechanics-generalized born surface area method (MM-GBSA) energy decomposition on RNAP II, were performed with a clinically used drug with chemical similarities to α-amanitin, polymyxin B. The obtained results show that polymyxin B potentially binds to RNAP II in the same interface of α-amanitin, preventing the toxin from binding to RNAP II without interfering with messenger ribonucleic acid (mRNA) synthesis. *In vivo* studies proved the efficacy of this potential antidote. A single dose of α-amanitin (0.33 mg/kg) followed by a multiple polymyxin B administration (3 × 2.5 mg/kg, at 4, 8 and 12 h post-α-amanitin as to mimic the real human intoxication scenario) was carried out. The short-term study (24 h) corroborated the *in silico* results since the inhibition of the mRNA transcripts in the kidneys elicited by α-amanitin was efficiently reverted by polymyxin B. Moreover, polymyxin B significantly decreased the hepatic and renal α-amanitin-induced injury as seen by the histology and plasma biomarkers. In the survival rate assay, all animals exposed to α-amanitin died within 5 days, whereas 50% survived up to 30 days when polymyxin B was administered 4, 8 and 12 h post α-amanitin. A single dose of polymyxin B (2.5 mg/kg) administered concomitantly with α-amanitin was able to guarantee 100% survival until the 30th day post exposure.

Taken together, these results demonstrate that polymyxin B acts on RNAP II, preventing α-amanitin binding to this crucial target. This effect protects RNAP II from inactivation leading to an effective increase of survival and a decrease in organ damage in α-amanitin-treated animals, prompting the use of polymyxin B as an antidote for *A. phalloides* poisoning in humans.

Keywords: α-amanitin, RNA polymerase II, polymyxin B, liver, kidney.

Abbreviations

ALT	Alanine aminotransferase
AST	Aspartate aminotransferase
Ct	Cycle threshold
DNA	Deoxyribonucleic acid
i.p.	Intraperitoneal
mRNA	Messenger ribonucleic acid
RNA	Ribonucleic acid
RNAP II	RNA polymerase II
ROS	Reactive oxygen species
RT-PCR	Real-time polymerase chain reaction
SD	Standard deviation

1. Introduction

The gathering and consumption of wild mushrooms has increased during recent years due to their delicate flavors and textures as well as their attributed high nutritional value (Cheung 2010). Despite warnings, edible and toxic mushrooms such as *A. phalloides* are frequently misidentified by mushroom collectors. This species is responsible for more than 90% of the fatalities caused by mushroom poisoning worldwide (Vetter 1998). The clinical importance of *A. phalloides* poisoning relies on the presence of powerful toxins such as cyclic octapeptides. These cyclic octapeptides are known as amatoxins and α-amanitin is the main responsible for the severe liver and kidney injury observed after *A. phalloides* poisoning. It is well established that α-amanitin inhibits RNA polymerase II (RNAP II), thereby interfering with the transcription process (Wieland 1983). However, other toxic mechanisms have been suggested, namely oxidative stress, which may play a critical role (Leist et al. 1997; Zheleva 2013; Zheleva et al. 2007). In addition, α-amanitin may also act synergically with endogenous cytokines (e.g. tumor necrosis factor-α) to promote apoptosis (Leist et al. 1997).

Unfortunately, so far, no consensual antidote for mushroom poisonings has been found and therefore amatoxin poisoning is generally associated with a poor outcome, mainly due to liver or kidney failure. Several treatments have been applied after human intoxications with *A. phalloides*, including hormones (*e.g.*, insulin, growth hormone, and glucagon), steroids, vitamin C, vitamin E, cimetidine, α-lipoic acid, antibiotics (benzylpenicillin, ceftazidime), N-acetylcysteine, and silybin. From these, only benzylpenicillin, ceftazidime, N-acetylcystein, and silybin proved to have some degree of therapeutic efficacy, though the death rate remains extremely high (Poucheret et al. 2010). The survival of individuals depends largely on the severity of liver damage, the rate of hepatic regeneration and the management of complications that may develop during the intoxication treatment course (Koda-Kimble et al. 2012). Liver transplantation is considered a last resort, however it remains the cornerstone of treatment in patients with fulminant hepatic failure (Broussard et al. 2001; Pinson et al. 1990).

Considering the main toxicity mechanism of amatoxins, the inhibition of RNAP II activity, the ideal therapeutic approach against *A. phalloides* intoxications would be to displace and / compete with amatoxins binding to RNAP II without impairing its normal transcription activity. Therefore, in the present study, we aimed to identify an effective antidote for *Amanita* mushroom species poisonings, by proposing an innovative *in silico* and *in vivo* approach based on the binding of α-amanitin to RNAP II and the screening of clinically used drugs that show bioisosterism with amatoxins. This bioisosterism will be tested in the same *in silico* models to assess a putative competition and displacement from amatoxins binding site with RNAP II. After *in silico* studies, one of the most promising

candidates, polymyxin B was chosen for further *in vivo* proof of concept, mainly focusing in the target organs of α-amanitin toxicity, kidney and liver in a mice model. Several parameters were evaluated, namely survival rate, histological damage, protein carbonylation, NF-κB nuclear activation, total RNA and specific mRNA quantification, in order to validate the effectiveness of polymyxin B in protecting mice against α-amanitin poisoning.

2. Material and methods

2.1. *In silico* study

2.1.1. Molecular docking on RNAP II

Molecular docking plays an important role in the rational design drugs and is helpful in elucidating key features of ligand–receptor interactions. This *in silico* method allows predicting the preferred orientation of putative antidotes when bound to RNAP II, forming a complex with overall minimum energy. Molecular docking studies were performed on polymyxin B according to our previous reported data (Garcia et al. 2014). The crystal structure of RNAP II complexed with α-amanitin (Protein Data Bank entry 3CQZ and 2VUM) was used to obtain the starting structures for the molecular docking (Bushnell et al. 2002) and only subunits Rpb1 and Rpb2 were used. The optimized Rpb1 and Rpb2 subunits were docked with polymyxin B. The docking procedure was made with the AutoDock 4 program (Morris et al. 2009; Mowry et al. 2013). This automated docking program uses a grid-based method for energy calculation of the flexible ligand in complex with a rigid protein. The program performs several runs in each docking experiment. Each run provides one predicted binding mode. The Lamarckian genetic algorithm (LGA) was used in all docking calculations. The 48×44×44 grid pointed along the x, y and z axes was centered on the α-amanitin, which was large enough to cover all possible rotations of the polymyxin B. The distance between two connecting grid points was 0.375 Å. The docking process was performed in 250 LGA runs. The population was 150, the maximum number of generations was 27,000 and the maximum number of energy evaluations was 2.5×10^6. After complete execution of AutoDock ten conformations of polymyxin B in complex with the receptor were obtained, which were finally ranked on the basis of binding energy. The resulting conformations were obtained in the Visual Molecular Dynamics (Humphrey et al. 1996). After analysis of all the solutions obtained, the best docking solution was chosen as starting structure for the subsequent minimization and molecular dynamic studies.

2.1.2. Optimization of polymyxin B

The structure of polymyxin B was constructed and optimized in Gaussian at the HF/6-31G* level of theory. Two optimizations were performed: in vacuum and in the condensed phase. The partial charges were calculated resorting to the RESP method.

2.1.3. Molecular dynamic simulations

The enzyme was first neutralized by adding Na^+ ions and solvated in a cubic box of TIP3P water molecules, such that there were at least 10.0 Å of water between the surface of the protein and the edge of the simulation box. The initial geometry optimization of the enzyme was minimized in two stages. In the first stage only the hydrogen and water atoms were minimized; in the second stage the entire system was minimized. The parameters of the chosen models were validated with molecular dynamics (MD) simulations in explicit solvent. The MDs were performed with ff99SB force field and the generalized amber force field (Gaff) (Case et al. 2005). An initial minimization was performed followed by an equilibration of 500 ps. The equilibration was performed in a NVT ensemble using Langevin dynamics with small restraints on the protein (100 kcal/mol). Then 10 ns of production simulation were performed. This represented a substantial computational effort, since each system is composed by ≈44000 atoms containing protein, deoxyribonucleic acid (DNA) and ribonucleic acid (RNA). Temperature was maintained at 300 K in the NPT ensemble using Langevin dynamics with a collision frequency of 1.0 ps^{-1}. The time step was set to 2 fs. The trajectories were saved every 500 steps for analysis. Constant pressure periodic boundary was used with an average pressure of 1 atm. Isotropic position scaling was used to maintain the pressure with a relaxation time of 2 ps. SHAKE constraints were applied to all bonds involving hydrogen. The particle mesh Ewald (PME) method was used to calculate electrostatic interactions with a cutoff distance of 8.0 Å.

2.1.4. Calculation of the binding energy

Molecular mechanics with generalized Born and surface area solvation (MM-GBSA) was applied to compute the binding energy between the RNAP II/polymyxin B complex and to decompose the interaction energies on a per residue basis by considering molecular mechanic energies and solvation energies (Kollman et al. 2000). The energy decomposition was performed for gas-phase energies, desolvation free energies calculated by GB model (Onufriev et al. 2000) and nonpolar contributions to desolvation using the linear combinations of pairwise overlaps (LCPO) method (Weiser et al. 1999).

2.2. Experimental studies

2.2.1. Chemical and drugs

α-Amanitin, polymyxin B, 1-octanesulfonic acid sodium salt, 2,4-dinitrophenylhydrazine, TRIzol and RNALater were purchased from Sigma-Aldrich (St. Louis, Missouri, USA). Methanol and xylene were obtained from Fisher Scientific (Waltham, Massachusetts,

USA). Sodium chloride, potassium chloride, sodium hydrogen phosphate, potassium dihydrogen phosphate, perchloric acid, Histosec paraffin pastilles, magnesium chloride, sodium hydroxide, ethylenediaminetetraacetic acid (EDTA) and disodium phosphate, were purchased from Merck (Darmstadt, Germany). Eosin 1% aqueous was obtained from Biostain (Traralgon, Australia) and Harris hematoxylin from Harris Surgipath (Richmond, Illinois, USA). Water was purified with a Milli-Q Plus ultra-pure water purification system (Millipore, Bedford, Massachusetts, USA). Bio-Rad DC protein assay kit, Clarity™ Western ECL Substrate, iScript cDNA Synthesis KitH, and SYBR Green PCR Master Mix were purchased from Bio-Rad Laboratories (Hercules, California, USA). Horseradish peroxidase conjugated anti-rabbit antibody, ECL chemiluminescence reagents, and 0.45 μm Amersham Protran nitrocellulose blotting membrane were purchased from GE Healthcare Bio-Science (Pittsburgh, Pennsylvania, USA). Dinitropenhyl-KLH rabbit IgG antibody was purchased from Invitrogen/Life Technologies (Grand Island, New York, USA). NF-κB p50 rabbit polyclonal IgG and goat anti-rabbit IgG F(ab')2 AP conjugated were purchased from Santa Cruz Biotechnology (Heidelberg, Germany). All primers were purified through high pressure liquid chromatography and purchased to STAB VIDA (Caparica, Lisboa, Portugal). The kit for DNase digestion step and the ultrapure water was obtained from Qiagen (Carnaxide, Portugal).

2.2.2. Animals

Male CD-1 mice (20-30 g) were purchased from Harlan (Udine, Italy), and kept in the vivarium of Faculty of Sports, University of Porto. Room temperature was maintained at 22 ± 2 ºC, relative humidity at 60 ± 10%, and a 12 h light/dark cycle. Water and standard rodent chow 4RF21 GLP certificate diet (Mucedola, 113 Settimo Milanese, Italy) were provided *ad libitum*. All procedures were carried out to provide appropriate animal care, minimizing their suffering. Housing and experimental treatment of the animals were in accordance with the guidelines defined by the European Council Directive (2010/63/EU) transposed into Portuguese law (Decreto-Lei n.º 113/2013, de 7 de Agosto). Moreover, the experiments were performed with the approval of the Ethical Committee of the Faculty of Pharmacy, University of Porto (nº 10/06/2013). Animals were acclimated for 5 days before starting the experiments.

2.2.3. *In vivo* study design

The murine model has been used as a reliable model for α-amanitin poisoning (Schneider et al. 1987; Schneider et al. 1992; Tong et al. 2007; Yamaura et al. 1986; Zhao et al. 2006), with similar hepatic toxic responses to amatoxins as humans (Tong et al. 2007). In this model, the intraperitoneal (i.p.) administration ensures the bioavailability of α-amanitin

and it has been the preferred route used in previous studies in mice in search for antidotes against amatoxins poisoning (Schneider et al. 1987; Schneider et al. 1992; Tong et al. 2007). In the present work, two *in vivo* studies were performed to evaluate the putative effectiveness of polymyxin B against α-amanitin toxicity: a short-term study (24 h) and a survival study (30 days). α-Amanitin and polymyxin B were always dissolved in 0.9% saline solution. In both studies, all α-amanitin-exposed animals received an i.p. dose of 0.33 mg/kg. This dose was chosen since it was previously reported to be the lethal dose (LD_{50}) of α-amanitin in mice (Wieland and Faulstich 1978) and it has been used in several studies aiming to test antidotes efficacy after amatoxin poisoning (Schneider et al. 1987; Schneider et al. 1992; Tong et al. 2007; Vogel et al. 1984).

2.2.3.1. Short-term study

Our work started with a short-term (24 h) study to evaluate the effectiveness of polymyxin B in protecting liver and kidney against the toxicity of α-amanitin. In order to create a real scenario of intoxication, since intoxicated people only arrive to emergency rooms hours or even days after mushrooms ingestion, polymyxin B was only administered to animals 4 h post α-amanitin administration. This 4-h delay in the administration was also used in several studies that aimed testing the efficacy of antidotal therapies in mice models (Schneider et al. 1992; Tong et al. 2007). Three consecutive doses of polymyxin B (2.5 mg/kg) with 4 h interval between each dosage were given to animals. According to the allometric scaling standardly used (West and Brown 2005), the 3 doses of 2.5 mg/kg of polymyxin B in mice, sums up to approximately 1 mg/kg in a 70 kg human. The current recommended dose of intravenous polymyxin B for patients with normal renal function is 1.5–2.5 mg/kg/day in two doses administered as 1 h infusions (Zavascki et al. 2007). Moreover, the three polymyxin B administrations at different time-points (4, 8 and 12 h) after α-amanitin injection are based on a previous pharmacokinetic study in mice with polymyxin B, in which the serum concentration of polymyxin B (3 mg/kg) is non-detectable at 4 h post-administration (He et al. 2013).

Animals were randomly divided into four groups that were treated as follows: (i) control group, animals subjected to four 0.9% saline solution i.p. administrations (0, 4, 8 and 12 h); (ii) α-amanitin group (Ama), animals exposed to one dose of α-amanitin (0.33 mg/kg i.p.) followed by three 0.9% saline solution i.p. administrations at different time points (4, 8 and 12 h) post α-amanitin administration; (iii) polymyxin B group (Pol), animals exposed to a 0.9% saline solution followed by three 2.5 mg/kg i.p. administrations of polymyxin B at different time-points (4, 8 and 12 h); (iv) α-amanitin plus polymyxin B (Ama+Pol), animals exposed to one dose of α-amanitin (0.33 mg/kg i.p.) followed by three

2.5 mg/kg i.p. administrations of polymyxin B at different time-points (4, 8 and 12 h). Twenty-four hours after α-amanitin administration, all animals were anesthetized with isoflurane and sacrificed by exsanguination. The blood, liver and kidney were collected for further analysis.

2.2.3.2. Survival rate study

Following the promising *in silico* and short term *in vivo* studies, the next step was to perform a long-term *in vivo* study, to evaluate survival rate and animals welfare of animals intoxicated with α-amanitin and treated with polymyxin B. In the α-amanitin group, animal suffering was expected, thus we reduced the number of animals to the minimum. Twenty four animals were randomly divided into five groups that were treated as follows: (i) control group, animals treated with 0.9% saline solution i.p.; (ii) α-amanitin group (Ama), animals exposed to one dose of α-amanitin (0.33 mg/kg i.p.); (iii) polymyxin B group (Pol), animals treated with 0.9% saline solution followed by 3 × 2.5 mg/kg administrations i.p. of polymyxin B at different time-points (4, 8 and 12 h); (iv); α-amanitin plus polymyxin B group (Ama+Pol conc), animals concomitantly exposed to administration of one dose of α-amanitin (0.33 mg/kg i.p.) and polymyxin B (1 × 2.5 mg/kg i.p.); (v) α-amanitin plus polymyxin B group (Ama+Pol), animals exposed to α-amanitin (0.33 mg/kg i.p.) followed by 3 × 2.5 mg/kg i.p. administrations of polymyxin B at different time-points (4, 8 and 12 h). Body weight, motor activity, dyspnea, and overall welfare of the animals were observed every day, for 30 days.

2.2.4. Short-term study (24 h) evaluations

2.2.4.1. Blood collection

In the short-term study, the blood was taken from the inferior vena cava into EDTA-containing tubes. The blood was immediately centrifuged at 920 *g* for 10 min (4°C). The plasma supernatant was collected into tubes and stored at -80°C until determination of aspartate aminotransferase (AST), alanine aminotransferase (ALT), creatinine, urea and total bilirubin. Plasma biochemical parameters were measured on an AutoAnalyzer (PRESTIGE 24i, PZ Cormay S.A.).

2.2.4.2. Tissue processing for biochemical analysis

After blood collection, liver and kidneys were removed, weighed, and processed as follows: (i) slices of liver and kidney were kept in RNAlater and stored at -80°C for future total RNA quantification and quantitative PCR analysis; (ii) segments of liver and kidney were placed in 4% paraformaldehyde [diluted in phosphate buffer solution (PBS) 1X, 2.5% sucrose, 0.1% glutaraldehyde, pH 7.2-7.4] and used for histological and

immunohistochemistry analysis; and (iii) a section of liver and kidney was placed in complete RIPA buffer [50 mM Tris–HCl, 150 mM NaCl, 1% Igepal CA-630 (v/v), 0.5% sodium deoxycholate (w/v) and 0.1% SDS (w/v), pH 7.4, (supplemented with 0.25 mM PMSF, 1 mM Na_3VO_4, 10 mM NaF and 0.5% (v/v) complete protease inhibitor cocktail)] and stored at -80°C for carbonyl quantification.

2.2.4.3. RNA extraction and real-time PCR

Total RNA isolation was performed by adding 500 μL of TRIzol reagent to liver and kidney samples according to the manufacturer's instructions. All specimens were homogenized by mechanical disruption using the Ultra-Turrax Mixer (IKAH) instrument and total RNA was extracted in RNAse-free environment. A DNase digestion step with RNase-Free DNase Set was included and the total RNA obtained was ressuspended in ultrapure water. The RNA concentration was determined by OD260 measurement using a NanoDropH ND-1000 Spectrophotometer (NanoDrop Technologies, USA), and the purity of the total RNA extracted was assessed by measuring the absorbance at 230 and 280 nm. 200 ng of total RNA was reverse-transcribed using the iScript Select cDNA Synthesis Kit (Bio-Rad, Hercules, California, USA) according to the manufacturer's protocol. All cDNA samples were stored at -20 °C until quantitative real-time PCR (qPCR) analysis. qPCR was performed in iQ™ 5 Real-Time PCR detection System (Bio-Rad, Hercules, California, USA) in 96-well plates with a reaction volume of 20 μL and runs up to 40 cycles using iQ™ SYBER® Green Supermix. The final PCR reaction mixture of 10 μL contained 0.25 μL of cDNA sample, 5 μL of iQ™ SYBR® Green Supermix, 0.25 μL of each primer and 4.25 μL of RNase-free water. The cycling conditions were set as follows: Taq DNA polymerase activation at 95 °C for 3 min, amplification steps: denaturation at 95 °C for 15 s, annealing at 60 °C for 15 s, and extension at 72 °C for 15 s with fluorescence acquisition. Two highly stable reference genes for RNAP II were chosen (β-actin, GAPDH) as well as two ribosomal 18S and 28S genes transcribed by RNA polymerase I. All cDNA samples were measured in duplicate, and the relative transcript levels were quantified by the threshold cycle (Ct) value. All primers were designed using the Beacon Designer Software (version 7.2, PREMIER Biosoft International, Palo Alto, CA, USA).

2.2.4.4. Histological analysis of liver and kidney

In the short-term study, routine histological procedures for qualitative structural analysis of the liver and kidney were performed in four mice from each group. The 4% paraformaldehyde-fixed transverse section of the liver and kidney was processed for the routine hematoxylin-eosin staining. The slides were examined and photographed with a Carl Zeiss Imager A1 light microscope equipped with an AxioCam MRc 5 digital camera

(Oberkochen, Germany). Histopathological evidences of tissue damage were calculated according to their severity and incidence in every slide (Dores-Sousa et al. 2015). Both liver and kidney, at least 50000 cells per slide were analyzed in a blind fashion in order to semi quantify the severity of the following parameters: i) cellular degeneration, ii) interstitial inflammatory cell infiltration, iii) necrotic zones, and iv) loss of tissue organization. The severity of cellular degeneration was scored according to the number of cells showing any alterations (dilatation, vacuolization, pyknotic nuclei, and cellular density) in the light microscopy visual field: grade 0 = no change from normal; grade 1 = a limited number of isolated cells (until 5% of the total cell number); grade 2 = groups of cells (5 to 30% of cell total number); and grade 3 = diffuse cell damage (30% of total cell number). The severity of necrosis was scored as follows: grade 0 = no necrosis; grade 1 = dispersed necrotic foci; grade 2 = confluence necrotic areas; grade 3 = massive necrosis. The inflammatory activity was graded semi-quantitatively into: grade 0 = no cellular infiltration; grade 1 = mild leukocyte infiltration (1 to 3 cells by visual field); grade 2 = moderate infiltration (4 to 6 leukocytes by visual field); and grade 3 = heavy infiltration by neutrophils. The severity of tissue disorganization was scored according to the percentage of the affected tissue: score 0 = normal structure; score 1 = less than one third of tissue; score 2 = greater than one third and less than two thirds; score 3 = grater of two thirds of tissue. For each visual field the highest possible score was 12 and the lowest was 0.

2.2.4.5. Determination of NF-κB through immunohistochemistry

In the short-term study, the determination of NF-κB nuclear translocation was performed both in the liver and kidney. The 4% paraformaldehyde-fixed transverse section of the liver and kidney was processed as indicated in 2.2.4.4 section and then the paraffin-embedded tissues were deparaffinized and re-hydrated. The slides were rinsed in distilled water and incubated in PBS for 10 min. Thereafter, antigens were unmasked by the microwave antigen retrieval procedure: slides were immersed in 10 mM citrate buffer, pH 6.0, at 100°C and placed in a full-powered microwave for 20 min and then cooled for 30 min. After washing four times (5 min each) with PBS solution, the sections were blocked with 3% bovine serum albumin (w/v) in PBS containing 0.05 % Tween 20 (v/v) (PBS-T), for 30 min to suppress nonspecific binding. Following the blocking step, each slide was incubated with anti-NF-kB p50 polyclonal rabbit antibody (1:50) in PBS-T overnight (4°C). After washing four times (5 min each) with PBS solution, the sections were incubated for 2 h, at 37°C with a goat anti-rabbit IgG alkaline phosphatase secondary antibody (1:100) in PBS-T. The sections were then washed four times (5 min) under gentle stirring and incubated with Fast Red reagent for 5 min. After washing, the slides were then counterstained with a solution of hematoxylin-water (1:5) for 3 min and once again

washed. Finally, slides were mounted in Crystal Mount medium with coverslips and analyzed by light microscopy. Negative controls were performed as described, with the omission of the primary antibody incubation step.

A minimum of 40 cells *per* area were evaluated and for each section six areas in each zone were seen. In the liver, cell quantification was possible and the number of nuclear staining in hepatocytes and macrophage-like cells were expressed in number of positive cells per area (μm^2).

2.2.4.6. Protein carbonylation assay

In the short-term study, protein carbonylation, an index of protein oxidation, was determined in the liver and kidney. Liver and kidney sections were homogenized in ice-cold RIPA buffer through sonication. The homogenates were centrifuged at 13000 *g*, for 10 min, at 4ºC, and supernatants were kept at -80 ºC until analysis. Samples containing 20 µg of protein were then processed as previously described (Barbosa et al. 2012). Immunoreactive bands were detected using the Clarity™ Western ECL Substrate, according to the supplier`s instructions, and digital images were acquired using a Molecular Imager® ChemiDocTM XRS+ System (Bio-Rad Laboratories, California, USA) and analyzed with Image LabTM Software (Bio-Rad Laboratories California, USA). Optical density results were expressed as % of control values.

2.2.5. Statistical analysis

All data obtained were expressed as mean ± standard deviation (SD). All statistical analysis was performed using GraphPad Prism® (version 6.00, GraphPad Software, San Diego, California, USA). Comparisons among the survival curves were performed using Log-rank (Mantel–Cox) test. The Shapiro-Wilk test was performed to check normality of the data. Statistical comparisons were done using the one-way ANOVA (in case of normal distribution) followed by the Bonferroni post hoc test or Kruskal-Wallis (in case not normal distribution) followed by the Dunn´s post hoc test. P values lower than 0.05 were considered as statistically significant.

3. Results

3.1. *In silico* study

3.1.1. Identification of critical residues for polymyxin B binding

A docking study with polymyxin B on RNAP II to determine the preferred orientation of the molecule on RNAP II was performed. To gain a broad insight of the most important residues in the polymyxin B dynamical interaction with RNAP II, we performed and analyzed MD simulations on docked complex of RNAP II/polymyxin B. Ten ns of MD simulation have been successfully performed for the polymyxin B/RNAP II complex. Figure 1 shows superposition of the average structures of α-amanitin polymyxin B during the simulations. The polymyxin B binding site is located in the same interface of α-amanitin. In order to more easily and accurately grasp the interactions between the RNAP II and polymyxin B, an energy decomposition analysis of the simulations was also done (Table 1). We resorted to the MM-GBSA method, since computational studies using MM-GBSA calculations on different complexes of protein/ligands showed good correlations with experimental data (Onufriev et al. 2000). Our aim was to investigate the interaction features in detail and obtain insights into the contribution of each component to the RNAP II/polymyxin B binding. The individual energy decompositions of all residues in the complex were calculated in order to identify key residues involved in polymyxin B binding to RNAP II.

Figure 2 depicts the relative position of the polymyxin B and important residues in the binding complex by using the lowest root-mean-square deviation RMSD structure in respect to the average of the simulation. The polymyxin B interacts with residues Arg720, Ala1087, Gly1088, Val1089, Val1094, Met1285, Ala1357, and Gly1360. The guanidinium group of Arg726 forms dipole-dipole interactions with L-α-γ-diaminobutyric acid (Dab) residue of polymyxin B, which corresponds to energy of -1.97 kcal/mol. The binding energy of residue Ala1087 is -1.41 kcal/mol, thus agreeing with a hydrogen bond between Ala1087 oxygen atom and polymyxin B N22 (Table 2). At the same time, Gly1088 oxygen atom also forms a hydrogen bond with polymyxin B N15 (-2.81 kcal/mol) (Table 2). Dipole-dipole interactions were observed between Val1089 and polymyxin B (-2.25 kcal/mol). Hydrophobic interactions may be the main force between Val1094 and side-chain leucine residue of polymyxin B, which correspond to energy of -2.25 kcal/mol. Met1285 alkyl group forms CH-π interactions with polymyxin B phenyl group (-1.83 kcal/mol). Finally, Ala1357 and Gly1360 alkyls groups interact with polymyxin B methyl-octanoic acid group by hydrophobic interactions (-0.63 kcal/mol).

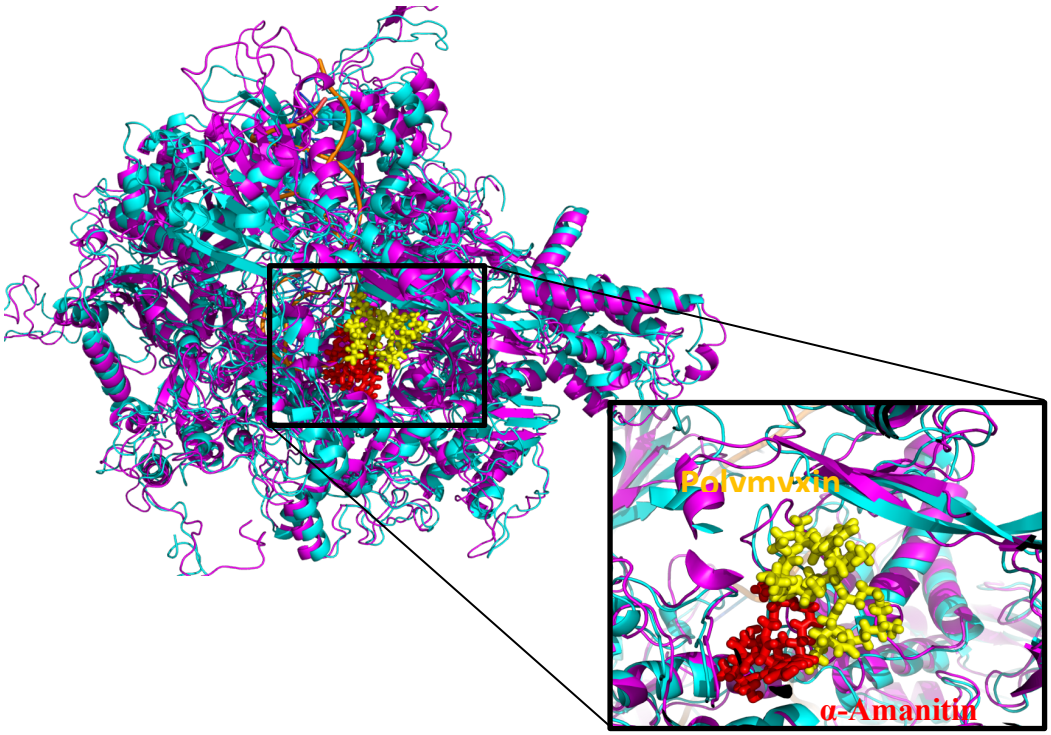

Figure 1. Superposition of RNAP II average structure/α-amanitin (cyan) and RNAP II average structure/ polymyxin B (magenta). (representation of α-Amanitin is in red and of polymyxin B is in yellow spheres).

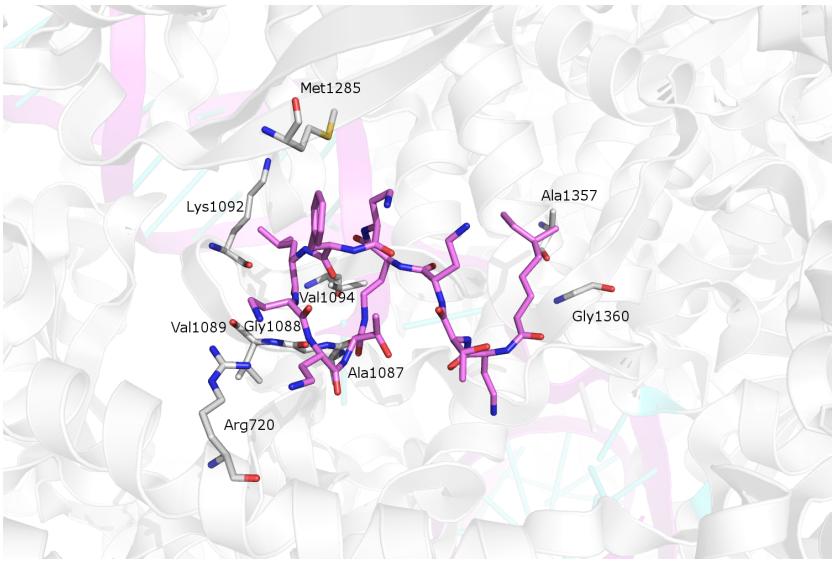

Figure 2. RNAP II geometries of key residues that produce some favorable interactions with polymyxin B, plotted in the complexes, according to the average structure from the MD trajectory.

Table 1. Binding energy calculation between the polymyxin B and Rpb1 and Rpb2 subunits (all energies are in kcal/mol)

Complex	ΔG_{ele}	ΔG_{vdw}	ΔG_{Int}	ΔG_{Gas}	ΔG_{GBSUR}	ΔG_{GB}	ΔG_{GBsol}	ΔG_{GBele}	ΔG_{tot}
RNAPII/Polymyxin B	-62.50	-57.64	0.00	-120.14	-8.45	110.40	101.95	47.90	-18.19

ΔG_{ele}: electrostatic energy. ΔG_{vdw}: van der waals energy; ΔG_{int}: internal energy; ΔG_{Gas}: total gas phase energy (sum ΔG_{ele}, ΔG_{vdw}, ΔG_{int}); ΔG_{GBSUR}: nonpolar contribution to solvation; ΔG_{GB}: the electrostatic contribution to the solvation free energy; ΔG_{GBSOL}: sum of nonpolar and polar contributions to solvation; ΔG_{GBELE}: sum of the electrostatic solvation free energy and electrostatic energy; ΔG_{TOT}: estimated total binding energy.

Table 2. Hydrogen bonds formed between the polymyxin B and RNA polymerase II[a]

Toxin/Antidote	Donor	AcceptorH	Acceptor	Distance[b](A)	Angle[b] (°)
Polymyxin B	Ala1087:O	Polymyxin B:2H14	PolymyxinB:N22	2.48	140.27
	Gly1088:O	Polymyxin B:2H10	PolymyxinB:N15	1.82	168.67
	Val1089:N	Polymyxin B:2H10	PolymyxinB:N15	2.11	148.55

[a]Hydrogen bonds were analyzed in the average structures from MD simulation. [b]The geometric criterion for the formation of H-bonds is common with an acceptor-donor distance less than 3.5 Å and the donor-H-acceptor angle larger than 120°.

3.2. Polymyxin B is able to prevent the hepatic and kidney damage induced by α-amanitin *in vivo*

3.2.1. Polymyxin B significantly abolished the increase of plasma aminotransferase elicited by α-amanitin

Plasma biomarkers were determined at 24 h after α-amanitin administration as shown in Figure 3. AST and ALT were significantly increased in the α-amanitin group (359.10 ± 190.40 and 120.20 ± 83.20 U/L for AST and ALT, respectively) as compared with control group (63.80 ± 8.63 and 37.80 ± 6.94 U/L for AST and ALT, respectively). This increase was prevented with the 3 × 2.5 mg/kg administration of polymyxin B (68.46 ± 23.92 and 32.70 ± 8.45 U/L for AST and ALT, respectively) (Figure 3A and 3B). On the other hand, urea and creatinine show a small tendency to increase in the α-amanitin group, however without reaching statistical significance (Figure 3C and 3D). The ratio AST/ALT and the total bilirubin showed no differences between treatments (Figure 3E and 3F).

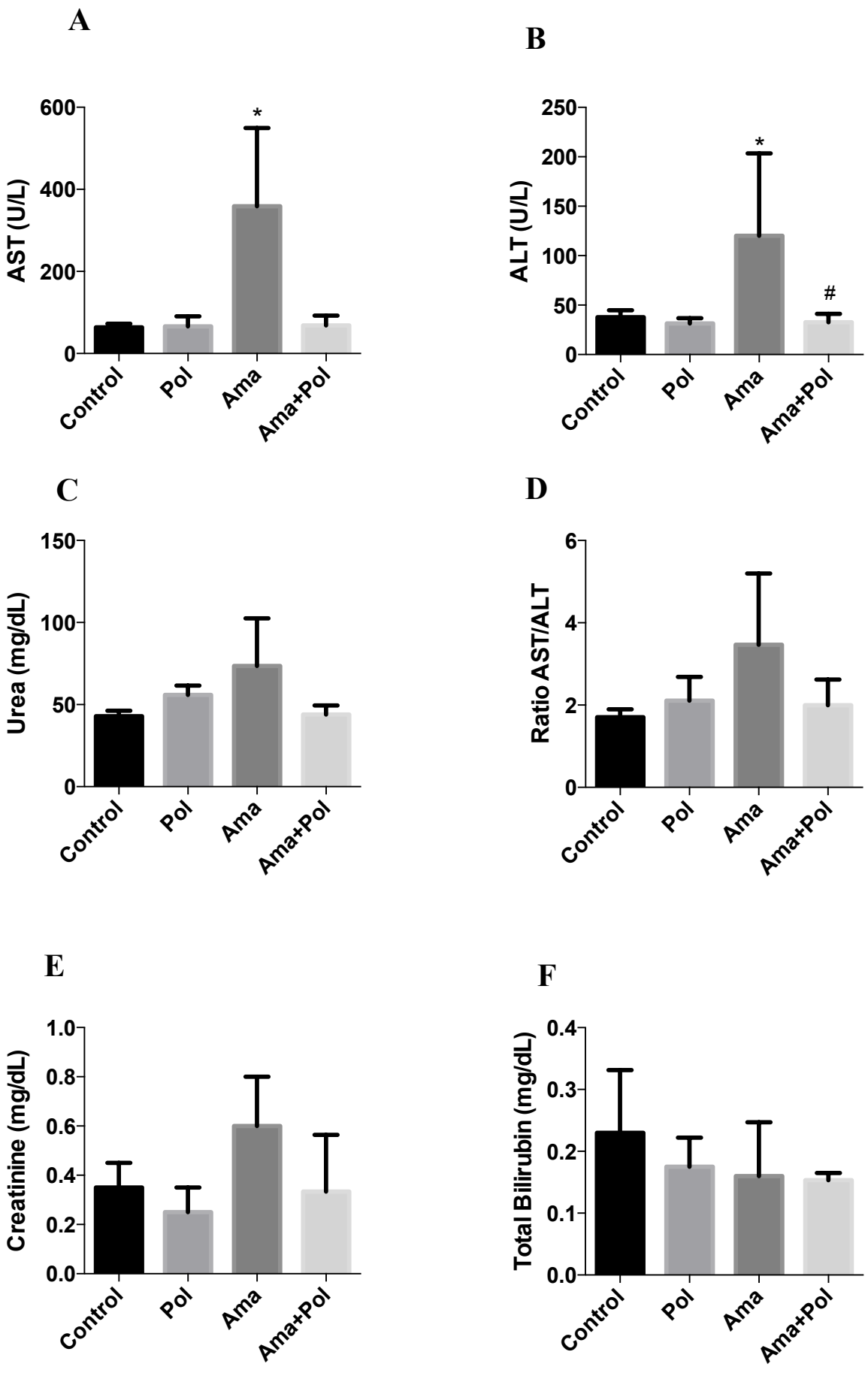
A
AST (U/L)
600
400
200
0
*
Control
Pol
Ama
Ama+Pol
B
ALT (U/L)
250
200
150
100
50
0
*
#
Control
Pol
Ama
Ama+Pol
C
Urea (mg/dL)
150
100
50
0
Control
Pol
Ama
Ama+Pol
D
Ratio AST/ALT
6
4
2
0
Control
Pol
Ama
Ama+Pol
E
Creatinine (mg/dL)
1.0
0.8
0.6
0.4
0.2
0.0
Control
Pol
Ama
Ama+Pol
F
Total Bilirubin (mg/dL)
0.4
0.3
0.2
0.1
0.0
Control
Pol
Ama
Ama+Pol

Figure 3. Plasma levels of **(A)** aspartate aminotransferase (AST), **(B)** alanine aminotransferase (ALT), **(C)** urea **(D)** ratio AST/ALT **(E)** creatinine and **(F)** total bilirubin in control, 3 × 2.5 mg/kg polymyxin B (Pol), 0.33 mg/kg α-amanitin (Ama), and α-amanitin plus polymyxin B (Ama+Pol) groups. Results are presented as means ± standard deviation, and were obtained from 4-5 animals from each treatment. Statistical comparisons were made using Kruskal-Wallis ANOVA on Ranks followed by the Dunn's *post hoc* test (*$p < 0.05$, Ama vs. control; #$p < 0.05$, Ama vs. Ama+Pol).

3.2.2. α-Amanitin caused significant decrease in hepatic weight

As an indirect measure of organ damage, we quantified the ratio of both liver and kidney weight to total body weight in the 24 h study (Table 3). The relative liver weight from the α-amanitin group showed a significant decrease (5.75 ± 0.58 mg/g) in comparison to control group (6.77 ± 0.64 mg/g), and the treatment with polymyxin B prevented this effect (5.94 ± 0.52 mg/g) (Table 3). No differences were seen in ratios of kidney weight/body weight values among control and treatment groups.

Table 3. Ratios of liver weight / body weight and kidney weight / body weight

	Control	Polymyxin B	α-Amanitin	α-Amanitin + polymyxin B
Liver	6.77 ± 0.64	6.04 ± 0.26	5.75 ± 0.58 *	5.94 ± 0.52
Kidney	0.97 ± 0.03	0.85 ± 0.11	0.92 ± 0.09	0.85 ± 0.10

3.2.3. Polymyxin B prevented the total RNA decrease in the kidney of α-amanitin treated animals

Since α-amanitin rapidly inactivates RNAP II with a consequent decrease on mRNA transcription, we quantified the total RNA content in the liver and kidney of animals in all experimental groups. These total RNA levels were further normalized to organ weight. Results from α-amanitin-intoxicated animals revealed that the kidney total RNA significantly decreased (0.981 ± 0.645 μg/mg kidney) compared with control (3.331 ± 0.466 μg/mg kidney) (Figure 4A). This effect was reverted in the α-amanitin plus

polymyxin B group (3.622 ± 1.550 μg/mg kidney). On the other hand, no differences were found for total RNA in the liver of α-amanitin-intoxicated animals (Figure 4B).

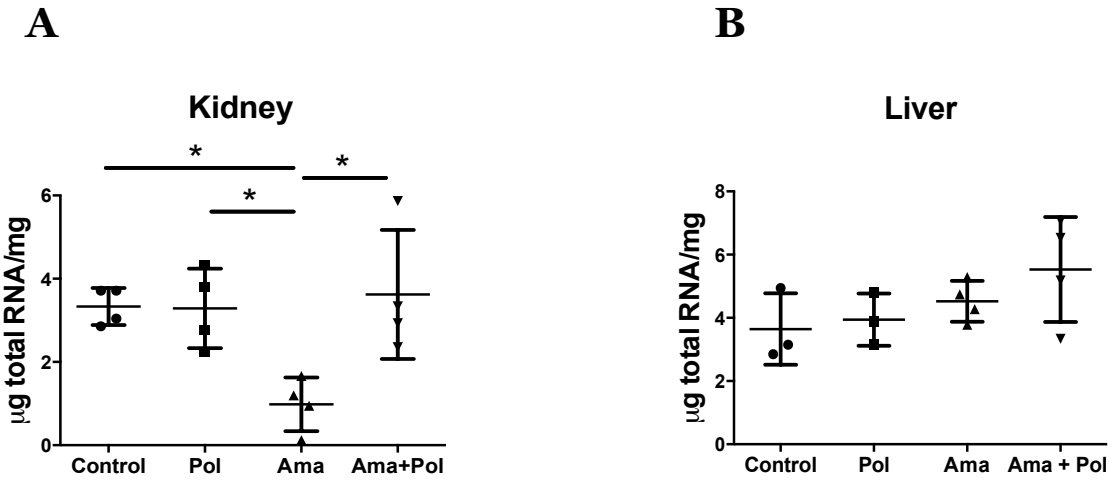

Figure 4. **(A)** Total RNA liver levels and **(B)** total RNA kidney levels of control, 3 × 2.5 mg/kg polymyxin B (Pol), 0.33 mg/kg α-amanitin (Ama), and α-amanitin plus polymyxin B (Ama+Pol) groups. Results were obtained from 4 animals from each treatment group. Statistical comparisons were made one-way ANOVA, followed by the Bonferroni *post hoc* test, (*$p < 0.05$, Ama vs. control; $^{\#}p < 0.05$, Ama vs. Ama +Pol).

3.2.4. Polymyxin B abrogated the α-amanitin-induced alteration of the transcription process

The evaluation of the genetic transcription by RNAP II was based on GAPDH and β-actin mRNA quantitative analysis. The relative transcript levels were quantified by the Ct value, which increases with a decreasing amount of template.

Data from α-amanitin-intoxicated kidney indicated that the transcription of GAPDH and β-actin mRNA significantly decreased (16.29 ± 1.31 and 17.83 ± 0.36, respectively) when compared with control group (12.98 ± 0.46 and 14.20 ± 0.3, respectively) (Table 4). This effect was reverted in the α-amanitin plus polymyxin B group (13.16 ± 0.30 and 15.08 ± 0.68 for GAPDH and β-actin mRNA, respectively).

Although the transcript levels of GAPDH mRNA in the liver samples of α-amanitin-treated showed a tendency to a decrease (17.28 ± 5.47), it failed to reach statistically significance. Nevertheless, this α-amanitin-treated tendency was reverted by the treatment with polymyxin B (14.80 ± 1.24).

On the other hand, no differences were found for β-actin mRNA levels for liver samples (Table 4). Importantly, RNA polymerase I was not affected by α-amanitin poisoning since the transcription of ribosomal proteins S18 and S28 by RNA polymerase I was always similar, regardless of the organ or experimental group analyzed (Table 4).

Table 4. Relative mRNA levels of S28, S18, GAPDH and β-actin genes in liver and kidney samples.

	RNAP I		RNAP II	
	S28	S18	GAPDH	β-Actin
Liver				
Control	34.3 ± 0.7	31.7 ± 1.4	14.5 ± 1.5	17.4 ± 2.5
Polymyxin B	34.9 ± 1.5	31.6 ±1.8	14.7 ± 1.4	17.3 ± 1.6
α-Amanitin	33.9 ± 0.4	30.7 ± 0.6	17.3 ± 5.5	16.1 ± 1.8
α-Amanitin+ polymyxin B	34.5 ± 0.4	31.0 ± 0.5	14.8 ± 1.2	16.5 ± 1.3
Kidney				
Control	34.9 ± 0.8	31.1 ± 0.8	13.0 ± 0.4	14.2 ± 0.4
Polymyxin B	33.8 ± 0.4	30.8 ± 0.3	12.5 ± 0.4	14.9 ± 0.4
α-Amanitin	34.4 ± 1.4	30.9 ± 1.7	16.3 ± 1.3****	17.8 ± 0.4****
α-Amanitin+ polymyxin B	32.8 ± 0.7	29.5 ± 0.9	13.2 ± 0.3$^{####}$	15.1 ± 0.7$^{####}$

3.2.5. Polymyxin B prevented α-amanitin-induced renal and hepatic damage

Given the known toxic effects of α-amanitin in the liver and kidney, we proceed to a histopathological analysis to evaluate the putative protective tissue effects of the polymyxin B antidote. As expected, liver samples from the control and polymyxin B groups presented a normal structure at light microscopy, without evidences of edema, necrosis or cellular infiltrations (Figure 5A and 5B, Table 5). On the other hand, α-amanitin caused prominent hepatic cellular edema, cytoplasmic vacuolization and interstitial inflammatory cell infiltration (Figure 5C, Table 5). Moreover, the α-amanitin group showed some necrotic foci in the liver (Figure 5C and Table 5), which were more evident in the centrilobular zone. The group of α-amanitin plus polymyxin B showed a significant decrease in α-amanitin-induced necrosis, edema and cytoplasmic vacuolization (Figure 5D, Table 5). However, polymyxin B was not able to prevent the α-amanitin-induced increase in interstitial infiltration of inflammatory cells (Figure 5D, Table 5).

Regarding the kidney, control and polymyxin B groups presented a normal renal structure at light microscopy (Figure 6A and 6B, Table 5). Histological examination of α-amanitin-treated kidney (Figure 6C, Table 5) revealed severe degenerative changes: 1) the renal

corpuscles appear heterogeneous, with a wide capsular space, and thickened external Bowman capsule; 2) proximal tubules showed necrotic cells vacuolization and edema; and 3) distal tubules cells had signs of atrophy and degeneration, while a large amount of a protein-related material caused enlargement and obstruction of these tubules (Figure 6C). Noteworthy, in the α-amanitin plus polymyxin group, the damage induced by α-amanitin was significantly attenuated, particularly the regarding the necrotic foci and the obstruction of distal tubules (Figure 6D, Table 5).

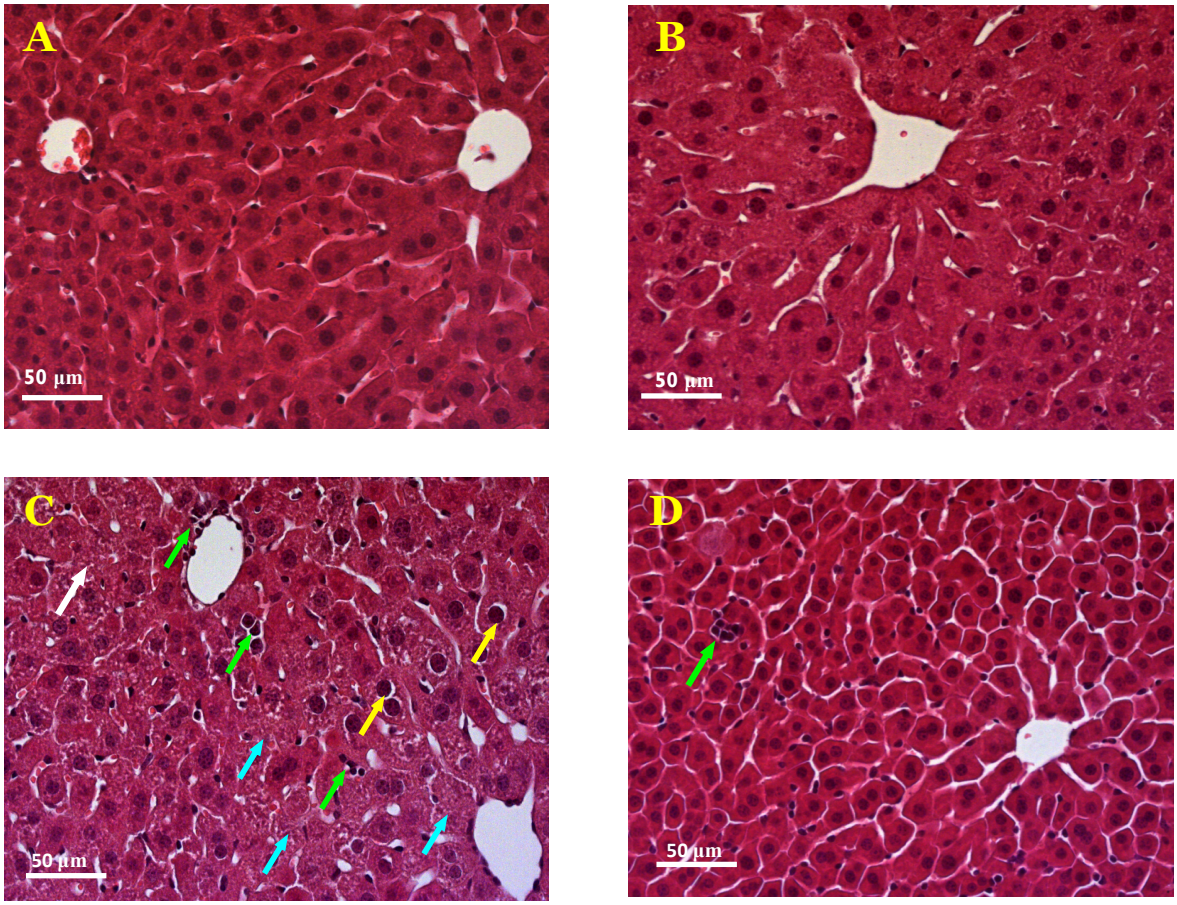

Figure 5. Liver histopathology: **(A)** Light micrograph from the control group, showing normal morphology and structure; **(B)** Light micrograph from the polymyxin B group, showing normal morphology and structure; **(C)** Light micrograph from α-amanitin group. The presence of cellular edema (yellow arrows), cytoplasmic vacuolization (white arrow), inflammatory cells (green arrows), as well as some necrotic zones can be seen (cyan arrows); **(D)** Light micrograph from α-amanitin plus polymyxin B group. The edema and cytoplasmic vacuolization and necrosis were significantly attenuated by polymyxin B.

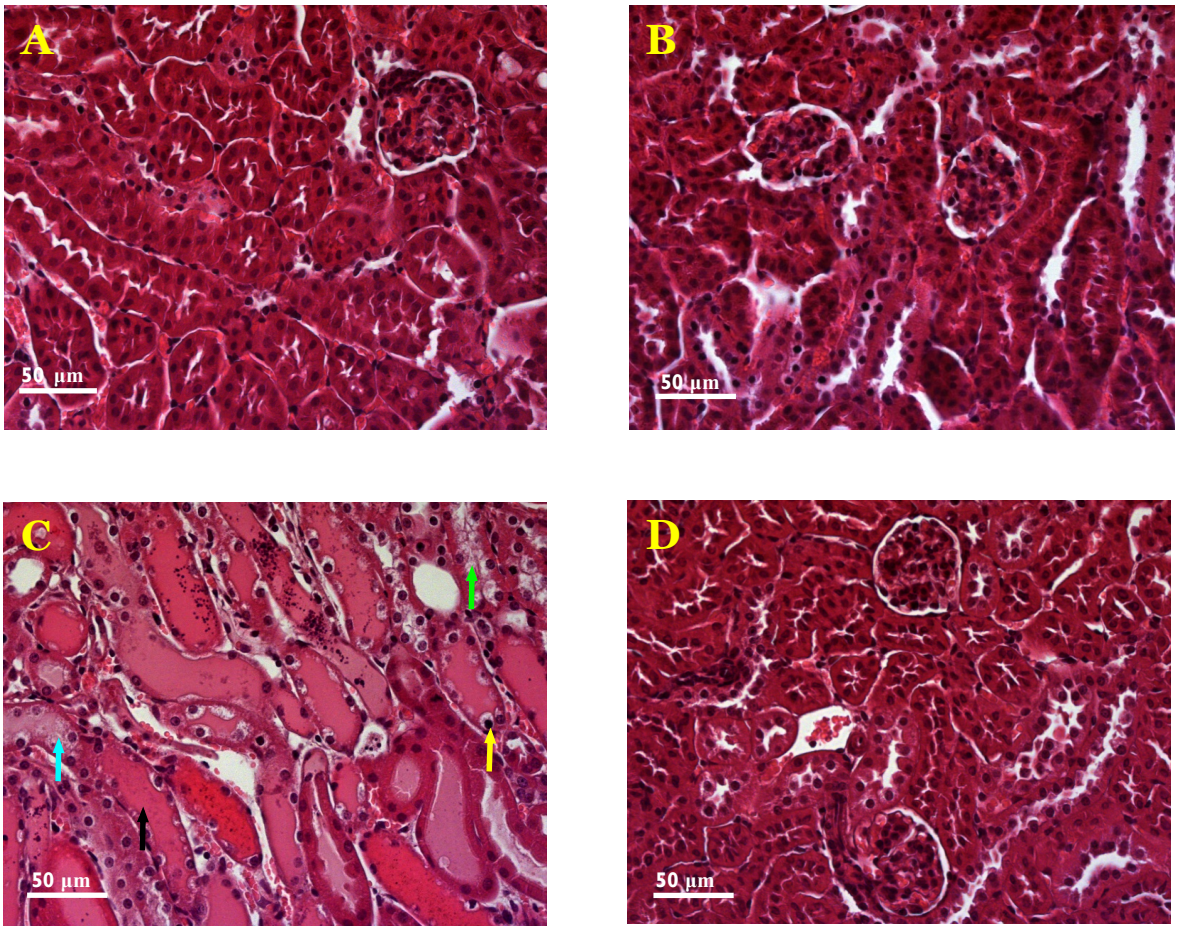

Figure 6. Kidney histopathology: **(A)** Light micrograph from the control group, showing normal morphology and structure; **(B)** Light micrograph from the polymyxin B group, showing normal morphology and structure; **(C)** Light micrograph from α-amanitin group. The presence of cellular edema (yellow arrow), cytoplasmic vacuolization (green arrow), large amounts of protein-related material cause enlargement and obstruction of distal tubules (black arrow), as well as some necrotic zones can be seen (cyan arrow); **(D)** Light micrograph from α-amanitin plus polymyxin B group. The obstruction of distal tubules, edema, cytoplasmic vacuolization and necrosis, were significantly attenuated after polymyxin B

Table 5. Semi-quantitative analysis of the morphological injury parameters of control, α-amanitin and α-amanitin plus polymyxin B groups.

Liver				
	Control	**Polymyxin B**	**α-Amanitin**	**α-Amanitin + polymyxin B**
Cellular degeneration	0.00 ± 0.00	0.25 ± 0. 44	2.02 ± 0.42****	0.44 ± 0.50$^{*\ ####}$
Necrosis	0.00 ± 0.00	0.16 ± 0.49*	1.62 ± 0.49****	0.42 ± 0.50$^{*\ ####}$
Inflammatory activity	0.25 ± 0.43	0.23 ± 0.42	2.09 ± 0.35****	2.04 ± 0.20****
Kidney				
Cellular degeneration	0.27 ±0.45	0.20 ± 0.41	2.26 ± 0.44****	1.08 ± 0.33$^{****\ ####}$
Necrosis	0.00 ± 0.00	0.00 ± 0.00	2.06 ± 0.62****	0.61 ± 0.55$^{****\ ####}$
Inflammatory activity	0.22 ± 0.42	0.19 ± 0.40	1.81 ± 0.42****	1.66 ± 0.48****

3.2.2.6. α-Amanitin caused NF-κB nuclear translocation that was not reverted by polymyxin B

The translocation of the NF-κB factor to the nuclei was assessed by immunohistochemistry in the liver and kidney (Figure 7 and 8) in the short term study. The liver of control and polymyxin B groups showed mainly cytoplasmic staining without marked nuclear staining cells (Figure 7A and 7B). On the other hand, α-amanitin caused significant nuclear translocation of NF-κB mainly in the macrophage-like cells (0.0397 ± 0.0168 cells/μm^2) when compared to control group (0.0018 ± 0.0027 cells/μm^2) (Figure 7C and 7E). Moreover, α-amanitin was also able to cause a significant increase of hepatocytes staining positive as a result of activated nuclear NF-κB (0.0151 ± 0.0093 cells/μm^2) (Figure 7C and 7F) when compared to the control group (0.0012 ± 0.0049 cells/μm^2). The α-amanitin plus polymyxin B group (0.0048 ± 0.0319 and 0.0019 ± 0.0129 cells/μm^2 for macrophage-like cells and hepatocytes, respectively) showed similar results to α-amanitin group, therefore polymyxin B was not able to revert the pro-inflammatory effects of α-amanitin (Figure 7D, 7E and 7F).

Regarding the kidneys, the results showed predominant cytoplasmic staining in control and polymyxin B groups (Figure 8A and 8B), whereas in both α-amanitin and α-amanitin plus polymyxin B groups an increase of macrophage-like cells staining positive for activated NF-κB was observed (Figure 8C and 8D). Due to the heterogeneity of the tissue, the accurate nuclear staining count of the type of cell marked was difficult, therefore only the representative light micrographs of the kidney (Figure 8) are presented.

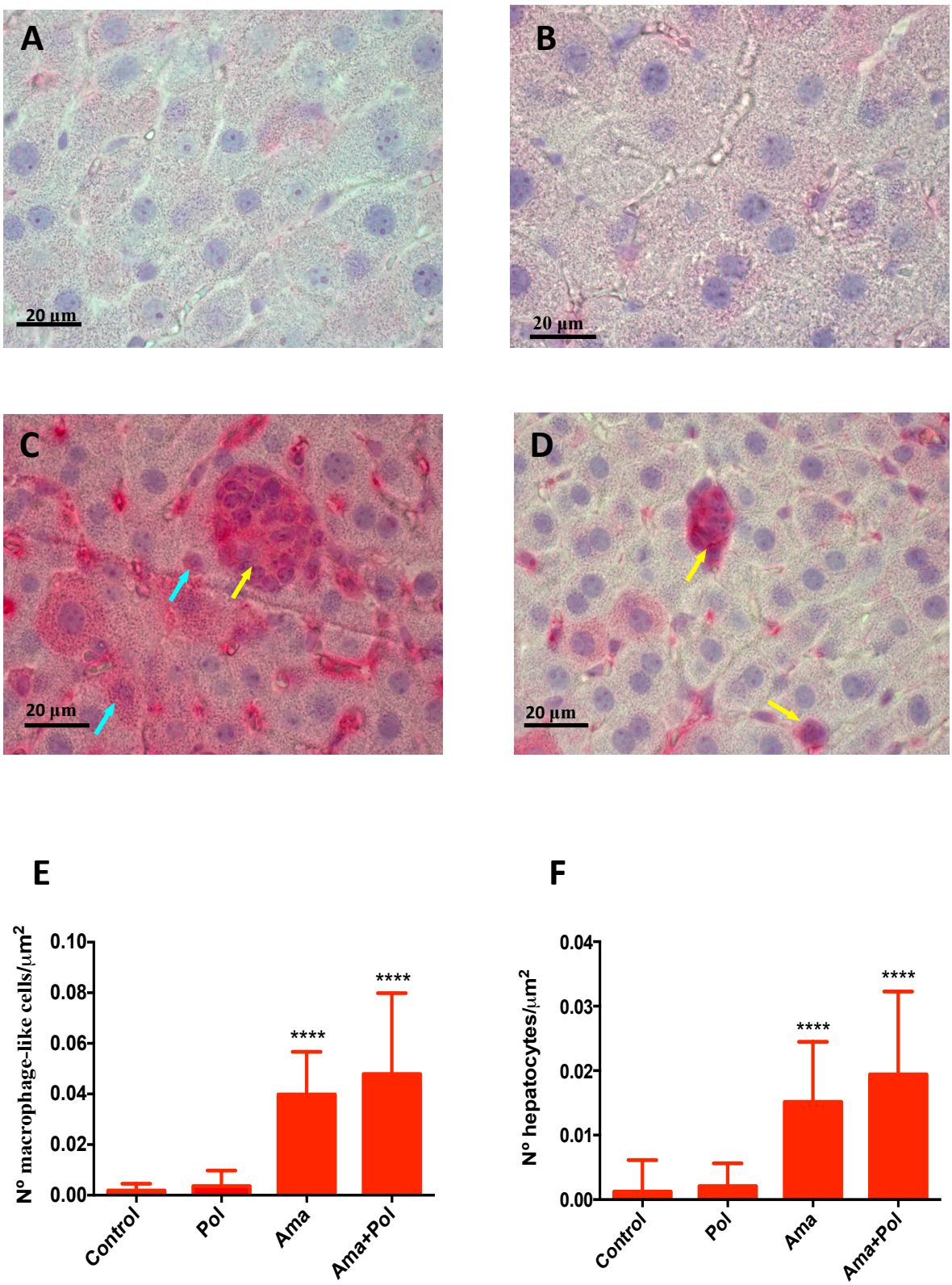

Figure 7. Immunohistochemistry of NF-κB activation in the liver by light microscopy: **(A)** Light micrograph from the control group, showing only cytoplasmic staining without

marked nuclear staining cells; **(B)** Light micrograph from polymyxin B group showing only cytoplasmic staining without marked nuclear staining cells; **(C)** Light micrograph from α-amanitin group showing a greater number of cell staining positive for activated NF-κB in the macrophage-like cells (yellow arrows) and in the hepatocytes (cyan arrows). **(D)** Light micrograph from α-amanitin plus polymyxin B group showing a greater number of cells staining positive for activated NF-κB in the macrophage-like cells (yellow arrow). **(E)** Number of macrophage-like cells staining positive for activated NF-κB. **(F)** Number of hepatocytes staining positive for activated NF-κB of control, 3 × 2.5 mg/kg polymyxin B (Pol), 0.33 mg/kg α-amanitin (Ama), and α-amanitin plus polymyxin B (Ama+Pol) groups. Results were expressed as means ± standard deviation. Results were obtained from 4 animals from each treatment group. Statistical comparisons were made using Kruskal-Wallis ANOVA on Ranks followed by the Dunn's *post hoc* test (****$p < 0.0001$, Ama and Ama+Pol vs. control).

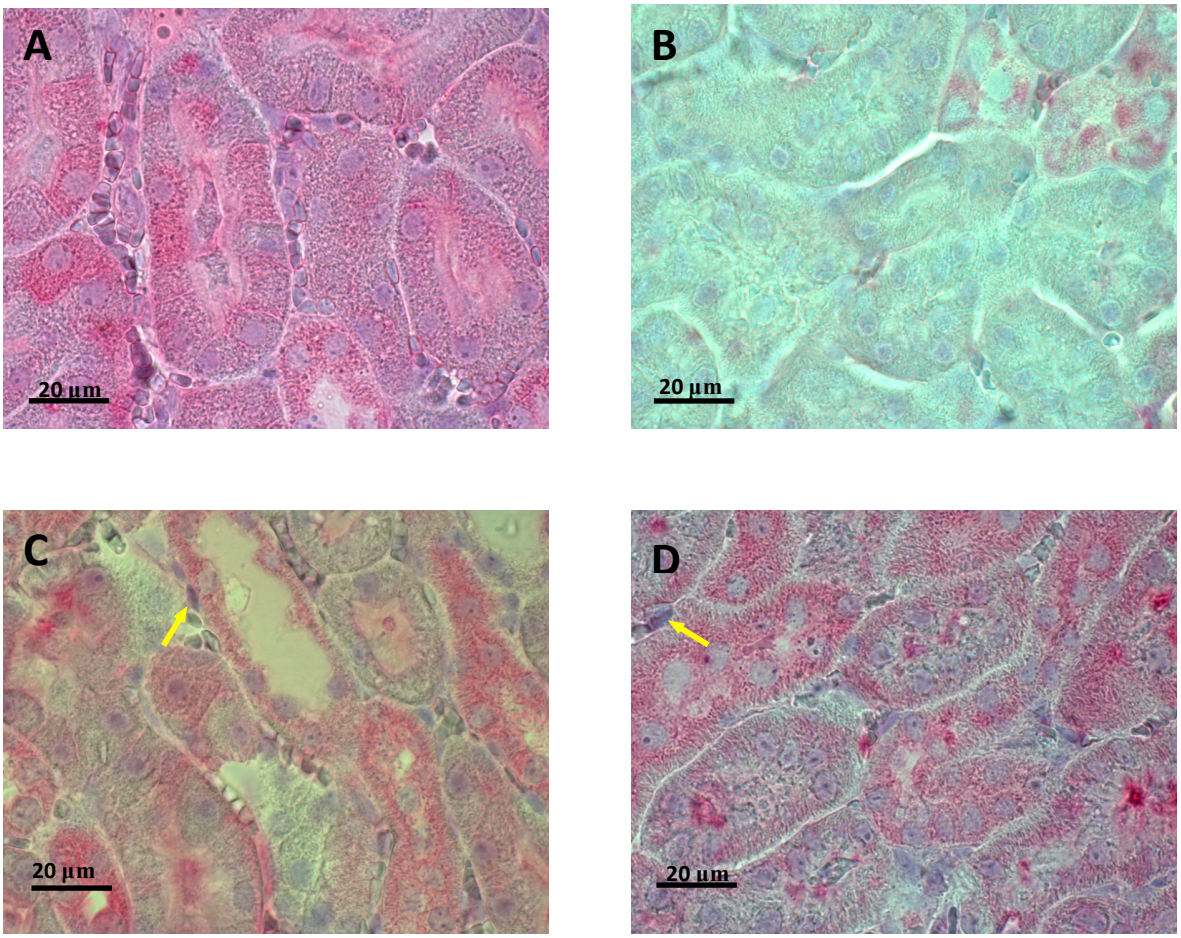

Figure 8. Immunohistochemistry of NF-κB activation in the kidney by light microscopy. **(A)** Light micrograph from the control group, showing only cytoplasmic staining without

marked nuclear staining cells. **(B)** Light micrograph from polymyxin B group showing only cytoplasmic staining without marked nuclear staining cells. **(C)** Light micrograph from α-amanitin group showing cell staining positive for activated NF-κB in the macrophage-like cells (yellow arrow). **(D)** Light micrograph from α-amanitin plus polymyxin B group showing cell staining positive for activated NF-κB in the macrophage-like cells (yellow arrow).

3.2.2.7. Polymyxin B prevented the α-amanitin increase of hepatic protein carbonylation

Protein carbonylation is an indicator of severe oxidative damage, which often leads to a loss of protein function. As shown in Figure 9A, liver protein carbonylation increased significantly in α-amanitin group (127.6 ± 7.1 %) when compared to control group (100.0 ± 10.1 %). Treatment with polymyxin B significantly attenuated hepatic α-amanitin-induced increase of protein carbonylation (107.8 ± 16.1 %). In the kidneys, although a tendency to increase was observed in the α-amanitin group (122.9 ± 34.3 %), when compared to control (100.0 ± 13.3 %), no statistical significance was reached (Figure 9B).

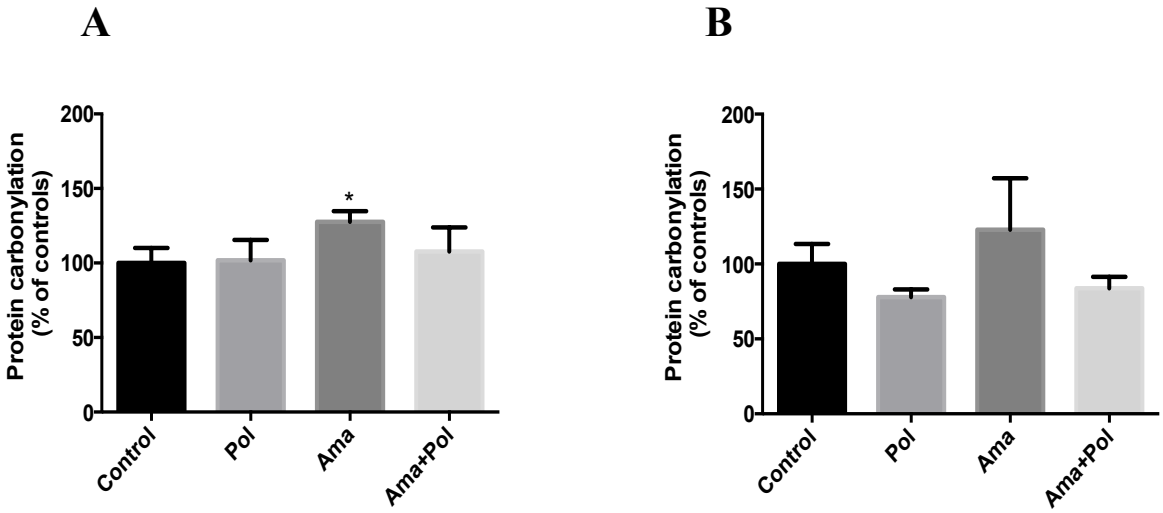

Figure 9. (A) Protein carbonylation levels in the liver; **(B)** Protein carbonylation levels in the kidney, in control, 3 × 2.5 mg/kg polymyxin B (Pol), 0.33 mg/kg α-amanitin (Ama), and α-amanitin plus polymyxin B (Ama+Pol) groups. Results were expressed as percentage variation of control values and expressed as means ± standard deviation. Results were obtained from 4 animals from each treatment group. Statistical comparisons were made one-way ANOVA, followed by the Dunn's *post hoc* test, (*$p < 0.05$, Ama vs. control; #$p < 0.05$, Ama vs. Ama +Pol).

3.2.3. Survival rate and welfare examination

A long-term survival study (30 days) was done with two different polymyxin B treatment regimens after α-amanitin (0.33 mg/kg i.p.): 1) polymyxin B was administered at 4, 8 and 12 h (3 × 2.5 mg/kg i.p.), and 2) polymyxin B (1 × 2.5 mg/kg) was concomitantly administered with α-amanitin.

All mice exposed to 0.33 mg/kg of α-amanitin died within 5 days (Figure 10). All deaths occurred within 2 to 5 days α-amanitin post administration. α-Amanitin treated animals became hunched and lethargic soon after dosing. Subsequently, mice showed apathy, reduced mobility, respiratory problems, seizures, and disorientation until death within 24 h of these symptoms arousal.

The concomitant administration of α-amanitin and polymyxin B resulted in 100% of survival. The group that received concomitant administration of polymyxin B with α-amanitin showed moderate signs of discomfort at day five, namely involuntary movements of the head that persisted without improvement until the end of the experiment.

The group that received multiple doses of polymyxin B and α-amanitin, a 50% survival rate was observed. All deaths occurred within 5 to 7 days. In the surviving animals that received multiple doses of polymyxin B and α-amanitin, no poisoning signs were observed. Neither the polymyxin B group (3 × 2.5 mg/kg i.p.) nor the control group showed any other signs of discomfort during the 30 days experiment.

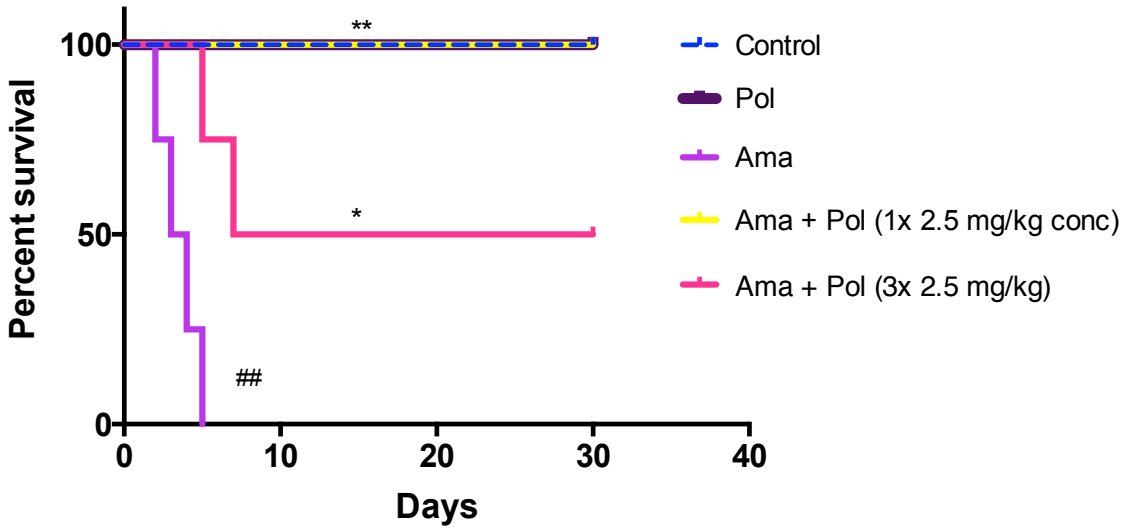

Figure 10. Survival rate curves after concomitant i.p. administration of 0.33 mg/kg of α-amanitin and polymyxin B (2.5 mg/kg) and administration of polymyxin B (2.5 mg/kg) 4, 8 and 12 h after initial administration of α-amanitin. Results are expressed as percent survival. Results were obtained from 4 animals from each treatment. Statistical

comparisons were made using Log-rank (Mantel-Cox) test (*p < 0.05, Ama + Pol 2.5 mg/kg vs. Ama; **p < 0.01, Ama + Pol 2.5 mg/kg vs. Ama; ##p < 0.01, Ama vs. control). Blue line represents saline-control treatment, dark purple represents polymyxin B treatment; violet line represents the treatment with α-amanitin, yellow line represents the concomitant treatment with α-amanitin and polymyxin B (2.5 mg/kg), magenta line represents the administration of polymyxin B (3x2.5 mg/kg) 4, 8 and 12 h after α-amaniti

4. Discussion

The present work reports the discovery of what we believe will be the first effective antidote for *A. phalloides* poisoning: polymyxin B. The present study provides unequivocal *in silico* and *in vivo* evidence that polymyxin B confers a potent protection against α-amanitin induced-toxicity, by interfering with its main mechanism of toxicity, the inhibition of RNAP II activity. Outstandingly, the *in silico* studies on RNAP II were shown to be of outmost importance in the development process, and the successful *in vivo* studies allow the suggestion of immediate use of the antidote in addition to the current therapeutic measures, as polymyxin B is a therapeutic drug with a well-established clinical use.

We started with the application of *in silico* methods, taking advantage of the description of the X-ray structure of α-amanitin with yeast RNAP II that revealed several key molecular interactions that may contribute to inhibition of RNAP II activity (Bushnell et al. 2002). Based on that structure, we have recently reported an *in silico* study in which we provided new insights into the inhibition mechanism of RNAP II by α-amanitin; additionally the mode of interaction of α-amanitin and three clinically used antidotes (benzylpenicillin, ceftazidime and silybin) with RNAP II, using docking methods and molecular dynamics simulations was investigated (Garcia et al. 2014). Multiple relevant interactions between α-amanitin and RNAP II are located in the bridge helix and the trigger loop. Thus, α-amanitin may block RNAP II translocation by interacting with the bridge helix, preventing the conformational change of the trigger loop and consequent transcriptional elongation. Benzylpenicillin, ceftazidime and silybin were shown to be able to bind to the same site as α-amanitin, although not replicating the unique α-amanitin binding mode. These drugs establish considerably less intermolecular interactions than α-amanitin and the ones that exist are essentially confined to the bridge helix and adjacent residues (Garcia et al. 2014). These results show that the therapeutic effect of these drugs does not seem to be directly related with the binding with RNAP II but to other mechanisms. Therefore, an antidote that regenerates the RNAP II or that prevents the α-amanitin binding to RNAP II does not

yet exists and clinical efficacy of the treatments after *A. phalloides* is still low (Garcia et al. 2015).

Herein, we have applied the same *in silico* methodology to a peptide with similar composition and molecular weight of amatoxins, polymyxin B, and confirmed its ability to displace α-amanitin from RNAP II. Polymyxin B was never tested as an antidote for α-amanitin. Docking and MD simulations (10 ns) were carried out to study the mode of interaction of RNAP II/polymyxin B complex using binding energy decomposition based on the MM-GBSA approach, as reported before for other molecules (Garcia et al. 2014). Three valuable findings could be observed *in silico*: (1) polymyxin B binding site is located in the same interface of α-amanitin, which can prevent the binding of the toxin; (2) polymyxin B does not interact with bridge helix residues allowing the transcription process; (3) hydrogen bonds, CH–π and hydrophobic interactions drive the bindings of polymyxin B to RNAP II. Therefore, the polymyxin B binding location on RNAP II can potentially protect RNAP II from the α-amanitin-induced impairment. In fact, competition between polymyxin B and α-amanitin and/or displacement of α-amanitin from RNAP II by polymyxin can occur depending on the affinity of each molecule for the RNAP II binding site.

To prove the applicability of our *in silico* results, we used an *in vivo* model often used to study α-amanitin toxicity (Schneider et al. 1987; Schneider et al. 1992; Tong et al. 2007; Yamaura et al. 1986; Zhao et al. 2006). Since RNAP II is considered the main target for α-amanitin toxicity, mRNA levels can be used as a measure of its inhibition (Larson 2011) and our results showed that inhibition of kidney GAPDH and β-actin mRNA transcription elicited by α-amanitin was efficiently reverted by polymyxin B. Still, in the liver changes on mRNA levels of GAPDH and β-actin did not reach significance. This apparent discrepancy between the liver and kidney could be explained, at least partially, by the process of mRNA turnover. The turnover of mRNA is complex, organ/cell specific, and the several critical mechanisms are not yet fully understood (Beelman and Parker 1995; Guhaniyogi and Brewer 2001; Ross 1995). Moreover, the mRNA half-live varies greatly between different cell types. In rat hepatocytes, the half-life for β-actin mRNA is 9 h (Reuner et al. 1995), whereas in HepG2 cells it is reported as 5-6 h (Gao et al. 2003). In addition, a half-life of 6.6 h and 13.5 h in human leukemia Nalm-6 (B-cell derived) and CCRF-CEM (T-cell derived) cells, respectively, was reported for the same mRNA transcript (Leclerc et al. 2002). Furthermore, the regulation of mRNA stability is likely to be an essential component in the tissue response to toxins exposure, and it differs among organs (Ross 1995). To the best of our knowledge, in CD-1 mice, the half-lives of hepatic or renal GAPDH and β-actin mRNA are not known. Moreover, in the present study, GAPDH

seemed to be a more sensitive marker for α-amanitin intoxication at 24 h in the kidney. However, organ differences of α-amanitin accumulation may also have an important influence in the observed results.

Polymyxin B not only had a strong impact on genetic expression, but it also caused a clear protection against α-amanitin-induced injury. Serum aminotransferases (ALT and AST) have been used as sensitive indicators for liver injury caused by amatoxins (Chang and Yamaura 1993; Yamaura et al. 1986; Zhao et al. 2006) and, in accordance, in our model, AST and ALT were significantly increased in the α-amanitin-intoxicated group. That α-amanitin-induced increased was totally reverted by administration of multiple doses of 2.5 mg/kg polymyxin B. Moreover, the plasma findings were corroborated by histological observations. The liver of mice administered with α-amanitin evidenced evident damage, with cellular edema, cytoplasmic vacuolization and interstitial inflammatory cell infiltration, as well as some centrilobular necrotic zones. These histological phenotypes are in agreement with previous reports of α-amanitin studies in mice (Kaya et al. 2014; Wills et al. 2005; Zhao et al. 2006). α-Amanitin (1 mg/kg i.p.)-treated Balb/c mice showed vacuolar degeneration of liver cells, 1 h and 6 h after poisoning (Kaya et al. 2014), whereas α-amanitin (0.327 mg/kg intravenous) caused liver fatty degeneration and necrosis 48 h after treatment in the same mice strain (Zhao et al. 2006). Moreover, histopathological hepatic damage in laboratory animals is similar to those found in humans after *A. phalloides* intoxication, namely regarding features of hepatic massive centrilobular necrosis and vacuolar degeneration (Fineschi et al. 1996).

Regarding the kidney, although less studied in humans, it is also a target organ for *A. phalloides* poisoning. Human data indicates that acute tubular necrosis with kidney failure occurs in amatoxins-intoxicated patients (Mydlik and Derzsiova 2006). In animal models, intense tubular necrosis was described in Balb/c mice 48 h after α-amanitin (0.327 mg/kg intravenous) (Zhao et al. 2006). In our work, the histological examination of α-amanitin-intoxicated kidney revealed extensive damage and a significant intratubular obstruction. Although the nature of that obstruction is unknown, the reduced tubular epithelial cell proliferation as a consequence of inhibition of RNAP II and cellular necrosis may lead to that material accumulation. Noteworthy, the administration of polymyxin B protected against the occurrence of the majority of the renal damage inflicted by α-amanitin, namely cellular edema, cytoplasmic vacuolization and necrosis. However, polymyxin B was not able to revert the hepatic and renal pro-inflammatory effect that occurred after α-amanitin. Indeed, in the present work, NF-κB was strongly activated in the liver and kidney exposed to α-amanitin, whereas polymyxin was not able to revert that NF-κB activation. The nuclear factor NF-κB pathway has been considered a prototypical

pro-inflammatory signaling, based on the role of NF-κB in the expression of pro-inflammatory genes including cytokines, chemokines, and adhesion molecules (Lawrence 2009). To the best of our knowledge, this was the first time that NF-κB factor was shown to play an important role on α-amanitin toxicity. Moreover, NF-κB activation can promote liver injury through the genetic transcription of TNF-α and IL-6 (Murr et al. 2002; Zhang et al. 2007; Zhao et al. 2005). In fact, TNF-α has been implicated in α-amanitin induced hepatotoxicity *in vivo*, since after α-amanitin (3 mg/kg i.p.), the levels of hepatic TNF-messenger RNA were shown to increase, concurring to hepatocytes apoptosis (Leist et al. 1997). Consistently, mice deficient for the 55-kilodalton TNF receptor were protected from α-amanitin–induced toxicity (Leist et al. 1997). The authors suggested that the synergism between TNF-α and α-amanitin may explain the highly hepatotoxic potential of α-amanitin *in vivo* (Leist et al. 1997). NF-κB could regulate TNF-α expression (Zhao et al. 2005), and therefore the development of therapies aimed to block TNF-α and/or NF-κB could be of outmost importance against amatoxins toxicity. In the present work, it is reasonable to assume that the pro-inflammatory effect of NF-κB may be responsible for some of the late deaths on the survival study when polymyxin B was only administered 4 h after α-amanitin. On the other hand, when administered concomitantly, polymyxin B possibly prevented α-amanitin to reach RNAP II, therefore avoiding any significant side effect. The link between α-amanitin RNAP II inhibition and NF-κB activation should be further investigated as it could stablish other pathways for antidotal therapy against this toxin.

α-Amanitin toxicity has been associated with oxidative stress and protein carbonylation is seen as a stable biomarker of oxidative stress as protein turnover can take hours or days (Dalle-Donne et al. 2003). Herein, protein carbonylation increased significantly in liver of mice exposed to α-amanitin, relatively to the control group, suggesting that α-amanitin is able to alter protein redox status. This effect was abrogated by the multiple administration of polymyxin B. Available data regarding α-amanitin ability to induce oxidative stress is elusive. Mice treated with α-amanitin (1 mg/kg i.p.) and sacrificed 20 h after poisoning showed liver superoxide dismutase activity increase (Zheleva et al. 2007). The authors concluded that *in vivo* α-amanitin liver accumulation could lead to reactive oxygen species (ROS) formation, in particular superoxide anion radical (Zheleva et al. 2007). Recently, the levels of ROS in kidney homogenates isolated from α-amanitin (1 mg/kg i.p.)-treated mice were found to be increased (Zheleva 2013), whereas *in vitro,* the formation of phenoxyl radical after oxidation of α-amanitin was demonstrated (Zheleva 2013). Although NF-κB pro-inflammatory activity is often associated with oxidative stress, in the present study, polymyxin B was able to abrogate α-amanitin induced protein

carbonylation and not NF-κB activation, suggesting that the mechanisms involved are dissimilar.

The hindrance of α-amanitin-overall toxicity by polymyxin B was established by a 30 days survival study. The administration of polymyxin B at 4, 8 and 12 h post α-amanitin resulted in a 50% of survival rate, whereas α-amanitin-treated animals died within 5 days. In this experimental approach, polymyxin B was administered 4 h after α-amanitin exposure, seeking a more realistic treatment approach, since hospitalization after *A. phalloides* human poisoning usually occurs only hours after ingestion. Importantly, the concomitant administration of polymyxin B and α-amanitin resulted in 100% survival until the 30th day post exposure, confirming the antidote efficacy.

Taken together, the *in silico* and the *in vivo* data obtained in the present study demonstrated that polymyxin B acts on RNAP II and prevents α-amanitin toxicity. The use of polymyxin B in human mushroom poisonings will be the main goal to prove the validity of the present work. Clinical assays in intoxicated humans are feasible with polymyxin B since the doses used in this pre-clinical study are considered safe (Zavascki et al. 2007), when allometric scaling is applied. The 3 doses of 2.5 mg/kg of polymyxin B in mice sums up to approximately 1 mg/kg in humans, according to the allometric scaling (West and Brown 2005). This polymyxin B dose is below the recommended dose of intravenous polymyxin B for the treatment of infections caused by *Pseudomonas aeruginosa* in patients with normal renal function (Zavascki et al. 2007). The data presented herein demonstrate that polymyxin B may be used as a novel pharmacological approach to the treatment of *A. phalloides* poisoning. Thus, its rapid introduction in the therapeutic antidotal response will be of the outmost importance to increase the patient's survival rate of the putative fatal *A. phalloides* intoxication. For ethical reasons, however, polymyxin B should be added to the ongoing therapeutic protocol to improve *A. phalloides* survival and not replace it as to guaranty the maximal efficacy of the clinical pharmacological weapons available.

Acknowledgements

Juliana Garcia, Vera Marisa Costa and Ricardo Dinis-Oliveira thank FCT - Foundation for Science and Technology - for their PhD grant (SFRH/BD/74979/2010), Post-doc grant (SFRH/BPD/63746/2009) and Investigator grant (IF/01147/2013), respectively. This work received financial support from the European Union (FEDER funds through COMPETE) and National Funds (FCT, Fundação para a Ciência e Tecnologia) through project Pest-C/EQB/LA0006/2013.

Table legends

Table 1. Binding energy calculation between the polymyxin B and Rpb1 and Rpb2 subunits (all energies are in kcal/mol).

Table 2. Hydrogen bonds formed between the polymyxin B and RNA polymerase II[a].

Table 3. Ratios of liver weight / body weight and kidney weight/body weight. Results are presented as means ± standard deviation from 4 animals of each treatment group. Statistical comparisons were made using the One-way ANOVA followed by Dunn's *post hoc* test (*$p < 0.05$ vs. control).

Table 4. Relative mRNA levels of S28, S18, GAPDH and β-actin genes in liver and kidney samples. Results are presented as mean ± standard deviation of threshold cycles from 4 animals from each treatment group. Statistical comparisons were made using ANOVA followed by Bonferroni *post hoc* test (****$p < 0.0001$, Ama and vs. Control; ####$p < 0.0001$, Ama and vs. Ama+Pol).

Table 5. Semi-quantitative analysis of the morphological injury parameters of control, α-amanitin and α-amanitin plus polymyxin B groups. Results of hematoxylin-eosin staining, given in scores, are presented as means ± standard deviation from 4 animals from each treatment group. Statistical comparisons were made using Kruskal-Wallis ANOVA on Ranks followed by the Dunn's *post hoc* test (*$p < 0.05$, ****$p < 0.0001$, treatment vs. control; ####$p < 0.0001$, Ama group vs Ama+ Pol).

REFERENCES

Barbosa DJ, Capela JP, Oliveira JM, et al. (2012) Pro-oxidant effects of Ecstasy and its metabolites in mouse brain synaptosomes. Br J Pharmacol 165(4b):1017-33

Beelman CA, Parker R (1995) Degradation of mRNA in eukaryotes. Cell 81(2):179-183

Bidnychenko Y (2001) Detecting Mushroom Peptide Toxins in Body Fluids by Capillary Electrophoresis. LCGC 19(9):1000-1002

Broussard CN, Aggarwal A, Lacey SR, et al. (2001) Mushroom poisoning--from diarrhea to liver transplantation. Am J Gastroenterol 96(11):3195-8

Bushnell DA, Cramer P, Kornberg RD (2002) Structural basis of transcription: alpha-amanitin-RNA polymerase II cocrystal at 2.8 A resolution. Proc Natl Acad Sci USA 99(3):1218-22

Case DA, Cheatham TE, 3rd, Darden T, et al. (2005) The Amber biomolecular simulation programs. J Comput Chem 26(16):1668-88

Chang I-M, Yamaura Y (1993) Aucubin: A new antidote for poisonous Amanita mushrooms. Phytother Res 7(1):53-56

Cheung PCK (2010) The nutritional and health benefits of mushrooms. Nutrition Bulletin 35(4):292-299

Dalle-Donne I, Rossi R, Giustarini D, Milzani A, Colombo R (2003) Protein carbonyl groups as biomarkers of oxidative stress. Clin Chim Acta 329(1-2):23-38

Dores-Sousa JL, Duarte JA, Seabra V, Bastos Mde L, Carvalho F, Costa VM (2015) The age factor for mitoxantrone's cardiotoxicity: Multiple doses render the adult mouse heart more susceptible to injury. Toxicology 329:106-19

Fineschi V, Di Paolo M, Centini F (1996) Histological criteria for diagnosis of amanita phalloides poisoning. J Forensic Sci 41(3):429-32

Gao C, Guo H, Downey L, Marroquin C, Wei J, Kuo PC (2003) Osteopontin-dependent CD44v6 expression and cell adhesion in HepG2 cells. Carcinogenesis 24(12):1871-8

Garcia J, Carvalho AT, Dourado DF, Baptista P, de Lourdes Bastos M, Carvalho F (2014) New in silico insights into the inhibition of RNAP II by alpha-amanitin and the protective effect mediated by effective antidotes. J Mol Graph Model 51:120-7

Garcia J, Costa V, Carvalho A, et al. (2015) Amanita phalloides poisoning: mechanisms of toxicity and treatment. submitted

Guhaniyogi J, Brewer G (2001) Regulation of mRNA stability in mammalian cells. Gene 265(1-2):11-23

He J, Gao S, Hu M, Chow DS, Tam VH (2013) A validated ultra-performance liquid chromatography-tandem mass spectrometry method for the quantification of polymyxin B in mouse serum and epithelial lining fluid: application to pharmacokinetic studies. J Antimicrob Chemother 68(5):1104-10

Humphrey W, Dalke A, Schulten K (1996) VMD: Visual molecular dynamics. J Mol Graph 14(1):33-38

Kaya E, Surmen MG, Yaykasli KO, et al. (2014) Dermal absorption and toxicity of alpha amanitin in mice. Cutan Ocul Toxicol 33(2):154-60

Kempe S, Kestler H, Lasar A, Wirth T (2005) NF- kB controls the global pro-inflammatory response in endothelial cells: evidence for the regulation of a pro-atherogenic program. Nucleic Acids Res 33(16):5308-5319

Koda-Kimble MA, Alldredge BK, Corelli RL, Ernst ME (2012) Koda-Kimble and Young's Applied Therapeutics: The Clinical Use of Drugs. Wolters Kluwer Health

Kollman PA, Massova I, Reyes C, et al. (2000) Calculating structures and free energies of complex molecules: combining molecular mechanics and continuum models. Acc Chem Res 33(12):889-97

Larson DR (2011) What do expression dynamics tell us about the mechanism of transcription? Current opinion in genetics & development 21(5):591-9

Lawrence T (2009) The Nuclear Factor NF- kB Pathway in Inflammation. Cold Harb Perspect Biol 1(6):a001651 Spring

Leclerc G, Leclerc G, Barredo J (2002) Real-time RT-PCR analysis of mRNA decay: half-life of Beta-actin mRNA in human leukemia CCRF-CEM and Nalm-6 cell lines. Cancer Cell Int 2(1):1

Leist M, Gantner F, Naumann H, et al. (1997) Tumor necrosis factor-induced apoptosis during the poisoning of mice with hepatotoxins. Gastroenterology 112(3):923-34

Morris GM, Huey R, Lindstrom W, et al. (2009) AutoDock4 and AutoDockTools4: Automated docking with selective receptor flexibility. J Comput Chem 30(16):2785-91

Mowry JB, Spyker DA, Cantilena LR, Jr., Bailey JE, Ford M (2013) 2012 Annual Report of the American Association of Poison Control Centers' National Poison Data System (NPDS): 30th Annual Report. Clin Toxicol 51(10):949-1229

Murr MM, Yang J, Fier A, Kaylor P, Mastorides S, Norman JG (2002) Pancreatic elastase induces liver injury by activating cytokine production within Kupffer cells via nuclear factor-Kappa B. J Gastrointest Surg 6(3):474-80

Mydlik M, Derzsiova K (2006) Liver and kidney damage in acute poisonings. Bantao Journal 4(1):30-32

Onufriev A, Bashford D, Case DA (2000) Modification of the Generalized Born Model Suitable for Macromolecules. J Phys Chem B 104(15):3712-3720

Pinson CW, Daya MR, Benner KG, et al. (1990) Liver transplantation for severe Amanita phalloides mushroom poisoning. Am J Surg 159(5):493-9

Poucheret P, Fons F, Dore JC, Michelot D, Rapior S (2010) Amatoxin poisoning treatment decision-making: pharmaco-therapeutic clinical strategy assessment using multidimensional multivariate statistic analysis. Toxicon 55(7):1338-45

Reuner KH, Wiederhold M, Dunker P, et al. (1995) Autoregulation of actin synthesis in hepatocytes by transcriptional and posttranscriptional mechanisms. European journal of biochemistry / FEBS 230(1):32-7

Ross J (1995) mRNA stability in mammalian cells. Microbiol Rev 59(3):423-50

Schneider SM, Borochovitz D, Krenzelok EP (1987) Cimetidine protection against alpha-amanitin hepatotoxicity in mice: a potential model for the treatment of Amanita phalloides poisoning. Ann Emerg Med 16(10):1136-40

Schneider SM, Michelson EA, Vanscoy G (1992) Failure of N-acetylcysteine to reduce alpha amanitin toxicity. J Appl Toxicol 12(2):141-2

Tong TC, Hernandez M, Richardson WH, 3rd, et al. (2007) Comparative treatment of alpha-amanitin poisoning with N-acetylcysteine, benzylpenicillin, cimetidine, thioctic acid, and silybin in a murine model. Ann Emerg Med 50(3):282-8

Vetter J (1998) Toxins of Amanita phalloides. Toxicon 36(1):13-24

Vogel G, Tuchweber B, Trost W, Mengs U (1984) Protection by silibinin against Amanita phalloides intoxication in beagles. Toxicol Appl Pharmacol 73(3):355-62

Weiser J, Shenkin PS, Still WC (1999) Approximate atomic surfaces from linear combinations of pairwise overlaps (LCPO). J Comput Chem 20(2):217-230

West GB, Brown JH (2005) The origin of allometric scaling laws in biology from genomes to ecosystems: towards a quantitative unifying theory of biological structure and organization. J Exp Biol 208(9):1575-1592

Wieland T (1983) The toxic peptides from Amanita mushrooms. Int J Pept Prot Res 22(3):257-276

Wieland T, Faulstich H (1978) Amatoxins, phallotoxins, phallolysin, and antamanide: the biologically active components of poisonous Amanita mushrooms. CRC Crit Rev Biochem 5(3):185-260

Wills BK, Haller NA, Peter D, White LJ (2005) Use of amifostine, a novel cytoprotective, in alpha-amanitin poisoning. Clin Toxicol (Phila) 43(4):261-7

Yamaura Y, Fukuhara M, Takabatake E, Ito N, Hashimoto T (1986) Hepatotoxic action of a poisonous mushroom, Amanita abrupta in mice and its toxic component. Toxicology 38(2):161-73

Zavascki AP, Goldani LZ, Li J, Nation RL (2007) Polymyxin B for the treatment of multidrug-resistant pathogens: a critical review. J Antimicrob Chemother 60(6):1206-15

Zhang XP, Zhang L, Chen LJ, et al. (2007) Influence of dexamethasone on inflammatory mediators and NF-kappaB expression in multiple organs of rats with severe acute pancreatitis. World J Gastroenterol 13(4):548-56

Zhao J, Cao M, Zhang J, Sun Q, Chen Q, Yang ZR (2006) Pathological effects of the mushroom toxin alpha-amanitin on BALB/c mice. Peptides 27(12):3047-52

Zhao YF, Zhai WL, Zhang SJ, Chen XP (2005) Protection effect of triptolide to liver injury in rats with severe acute pancreatitis. Hepatobiliary Pancreat Dis Int 4(4):604-8

Zheleva A (2013) Phenoxyl radicals formation might contribute to severe toxicity of mushrooms toxin alpha-amanitin-an electron paramagnetic resonance study. TJS 11(1):33-38

Zheleva A, Tolekova A, Zhelev M, Uzunova V, Platikanova M, Gadzheva V (2007) Free radical reactions might contribute to severe alpha amanitin hepatotoxicity-a hypothesis. Med Hypotheses 69(2):361-7

CHAPTER IV

DISCUSSION AND CONCLUSIONS

4.1 Discussion and conclusions

In this section, the results obtained and included in this dissertation are discussed and integrated. The conclusions will be inferred considering the overall results of the dissertation and the findings of other published reports.

The key findings of this thesis were: 1) Amatoxins and phallotoxins are not equally distributed in the *A. phalloides* fruiting body and environmental conditions play a significant role in the mushrooms content of these toxins; 2) A new HPLC method using DAD and EC detectors was successfully applied to measure α-amanitin in rat liver and kidney allowing, in a clinical case, to confirm the diagnosis of amatoxins poisoning; 4) RNAP II α-amanitin binding was characterized *in silico* and can be divided into specific zones with different properties. The model developed provided a reliable platform for the structure-based drug design of novel antidotes for amatoxins poisoning. 5) α-Amanitin affects RNAP II transcription by compromising the trigger loop and bridge helix functions. 6) The therapeutic effect of the antidotes (benzylpenicillin, ceftazidime and silybin) used in amatoxins poisoning does not seem to be directly related with RNAP II binding. 7) *In silico* studies showed that polymyxin B binding site is located in the same interface of α-amanitin, which may prevent the toxin from binding to RNAP II without interfering with mRNA synthesis. 8) *In vivo,* the inhibition of the transcription specific kidney genes elicited by α-amanitin (0.33 mg/kg) was efficiently reverted by multiple doses of polymyxin B (3 × 2.5 mg/kg). 9) Polymyxin B significantly decreased the hepatic and renal α-amanitin-induced injury as supported by the histology and plasma damage biomarkers data. 10) Fifty percent of animal exposed to polymyxin B (3 × 2.5 mg/kg) 4, 8 and 12 hours after α-amanitin (0.33 mg/kg) survived, while all animals treated with α-amanitin died until day 5. 11) A single dose of polymyxin B (2.5 mg/kg) administered concomitantly with α-amanitin (0.33 mg/kg) was able to guaranty 100% survival until the 30th day post exposure.

Amanita phalloides poisoning is a global problem arising from the naturally fruiting of the body in many parts of the globe. It is one of the most poisonous known toadstools, being associated with severe symptoms, high morbidity and mortality (85, 125). Despite warnings, wild edible and *A. phalloides* mushrooms are frequently mistaken and every year several cases of intoxications are reported (6, 50, 120, 126, 127). Other authors has indicated a potentially significant variation in the amount of amatoxins contained in mushrooms collected at different geographical areas (27). Therefore, it is of great importance to characterize the toxicological profile of *A. phalloides* mushrooms throughout the world. Taking into account that no works are available regarding toxins'

composition of *A. phalloides* growing in Portugal, the composition of Portuguese *A. phalloides* carpophores collected from two different sites of Trás-os-Montes (Vinhais and Mogadouro) were analyzed (study I). Since α-amanitin is the main toxin responsible for the toxic effects of *A. phalloides*, the study I was focused on the quantification of this toxin. The analysis was made in 3 separated parts of the fruit body; caps, stipe, and volva. The results showed that the caps contained the highest amount of α-amanitin (783.94 ± 2.66 μg/g and 666.00 ± 1.45 μg/g in caps from Vinhais and Mogadouro, respectively), whereas the volva had the lowest content (103.87 ± 1.84 μg/g and 73.16 ± 1.66 μg/g in volva from Vinhais and Mogadouro, respectively), which are consistent with previous data (27). Qualitative analyses of the β-, γ-amanitin, phalloidin, phallisin, and phallacidin based on LC-MS and HPLC-DAD were also performed. The results showed that the contents and distribution of amatoxins and phallotoxins in the different carpophore tissues are markedly different and vary from one area to another. In fact, caps have the highest content of amatoxins, whereas the volva was richest in phallotoxins, which is in accordance with previous reports (27-29). Moreover, our study supports the hypothesis that environmental conditions (mainly the soil type) clearly have an effect on the phallotoxin composition of *A. phalloides* carpophores. Vinhais and Mogadouro have significant topographic (128) and climatic differences (129) that have a significant impact in the soil type where the mushrooms grow. Leptosols are dominant in Mogadouro, whereas cambisols are the most representative soils of Vinhais (130). The highest phalloidin concentration was found in the stipe from Mogadouro, whereas the highest phallisin concentration was found in the stipe from Vinhais. These results corroborated a previous report indicating that the soil characteristics appear to have higher influence on phallotoxin composition than on amatoxins composition (29).

A lack of analytical methods to quantify α-amanitin in biological samples hinders the quantification of this toxin in tissues. According to the literature, liquid chromatography is the method of excellence for α-amanitin quantification (131, 132). Despite the availability of several HPLC methods in the literature for the analysis and quantification of α-amanitin in different matrices, they have been mainly applied in mushrooms (27-29, 75, 76), plasma (131, 133) and urine (134). Besides, these methods seem matrix specific. To the best of our knowledge, only two studies have been validated, namely a LC method for α-amanitin analyses in tissues. Leite *et al.* developed an analytical methodology of ultra performance liquid chromatography-tandem mass spectrometry (UPLC–MS/MS), following liver sample preparation by protein precipitation with organic solvents, and solid phase extraction procedure with a limit of detection of 10.9 ng/g (135). Filigenzi *et al.* described a LC-MS/MS/MS method for the analysis of α-amanitin in liver

(131). Liver was prepared by homogenization with aqueous acetonitrile and subsequent removal of acetonitrile was done using methylene chloride. The aqueous phase was then extracted using mixed-mode C18/cation exchange solid phase extraction cartridges. The detection limit of this method was 0.50 ng/g (131). These methods are time consuming and use equipment not common in all Toxicology Laboratories with

use of organic and environmentally detrimental reagents. Moreover, to date there are no published HPLC with EC detection methods for the analysis of α-amanitin in biological tissues. The determination of amatoxins in serum by HPLC was greatly improved by using EC detection, particularly as far as minimum detectable amounts are concerned (136). Consequently, we developed a simple and efficient analytical method for quantification of α-amanitin in liver and kidney tissues, since they are the α-amanitin main target organs (study II). The study II was focused on the development, optimization and application of a HPLC method with in-line connected DAD and EC detectors to quantify α-amanitin in biological samples (namely liver and kidney). Kidney and liver samples preparation was achieved by a simple and unique deproteinization step with perchloric acid. Specificity, linearity, recovery, intra and inter-assay precision, and detection and quantification limits were determined, in order to guarantee reliability of the analytical results. The developed method proved to be specific and linear in the range of 0.025-10 μg/mL, and showed coefficients of correlation greater than 0.994. The extraction recovery presented good results for the concentrations analyzed, with values ranging from 96.87 to 101.45% for both matrices. Precision was checked at three levels and in three different days over 3 weeks, with intra-day and inter-day coefficients of variation lower than 15.3%. The limit of detection values for α-amanitin based on visual evaluation ranged from 0.05 (DAD) to 0.025 μg/mL (EC) in liver and 0.125 (DAD) to 0.100 μg/mL (EC) in kidney. Limit of quantification values based on visual evaluation ranged from 0.250 (DAD) to 0.025 μg/mL (EC) in liver and 0.250 (DAD)–0.100 μg/mL (EC) in kidney. This method was also successfully applied to quantify α-amanitin in human plasma since there were no endogenous substances in the samples co-eluting with α-amanitin. To prove the applicability of our method, we performed an *in vivo* study (Wistar rats) with different α-amanitin doses (10 and 21,4 mg/kg, i.p.) and sacrifice times (2 and 4 hours). Our results showed higher levels of total α-amanitin in kidney than in liver, explained by the fact that the kidney serves as an elimination organ of α-amanitin. Therefore the validated analytical method was able to be successfully applied to toxicokinetics studies. Importantly, we validated the method using two detectors (DAD and EC) since HPLC-EC instruments are not available in many laboratories. Noteworthy, the results showed that the limits of detection and quantification for α-amanitin could be improved through the use of an EC

detector. The validated analytical method presents a high potential in the identification, detection and determination of α-amanitin in hepatic and renal samples offering a significant improvement in diagnosis, postmortem confirmation of amatoxin intoxications, tissues analysis and other toxicokinetics studies (study II). Moreover, it can be also successfully applied to other matrices like urine and gastric juice samples as we demonstrated in a clinical case of amatoxins poisoning (study III). This was an unusual case of amatoxins poisoning since no amatoxin symptoms and toxicity were observed. The patient was taken to the hospital emergency room 3 hours after mushrooms ingestion due to the rapid hallucinogenic symptoms. These hallucinogenic symptoms lead to the suspicion of isoxazoles-containing mushrooms poisoning, which was confirmed by the presence of muscimol in the urine analyzed by GC-MS. Our validated HPLC-DAD method was applied to the gastric juice sample, revealing the presence of α-amanitin at 1.12 μg/mL concentration. The rapid hospitalization and the history of mushrooms ingestion, led to an early therapeutic intervention for amatoxins poisoning, which consisted of gastric lavage, oral-activated charcoal, silybin and N-acetylcysteine administration. Usually, the amatoxins' intoxicated patients arrive at the emergency room hours or even days after mushrooms ingestion when clinical symptoms are evident. The most widely used antidotes are benzylpenicillin, ceftadizime, silybin and N-acetylcysteine (5), although their precise mechanisms of action remain to be elucidated. Benzylpenicillin appears to inhibit uptake of amatoxins by hepatocytes (137), but high doses are required for that pharmacological action, which narrows the therapeutic/safety margin (97). Ceftazidime is stated to have the same pharmacological mechanisms of benzylpenicillin (97), but no study was conducted to prove it. Silybin and N-acetylcysteine have been used due to their antioxidant proprieties; however other mechanisms may be involved. So far, none of these antidotes have proven to be of clinical efficacy as controlled studies are lacking and experimental data in animals are equivocal. Thus, the main objective of this dissertation was to discover an effective antidote for amatoxins poisoning. For that purpose, the most known toxic mechanism of α-amanitin was explored (study IV). α-Amanitin inhibits RNAP II, a vital enzyme in the transcription process, being responsible for the synthesis of mRNA (explained in the theoretical background of this dissertation) (9). With this in mind, the elucidation of the inhibition mechanism of RNAP II by α-amanitin, using *in silico* studies, was performed (study IV). *In silico* methodologies have become a crucial component to study the interactions between biomolecules and their environment (138) allowing to elucidate the mechanisms of action of many compounds and to identify innovative therapeutic treatments (139). Another main advantage of the *in silico* techniques is their effectiveness in reducing costs and the number of experimental animals (140). Therefore, firstly, we used *in silico* studies to elucidate RNAP II structure and its

interaction with α-amanitin and with classically-used antidotes. The structure of RNAP II in a complex with α-amanitin has been determined by X-ray crystallography (56). The structure of the complex indicated the likely basis of inhibition and gives unexpected insights into the transcription mechanism (56). Bushnell *et al.* suggested that α-amanitin interferes with bridge helix movement during translocation since it binds to the free RNAP II core adjacent to the bridge helix (56). This X-ray structure allowed us to study *in silico* the mode of interaction of α-amanitin with RNAP II. Study IV started with molecular docking, an effective tool for unveiling RNAP II-α-amanitin molecular recognition (141). This procedure allowed to predict the α-amanitin conformation and orientation (or posing) within the RNAP II binding site. However, the docking process considered the target binding site and the ligand as rigid elements. The incorporation of flexibility properties in the molecular recognition process was achieved by using MD (142). MD was applied to study the physical movements of atoms that composed the complex (RNAP II-α-amanitin) interacting for a period of time, giving a view of the motion of the atoms. Moreover, MD simulations allowed exploring of additional druggable binding sites (cryptic or allosteric) in the RNAP II. To provide a more detailed understanding of molecular recognition in RNAP II-α-amanitin interactions, we resorted to the MM-GBSA method. This is one of the most important post processing methods for free-energy estimation (143). The binding free energies obtained from molecular mechanics with MM-GBSA calculations using MD trajectories is the most popular procedure to measure the strength of interactions between a ligand and its receptor (143). The results showed that α-amanitin affects RNAP II transcription by compromising trigger loop and bridge helix functions. The observed direct interactions between α-amanitin and trigger loop residues (Leu1081, Asn1082, Thr1083, His1085 and Gly1088) and bridge helix residues (Gly819, Gly820, Glu822, His816 and Phe815) interfere with the elongation process and thus impair the transcription process. These results clearly corroborated the hypothesis of an important role of the bridge helix and trigger loop as fundamental elements in the synthesis of mRNA (58). Moreover, previous findings suggested that α-amanitin affects the trigger loop movement, which closes over the active site during nucleotide incorporation (58). To provide a new insight into the plausible mechanism of action of the three classically-used antidotes in amatoxins poisoning (benzylpenicillin, ceftazidime and silybin), we used the same *in silico* methodologies described above. The results showed that the antidotes are able to bind to the same site as α-amanitin in RNAP II, although not reproducing the distinctive α-amanitin binding mode. It is not surprising that these drugs fail to reproduce the binding mode of α-amanitin, since the ligands are small molecules that establish much less intermolecular interactions with RNAP II than α-amanitin. From

the *in silico* study (study IV), we demonstrated that the therapeutic effect of these antidotes does not seem to be directly related with competition to RNAP II. From the knowledge of the recognition modes of RNAP II/α-amanitin binding, we began to search novel ligands with therapeutic potential against amatoxins poisoning (study V). Molecular docking with putative ligands began with a database of peptide compounds with similar composition and molecular weight to that of amatoxins, to predict relative ligand binding affinities. Then MD and mm-GBSA methodologies were applied in order to provide new insights into the possible therapeutic mechanism of action of the chosen compounds. This study provided, for the first time, a promising compound in amatoxins poisoning, polymyxin B. *In silico* results showed that polymyxin B binding site is located in the same interface of α-amanitin, which can prevent the toxin from binding, and hence possibly protect RNAP II from α-amanitin-induced impairment. To validate these results, a rodent model (CD-1 mice) was used. Mice have been used in several studies of amatoxins poisoning since their response to hepatic toxins is considered analogous to that of humans, mainly with renal and hepatic impairment (101, 144-147). As oral absorption of amatoxins in mice is poor, the bioavailability was guaranteed by intraperitoneal administration. Moreover, the intraperitoneal administration has been the preferred route in previous studies that evaluate putative new and the classical antidotes used against amatoxins poisoning (101, 112, 144, 145, 148). The selected dose of α-amanitin to be assayed (0.33 mg/kg) was based on LD_{50} in white mice (the strain was not specified) (36), however other doses have been reported in mice (0.15 to 0.5 mg/kg) (149). The previously described i.p. LD_{50} of α-amanitin in male Swiss mice (20-25 g) was 0.8 mg/kg, and the LD_{95} was 1.2 mg/kg (150). In a study conducted by Wills *et al.* the i.p. 0.68 mg/kg dose represented a LD_{90} in female Swiss mice (21-24 g) (145), whereas the intravenous LD_{50} dose of α-amanitin was 0.327 mg/kg in male BALB/c mice (20 ±2.0 g) (147). These differences may be due to the sex, age, and mouse strains suggesting that these are important factors determining the susceptibility of mice to the toxic action of α-amanitin.

In this dissertation, two types of *in vivo* studies were performed in order to prove the efficacy of polymyxin B against α-amanitin intoxication: a short-term study (sacrifice time at 24 hours) and a survival study. The first study was conducted to examine histological damage, protein carbonylation, NF-κB activation, total RNA and specific mRNA quantification in liver and kidney. The subsequent survival study aimed to evaluate the long-term effectiveness of polymyxin B.

In the short-term study, all polymyxin B-treated animals received three i.p. doses of 2.5 mg/kg (4, 8 and 12 hours after α-amanitin injection). This dose regimen was chosen based on a previous pharmacokinetic study, in which an UPLC–MS/MS method was used

for the quantification of polymyxin B in mice serum samples after a intravenous dose of 3 mg/kg, showing that polymyxin B is non-detectable at 4 h post-administration (151). In our study, the regimen of polymyxin B was initiated 4 hours after intoxication of mice with α-amanitin, a lag time that confers realism to a possible therapeutic scheme to be applied to intoxicated humans. The interaction of polymyxin B and RNAP II seen *in silico* was corroborated in this *in vivo* study, as mRNA quantification revealed that inhibition of specific mRNAs transcripts elicited by α-amanitin was efficiently reverted by polymyxin B in the kidney. Therefore, a competition between α-amanitin and polymyxin B and/or displacement of α-amanitin from its RNAP II binding site by polymyxin B may occur. For the first time, a competitive RNAP II binder has been reported.

As the hepatic damage is the main concern after amatoxins poisoning, plasma liver damage biomarkers were assessed, namely plasma aminotransferases (AST and ALT). Plasma aminotransferases have been used as sensitive indicators for liver injury caused by amatoxins in animals and humans. In humans, plasma levels of hepatic aminotransferases have been the most accurate predictive indicators of recovery or death (18), whereas in mice studies they have been used as indicators to demonstrate the putative benefits of treatments (101, 152). Our results demonstrate that the increase on plasma aminotransferases after α-amanitin administration was abrogated by polymyxin B. This lower damage was accompanied by a marked decrease in histological hepatic damage namely necrosis, cytoplasmic vacuolation and cellular edema that occurred after α-amanitin.

While our study showed that polymyxin B prevented aminotransferase rise after α-amanitin, in a study conducted to analyze the efficacy of the classical antidotes used in amatoxin poisoning namely benzylpenicillin, silybin, and N-acetylcysteine, none of them prevented such α-amanitin-induced increase of aminotransferases in mice (101). In that study, the classical antidotes (benzylpenicillin, silybin and N-acetylcysteine) were administered 4 hours after the i.p. LD_{50} (0.6 mg/kg) of α-amanitin and plasma aminotransferases were analyzed 48 hours after α-amanitin administration (101). Based on that data, the authors concluded that these antidotal therapies were not effective in limiting hepatic injury after α-amanitin poisoning (101).

In our *in vivo* study, kidney damage was also evaluated, since it is also a target organ of toxicity of α-amanitin. Our results showed extensive cell damage (tubular necrosis, edema and cytoplasmic vacuolation) with a significant intratubular obstruction and inflammation in α-amanitin-intoxicated kidney. Amatoxins are excreted in large quantities in urine during the first days after mushrooms ingestion and remain high in the kidney for long periods (96 hours after ingestion of mushrooms) (19), which results in

kidney damage. That injury leads to high values of plasma creatinine and urea, culminating in renal failure (153, 154). Human kidney biopsy of amatoxins' intoxicated patients showed massive acute tubular necrosis, mainly in the proximal convoluted tubule, and mild interstitial infiltration by mononuclear cells (155). Thus, our mice model also closely mimics human renal injury induced by α-amanitin. Moreover, the renal damage was drastically attenuated by the multiple administration of polymyxin B. This finding demonstrates that this antidote provides protection to both target organs of amatoxins: liver and kidney.

In study V, it was observed that the inflammatory activity elicited by α-amanitin was not prevented by polymyxin B. In fact, a powerful activation of NF-κB in both organs (liver and kidney) was observed after α-amanitin administration. This effect was not prevented by polymyxin B. NF-kB is a pivotal transcription factor implicated in the regulation of many genes, particularly those of the inflammatory and immune responses and has both cytoprotective and cell death promoting effects (156). To the best of our knowledge, this was the first time that an association between NF-κB activation in liver and kidney with α-amanitin administration was described.

After an *in vivo* administration of α-amanitin (i.p. 3 mg/kg), the levels of hepatic TNF-messenger RNA increased, suggesting that the synergism between TNF-α and α-amanitin may increase the hepatotoxicity of α-amanitin (65). Moreover, an association between NF-κB activation and TNF-α may also exist, since TNF-α is known to be regulated by NF-κB activation (157). A study that aimed to investigate the effect of the inflammatory response and NF-kB activation in mice renal injury concluded that in the acute inflammatory response induced by ischemia/reperfusion, the activation of the TNF-α/NF-kB signal pathway plays a key role in renal injury (158). Moreover, the activation of NF-kB can promote liver injury in rats with acute pancreatitis by inducing the genetic expression of TNF-α (159). These findings favor the research of novel treatments targeting the NF-κB inhibition, since it may play an important role in the protection against α-amanitin-induced hepatic and renal toxicity. A finding that supports our hypothesis concerns triptolide (an anti-inflammatory and immunosuppressive compound) that was able to reduce pathological damage in the liver by inhibiting the activation of NF-κB and therefore decrease the release of inflammatory mediators in mice with severe pancreatitis (160).

Oxidative stress has also been implicated in α-amanitin-induced liver injury (explained in the theoretical background of this thesis) (67, 68). In this dissertation, carbonylation was used as a stress oxidative biomarker, since protein carbonylation occurs early after oxidative stress and is relatively stable (161). In our *in vivo* study, it was

performed, by the first time the protein carbonylation analysis after α-amanitin administration. The results showed that protein carbonylation levels increased significantly in liver of mice exposed to α-amanitin relatively to the control group, an effect that was prevented by polymyxin B. Our results corroborate previous findings, suggesting that ROS may have an important role in α-amanitin-induced liver toxicity (67, 68). Although ROS are commonly involved in mechanisms that drive to NF-kB nuclear activation (162), polymyxin B was able to hinder α-amanitin induced protein carbonylation but not NF-κB activation, suggesting that the mechanisms involved in the two pathways are different.

The survival study used the same dose regimen and scheme of the short-term study as well as a concomitant regimen, in which a single polymyxin B (2.5 mg/kg) was administered concomitantly with α-amanitin. The results showed 50% of survival of the polymyxin B-treated mice in comparison with 100% of mortality of α-amanitin-exposed mice. Moreover, a single dose of polymyxin B (2.5 mg/kg) concomitantly administered with α-amanitin resulted in the full survival of the α-amanitin treated animals. These results secure the potential use of polymyxin B as an antidote against α-amanitin-induced liver and kidney toxicity. To the best of our knowledge, no survival study was done with the classical antidotes and these studies are the gold standard for evaluating the long-term efficacy of the antidotes.

The–findings of our *in vivo* study, allow proposing polymyxin B as novel therapeutic approach for amatoxins poisoning. Since polymyxin B is already clinically used as an antibiotic, the rapid introduction as an antidote may be of the outmost importance to increase patient survival on the putative fatal *A. phalloides* intoxication. For ethical reasons, however, polymyxin B should be added to the present protocol on *A. phalloides* intoxication and it should not replace the current protocol. We believe that this addition will improve the overall survival of intoxicated patients.

With this study, it was given an important step in the treatment of α-amanitin poisoning. Due to the importance of this study, the pharmacological use of polymyxin B as antidote in α-amanitin intoxication is being patented.

Conclusions and future perspectives

In summary, from the experimental, the *in silico* and the *in vivo* studies herein described, it was possible to conclude that:

- The toxins composition of *A. phalloides* varies greatly, depending on the soil and environmental conditions.

- HPLC with DAD and EC detectors is able to accurately and specifically measure α-amanitin in liver and kidney samples.

- α-Amanitin compromises the trigger loop and the bridge helix functions of RNAP II, which alters the elongation process contributing to the inhibition of this enzyme.

- The action mechanisms of the current antidotes (benzylpenicillin, ceftazidime and silybin) used in amatoxins poisoning do not seem to be directly related with binding to RNAP II.

- Polymyxin B binding site is located in the same interface of α-amanitin, which can prevent the toxins from binding, and hence protect RNAP II from α-amanitin-induced impairment.

- mRNA analysis was in agreement with *in silico* results showing that polymyxin B may compete and/or displace α-amanitin from its RNAP II binding site.

- The effectiveness of polymyxin B was confirmed by the reversion of the increases of plasmatic aminotransferases elicited by α-amanitin as well as attenuation of α-amanitin-induced liver and kidney damage.

- Multiple dose therapy of polymyxin B iniciated 4 hours after α-amanitin administration resulted in 50% of survival rate of the treated mice vs 0% in α-amanitin control group.

- Concomitant administration of polymyxin B with α-amanitin resulted in full survival of the animals.

- Polymyxin B should be introduced as therapeutic drug to be used against α-amanitin toxicity and it has high potential to be immediately applied in humans, since it is already in clinical use for other pathologies.

Concerning future perspectives, the pathway of the trigger loop is still missing. Thus it will be of great value to unveil the full trigger loop movement using *in silico* studies to confirm if α-amanitin impairs it. Moreover, the role of NF-κb in α-amanitin-induced inflammation should be further investigated. Additionally, other inflammation pathways should be explored. The putative pro-inflammatory properties of α-amanitin may be due to its interactions with cellular signaling cascades involving cytokines, regulatory transcription factors, and the expression of pro-inflammatory genes. Cytokines (IL-1α, IL-1β, IL-6, IL-8, and TNF-α) deserves experimental evaluation.

Future projects are required to continue with the pre-clinical studies to explain, in more detail, the mode of action of polymyxin B in the protection against α-amanitin - induced liver and kidney injury, but also pre-clinical studies, particularly those aimed to synthesize new polymyxin B derivatives in attempt to guarantee full animals survival or the use of polimedication, namely polymyxin B together with anti-inflammatory drugs.

CHAPTER V

REFERENCES

References

1. Cheung PCK. The nutritional and health benefits of mushrooms. Nutr Bull. 2010;35(4):292-9.
2. Pilz D, Molina R. Commercial harvests of edible mushrooms from the forests of the Pacific Northwest United States: issues, management, and monitoring for sustainability. Forest Ecol Manag. 2002;155(1–3):3-16.
3. Eren SH, Demirel Y, Ugurlu S, Korkmaz I, Aktas C, Güven FMK. Mushroom poisoning: retrospective analysis of 294 cases. Clinics. 2010;65(5):491-6.
4. Karlson-Stiber C, Persson H. Cytotoxic fungi--an overview. Toxicon. 2003;42(4):339-49.
5. Enjalbert F, Rapior S, Nouguier-Soule J, Guillon S, Amouroux N, Cabot C. Treatment of amatoxin poisoning: 20-year retrospective analysis. J Toxicol Clin Toxicol. 2002;40(6):715-57.
6. Alves A, Gouveia Ferreira M, Paulo J, Franca A, Carvalho A. Mushroom poisoning with Amanita phalloides - a report of four cases. Eur J Intern Med. 2001;12(1):64-6.
7. Bonnet MS, Basson PW. The toxicology of Amanita phalloides. Homeopathy. 2002;91(4):249-54.
8. Diaz JH. Syndromic diagnosis and management of confirmed mushroom poisonings. Crit Care Med. 2005;33(2):427-36.
9. Vetter J. Toxins of Amanita phalloides. Toxicon. 1998;36(1):13-24.
10. Escudie L, Francoz C, Vinel JP, Moucari R, Cournot M, Paradis V, et al. Amanita phalloides poisoning: reassessment of prognostic factors and indications for emergency liver transplantation. J Hepatol. 2007;46(3):466-73.
11. Ganzert M, Felgenhauer N, Zilker T. Indication of liver transplantation following amatoxin intoxication. J Hepatol. 2005;42(2):202-9.
12. Koda-Kimble MA, Alldredge BK, Corelli RL, Ernst ME. Koda-Kimble and Young's Applied Therapeutics: The Clinical Use of Drugs: Wolters Kluwer Health; 2012.
13. Broussard CN, Aggarwal A, Lacey SR, Post AB, Gramlich T, Henderson JM, et al. Mushroom poisoning--from diarrhea to liver transplantation. Am J Gastroenterol. 2001;96(11):3195-8.
14. Pinson CW, Daya MR, Benner KG, Norton RL, Deveney KE, Kurkchubasche AG, et al. Liver transplantation for severe Amanita phalloides mushroom poisoning. Am J Surg 1990;159(5):493-9.
15. Brandão JL, Pinheiro J, Pinho D, Correia da Silva D, Fernandes E, Fragoso G, et al. Intoxicação por cogumelos em portugal. Acta Med Port. 2011;24(S2):269-78.
16. Mowry JB, Spyker DA, Cantilena LR, Jr., Bailey JE, Ford M. 2012 Annual Report of the American Association of Poison Control Centers' National Poison Data System (NPDS): 30th Annual Report. Clin Toxicol (Phila). 2013;51(10):949-1229.
17. Schenk-Jaeger KM, Rauber-Luthy C, Bodmer M, Kupferschmidt H, Kullak-Ublick GA, Ceschi A. Mushroom poisoning: a study on circumstances of exposure and patterns of toxicity. Eur J Intern Med. 2012;23(4):e85-91.
18. Giannini L, Vannacci A, Missanelli A, Mastroianni R, Mannaioni PF, Moroni F, et al. Amatoxin poisoning: A 15-year retrospective analysis and follow-up evaluation of 105 patients. Clin Toxicol. 2007;45(5):539-42.
19. Jaeger A, Jehl F, Flesch F, Sauder P, Kopferschmitt J. Kinetics of amatoxins in human poisoning: therapeutic implications. J Toxicol Clin Toxicol. 1993;31(1):63-80.
20. Barceloux DG. Medical Toxicology of Natural Substances: Foods, Fungi, Medicinal Herbs, Plants, and Venomous Animals: Wiley; 2008.
21. Block SS, Stephens RL, Murrill WA. Natural Food Poisons, Amanita Toxins in Mushrooms. J Agr Food Chem. 1955;3(7):584-7.
22. Kaneko H, Tomomasa T, Inoue Y, Kunimoto F, Fukusato T, Muraoka S, et al. Amatoxin poisoning from ingestion of Japanese Galerina mushrooms. J Toxicol Clin Toxicol. 2001;39(4):413-6.

23. Olson KR, Pond SM, Seward J, Healey K, Woo OF, Becker CE. Amanita phalloides-type mushroom poisoning. West J Med. 1982;137(4):282-9.
24. Pond SM, Olson KR, Woo OF, Osterloh JD, Ward RE, Kaufman DA, et al. Amatoxin poisoning in northern California, 1982-1983. West J Med. 1986;145(2):204-9.
25. Trim GM, Lepp H, Hall MJ, McKeown RV, McCaughan GW, Duggin GG, et al. Poisoning by Amanita phalloides ("deathcap") mushrooms in the Australian Capital Territory. Med J Aust. 1999;171(5):247-9.
26. Reid DA, Eicker A. South African fungi: the genus Amanita. Mycol Res. 1991;95(1):80-95.
27. Enjalbert F, Cassanas G, Guinchard C, Chaumont JP. Toxin composition of Amanita phalloides tissues in relation to the collection site. Mycologia. 1996;88(6):909-21.
28. Enjalbert F, Cassanas G, Salhi SL, Guinchard C, Chaumont JP. Distribution of the amatoxins and phallotoxins in Amanita phalloides. Influence of the tissues and the collection site. C R Acad Sci III. 1999;322(10):855-62.
29. Enjalbert F, Gallion C, Jehl F, Monteil H. Toxin content, phallotoxin and amatoxin composition of Amanita phalloides tissues. Toxicon. 1993;31(6):803-7.
30. Hu J, Zhang P, Zeng J, Chen Z. Determination of amatoxins in different tissues and development stages of Amanita exitialis. J Sci Food Agric. 2012;92(13):2664-7.
31. Lynen F, Wieland U. Über die Giftstoffe des Knollenblätterpilzes. IV. Justus Liebigs Annalen der Chemie. 1938;533(1):93-117.
32. Cooper JA. Effects of cytochalasin and phalloidin on actin. J Cell Biol. 1987;105(4):1473-8.
33. Dancker P, Low I, Hasselbach W, Wieland T. Interaction of actin with phalloidin: polymerization and stabilization of F-actin. Biochim Biophys Acta. 1975;400(2):407-14.
34. Gabbiani G, Montesano R, Tuchweber B, Salas M, Orci L. Phalloidin-induced hyperplasia of actin filaments in rat hepatocytes. Lab Invest. 1975;33(5):562-9.
35. Wieland T. Interaction of phallotoxins with actin. Adv Enzyme Regul. 1976;15:285-300.
36. Wieland T, Faulstich H. Amatoxins, phallotoxins, phallolysin, and antamanide: the biologically active components of poisonous Amanita mushrooms. CRC Crit Rev Biochem. 1978;5(3):185-260.
37. Derelanko MJ, Hollinger MA. Handbook of Toxicology, Second Edition: Taylor & Francis; 2001.
38. Brossi A. The Alkaloids: Chemistry and Pharmacology Elsevier Science; 1991.
39. Turcotte A, Gicquaud C, Gendreau M, St-Pierre S. Séparation des virotoxines du champignon Amanita virosa et étude comparative de leur interaction sur l'actine in vitro. Can J Biochemi Cell B. 1984;62(12):1327-34.
40. Wong JH. Chapter 25 - Fungal Toxins. In: Kastin AJ, editor. Handbook of Biologically Active Peptides (Second Edition). Boston: Academic Press; 2013. p. 166-8.
41. Faulstich H, Buku A, Bodenmuller H, Wieland T. Virotoxins: actin-binding cyclic peptides of Amanita virosa mushrooms. Biochemistry. 1980;19(14):3334-43.
42. Loranger A, Tuchweber B, Gicquaud C, St-Pierre S, Cote MG. Toxicity of peptides of Amanita virosa mushrooms in mice. Fundam Appl Toxicol. 1985;5(6 Pt 1):1144-52.
43. Himmelmann A, Mang G, Schnorf-Huber S. Lethal ingestion of stored Amanita phalloides mushrooms. Swiss Med Wkly. 2001;131(41-42):616-7.
44. Deshpande SS. Handbook of Food Toxicology: Taylor & Francis; 2002.
45. Faulstich H, Talas A, Wellhoner HH. Toxicokinetics of labeled amatoxins in the dog. Arch Toxicol. 1985;56(3):190-4.
46. Homann J, Rawer P, Bleyl H, Matthes KJ, Heinrich D. Early detection of amatoxins in human mushroom poisoning. Arch Toxicol. 1986;59(3):190-1.
47. Mydlik M, Derzsiova K. Liver and kidney damage in acute poisonings. Bantao Journal. 2006;4(1):30-2.
48. Becker CE, Tong TG, Boerner U, Roe RL, Sco TA, MacQuarrie MB, et al. Diagnosis and treatment of Amanita phalloides-type mushroom poisoning: use of thioctic acid. West J Med. 1976;125(2):100-9.

49. Faulstich H. New aspects of amanita poisoning. Klin Wochenschr. 1979;57(21):1143-52.
50. Amini M, Ahmadabadi A, Kazemifar AM, Solhi H, Jand Y. Amanita Phalloides Intoxication Misdiagnosed as Acute Appendicitis: A Case Report. Iran J Toxicol. 2011;5(14):527-30.
51. Serne EH, Toorians AW, Gietema JA, Bronsveld W, Haagsma EB, Mulder PO. Amanita phalloides, a potentially lethal mushroom: its clinical presentation and therapeutic options. Neth J Med. 1996;49(1):19-23.
52. Wieland T. The toxic peptides from Amanita mushrooms. Int J Pept Protein Res. 1983;22(3):257-76.
53. Cochet-Meilhac M, Chambon P. Animal DNA-dependent RNA polymerases. 11. Mechanism of the inhibition of RNA polymerases B by amatoxins. Biochim Biophys Acta. 1974;353(2):160-84.
54. Nguyen VT, Giannoni F, Dubois M-F, Seo S-J, Vigneron M, Kédinger C, et al. In Vivo Degradation of RNA Polymerase II Largest Subunit Triggered by α-Amanitin. Nucleic Acids Res. 1996;24(15):2924-9.
55. Rudd MD, Luse DS. Amanitin Greatly Reduces the Rate of Transcription by RNA Polymerase II Ternary Complexes but Fails to Inhibit Some Transcript Cleavage Modes. J Biol Chem. 1996;271(35):21549-58.
56. Bushnell DA, Cramer P, Kornberg RD. Structural basis of transcription: α-Amanitin–RNA polymerase II cocrystal at 2.8 Å resolution. Proc Natl Acad Sci USA. 2002;99(3):1218-22.
57. Kaplan CD, Larsson KM, Kornberg RD. The RNA polymerase II trigger loop functions in substrate selection and is directly targeted by alpha-amanitin. Mol Cell. 2008;30(5):547-56.
58. Wang D, Bushnell DA, Westover KD, Kaplan CD, Kornberg RD. Structural basis of transcription: role of the trigger loop in substrate specificity and catalysis. Cell. 2006;127(5):941-54.
59. Magdalan J, Ostrowska A, Piotrowska A, Izykowska I, Nowak M, Gomulkiewicz A, et al. alpha-Amanitin induced apoptosis in primary cultured dog hepatocytes. Folia Histochem Cytobiol. 2010;48(1):58-62.
60. Magdalan J, Piotrowska A, Gomulkiewicz A, Sozanski T, Podhorska-Okolow M, Szelag A, et al. Benzylpenicyllin and acetylcysteine protection from alpha-amanitin-induced apoptosis in human hepatocyte cultures. Exp Toxicol Pathol. 2011;63(4):311-5.
61. Magdalan J, Ostrowska A, Piotrowska A, Gomulkiewicz A, Podhorska-Okolow M, Patrzalek D, et al. Benzylpenicillin, acetylcysteine and silibinin as antidotes in human hepatocytes intoxicated with alpha-amanitin. Exp Toxicol Pathol. 2010;62(4):367-73.
62. Ljungman M, Zhang F, Chen F, Rainbow AJ, McKay BC. Inhibition of RNA polymerase II as a trigger for the p53 response. Oncogene. 1999;18(3):583-92.
63. Arima Y, Nitta M, Kuninaka S, Zhang D, Fujiwara T, Taya Y, et al. Transcriptional Blockade Induces p53-dependent Apoptosis Associated with Translocation of p53 to Mitochondria. J Biol Chem. 2005;280(19):19166-76.
64. Leu JI, George DL. Hepatic IGFBP1 is a prosurvival factor that binds to BAK, protects the liver from apoptosis, and antagonizes the proapoptotic actions of p53 at mitochondria. Genes Dev. 2007;21(23):3095-109.
65. Leist M, Gantner F, Naumann H, Bluethmann H, Vogt K, Brigelius-Flohe R, et al. Tumor necrosis factor-induced apoptosis during the poisoning of mice with hepatotoxins. Gastroenterology. 1997;112(3):923-34.
66. El-Bahay C, Gerber E, Horbach M, Tran-Thi QH, Rohrdanz E, Kahl R. Influence of tumor necrosis factor-alpha and silibin on the cytotoxic action of alpha-amanitin in rat hepatocyte culture. Toxicol Appl Pharmacol. 1999;158(3):253-60.
67. Zheleva A. Phenoxyl radicals formation might contribute to severe toxicity of mushrooms toxin alpha-amanitin- an electron paramagnetic resonance study. TJS. 2013;11(1):33-8.

68. Zheleva A, Tolekova A, Zhelev M, Uzunova V, Platikanova M, Gadzheva V. Free radical reactions might contribute to severe alpha amanitin hepatotoxicity-a hypothesis. Med Hypotheses. 2007;69(2):361-7.
69. Fineschi V, Di Paolo M, Centini F. Histological criteria for diagnosis of amanita phalloides poisoning. J Forensic Sci. 1996;41(3):429-32.
70. Kucuk HF, Karasu Z, Kılıc M, Nart D. Liver Failure in Transplanted Liver Due to Amanita Falloides. Transplantat Proc. 2005;37(5):2224-6.
71. Sanz P, Reig R, Borras L, Martinez J, Manez R, Corbella J. Disseminated intravascular coagulation and mesenteric venous thrombosis in fatal Amanita poisoning. Hum Toxicol. 1988;7(2):199-201.
72. Soysal D, Cevik C, Saklamaz A, Yetimalar Y, Unsal B. Coagulation disorders secondary to acute liver failure in Amanita phalloides poisoning: a case report. Turk J Gastroenterol. 2006;17(3):198-202.
73. Ytrebo LM, Sen S, Rose C, Ten Have GA, Davies NA, Hodges S, et al. Interorgan ammonia, glutamate, and glutamine trafficking in pigs with acute liver failure. Am J Physiol Gastrointest Liver Physiol. 2006;291(3):G373-81.
74. Diaz JH. Evolving global epidemiology, syndromic classification, general management, and prevention of unknown mushroom poisonings. Crit Care Med. 2005;33(2):419-26.
75. Enjalbert F, Cassanas G, Rapior S, Renault C, Chaumont JP. Amatoxins in wood-rotting Galerina marginata. Mycologia. 2004;96(4):720-9.
76. Enjalbert F, Gallion C, Jehl F, Monteil H, Faulstich H. Simultaneous assay for amatoxins and phallotoxins in Amanita phalloides Fr. by high-performance liquid chromatography. J Chromatogr. 1992;598(2):227-36.
77. Rittgen J, Putz M, Pyell U. Identification of toxic oligopeptides in Amanita fungi employing capillary electrophoresis-electrospray ionization-mass spectrometry with positive and negative ion detection. Electrophoresis. 2008;29(10):2094-100.
78. Chung WC, Tso SC, Sze ST. Separation of polar mushroom toxins by mixed-mode hydrophilic and ionic interaction liquid chromatography-electrospray ionization-mass spectrometry. J Chromatogr Sci. 2007;45(2):104-11.
79. Jansson D, Fredriksson SA, Herrmann A, Nilsson C. A concept study on identification and attribution profiling of chemical threat agents using liquid chromatography-mass spectrometry applied to Amanita toxins in food. Forensic Sci Int. 2012;221(1-3):44-9.
80. Ahmed W, Gonmori K, Suzuki M, Watanabe K, Suzuki O. Simultaneous analysis of α-amanitin, α-amanitin, and phalloidin in toxic mushrooms by liquid chromatography coupled to time-of-flight mass spectrometry. Forensic Toxicol. 2010;28(2):69-76.
81. Bleuter JA, Vergeer AA. Amatoxins in American mushrooms: evaluation of the meixner test. Mycologia. 1980;72(6):1142-9.
82. Beuhler M, Lee DC, Gerkin R. The Meixner test in the detection of alpha-amanitin and false-positive reactions caused by psilocin and 5-substituted tryptamines. Ann Emerg Med. 2004;44(2):114-20.
83. Butera R, Locatelli C, Coccini T, Manzo L. Diagnostic accuracy of urinary amanitin in suspected mushroom poisoning: a pilot study. J Toxicol Clin Toxicol. 2004;42(6):901-12.
84. Albertson TE, Owen KP, Sutter ME, Chan AL. Gastrointestinal decontamination in the acutely poisoned patient. Int J Emerg Med. 2011;4:65.
85. Santi L, Maggioli C, Mastroroberto M, Tufoni M, Napoli L, Caraceni P. Acute Liver Failure Caused by Amanita phalloides Poisoning. Int J Hepatol. 2012;2012:6.
86. Seymour FK, Henry JA. Assessment and management of acute poisoning by petroleum products. Hum Exp Toxicol 2001;20(11):551-62.
87. Vale JA. Position statement: gastric lavage. American Academy of Clinical Toxicology; European Association of Poisons Centres and Clinical Toxicologists. J Toxicol Clin Toxicol. 1997;35(7):711-9.

88. Vale JA, Kulig K, American Academy of Clinical T, European Association of Poisons C, Clinical T. Position paper: gastric lavage. J Toxicol Clin Toxicol. 2004;42(7):933-43.
89. TOXBASE Clinical toxicology database of the United Kingdom national poisons information service: Amanita phalloides-features and management [www.toxbase.org accessed 7th February 2015]. 2008.
90. CIAV. Centro de informação antivenenos: Protocolo terapêutico preconizado pelo CIAV nos casos de intoxicação por Amanita Phalloides. In: Instituto Nacional de Emergência Médica - INEM IP, 2014.
91. Mas A. Mushrooms, amatoxins and the liver. J Hepatol. 2005;42(2):166-9.
92. National Poisons Centre, New Zealand: Amanita phalloides [www.toxinz.com accessed 7th February 2015]. 2013.
93. Koppel C. Clinical symptomatology and management of mushroom poisoning. Toxicon. 1993;31(12):1513-40.
94. Lionte C, Sorodoc L, Simionescu V. Successful treatment of an adult with Amanita phalloides-induced fulminant liver failure with molecular adsorbent recirculating system (MARS). Rom J Gastroenterol. 2005;14(3):267-71.
95. Shi Y, He J, Chen S, Zhang L, Yang X, Wang Z, et al. MARS: optimistic therapy method in fulminant hepatic failure secondary to cytotoxic mushroom poisoning--a case report. Liver. 2002;22 Suppl 2:78-80.
96. Bergis D, Friedrich-Rust M, Zeuzem S, Betz C, Sarrazin C, Bojunga J. Treatment of Amanita phalloides intoxication by fractionated plasma separation and adsorption (Prometheus(R)). J Gastrointestin Liver Dis. 2012;21(2):171-6.
97. Poucheret P, Fons F, Dore JC, Michelot D, Rapior S. Amatoxin poisoning treatment decision-making: pharmaco-therapeutic clinical strategy assessment using multidimensional multivariate statistic analysis. Toxicon. 2010;55(7):1338-45.
98. Moroni F, Fantozzi R, Masini E, Mannaioni PF. A trend in the therapy of Amanita phalloides poisoning. Arch Toxicol. 1976;36(2):111-5.
99. Magdalan J, Ostrowska A, Piotrowska A, Gomulkiewicz A, Szelag A, Dziedgiel P. Comparative antidotal efficacy of benzylpenicillin, ceftazidime and rifamycin in cultured human hepatocytes intoxicated with alpha-amanitin. Arch Toxicol. 2009;83(12):1091-6.
100. Floersheim GL, Eberhard M, Tschumi P, Duckert F. Effects of penicillin and silymarin on liver enzymes and blood clotting factors in dogs given a boiled preparation of Amanita phalloides. Toxicol Appl Pharmacol. 1978;46(2):455-62.
101. Tong TC, Hernandez M, Richardson WH, 3rd, Betten DP, Favata M, Riffenburgh RH, et al. Comparative treatment of alpha-amanitin poisoning with N-acetylcysteine, benzylpenicillin, cimetidine, thioctic acid, and silybin in a murine model. Ann Emerg Med. 2007;50(3):282-8.
102. Kaya E, Surmen MG, Yaykasli KO, Karahan S, Oktay M, Turan H, et al. Dermal absorption and toxicity of alpha amanitin in mice. Cutan Ocul Toxicol. 2014;33(2):154-60.
103. Floersheim GL. Toxins and intoxications from the toadstool Amanita phalloides. Trends Pharmacol Sci. 1983;4(0):263-6.
104. Kroncke KD, Fricker G, Meier PJ, Gerok W, Wieland T, Kurz G. alpha-Amanitin uptake into hepatocytes. Identification of hepatic membrane transport systems used by amatoxins. J Biol Chem. 1986;261(27):12562-7.
105. Luper S. A review of plants used in the treatment of liver disease: part 1. Altern Med Rev. 1998;3(6):410-21.
106. Mengs U, Pohl RT, Mitchell T. Legalon(R) SIL: the antidote of choice in patients with acute hepatotoxicity from amatoxin poisoning. Curr Pharm Biotechnol. 2012;13(10):1964-70.
107. Vogel G, Tuchweber B, Trost W, Mengs U. Protection by silibinin against Amanita phalloides intoxication in beagles. Toxicol Appl Pharmacol. 1984;73(3):355-62.
108. Fraschini F, Demartini G, Esposti D. Pharmacology of Silymarin. Clin Drug Invest. 2002;22(1):51-65.
109. Pradhan SC, Girish C. Hepatoprotective herbal drug, silymarin from experimental pharmacology to clinical medicine. Indian J Med Res. 2006;124(5):491-504.

110. James LP, Mayeux PR, Hinson JA. Acetaminophen-induced hepatotoxicity. Drug Metab Dispos. 2003;31(12):1499-506.
111. Akin A, Ozgur S, Kiliç D, Aliustaoglu M, Keskek N. The Effects of N-acetylcysteine in Patients with Amanita phalloides intoxication. J Drug Toxicol. 2013;4(5):3.
112. Schneider SM, Michelson EA, Vanscoy G. Failure of N-acetylcysteine to reduce alpha amanitin toxicity. J Appl Toxicol. 1992;12(2):141-2.
113. Floersheim GL, Weber O, Tschumi P, Ulbrich M. [Clinical death-cap (Amanita phalloides) poisoning: prognostic factors and therapeutic measures. Analysis of 205 cases]. Schweiz Med Wochenschr. 1982;112(34):1164-77.
114. Hruby K, Csomos G, Fuhrmann M, Thaler H. Chemotherapy of Amanita phalloides poisoning with intravenous silibinin. Hum Toxicol. 1983;2(2):183-95.
115. Fantozzi R, Ledda F, Caramelli L, Moroni F, Blandina P, Masini E, et al. Clinical findings and follow-up evaluation of an outbreak of mushroom poisoning--survey of Amanita phalloides poisoning. Klin Wochenschr. 1986;64(1):38-43.
116. Feinfeld DA, Mofenson HC, Caraccio T, Kee M. Poisoning by amatoxin-containing mushrooms in suburban New York-report of four cases. J Toxicol Clin Toxicol. 1994;32(6):715-21.
117. Jander S, Bischoff J, Woodcock BG. Plasmapheresis in the treatment of Amanita phalloides poisoning: II. A review and recommendations. Ther Apher. 2000;4(4):308-12.
118. Krenova M, Pelclova D, Navratil T. Survey of Amanita phalloides poisoning: clinical findings and follow-up evaluation. Hum Exp Toxicol. 2007;26(12):955-61.
119. Ahishali E, Boynuegri B, Ozpolat E, Surmeli H, Dolapcioglu C, Dabak R, et al. Approach to mushroom intoxication and treatment: can we decrease mortality? Clin Res Hepatol Gastroenterol. 2012;36(2):139-45.
120. Ward J, Kapadia K, Brush E, Salhanick SD. Amatoxin poisoning: case reports and review of current therapies. J Emerg Med. 2013;44(1):116-21.
121. Roberts DM, Hall MJ, Falkland MM, Strasser SI, Buckley NA. Amanita phalloides poisoning and treatment with silibinin in the Australian Capital Territory and New South Wales. Med J Aust. 2013;198(1):43-7.
122. Larson AM. Acute liver failure. Dis Mon. 2008;54(7):457-85.
123. O'Grady JG, Alexander GJ, Hayllar KM, Williams R. Early indicators of prognosis in fulminant hepatic failure. Gastroenterology. 1989;97(2):439-45.
124. Bernuau J. Selection for emergency liver transplantation. J Hepatol. 1993;19(3):486-7.
125. Klein AS, Hart J, Brems JJ, Goldstein L, Lewin K, Busuttil RW. Amanita poisoning: Treatment and the role of liver transplantation. Am J Med. 1989;86(2):187-93.
126. Chen W-C, Kassi M, Saeed U, Frenette CT. A Rare Case of Amatoxin Poisoning in the State of Texas. Case Rep Gastroenterol. 2012;6(2):350-7.
127. Das RN, Parajuli S, Jayakumar J. “Last supper with mushroom soup”: a case report of amatoxin poisoning. Mcgill J Med. 2007;10(2):93-5.
128. Dias LG, Pereira AP, Estevinho LM. Comparative study of different Portuguese samples of propolis: pollinic, sensorial, physicochemical, microbiological characterization and antibacterial activity. Food Chem Toxicol. 2012;50(12):4246-53.
129. Evelpidou N, Figueiredo T, Mauro F, Tecim V, vassilopoulos A. Natural Heritage from East to West: case studies from 6 EU countries. Berlin: Springer Verlag; 2010.
130. Agroconcultores, Coba. Carta darta dos Solos. Carta do Uso Actual da Terra e Carta de Aptidão da Terra do Nordeste de Portugal. Vila Real: UTAD/PDRITM; 1991.
131. Filigenzi MS, Poppenga RH, Tiwary AK, Puschner B. Determination of alpha-amanitin in serum and liver by multistage linear ion trap mass spectrometry. J Agric Food Chem. 2007;55(8):2784-90.
132. Tanahashi M, Kaneko R, Hirata Y, Hamajima M, Arinobu T, Ogawa T, et al. Simple analysis of α-amanitin and β-amanitin in human plasma by liquid chromatography-mass spectrometry. Forensic Toxicol. 2010;28(2):110-4.
133. Tagliaro F, Schiavon G, Bontempelli G, Carli G, Marigo M. Improved high-performance liquid chromatographic determination with amperometric detection of

alpha-amanitin in human plasma based on its voltammetric study. J Chromatogr. 1991;563(2):299-311.
134. Defendenti C, Bonacina E, Mauroni M, Gelosa L. Validation of a high performance liquid chromatographic method for alpha amanitin determination in urine. Forensic Sci Int. 1998;92(1):59-68.
135. Leite M, Freitas A, Azul AM, Barbosa J, Costa S, Ramos F. Development, optimization and application of an analytical methodology by ultra performance liquid chromatography-tandem mass spectrometry for determination of amanitins in urine and liver samples. Anal Chim Acta. 2013;799:77-87.
136. Tagliaro F, Chiminazzo S, Maschio S, Alberton F, Marigo M. Improved high performance liquid chromatographic determination of amanitins with electrochemical detection. Chromatographia. 1987;24(1):482-6.
137. Letschert K, Faulstich H, Keller D, Keppler D. Molecular characterization and inhibition of amanitin uptake into human hepatocytes. Toxicological sciences : an official journal of the Society of Toxicology. 2006;91(1):140-9.
138. Cho H, Wu M, Bilgin B, Walton SP, Chan C. Latest developments in experimental and computational approaches to characterize protein–lipid interactions. Proteomics. 2012;12(22):3273-85.
139. Kitchen DB, Decornez H, Furr JR, Bajorath J. Docking and scoring in virtual screening for drug discovery: methods and applications. Nat Rev Drug Discov. 2004;3(11):935-49.
140. Alonso H, Bliznyuk AA, Gready JE. Combining docking and molecular dynamic simulations in drug design. Med Res Rev. 2006;26(5):531-68.
141. Azam SS, Abbasi SW. Molecular docking studies for the identification of novel melatoninergic inhibitors for acetylserotonin-O-methyltransferase using different docking routines. Theor Biol Med Model. 2013;10:63.
142. Ilizaliturri-Flores I, Rosas-Trigueros J, Carrilho-Vazquez J, Vique-Snchez J, Carrillo-Ibarra N, Zamora-Lopez B, et al. Identification of pharmacological targets combining docking and molecular dynamics simulations. Am J Agric Biol Sci. 2013;8:89-106.
143. Srivastava HK, Sastry GN. Molecular Dynamics Investigation on a Series of HIV Protease Inhibitors: Assessing the Performance of MM-PBSA and MM-GBSA Approaches. J Chem Inf Model. 2012;52(11):3088-98.
144. Schneider SM, Borochovitz D, Krenzelok EP. Cimetidine protection against alpha-amanitin hepatotoxicity in mice: a potential model for the treatment of Amanita phalloides poisoning. Ann Emerg Med. 1987;16(10):1136-40.
145. Wills BK, Haller NA, Peter D, White LJ. Use of amifostine, a novel cytoprotective, in alpha-amanitin poisoning. Clin Toxicol (Phila). 2005;43(4):261-7.
146. Yamaura Y, Fukuhara M, Takabatake E, Ito N, Hashimoto T. Hepatotoxic action of a poisonous mushroom, Amanita abrupta in mice and its toxic component. Toxicology. 1986;38(2):161-73.
147. Zhao J, Cao M, Zhang J, Sun Q, Chen Q, Yang ZR. Pathological effects of the mushroom toxin alpha-amanitin on BALB/c mice. Peptides. 2006;27(12):3047-52.
148. Chang LM, Yun HS, Kim YS, Ahn JW. Aucubin: potential antidote for alpha-amanitin poisoning. J Toxicol Clin Toxicol. 1984;22(1):77-85.
149. Bidnychenko Y. Detecting Mushroom Peptide Toxins in Body Fluids by Capillary Electrophoresis. LCGC. 2001;19(9):1000-2.
150. Floersheim GL. Antagonistic effects to phalloidin, alpha-amanitin and extracts of Amanita phalloides. Agents Actions. 1971;2(3):142-9.
151. He J, Gao S, Hu M, Chow DS, Tam VH. A validated ultra-performance liquid chromatography-tandem mass spectrometry method for the quantification of polymyxin B in mouse serum and epithelial lining fluid: application to pharmacokinetic studies. J Antimicrob Chemother. 2013;68(5):1104-10.
152. Chang I-M, Yamaura Y. Aucubin: A new antidote for poisonous Amanita mushrooms. Phytother Res. 1993;7(1):53-6.

153. Mendez-Navarro J, Ortiz-Olvera NX, Villegas-Rios M, Mendez-Tovar LJ, Andersson KL, Moreno-Alcantar R, et al. Hepatotoxicity from ingestion of wild mushrooms of the genus Amanita section Phalloideae collected in Mexico City: two case reports. Ann Hepatol. 2011;10(4):568-74.
154. Unverir P, Soner BC, Dedeoglu E, Karcioglu O, Boztok K, Tuncok Y. Renal and hepatic injury with elevated cardiac enzymes in Amanita phalloides poisoning: a case report. Hum Exp Toxicol. 2007;26(9):757-61.
155. Garrouste C, Hemery M, Boudat AM, Kamar N. Amanita phalloides poisoning-induced end-stage renal failure. Clin Nephrol. 2009;71(5):571-4.
156. Leclercq IA, Farrell GC, Sempoux C, Peña Ad, Horsmans Y. Curcumin inhibits NF-□B activation and reduces the severity of experimental steatohepatitis in mice. J Hepatol. 2004;41(6):926-34.
157. Rodriguez M, Cabal-Hierro L, Carcedo MT, Iglesias JM, Artime N, Darnay BG, et al. NF-kappaB signal triggering and termination by tumor necrosis factor receptor 2. J Biol Chem. 2011;286(26):22814-24.
158. Jung HS, Joo JD, Kim DW, In JH, Roh M, Jeong JT, et al. Effect of milrinone on the inflammatory response and NF-kB activation in renal ischemia-reperfusion injury in mice. Korean J Anesthesiol. 2014;66(2):136-42.
159. Murr MM, Yang J, Fier A, Kaylor P, Mastorides S, Norman JG. Pancreatic elastase induces liver injury by activating cytokine production within Kupffer cells via nuclear factor-Kappa B. J Gastrointest Surg. 2002;6(3):474-80.
160. Zhao YF, Zhai WL, Zhang SJ, Chen XP. Protection effect of triptolide to liver injury in rats with severe acute pancreatitis. Hepatobiliary Pancreat Dis Int. 2005;4(4):604-8.
161. Dalle-Donne I, Rossi R, Giustarini D, Milzani A, Colombo R. Protein carbonyl groups as biomarkers of oxidative stress. Clin Chim Acta. 2003;329(1-2):23-38.
162. Morgan MJ, Liu Z-g. Crosstalk of reactive oxygen species and NF-κB signaling. Cell Research. 2011;21(1):103-15.